

Mechanically triggered on-demand degradation of polymers synthesized by radical polymerizations

In the format provided by the
authors and unedited

Table of Contents

Experimental Section.....	3
Materials	3
Instrumentation.....	3
Synthesis of ethyl 3-hexyl-2,4-dioxo-3-azabicyclo[3.2.0]hept-6-ene-6-carboxylate (HCBI).....	6
Synthesis of ethyl 3-methyl-2,4-dioxo-3-azabicyclo[3.2.0]hept-6-ene-6-carboxylate (MCBI)	6
Synthesis of diethyl 3,3'-(hexane-1,6-diyl)bis(2,4-dioxo-3-azabicyclo[3.2.0]hept-6-ene-6-carboxylate) (DCBI)	7
Synthesis of ethyl 3,4-dipropylcyclobut-1-ene-1-carboxylate (CBO)	8
Determination of reactivity ratio	13
Ultrasonication of polymers followed by ^1H NMR and FT-IR measurements.....	13
Ultrasonication of polymers followed by treatment with NaOH solution.....	13
NaOH solution treatment of polymers followed by ultrasonication.....	14
Cryo-milling of polymers followed by treatment with NaOH solution	14
Ball-milling of polymers followed by treatment with NaOH solution.....	14
Ball-milling of dry polymers with solid NaOH.....	14
Ultrasonication of polymer followed by treatment with NaOH solutions of different concentrations.....	15
Degradation products analysis.....	15
Thermal stability experiments of PHCBI and PS-<i>co</i>-PHCBI.....	15
Supporting Data	16
Determination of copolymer type by NMR experiments.....	16
Determination of monomer reactivity ratios	18
TGA and DSC data	21
Dynamic mechanical analysis (DMA) data.....	26
Thermal stability experiments of PHCBI and PS-<i>co</i>-PHCBI.....	30
Effect of ultrasonication on polymers monitored by ^1H NMR and FT-IR measurements	32
Treatment of polymers with NaOH solution followed by ultrasonication	47

Cryo-milling of polymers followed by treatment with NaOH solution	47
Treatment of polymers with different mechanical methods and hydrolysis	50
Ball-milling of dry polymers with solid NaOH.....	51
Ultrasonication of polymer followed by treatment with NaOH solutions of different concentrations.....	52
Chromatographic isolation and characterization of degradation products of PS ₅₀ -co-PHCBI ₅₀	52
Characterization of the degradation products	54
CoGEF Calculation.....	62
NMR spectra.....	88
<i>Reference</i>	120

Experimental Section

Materials

Styrene, methyl acrylate and methyl methacrylate were purchased from Sigma-Aldrich and passed through a short basic alumina column before use. 1,3-Butadiene (2 mol L⁻¹ in THF) was purchased from TCI and passed through a short basic alumina column before use. Azobisisobutyronitrile (AIBN) was purchased from Sigma-Aldrich and recrystallized in methanol before use. Hexylamine, hexamethylenediamine, maleic anhydride, (Z)-oct-4-ene, aluminium chloride (AlCl₃), trifluoroacetic acid (TFA), acetic acid, acetic anhydride, nickel (II) acetate tetrahydrate, trimethylamine (Et₃N), cross-linked polystyrene (Poly(styrene-*co*-divinylbenzene)) and 1,3,5-trimethoxybenzene were purchased from Sigma-Aldrich and used without further purification. *N*-methylmaleimide was purchased from TCI and used without further purification. Ethyl propiolate was purchased from Fluorochem and used without further purification. Polystyrene (M.W. 50 kg mol⁻¹, $D = 1.06$) was purchased from Alfa Aesar. Solvents were purchased from Acros Organics, Sigma Aldrich, Fischer Scientific, and Reactolab and were used without further purification. Deuterated chloroform (CDCl₃) was purchased from Cambridge Isotope Laboratories. *N*-hexyl maleimide is commercial available and here we synthesized it following the literature¹. 1,1'-(hexane-1,6-diyl)bis(1H-pyrrole-2,5-dione) was synthesized following the literature².

Instrumentation

NMR spectra were recorded on a Bruker Avance III 300 MHz NMR spectrometer (¹H NMR 300 MHz, ¹³C NMR 75 MHz) or Bruker Avance III 400 MHz NMR spectrometer (¹H NMR 400 MHz, ¹³C NMR 101 MHz) or Bruker Avance III 400 MHz NMR spectrometer (¹H NMR 400 MHz, ¹³C NMR 101 MHz) with Prodigy Cryoprobe. Data were evaluated with the MestReNova software suite and all chemical shifts δ are reported in parts per million (ppm) with coupling constant in Hz. IR spectra were measured on a PerkinElmer Spectrum 65 FT-IR spectrometer with an ATR set-up. The polymer solution was pipetted onto the crystal, and the solvent was allowed to evaporate before a measurement.

Relative molecular weights and molecular weight distributions of polymers were measured by size exclusion chromatography (SEC) on either A or B. (A) An Agilent 1200 series HPLC system equipped with an Agilent PLgel mixed guard column (particle size = 5 μ m) and two Agilent PLgel mixed-D columns (ID = 7.5 mm, L = 300 mm, particle size = 5 μ m). Signals were recorded by an UV detector (Agilent 1200 series, 346 nm), an Optilab REX interferometric refractometer, and a miniDawn TREOS light scattering detector (Wyatt Technology Corp.). Samples were run using THF as the eluent at 30 °C and a flow rate of 1.0 mL min⁻¹. The sample solutions were filtered through a 13 mm syringe filter (Nylon 66, nonsterile, pore size 0.22 μ m, Swiss Labs) before injection. (B) An Agilent 1260 series pump equipped with two Agilent PLgel MIXED-B columns (ID = 7.5 mm, L = 300 mm, particle size = 10 μ m), an Agilent 1200 series diode array detector (254 nm and 320 nm), a Wyatt 18-angle

DAWN HELEOS light scattering detector, and an Optilab rEX differential refractive index detector. The mobile phase was THF at room temperature and a flow rate of 1.0 mL min⁻¹. The sample solutions were filtered through a 13 mm syringe filter (PTFE, nonsterile, pore size 0.22 µm, Filtrous) before injection. Data analyses were carried out on Astra software (Wyatt Technology Corp.) and molecular weights were determined based on narrow molecular weight polystyrene standards calibration.

Thermogravimetric analysis (TGA) was conducted on a Mettler Toledo TGA/DSC 1 STAR system under nitrogen up to 600 °C with a heating rate of 10 °C min⁻¹. The reported degradation temperature (T_d) was taken at the extrapolated onset temperature. Differential scanning calorimetry (DSC) was conducted on a Mettler Toledo DSC 2 STAR system under nitrogen up to 250 °C with a heating and cooling rate of 20 °C min⁻¹. The glass transition temperature (T_g) was taken from the mid-point of the thermal transition in the second heating cycle (T_g of PCBI was taken from the first heating cycle). Dynamic mechanical analysis (DMA) measurements were performed using a TA Instruments DMA Q800 in tensile mode. The polymer films were cut into rectangular strips of a width of 2.8 mm and a length of ≈12 mm so that the measurement length of the sample was maintained at ≈10 mm. Experiments were conducted in a range of -70 °C to 200 °C. The heating rate of 3 °C min⁻¹ and a strain amplitude of 5 µm at a frequency of 1 Hz was applied.

Ultrasonication was performed with a Branson 450 digital sonifier using a 13 mm tip. Pulsed ultrasound (1 s on, 1 s off, 20 kHz, 20% amplitude) was applied at 0 °C with a chiller.

Cryo-milling was conducted on a SPEX SamplePrep 6770 Freezer/mill. The grinding was performed in a polycarbonate vial with 2 min-grinding-2 min-cooling setting at a rate of 12 cycles per second, under liquid nitrogen.

Ball-milling was conducted in a 10 ml screw-top grinding jar with stainless steel grinding balls with a diameter of 2 mm on a Retsch Mixer Mill MM400 with a frequency of 30 Hz.

Electrospray ionization mass spectrometry (ESI-MS) of synthesized compounds was carried out on a Bruker 4.7T BioAPEX II or an Agilent 6140 series Quadrupole LCMS Spectrometer system.

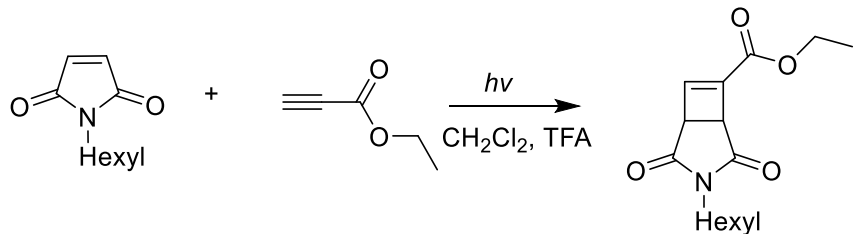
The high-resolution LC-MS analysis was performed by ultra-performance liquid chromatography coupled to a hybrid quadrupole, orthogonal acceleration time-of-flight high-resolution mass spectrometer (UPLC-QToF). A Waters ACQUITY™ UPLC™ I-Class coupled to a Waters Xevo™ G2-XS QTof (Waters Corporation, Wilmslow, UK) system was used in the Waters laboratory in Eschborn, Germany. The sample solutions were separated by reversed phase liquid chromatography using an ACQUITY UPLC I-Class system on a Waters ACQUITY UPLC BEH C18 analytical column (100 mm x 2.1 mm, 1.7 µm). In positive ionization mode, the injection volume was 2 µL (Solvent, PS₄₉-co-PHCBI₅₁, PS₄₉-co-PHCBI₅₁-cryo-milling-hydrolysis, PS₄₉-co-PHCBI₅₁-sonication-hydrolysis) and 8 µL (blank matrix). The higher injection volume of the blank matrix sample is to take into account the lower initial weight by a factor of four.

Due to the acidic chromatographic conditions and the therefore lower expected response in the negative ionization mode, the injection volume was 4 μ L and 10 μ L respectively. The UPLC parameters were as follows: column temperature 50 °C; flow rate 0.40 mL/min; temperature of the autosampler 8 °C; mobile phase, solvent A (0.1% formic acid in water, Biosolve, LCMS grade) and solvent B (0.1% formic acid in acetonitrile, Biosolve LCMS grade). The chromatographic separation started at 10% B for 0.5 min. The gradient was then increased to 98% B in 9 min and kept isocratic for 6 min. At 15.1 min the mobile phase ratio changed back to the initial conditions and was re-equilibrated for 2.4 min. The total run time per sample was 17 min. The LC-MS analysis was performed using the Xevo G2-XS QToF system with an electrospray (ESI) source operated in both positive (ESI⁺) and negative (ESI⁻) ion modes. The mass spectrometer operating conditions were as follows: cone voltage, 20 V; capillary voltage in ESI⁺ mode 3.0 kV; capillary voltage in ESI⁻ mode -2.5 kV; source temperature 120 °C; desolvation temperature 550 °C; nitrogen cone gas flow rate 50 L/h; and nitrogen desolvation gas flow of 950 L/h. The high resolution time of flight mass analyzer was operated at 30,000 resolution (defined as FWHM at *m/z* 956) with an acquisition time of 0.15s. The mass spectrometer was calibrated using a solution of sodium formate over a mass range of 50–2000 Da. The MS^E mode was used for data collection, meaning alternating scans between a low-energy full scan and a high-energy full scan. The collision voltage was set as 6.0 eV for the low-energy scan and a 15–55 eV ramp for the high-energy scan. Data were acquired over a mass range of 50–2000 *m/z*. The acquired data were centroided and lock mass corrected during data acquisition using an external reference (Lock-Spray™) consisting of a 200 pg/mL solution of leucine enkephalin infused at a flow rate of 20 μ L/min via a lockspray interface, generating a realtime reference ion of [M+H]⁺ (*m/z* 556.2766) in positive ion mode and [M-H]⁻ (*m/z* 554.2620) in negative ion mode to ensure accurate MS analyses. Data acquisition and data processing was performed using the waters_connect informatics platform and UNIFI™ (Waters Corporation, Wilmslow, UK). Peaks detection was performed by an Apex peak detection algorithm using the 3 dimensional peak shape³. An in-house, self-built compounds library (containing compound name, molecular formula, proposed chemical structure, and accurate molecular mass) of 18 selected target compounds was developed (Fig. S96) and used in waters_connect software. An accurate mass window of \pm 5 ppm was used as criteria for compounds confirmation on molecular ion masses. Typical adduct ions were selected including H⁺, Na⁺, HCOO⁻ and H⁻, and used for molecular ion confirmation purposes. The LC-MS system performance was assessed for mass accuracy, repeatability and sensitivity using a system suitability standard solution consisting of a 9 component mixture (acetaminophen, caffeine, leucine enkephalin, reserpine, sulfaguanidine, sulfadimethoxine, terfenadine, Val-Tyr-Val, verapamil) for both ionisation modes before measuring the actual samples of interest. Each sample was analysed in five replicate measurements.

UV reactions were conducted under a mercury lamp (36 W or 400 W) with cooling fans.

Silica flash column chromatography was performed on a Biotage Isolera system using SiliCycle SiliaSep HP flash cartridges.

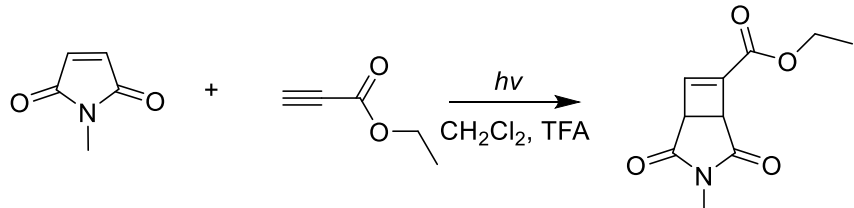
Synthesis of ethyl 3-hexyl-2,4-dioxo-3-azabicyclo[3.2.0]hept-6-ene-6-carboxylate (HCBI)



HCBI was synthesized following the literature⁴ with some modifications. *N*-hexyl maleimide (1.81g, 10 mmol, 1.0 eq), ethyl propiolate (2.45 g, 25 mmol, 2.5 eq.) and trifluoroacetic acid (1.2 g, 11 mmol, 1.1 eq.) were dissolved in 60 mL methylene chloride in a 100 mL flask. After sparging the solution for 30 min with N₂, the flask was sealed by septum and stirred under UV irradiation (mercury lamp, 400 W) for 48 h. After completion of the reaction (thin layer chromatography (TLC) monitoring), the solvent was removed under vacuum. The crude residue was purified by silica column chromatography (5-50% ethyl acetate/hexane) to afford the product as a light yellow liquid.

Yield: 62%. ¹H NMR (400 MHz, Chloroform-d) δ 7.03 (d, *J* = 1.3 Hz, 1H), 4.26 (q, *J* = 7.1 Hz, 2H), 4.01 (d, *J* = 3.2 Hz, 1H), 3.75 (dd, *J* = 3.2, 1.3 Hz, 1H), 3.40 – 3.48 (m, 2H), 1.45 – 1.57 (m, 2H), 1.32 (t, *J* = 7.1 Hz, 3H), 1.18 – 1.28 (m, 6H), 0.80 – 0.95 (m, 3H). ¹³C NMR (101 MHz, Chloroform-d) δ 172.77, 172.26, 160.19, 145.29, 141.29, 61.35, 46.73, 44.29, 38.94, 31.25, 27.38, 26.36, 22.45, 14.13, 13.93. ESI-MS: 302.0 (M + Na⁺).

Synthesis of ethyl 3-methyl-2,4-dioxo-3-azabicyclo[3.2.0]hept-6-ene-6-carboxylate (MCBI)

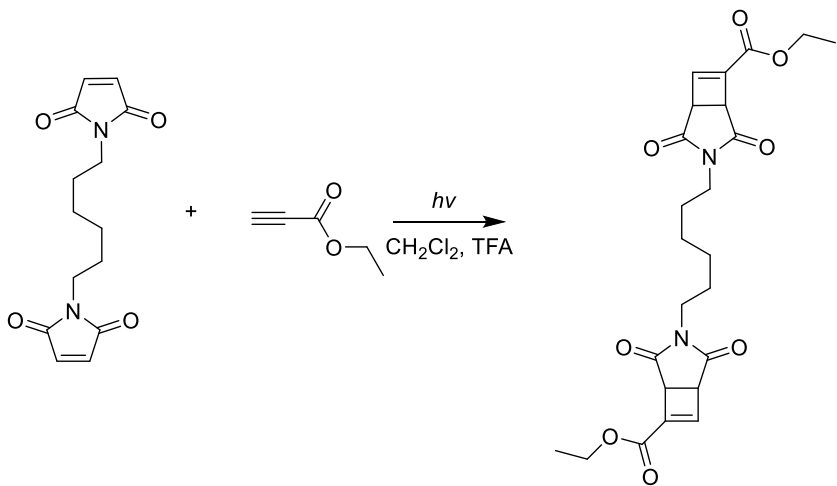


MCBI was synthesized following the literature⁴ with some modifications. *N*-methylmaleimide (3.0 g, 27 mmol, 1.0 eq), ethyl propiolate (6.6 g, 67 mmol, 2.6 eq.) and trifluoroacetic acid (3.2 g, 28 mmol, 1.1 eq.) were dissolved in 80 mL methylene chloride in a 100 mL flask. After sparging the solution for 30 min with N₂, the flask

was sealed by septum and stirred under UV irradiation (mercury lamp, 400 W) for 48 h. After completion of the reaction (thin layer chromatography (TLC) monitoring), the solvent was removed under vacuum. The crude residue was purified by silica column chromatography (5-50% ethyl acetate/hexane) to afford the product as a light yellow liquid.

Yield: 77%. ^1H NMR (400 MHz, Chloroform-*d*) δ 6.94 (d, J = 1.3 Hz, 1H), 4.14 (q, J = 7.1 Hz, 2H), 3.97 (d, J = 3.2 Hz, 1H), 3.72 (dd, J = 3.2, 1.3 Hz, 1H), 2.85 (s, 1H), 1.21 (t, J = 7.1 Hz, 3H). ^{13}C NMR (101 MHz, Chloroform-*d*) δ 172.81, 172.38, 160.13, 145.21, 140.94, 61.22, 46.80, 44.36, 24.93, 14.05. ESI-MS: 210.1 ($M + \text{H}^+$).

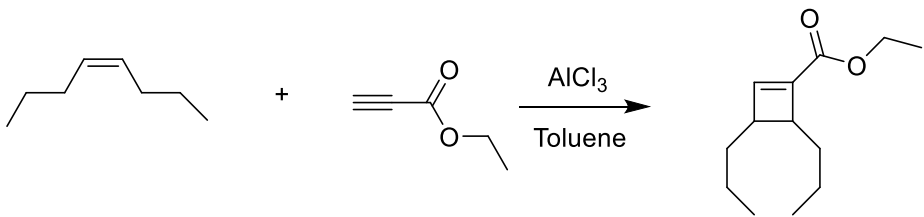
Synthesis of diethyl 3,3'-(hexane-1,6-diyl)bis(2,4-dioxo-3-azabicyclo[3.2.0]hept-6-ene-6-carboxylate) (DCBI)



DCBI was synthesized following the literature⁴ with some modifications. 1,1'-(hexane-1,6-diyl)bis(1H-pyrrole-2,5-dione) (3.0 g, 27 mmol, 1.0 eq), ethyl propiolate (6.6 g, 67 mmol, 2.6 eq.) and trifluoroacetic acid (3.2 g, 28 mmol, 1.1 eq.) were dissolved in 80 ml methylene chloride in a 100 mL flask. After sparging the solution for 30 min with N_2 , the flask was sealed by septum and stirred under UV irradiation (mercury lamp, 36 W) for 48 h. After completion of the reaction (thin layer chromatography (TLC) monitoring), the solvent was removed under vacuum. The crude residue was purified by silica column chromatography (5-50% ethyl acetate/hexane) to afford the product as a light yellow liquid.

Yield: 19%. ^1H NMR (400 MHz, Chloroform-*d*) δ 7.01 (d, J = 1.3 Hz, 2H), 4.23 (q, J = 7.1 Hz, 4H), 4.01 (dd, J = 3.3, 1.7 Hz, 2H), 3.75 (d, J = 3.4 Hz, 2H), 3.40 (t, J = 7.3 Hz, 4H), 1.45 – 1.51 (m, 4H), 1.22 – 1.32 (m, 10H). ^{13}C NMR (101 MHz, Chloroform-*d*) δ 170.88, 170.41, 158.29, 143.41, 139.28, 59.44, 44.82, 42.39, 36.73, 25.29, 24.16, 24.15, 12.22. ESI-MS: 473.2 ($M + \text{H}^+$).

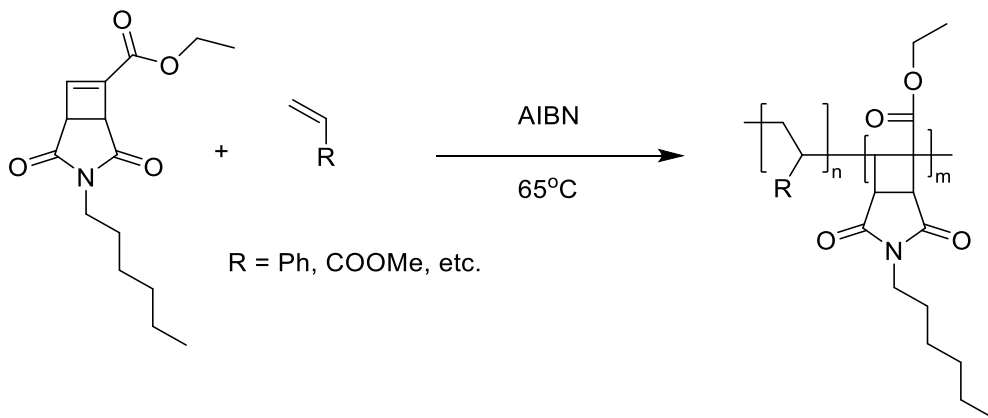
Synthesis of ethyl 3,4-dipropylcyclobut-1-ene-1-carboxylate (CBO)



CBO was synthesized following the literature⁵ with some modifications. Anhydrous aluminum chloride (1.79 g, 13.4 mmol, 0.5 eq.) was charged to a 100 mL flame-dried round bottom flask under N_2 , followed by 20 mL anhydrous toluene. Ethyl propiolate (3.1 g, 32.1 mmol, 1.2 eq.) was then added dropwise, followed by (*Z*)-oct-4-ene (3 g, 26.7 mmol, 1.0 eq.). The reaction was stirred for 7 days at room temperature, then poured into an aqueous solution of KH_2PO_4 (0.2 M, 60 ml) with stirring, resulting in the formation of a white precipitate. 20 mL of a 10% HCl solution was added to dissolve the precipitate. The aqueous layer was extracted with 3 x 20 mL portions of diethyl ether. The combined organic layers were washed with brine and dried over MgSO_4 . Solvent was removed under reduced pressure. The crude residue was purified by silica column chromatography (0-20% ethyl acetate/hexane) to afford the product as a colorless liquid.

Yield: 55 %. ^1H NMR (400 MHz, Chloroform-*d*) δ 6.88 (d, $J = 1.3$ Hz, 1H), 4.12 – 4.22 (m, 2H), 3.04 (td, $J = 6.9, 4.4$ Hz, 1H), 2.73 – 2.78 (m, 1H), 1.25 – 1.59 (m, 11H), 0.87 – 0.95 (m, 6H). ^{13}C NMR (101 MHz, Chloroform-*d*) δ 162.92, 149.39, 142.04, 59.89, 45.32, 43.65, 30.95, 30.76, 21.63, 21.18, 14.37, 14.28, 14.23. ESI-MS: 211.2 ($\text{M} + \text{H}^+$).

Polymerizations



PHCBI. HCBI (8 g, 29 mmol), AIBN (3 mg, 0.018 mmol), and 10 mL 1,4-dioxane were added into a Schlenk flask. The mixture was sparged with Ar for 60 min, before heating to 65 °C. After stirring for 72 h at 65 °C, the reaction solution was cooled to room temperature and precipitated into cold methanol (200 mL x 5). The precipitate was filtered off and dried under vacuum, and the title polymer was isolated as a white powder.

¹H NMR (400 MHz, Chloroform-*d*) δ 3.75-4.54 (m), 1.89-3.68 (m), 1.08-1.62 (m), 0.76-0.95 (m). ¹³C NMR (101 MHz, Chloroform-*d*) δ 177.02, 176.14, 62.94, 62.23, 39.16, 31.36, 29.70, 27.28, 26.57, 22.54, 13.97, 13.33.

PS-*co*-PHCBI ($F_{\text{CBI}} = 18\%, 25\%, 40\%, 45\%$). Styrene (6.25 g, 60 mmol), HCBI (0.84 g, 4.32 mmol or 1.68 g, 8.65 mmol or 3.36 g, 17.30 mmol or 5.04 g, 25.95 mmol), and AIBN (3 mg, 0.018 mmol) were added into a Schlenk flask. The mixture was degassed by three freeze-pump-thaw degassing cycles, before taking 0.1 mL solution for ¹H NMR measurement. After stirring for 60 h at 65 °C under Ar, the reaction solution was cooled to room temperature and precipitated into cold methanol (200 mL x 5). The precipitate was filtered off and dried under vacuum, and the title polymer was isolated as a white solid.

PS₈₂-*co*-PHCBI₁₈: ¹H NMR (400 MHz, Chloroform-*d*) δ 6.26-7.29 (m), 3.03-3.95 (m), 1.09-2.60 (m), 0.68-1.07 (m). ¹³C NMR (101 MHz, Chloroform-*d*) δ 175.74, 172.08, 146.01, 145.21, 144.92, 127.96, 127.32, 125.65, 125.50, 60.92, 45.68, 43.85, 40.79, 40.54, 40.44, 31.35, 29.72, 27.69, 26.61, 22.52, 22.50, 14.05.

PS₇₅-*co*-PHCBI₂₅: ¹H NMR (400 MHz, Chloroform-*d*) δ 6.25-7.23 (m), 3.08-3.86 (m), 1.09-2.68 (m), 0.63-1.09 (m). ¹³C NMR (101 MHz, Chloroform-*d*) δ 175.64, 172.12, 145.38, 145.17, 128.56, 127.95, 127.84, 127.42, 125.93, 125.61, 60.93, 40.62, 40.30, 40.06, 31.33, 27.70, 27.68, 26.56, 26.50, 22.54, 22.52, 14.04.

PS₆₀-*co*-PHCBI₄₀: ¹H NMR (400 MHz, Chloroform-*d*) δ 6.28-7.23 (m), 3.01-3.79 (m), 1.10-2.65 (m), 0.60-1.10 (m). ¹³C NMR (101 MHz, Chloroform-*d*) δ 176.16, 174.45, 144.97, 143.45, 128.31, 127.82, 127.61, 125.64, 61.40, 60.65, 42.26, 40.67, 40.39, 38.77, 31.34, 27.68, 27.28, 26.54, 22.50, 14.03.

PS₅₅-*co*-PHCBI₄₅: ¹H NMR (400 MHz, Chloroform-*d*) δ 6.31-7.25 (m), 3.00-3.85 (m), 1.10-2.98 (m), 0.59-1.08 (m). ¹³C NMR (101 MHz, Chloroform-*d*) δ 175.94, 172.34, 144.12, 128.57, 128.27, 127.49, 125.73, 60.71, 42.87, 40.00, 38.77, 31.35, 27.72, 27.48, 26.54, 22.50, 14.02.

PS-*co*-PHCBI ($F_{\text{HCBI}} = 50\%, 51\%, 55\%, 62\%$). Styrene and HCBI (For $F_{\text{HCBI}} = 50\%$, 55 mmol in total, styrene: HCBI = 20:80, for $F_{\text{CBI}} = 51\%, 55\%, 62\%$, 60 mmol in total, styrene: HCBI = 20:80, 40:60, 70:30), as well as AIBN (3 mg, 0.018 mmol) were added into a Schlenk flask. The mixture was degassed by three freeze-pump-thaw degassing cycles, before taking 0.1 mL solution for ¹H NMR measurement. After stirring 24 h at 65 °C under Ar, the reaction solution was cooled to room temperature and precipitated into cold methanol (200 mL x 5). The precipitate was filtered off and dried under vacuum, and the title polymer was isolated as a white solid.

PS₅₀-co-PHCBI₅₀: Yield: 37%. ¹H NMR (400 MHz, Chloroform-*d*) δ 6.38-7.67 (m), 1.89-4.28 (m), 0.34-1.67 (m). ¹³C NMR (101 MHz, Chloroform-*d*) δ 128.58, 61.78, 31.36, 28.00, 26.58, 22.53, 14.04.

PS₄₉-co-PHCBI₅₁: ¹H NMR (400 MHz, Chloroform-*d*) δ 6.28-7.40 (m), 1.10-4.20 (m), 0.55-1.09 (m). ¹³C NMR (101 MHz, Chloroform-*d*) δ 176.59, 175.80, 172.10, 128.11, 126.90, 61.01, 42.25, 39.03, 31.48, 27.70, 27.39, 26.58, 26.46, 22.49, 14.02.

PS₄₅-co-PHCBI₅₅: ¹H NMR (400 MHz, Chloroform-*d*) δ 6.28-7.52 (m), 1.10-4.30 (m), 0.55-1.09 (m). ¹³C NMR (101 MHz, Chloroform-*d*) δ 176.92, 128.86, 127.70, 126.79, 60.84, 43.03, 40.91, 38.66, 31.35, 27.52, 26.65, 22.50, 14.01.

PS₃₈-co-PHCBI₆₂: ¹H NMR (400 MHz, Chloroform-*d*) δ 6.69-7.80 (m), 1.83-4.32 (m), 1.10-1.82, 0.55-1.09 (m). ¹³C NMR (101 MHz, Chloroform-*d*) δ 177.04, 175.59, 172.70, 128.42, 127.10, 60.92, 42.20, 40.66, 38.88, 31.37, 31.32, 27.67, 27.47, 26.61, 22.52, 22.50, 14.02.

PS₇₃-co-PHCBI₂₇. Styrene (5.2 g, 50 mmol), HCBI (2.5 g, 9 mmol), 4-cyano-4-(phenylcarbonothioylthio)pentanoic acid (16 mg, 0.06 mmol), and AIBN (3 mg, 0.018 mmol) were added into a Schlenk flask. The mixture was degassed by three freeze-pump-thaw degassing cycles, before taking 0.1 mL solution for ¹H NMR measurement. After stirring 168 h at 65 °C under Ar, the reaction solution was cooled to room temperature and precipitated into cold methanol (200 mL x 5). The precipitate was filtered off and dried under vacuum, and the title polymer was isolated as a pink solid. ¹H NMR (400 MHz, Chloroform-*d*) δ 6.30-7.20 (m), 3.02-3.84 (m), 1.08-2.60 (m), 0.7-1.06 (m). ¹³C NMR (101 MHz, Chloroform-*d*) δ 176.47, 175.47, 146.22, 145.08, 128.26, 127.95, 127.82, 127.78, 125.49, 47.34, 40.52, 39.76, 38.55, 31.40, 31.33, 27.49, 26.63, 26.55, 22.48, 14.03, 13.61.

PMA₈₇-co-PHCBI₁₃. Methyl acrylate (4.13 g, 48 mmol), HCBI (3.35 g, 12 mmol), and AIBN (3 mg, 0.018 mmol) were added into a Schlenk flask. The mixture was degassed by three freeze-pump-thaw degassing cycles, before heating to 65 °C. After stirring 15 h at 65 °C under Ar, the reaction solution was cooled to room temperature and precipitated into cold methanol (200 mL x 5). The precipitate was filtered off and dried under vacuum, and the title polymer was isolated as a colorless gel.

¹H NMR (400 MHz, Chloroform-*d*) δ 3.98-4.35 (m), 3.55-3.80 (m), 3.41-3.50 (m), 2.86-3.28 (m), 2.13-2.62 (m), 1.07-2.03 (m), 0.76-0.90 (m). ¹³C NMR (101 MHz, Chloroform-*d*) δ 174.89, 61.84, 53.42, 51.71, 50.81, 41.53, 41.31, 41.12, 35.16, 31.30, 31.27, 27.59, 26.52, 22.49, 13.98, 13.59.

PMA₉₇-co-PHCBI₃. Methyl acrylate (5.2 g, 60 mmol), HCBI (0.84 g, 3 mmol), AIBN (3 mg, 0.018 mmol), and 6 mL 1,4-dioxane were added into a Schlenk flask. The

mixture was degassed by three freeze-pump-thaw degassing cycles, before heating to 65 °C. After stirring 15 h at 65 °C, the reaction solution was cooled to room temperature and precipitated into cold methanol (200 mL x 5). The precipitate was filtered off and dried under vacuum, and the title polymer was isolated as a colorless gel.

¹H NMR (400 MHz, Chloroform-*d*) δ 3.98-4.37 (m), 3.55-3.82 (m), 2.86-3.51 (m), 1.04-2.44 (m), 0.77-0.92 (m). ¹³C NMR (101 MHz, Chloroform-*d*) δ 174.89, 51.84, 51.81, 51.71, 50.83, 41.39, 41.31, 41.13, 35.84, 35.82, 35.56, 35.16, 34.96, 34.95, 34.74, 34.46, 34.26, 31.27, 27.60, 26.50, 22.50, 13.98.

PMMA₉₈-co-PHCBI₂. Methyl methacrylate (6.01 g, 60 mmol), HCBI (0.84 g, 3 mmol), AIBN (3 mg, 0.018 mmol), and 6 mL 1,4-dioxane were added into a Schlenk flask. The mixture was degassed by three freeze-pump-thaw degassing cycles, before heating to 65 °C. After stirring 15 h at 65 °C, the reaction solution was cooled to room temperature and precipitated into cold methanol (200 mL x 5). The precipitate was filtered off and dried under vacuum, and the title polymer was isolated as a white solid.

¹H NMR (400 MHz, Chloroform-*d*) δ 4.02-4.27 (m), 3.36-3.96 (m), 3.01-2.21 (m), 2.35-2.85 (m), 1.52-2.12 (m), 1.15-1.46 (m), 0.67-1.12 (m). ¹³C NMR (101 MHz, Chloroform-*d*) δ 178.08, 177.78, 176.97, 176.93, 54.49, 54.18, 52.70, 44.92, 44.57, 18.76, 16.51, 16.48.

PS₃₄-co-PB₄₉-co-PHCBI₁₇. Styrene (3.12 g, 30 mmol), 1,3-butadiene (15 mL of a 2 mol L⁻¹ solution in THF, 30 mmol), HCBI (0.84 g, 3 mmol), and AIBN (3 mg, 0.018 mmol) were added into a Schlenk flask. The mixture was degassed by three freeze-pump-thaw degassing cycles, before transferring into a 100 mL ACE pressure tube under Ar. After stirring 72 h at 65 °C in the pressure flask, the reaction solution was cooled to room temperature and precipitated into cold methanol (200 mL x 5). The precipitate was filtered off and dried under vacuum, and the title polymer was isolated as a colorless gel.

¹H NMR (400 MHz, Chloroform-*d*) δ 6.71-7.56 (m), 4.77-5.62 (m), 3.03-4.24 (m), 1.38-3.01 (m), 0.67-1.37 (m). ¹³C NMR (101 MHz, Chloroform-*d*) δ 178.33, 176.47, 172.21, 145.36, 145.00, 131.43, 130.01, 129.98, 128.14, 127.79, 125.85, 125.81, 61.31, 53.42, 45.73, 43.46, 40.07, 38.89, 32.68, 31.32, 30.46, 27.71, 27.37, 26.59, 22.51, 14.01.

PS. Commercially available polystyrene was used. ¹H NMR (400 MHz, Chloroform-*d*) δ 6.90-7.20 (m), 6.30-6.58 (m), 1.26-1.57 (m), 1.84-2.06 (m). ¹³C NMR (101 MHz, Chloroform-*d*) δ 145.22, 128.03, 127.95, 127.59, 127.42, 125.63, 125.48, 40.71m 40.41, 40.26.

PMA. Methyl acrylate (12 g, 140 mmol), AIBN (3 mg, 0.018 mmol), 4-cyano-4-(phenylcarbonothioylthio)pentanoic acid (4.8 mg, 0.017 mmol), and 10 mL 1,4-dioxane were added into a Schlenk flask. The mixture was degassed by three freeze-pump-thaw degassing cycles, before heating to 65 °C. After stirring 15 h at 65 °C, the reaction

solution was cooled to room temperature and precipitated into cold methanol (200 mL x 5). The precipitate was filtered off and dried under vacuum, and the title polymer was isolated as a colorless gel.

¹H NMR (400 MHz, Chloroform-*d*) δ 3.46-3.82 (m), 2.23-2.38 (m), 1.87-1.96 (m), 1.60-1.77 (m), 1.38-1.56 (m). ¹³C NMR (101 MHz, Chloroform-*d*) δ 174.87, 67.08, 51.79, 51.70, 41.30, 41.12, 35.81, 35.16, 34.26.

PMMA. Methyl methacrylate (11 g, 110 mmol), AIBN (3 mg, 0.018 mmol), 4-cyano-4-(phenylcarbonothioylthio)pentanoic acid (4.8 mg, 0.017 mmol), and 10 mL 1,4-dioxane were added into a Schlenk flask. The mixture was degassed by three freeze-pump-thaw degassing cycles, before heating to 65 °C. After stirring 15 h at 65 °C, the reaction solution was cooled to room temperature and precipitated into cold methanol (200 mL x 5). The precipitate was filtered off and dried under vacuum, and the title polymer was isolated as a white solid.

¹H NMR (400 MHz, Chloroform-*d*) δ 3.40-3.76 (m), 1.62-2.06 (m), 1.35-1.48 (m), 1.15-1.22 (m), 0.74-1.08 (m). ¹³C NMR (101 MHz, Chloroform-*d*) δ 178.11, 178.08, 177.78, 176.97, 176.90, 67.08, 54.43, 54.21, 52.72, 51.81, 44.91, 44.56, 18.74, 16.50.

PS₄₇-co-PB₅₃. Styrene (4.5 g, 43 mmol), 1,3-butadiene (15 mL of a 2 mol L⁻¹ solution in THF, 30 mmol), 4-cyano-4-(phenylcarbonothioylthio)pentanoic acid (2.5 mg, 0.009 mmol), and AIBN (3 mg, 0.018 mmol) were added into a Schlenk flask. The mixture was degassed by three freeze-pump-thaw degassing cycles, before transferring into a 100 mL ACE pressure tube under Ar. After stirring 72 h at 65 °C in the pressure tube, the reaction solution was cooled to room temperature and precipitated into cold methanol (200 mL x 5). The precipitate was filtered off and dried under vacuum, and the title polymer was isolated as a pink gel.

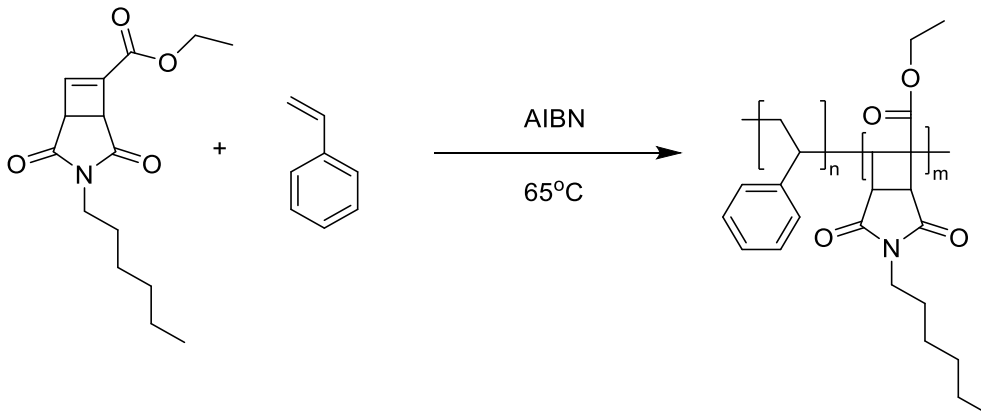
¹H NMR (400 MHz, Chloroform-*d*) δ 6.46-7.31 (m), 4.74-5.51 (m), 1.00-2.52 (m). ¹³C NMR (101 MHz, Chloroform-*d*) δ 145.31, 136.88, 131.55, 130.20, 128.51, 127.63, 126.20, 125.84, 113.79, 53.42, 50.85, 45.30, 43.39, 39.98, 35.82, 32.66, 30.32, 27.28, 25.26.

PS₆₅-co-PCBO₃₅. Styrene (1.24 g, 11.9 mmol) and CBO (1 g, 4.75 mmol), as well as AIBN (1 mg, 6 μmol) were added into a Schlenk flask. The mixture was degassed by three freeze-pump-thaw degassing cycles, before taking 0.1 mL solution for ¹H NMR measurement. After stirring 48 h at 65 °C under N₂, the reaction solution was cooled to room temperature and precipitated into cold methanol (100 mL x 5). The precipitate was filtered off and dried under vacuum, and the title polymer was isolated as a white solid.

1.02 g, 45%. ¹H NMR (400 MHz, Chloroform-*d*) δ 6.26-7.36 (m), 2.31-4.23 (m), 0.11-2.26 (m). ¹³C NMR (101 MHz, Chloroform-*d*) δ 145.71, 127.93, 125.60, 59.28, 40.41, 14.49, 13.78. *M_n*: 26 kg mol⁻¹, *D*: 2.2.

(PS-*co*-PMCBI)-*I*-PDCBI Styrene (2.29 g, 21.98 mmol), MCBI (0.84 g, 4.01 mmol), DCBI (0.57 g, 1.2 mmol), and AIBN (1 mg, 6 μ mol) were added into a Schlenk flask. The mixture was degassed by three freeze-pump-thaw degassing cycles, before taking 0.1 mL solution for ^1H NMR measurement. After stirring overnight at 65 °C under N_2 , the reaction mixture was cooled to room temperature. The insoluble solid was washed by THF and dried under vacuum to give the title polymer.

Determination of reactivity ratio



Styrene, HCBI (styrene and HCBI, overall amount 50 mmol), and AIBN (3 mg, 0.018 mmol) were added into a Schlenk flask. The mixture was degassed by three freeze-pump-thaw degassing cycles, before heating to 65 °C. After 2 h (or 1.5 h), the reaction solution was cooled to room temperature, 0.1 mL was taken for ^1H NMR measurements, and the rest was precipitated into cold methanol (100 mL x 5). The precipitate was filtered off and dried under vacuum, and the polymer was isolated as a white solid.

Ultrasonication of polymers followed by ^1H NMR and FT-IR measurements

A solution of PS₅₀-*co*-PHCBI₅₀ (80 mg polymer in 20 mL THF) was placed in a Suslick reaction vessel and sparged with N_2 for 15 min prior to sonication. Pulsed ultrasound was applied (1 s on, 1 s off, 20 % amplitude) while the was solution kept in an ice/water bath. At 1 h, 2 h, 3 h and 4 h sonication time (on time), an aliquot (2.0 mL) was taken from the solution. After removing the solvent under reduced pressure, the samples were subjected to ^1H NMR analysis. Furthermore, for PS₄₉-*co*-PHCBI₅₁, 0.5 mL of withdrawn solution (4 h sonication) was subjected to FT-IR analysis.

Ultrasonication of polymers followed by treatment with NaOH solution

For a typical pulsed ultrasonication experiment, a solution of polymer (80 mg polymer in 20 mL THF) was placed in a Suslick reaction vessel and sparged with N_2 for 15 min prior to sonication. Pulsed ultrasound was applied (1 s on, 1 s off, 20 % amplitude) while the was solution kept in an ice/water bath. At each sonication time (0, 30, 60, 120, 180 and 240 min, on time), an aliquot (1.5 mL) was taken from the solution and directly subjected to SEC analysis. After measurement, 150 μ L NaOH solution (1 mol L⁻¹ or 0.5 mol L⁻¹ for PMA) was added into the aliquot. After stirring overnight (0.5 h for PMA), the NaOH treated solution was further analyzed by SEC.

NaOH solution treatment of polymers followed by ultrasonication

A solution of PS₄₉-*co*-PHCBI₅₁ (120 mg polymer in 30 mL THF) was placed in a 50 mL beaker. Then, 3 mL NaOH solution (1 mol L⁻¹) was added and the solution was kept stirring overnight at room temperature. In the next day, after stopping stirring, the solution separated into two phases, the aqueous phase was removed with a separatory funnel. An aliquot (1.5 mL) was taken from the THF phase and directly subjected to SEC analysis. The rest of the THF phase was subjected to pulsed ultrasound (1 s on, 1 s off, 20 % amplitude) while the solution was kept at 0 °C with a chiller. At each sonication time point (0, 30, 60, 120, 180, and 240 min, on time), an aliquot (1.5 mL) was taken from the solution and directly subjected to SEC analysis.

Cryo-milling of polymers followed by treatment with NaOH solution

200 mg PS, PS₄₉-*co*-PHCBI₅₁, PS₆₀-*co*-PHCBI₄₀, PS₅₀-*co*-PHCBI₅₀, PS₆₅-*co*-PCBO₃₅, (PS-*co*-PMCB_I)-*l*-PDCBI or cross-linked PS was placed in a cryo-milling machine. After cryo-milling (30 and 60 min for PS and PS₄₉-*co*-PHCBI₅₁, 60 min for PS₆₀-*co*-PHCBI₄₀, PS₅₀-*co*-PHCBI₅₀, PS₆₅-*co*-PCBO₃₅, (PS-*co*-PMCB_I)-*l*-PDCBI, and cross-linked PS on time), a sample (2 mg) was taken and dissolved in 1.5 mL THF, filtered through a syringe filter (0.22 µm) and then directly subjected to SEC analysis. Another 2 mg sample was taken and dissolved in 1.5 mL THF. Then, 150 µL NaOH solution (1 mol L⁻¹) was added into the polymer solution. After stirring overnight at room temperature, the NaOH treated solution was further analyzed by SEC.

Ball-milling of polymers followed by treatment with NaOH solution

350 mg PS₆₀-*co*-PHCBI₄₀ (or PS) was placed in a 10 mL top screwed stainless steel grinding jar with stainless steel grinding balls with a diameter of 2 mm. The polymer was grinded for 60 min with 30 Hz frequency. Thereafter, a sample (2 mg) was taken and dissolved in 1.5 mL THF, filtered through a syringe filter (0.22 µm) and then directly subjected to SEC analysis. Another 2 mg sample was taken and dissolved in 1.5 mL THF. Then, 150 µL NaOH solution (1 mol L⁻¹) was added into the polymer solution. After stirring overnight at room temperature, the NaOH treated solution was further analyzed by SEC.

Ball-milling of dry polymers with solid NaOH

300 mg PS₅₀-*co*-PHCBI₅₀ (or PS) and 300 mg of solid NaOH were placed in a 10 mL top screwed stainless steel grinding jar with stainless steel grinding balls with a diameter of 2 mm. The polymer was grinded for 60 min with 30 Hz frequency. Thereafter, a sample (2 mg) was taken and dissolved in 1.5 mL THF, filtered through a syringe filter (0.22 µm) and then directly subjected to SEC analysis.

Ultrasonication of polymer followed by treatment with NaOH solutions of different concentrations

For a typical pulsed ultrasonication experiment, a solution of PS₄₉-*co*-PHCBI₅₁ (120 mg polymer in 30 mL THF) was placed in a 50 mL beaker. Pulsed ultrasound was applied (1 s on, 1 s off, 20 % amplitude) while the solution was kept at 0 °C. After 240 min sonication, six aliquots (1.5 mL each) were taken from the solution and 150 µL NaOH solution of different concentrations (1.0 M, 0.5 M, 0.1 M, 0.05 M, 0.01 M, 0.001 M) was added into each of the aliquots. After stirring overnight at room temperature, the NaOH treated solutions were analyzed by SEC.

Degradation products analysis

For ultrasonication products: After sonication (240 min) and NaOH treatment, 0.1 mL of the PS₅₀-*co*-PHCBI₅₀ mixture was taken for mass analysis, the remainder of the mixture was purified by flash silica column chromatography (0-100% MeOH/DCM) to afford two fractions, F₁ (26 mg, 34%, M_n : 10 kg mol⁻¹) and F₂ (49 mg, 58%, M_n < 1 kg mol⁻¹). The fractions were further analyzed by ¹H NMR, SEC and Mass Spectrometry.

For cryo-milling products: After cryo-milling (60 min) and NaOH treatment, 0.1 mL of the PS₅₀-*co*-PHCBI₅₀ mixture was taken for mass analysis and the remainder of the mixture was purified by silica flash column chromatography (0-100% MeOH/DCM) to afford two fractions, F₁ (63 mg, 69%, M_n < 1 kg mol⁻¹) and F₂ (28 mg, 26%, M_n < 1 kg mol⁻¹). The fractions were further analyzed by ¹H NMR, SEC and Mass Spectrometry.

High-Resolution LC-MS Analysis: Several samples were provided for LC-MS analysis: the non-degraded PS₄₉-*co*-PHCBI₅₁, and the samples PS₄₉-*co*-PHCBI₅₁-cryo-milling-hydrolysis, PS₄₉-*co*-PHCBI₅₁-sonication-hydrolysis after degradation. Furthermore, a procedural blank sample (blank matrix) that did not contain the polymeric material used to assess possible artifacts/impurities generated from the sample preparation procedure (solvents, vessels and chemicals), and a solvent sample that took into account the solvents used to dissolve and dilute the polymeric samples. Material was taken from the sample vessels and weighed into Eppendorf vials. The weights were 0.80 mg for the non-degraded PS₄₉-*co*-PHCBI₅₁, 0.80 mg for the PS₄₉-*co*-PHCBI₅₁-cryomilling-hydrolysis, 0.70 mg for the PS₄₉-*co*-PHCBI₅₁-sonication-hydrolysis and 0.20 mg for the blank matrix sample. The samples were dissolved in 1.0 mL tetrahydrofuran/water 70/30 (v/v) prior to diluting 1:10 with acetonitrile/water 90/10 (v/v) for LC-MS analysis.

Thermal stability experiments of PHCBI and PS-*co*-PHCBI

20 mg of PHCBI or PS₄₉-*co*-PHCBI₅₁ was added into a dry 10 mL round bottom flask. The flask was vacuum degassed and refilled with Ar three times and then, while being under Ar, dipped into a heated oil bath (180 °C). After heating for 30 min, the flask was cooled down to room temperature. Then, samples were characterized by ¹H NMR spectroscopy and SEC.

Supporting Data

Determination of copolymer type by NMR experiments

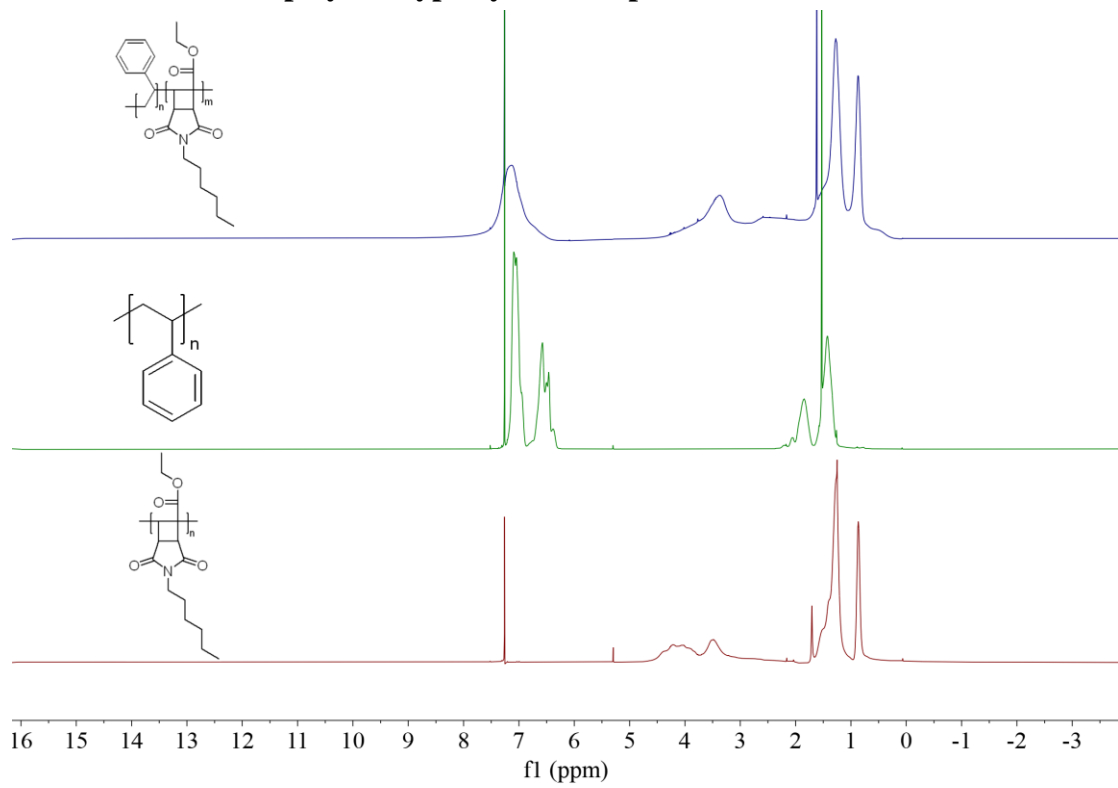


Fig. S1 ¹H NMR spectra (400 MHz, Chloroform-*d*) of PS₅₅-co-PHCBI₄₅, PS and PHCBI.

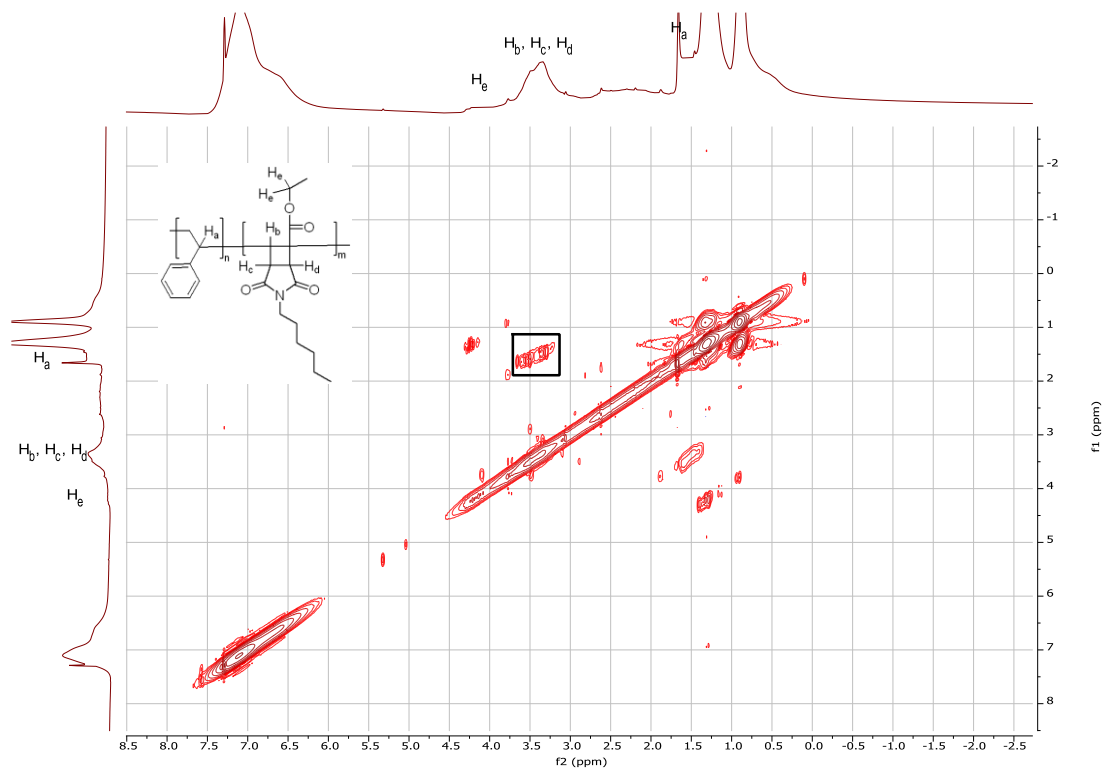


Fig. S2 NOESY NMR spectra (400 MHz, Chloroform-*d*) of $\text{PS}_{55}\text{-}co\text{-}\text{PHCBI}_{45}$. The strong correlation signals shown in the box between protons H_a and $\text{H}_b, \text{H}_c, \text{H}_d, \text{H}_e$ prove that the copolymer did not contain blocks of the individual monomers (There would not be such strong correlation signals for a block copolymer).

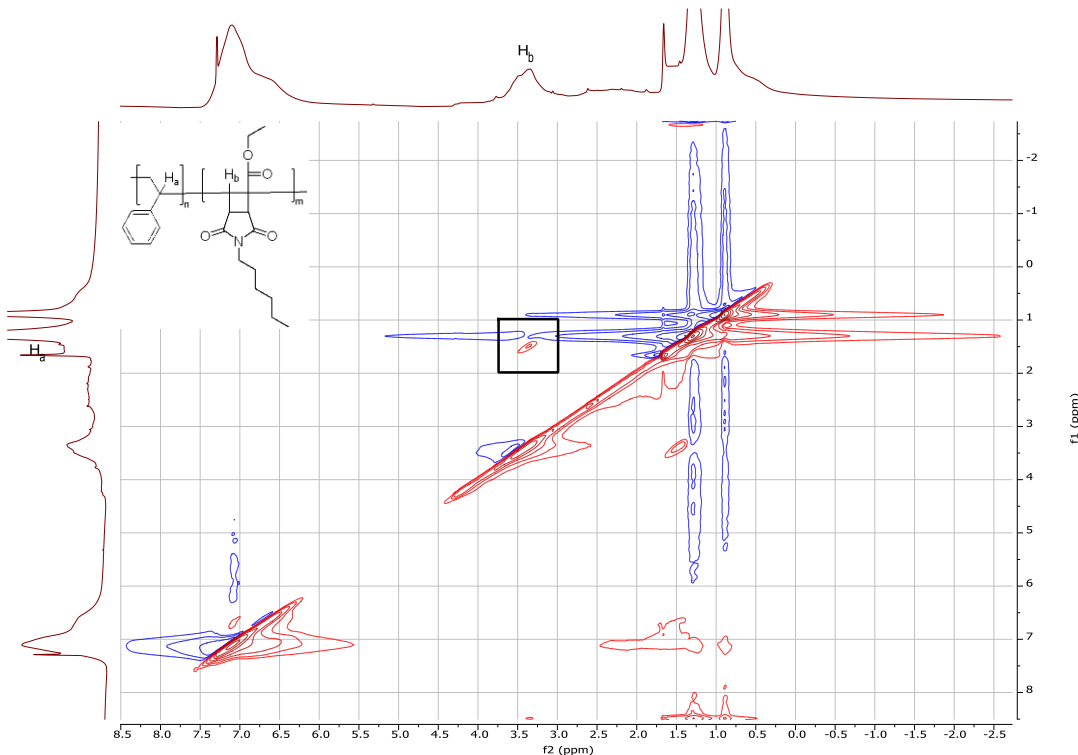


Fig. S3 COSY NMR spectra (400 MHz, Chloroform-*d*) of PS₅₂-co-PHCBI₄₈. The strong correlation signals shown in box between protons H_a and H_b prove that the copolymer did not contain blocks of the individual monomers (There would not be such strong correlation signals for a block copolymer).

Determination of monomer reactivity ratios

Table S1 Free radical copolymerizations of CBI and styrene to determine monomer reactivity ratios

Entry	$f_{\text{HCBI}}/f_{\text{styrene}}^{\text{a}}$	React. time (h)	Conversion ^a			$F_{\text{HCBI}}/F_{\text{styrene}}^{\text{a}}$	Yield ^b	SEC	
			Styrene	HCBI	Total			M_n (kg·mol ⁻¹)	D
1	6/94	2	12%	18%	18%	36/64	3.1%	76	1.72
2	12/88	2	9%	8%	8%	46/54	1.3%	67	1.78
3	19/81	2	15%	10%	11%	50/50	1.7%	72	1.65
4	25/75	2	16%	9%	11%	53/47	1.5%	65	1.74
5	35/65	1.5	20%	12%	15%	57/43	2.3%	55	1.69
6	40/60	1.5	20%	7%	12%	58/42	1.8%	45	1.73

^a Determined by ¹H NMR spectroscopy with 1,3,5-trimethoxybenzene as internal standard. ^b Determined after precipitation.

The mole fractions of HCBI and styrene in the monomer feed are represented by f_{HCBI} and f_{styrene} . F_{HCBI} and F_{styrene} are the mole fractions of the corresponding residues in the copolymers.

The analysis according to the Fineman-Ross linearization method⁶ was based on:

$$f(F-1)/F = r_{\text{HCBI}}(f^2/F) - r_{\text{styrene}}$$

where $f = f_{\text{HCBI}}/f_{\text{styrene}}$ and $F = F_{\text{HCBI}}/F_{\text{styrene}}$. r_{HCBI} and r_{styrene} are the reactivity ratios of the two monomers.

The analysis according to Fineman-Ross (Fig. S4) affords a reactivity ratio $r_{\text{CBI}} = 0.74$ for HCBI and a reactivity ratio $r_{\text{styrene}} = 0.04$ for styrene.

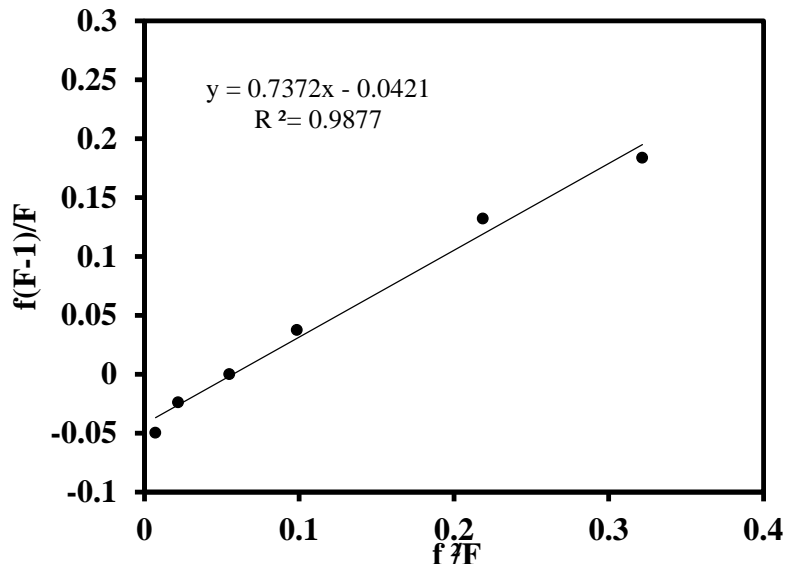


Fig. S4 Fineman-Ross plot for the free radical copolymerization of HCBI and styrene (The data shown here is also presented in Fig. 2 of the main manuscript) under bulk condition at 65 °C with AIBN as initiator.

The analysis according to the Kelen-Tüdös linearization method⁷ was based on:

$$\eta = (r_{\text{HCBI}} + (r_{\text{styrene}}/\alpha)) \zeta - (r_{\text{styrene}}/\alpha)$$

where $\eta = (f(F-1))/(F(\alpha + (f^2/F)))$, $\zeta = (f^2/F)/(\alpha + (f^2/F))$

and $\alpha = ((f^2/F)_{\max} \times (f^2/F)_{\min})^{0.5}$.

The analysis according to Kelen-Tüdös affords a reactivity ratio $r_{\text{HCBI}} = 0.82$ for HCBI and a reactivity ratio $r_{\text{styrene}} = 0.05$ for styrene.

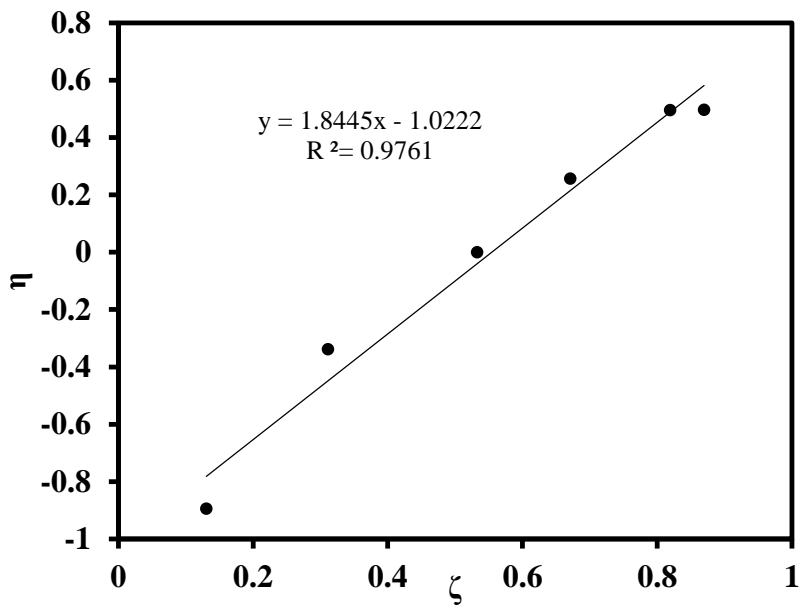


Fig. S5 Kelen-Tüdös plot for the free radical copolymerization of HCBI and styrene (The data shown here is also presented in Fig. 2 of the main manuscript) under bulk condition at 65 °C with AIBN as initiator.

The analysis according to the Mayo-Lewis nonlinear least-squares method^{8,9} was based on:

$$F_{\text{HCBI}} = (r_{\text{HCBI}} f_{\text{HCBI}}^2 + f_{\text{HCBI}} f_{\text{styrene}}) / (r_{\text{HCBI}} f_{\text{HCBI}}^2 + 2f_{\text{HCBI}} f_{\text{styrene}} + r_{\text{styrene}} f_{\text{styrene}}^2)$$

The analysis according to Mayo-Lewis affords a reactivity ratio $r_{\text{HCBI}} = 0.81$ for HCBI and a reactivity ratio $r_{\text{styrene}} = 0.05$ for styrene.

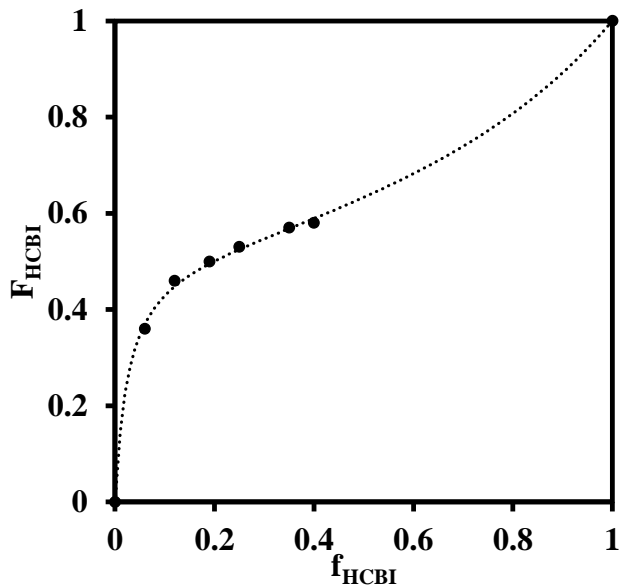


Fig. S6 Mayo-Lewis plot for the free radical copolymerization of HCBI and styrene (The data shown here is also presented in Fig. 2 of the main manuscript) under bulk condition at 65 °C with AIBN as initiator.

TGA and DSC data

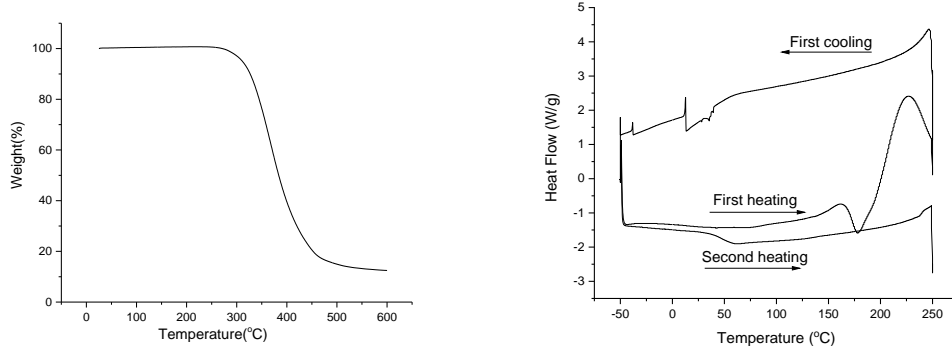


Fig. S7 TGA (left) and DSC (right) traces of PHCBI.

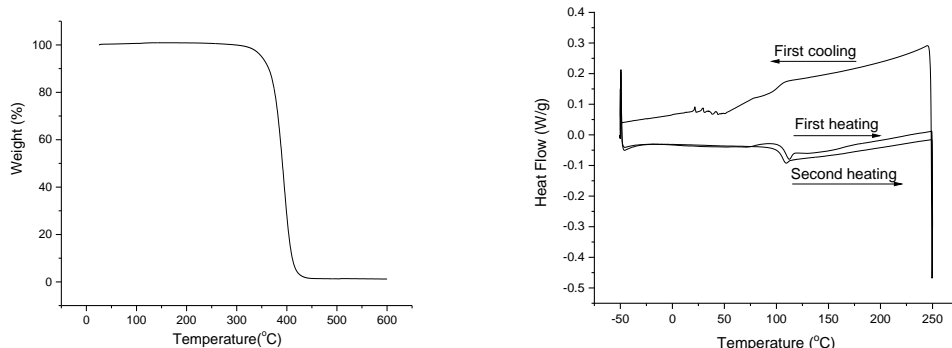


Fig. S8 TGA (left) and DSC (right) traces of PS₈₂-co-PHCBI₁₈.

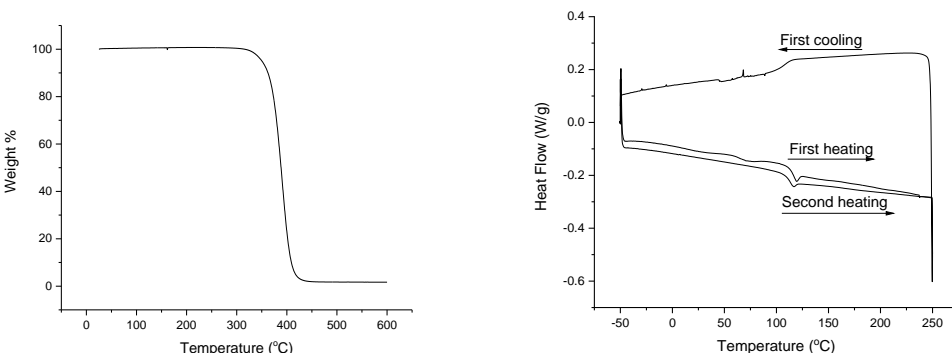


Fig. S9 TGA (left) and DSC (right) traces of PS₇₅-co-PHCBI₂₅.

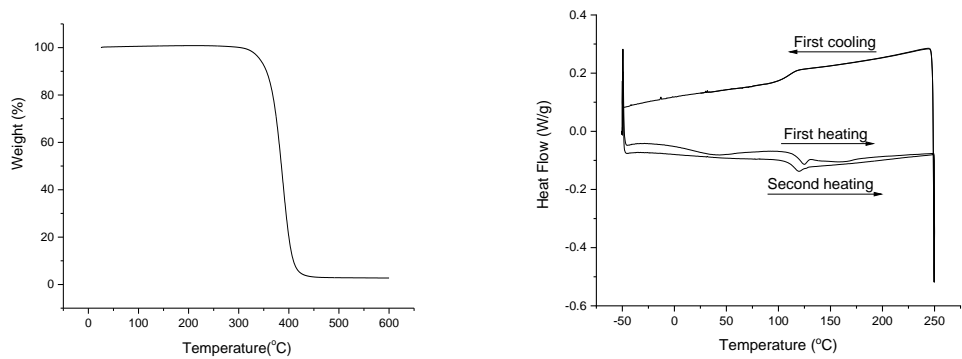


Fig. S10 TGA (left) and DSC (right) traces of $\text{PS}_{60}\text{-}co\text{-}\text{PHCBI}_{40}$.

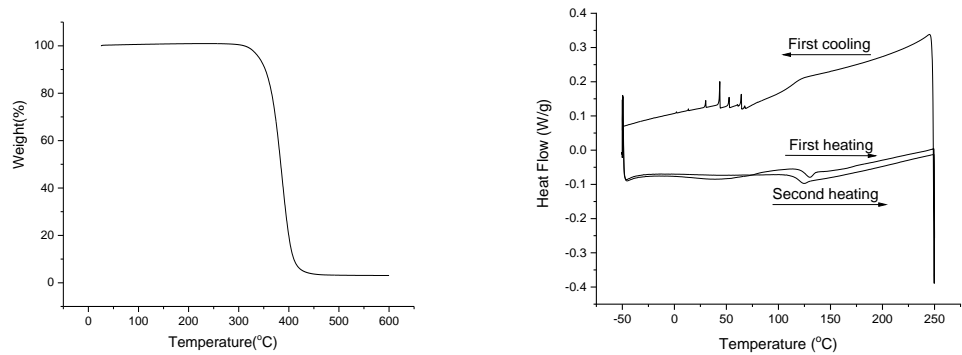


Fig. S11 TGA (left) and DSC (right) traces of $\text{PS}_{55}\text{-}co\text{-}\text{PHCBI}_{45}$.

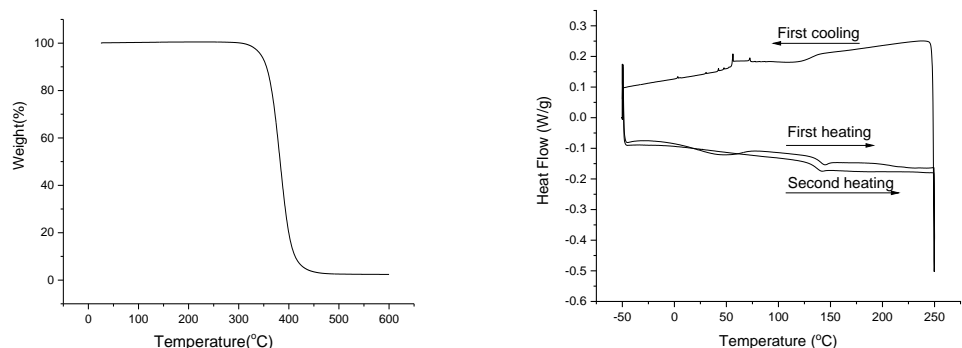


Fig. S12 TGA (left) and DSC (right) traces of $\text{PS}_{49}\text{-}co\text{-}\text{PHCBI}_{51}$.

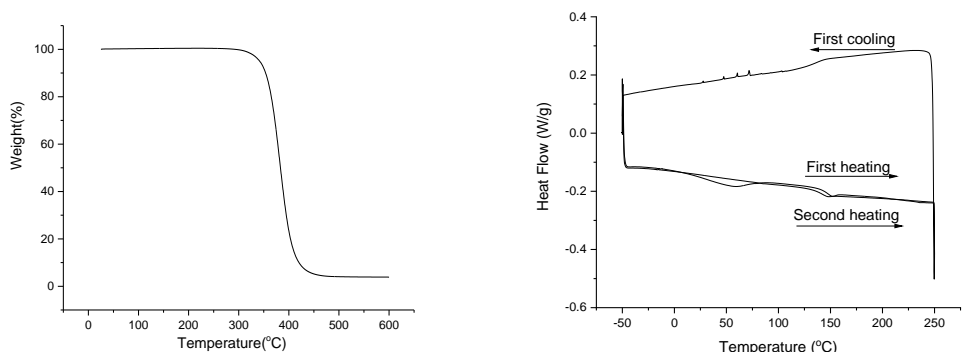


Fig. S13 TGA (left) and DSC (right) traces of PS₄₅-*co*-PHCBI₅₅.

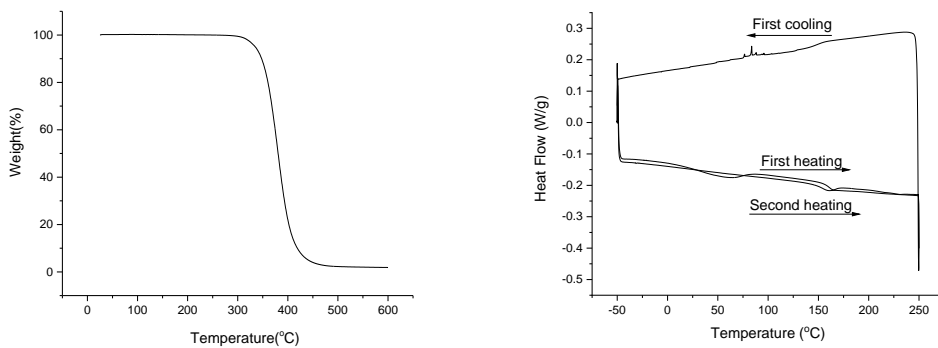


Fig.S14 TGA (left) and DSC (right) traces of PS₃₈-*co*-PHCBI₆₂.

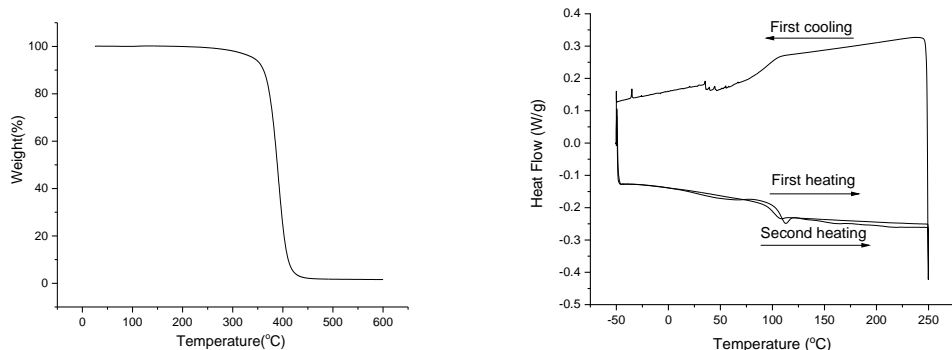


Fig. S15 TGA (left) and DSC (right) traces of PS₇₃-*co*-PHCBI₂₇.

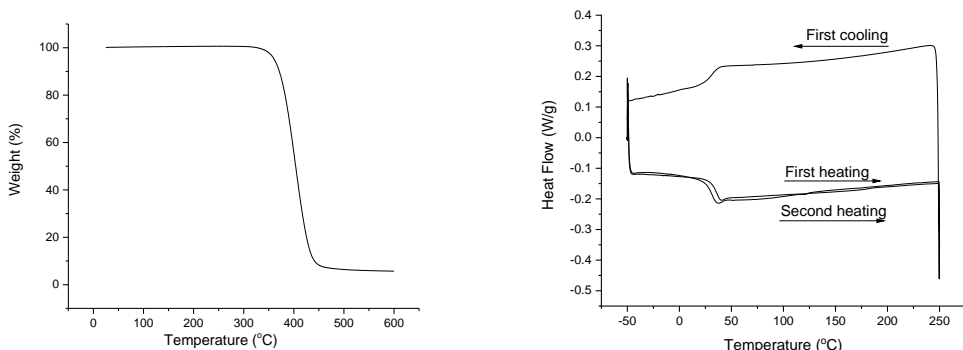


Fig. S16 TGA (left) and DSC (right) traces of PMA₈₇-*co*-PHCBI₁₃.

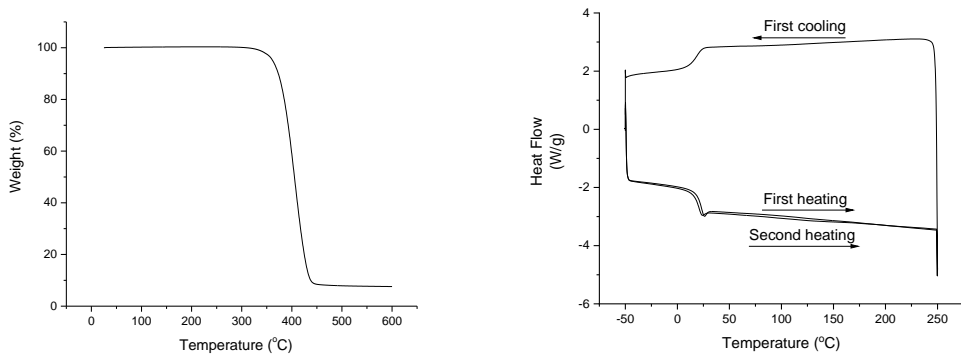


Fig. S17 TGA (left) and DSC (right) traces of $\text{PMA}_{97}\text{-}co\text{-}\text{PHCBI}_3$.

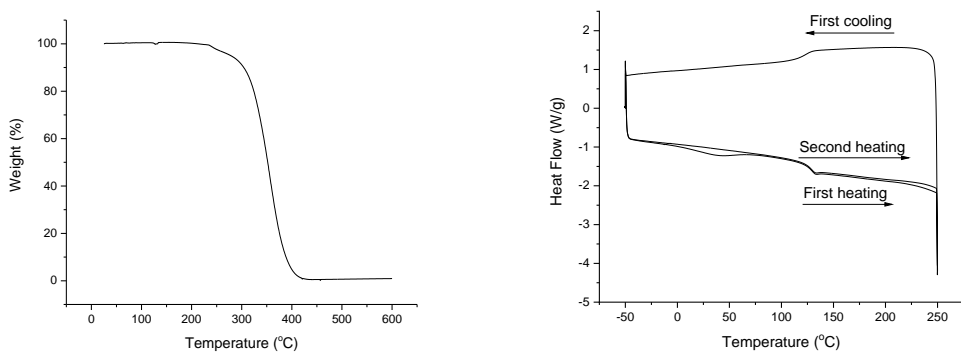


Fig. S18 TGA (left) and DSC (right) traces of $\text{PMMA}_{98}\text{-}co\text{-}\text{PHCBI}_2$.

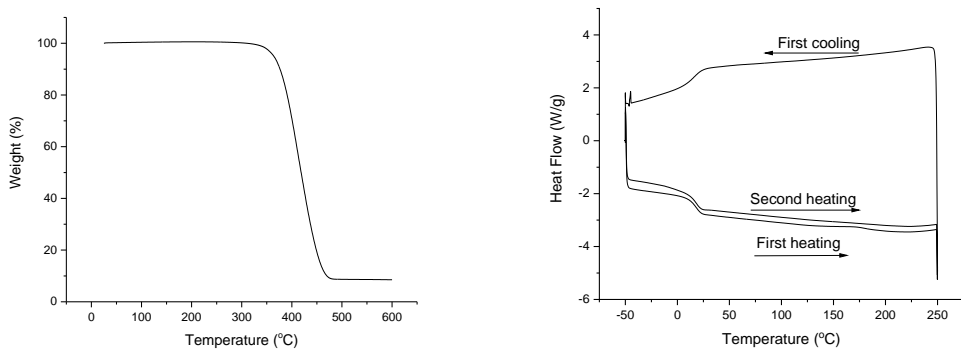


Fig. S19 TGA (left) and DSC (right) traces of $\text{PS}_{34}\text{-}co\text{-}\text{PB}_{49}\text{-}co\text{-}\text{PHCBI}_{17}$.

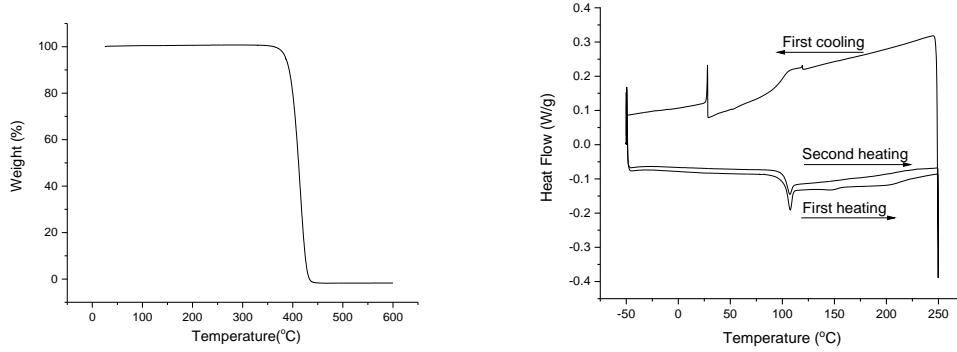


Fig. S20 TGA (left) and DSC (right) traces of PS.

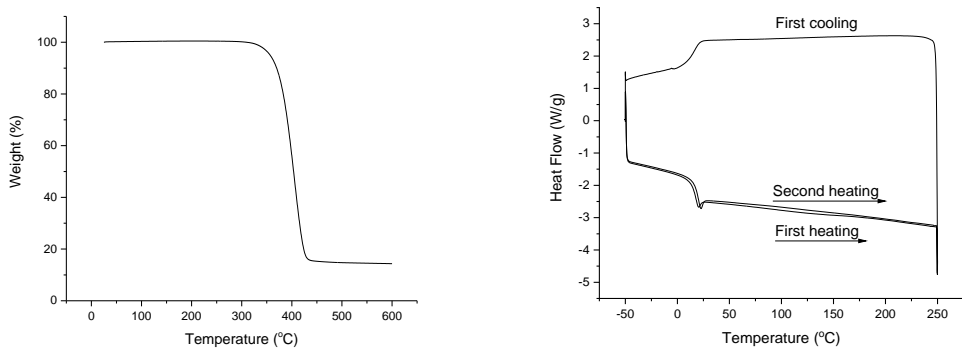


Fig. S21 TGA (left) and DSC (right) traces of PMA.

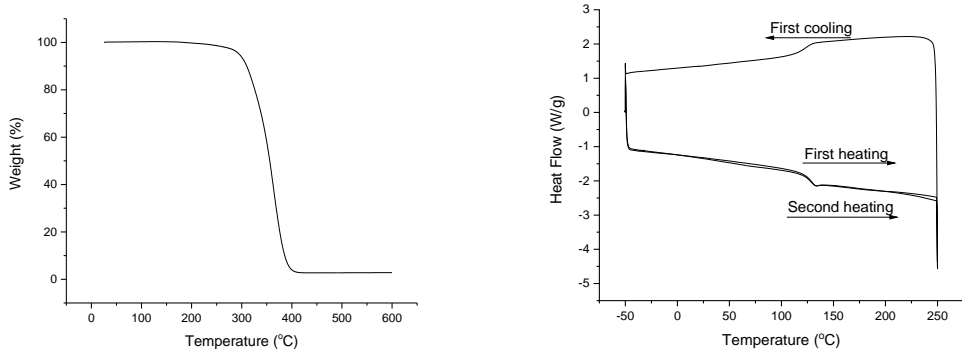


Fig. S22 TGA (left) and DSC (right) traces of PMMA.

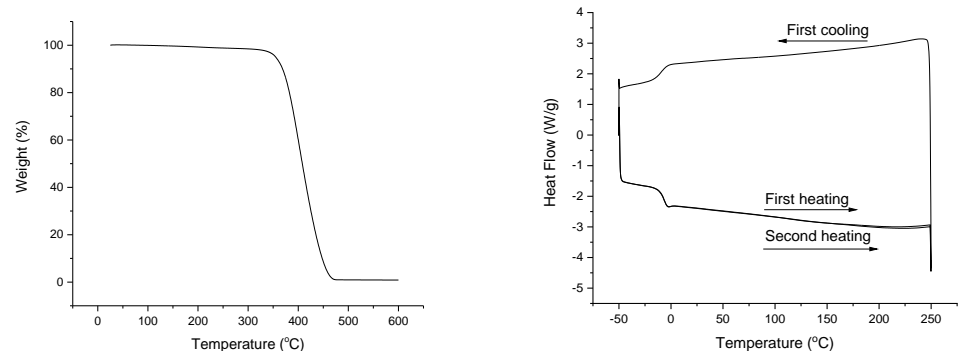


Fig. S23 TGA (left) and DSC (right) traces of PS₄₇-co-PB₅₃.

Dynamic mechanical analysis (DMA) data

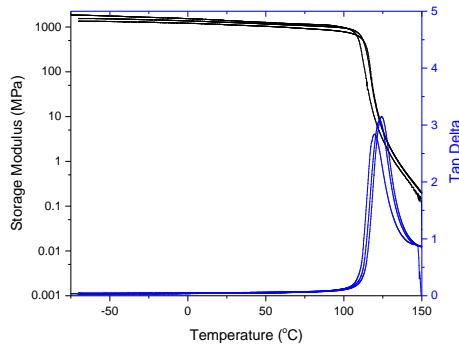


Fig. S24 DMA traces (three different samples) of $\text{PS}_{82}\text{-}co\text{-}\text{PHCBI}_{18}$.

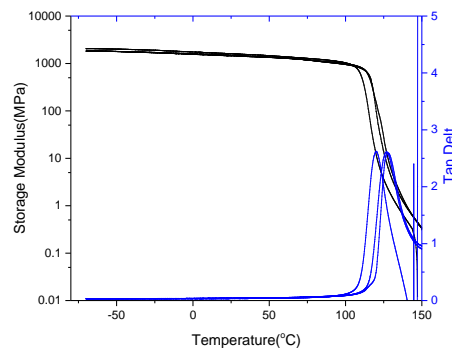


Fig. S25 DMA traces (three different samples) of $\text{PS}_{75}\text{-}co\text{-}\text{PHCBI}_{25}$.

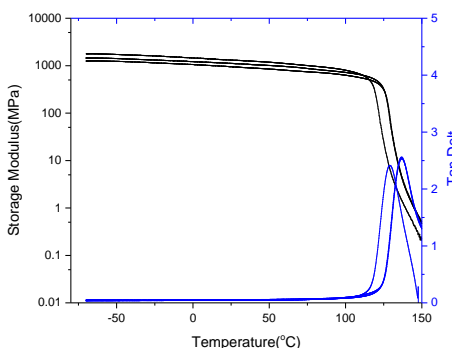


Fig. S26 DMA traces (three different samples) of $\text{PS}_{60}\text{-}co\text{-}\text{PHCBI}_{40}$.

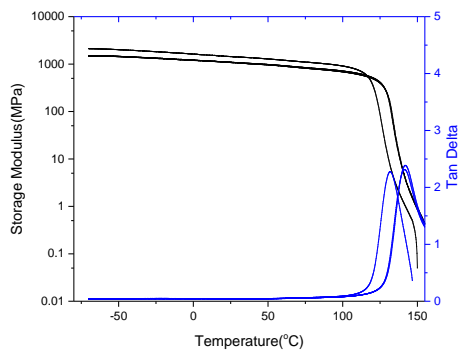


Fig. S27 DMA traces (three different samples) of $\text{PS}_{55}\text{-}co\text{-}\text{PHCBI}_{45}$.

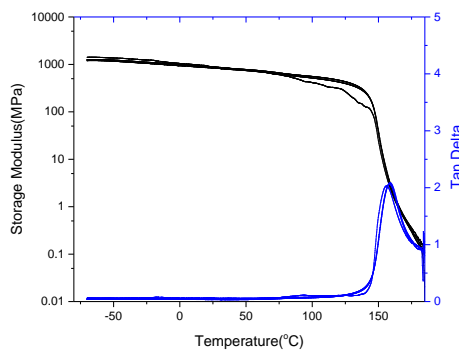


Fig. S28 DMA traces (three different samples) of $\text{PS}_{49}\text{-}co\text{-}\text{PHCBI}_{51}$.

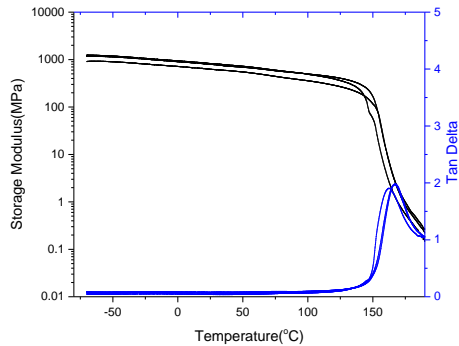


Fig. S29 DMA traces (three different samples) of $\text{PS}_{45}\text{-}co\text{-}\text{PHCBI}_{55}$.

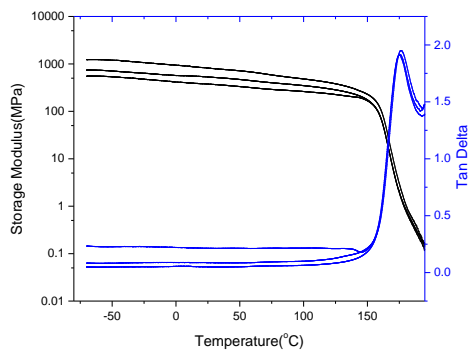


Fig. S30 DMA traces (three different samples) of PS₃₈-co-PHCBI₆₂.

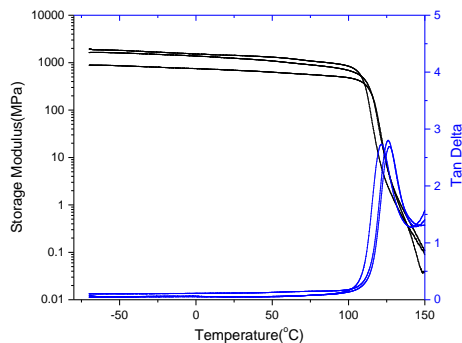


Fig. S31 DMA traces (three different samples) of PS₇₃-co-PHCBI₂₇.

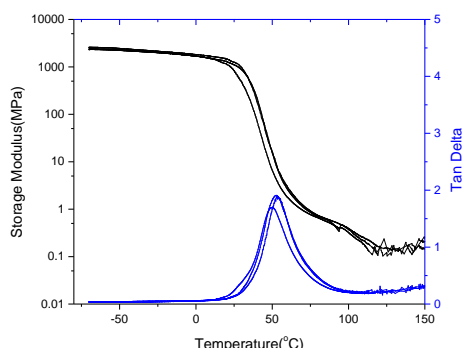


Fig. S32 DMA traces (three different samples) of PMA₈₇-co-PHCBI₁₃.

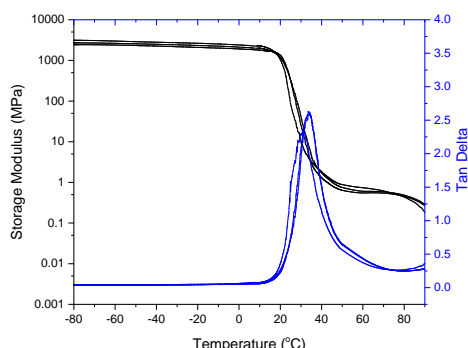


Fig. S33 DMA traces (three different samples) of PMA₉₇-co-PHCBI₃.

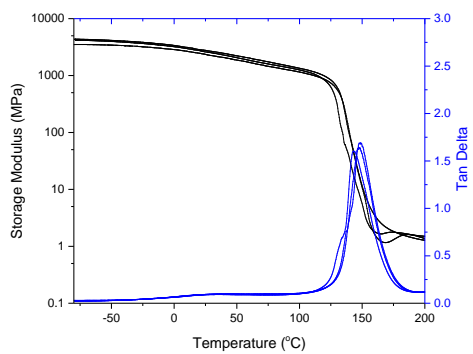


Fig. S34 DMA traces (three different samples) of PMMA₉₈-co-PHCBI₂.

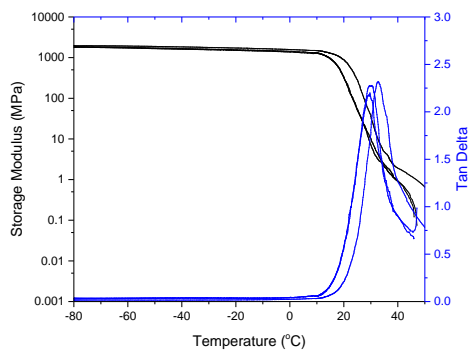


Fig. S35 DMA traces (three different samples) of PS₃₄-co-PB₄₉-co-PHCBI₁₇.

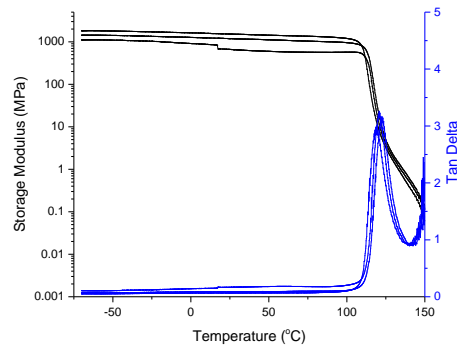


Fig. S36 DMA traces (three different samples) of PS.

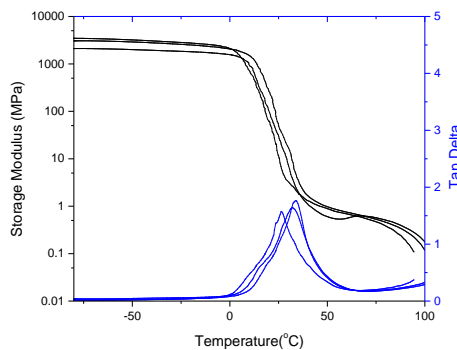


Fig. S37 DMA traces (three different samples) of PMA.

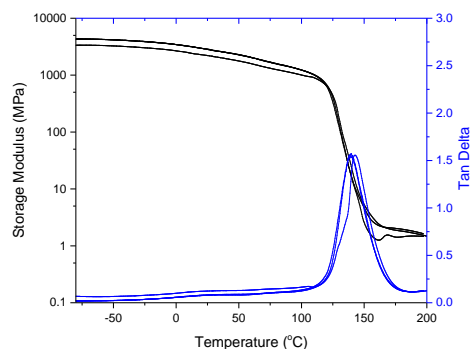


Fig. S38 DMA traces (three different samples) of PMMA.

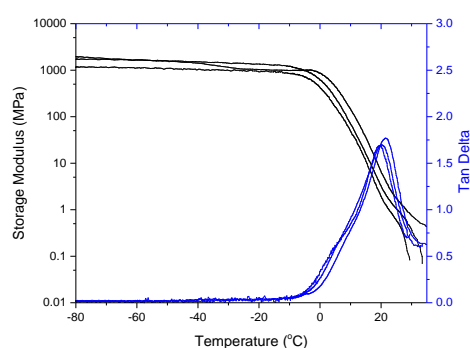


Fig. S39 DMA traces (three different samples) of PS₄₇-co-PB₅₃.

Thermal stability experiments of PHCBI and PS-co-PHCBI

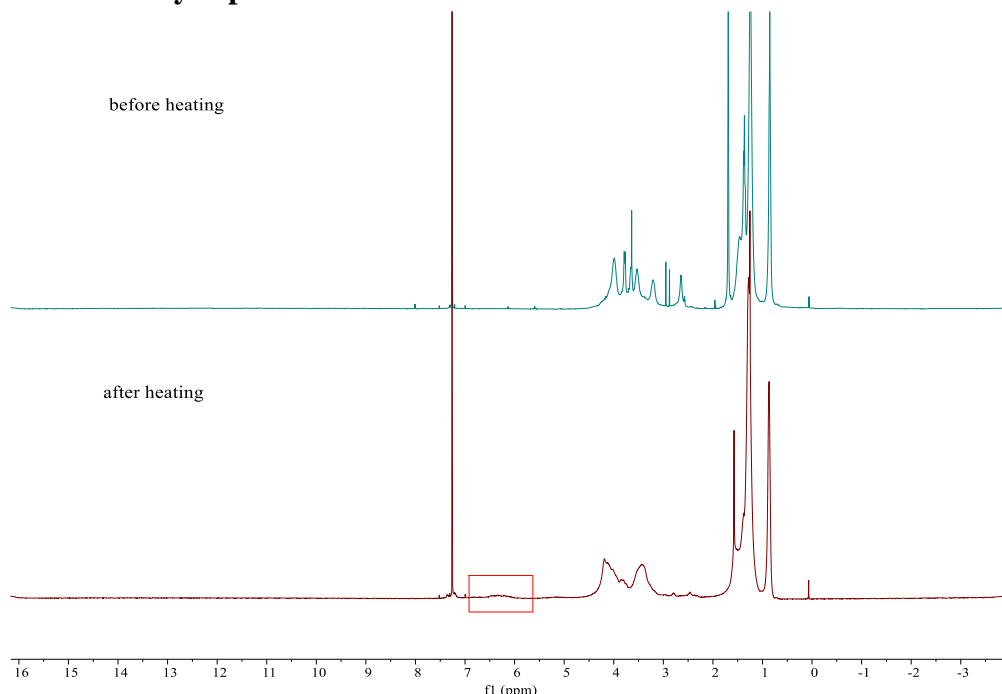


Fig. S40 ¹H NMR spectra (400 MHz, CDCl₃) of PHCBI before and after heating under Ar atmosphere for 30 min at 180 °C. New signals in the red box are assigned to ring-opened cyclobutanes. Other proton signals change can also be seen between 3 and 4.5 ppm.

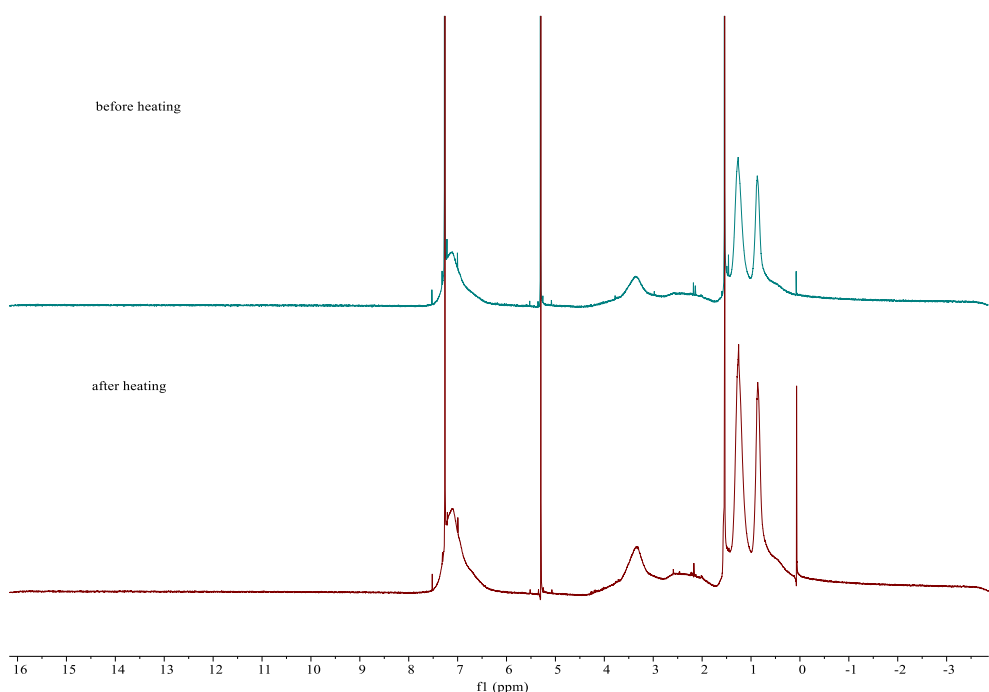


Fig. S41 ¹H NMR spectra (400 MHz, CDCl₃) of PS₄₉-co-PHCBI₅₁ before and after heating under Ar atmosphere for 30 min at 180 °C. The similarity between the two spectra indicates that the copolymers are stable at 180 °C.

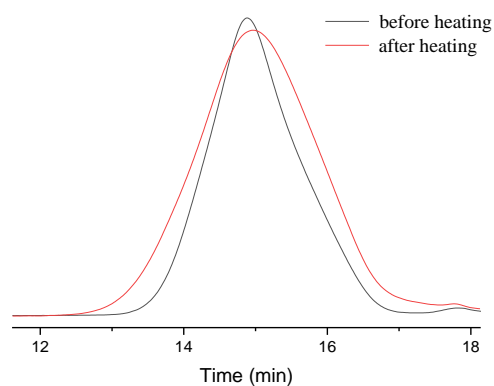


Fig. S42 SEC trace of PHCBI before and after heating under Ar atmosphere for 30 min at 180 °C.

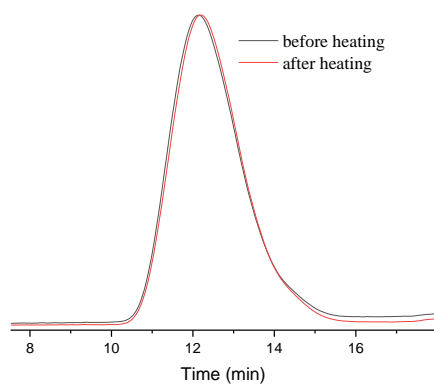


Fig. S43 SEC trace of $\text{PS}_{49}\text{-}co\text{-}\text{PHCBI}_{51}$ before and after heating under Ar atmosphere for 30 min at 180 °C. The similarity between the two SEC traces indicates that the copolymers are stable at 180 °C.

Effect of ultrasonication on polymers monitored by ^1H NMR and FT-IR measurements

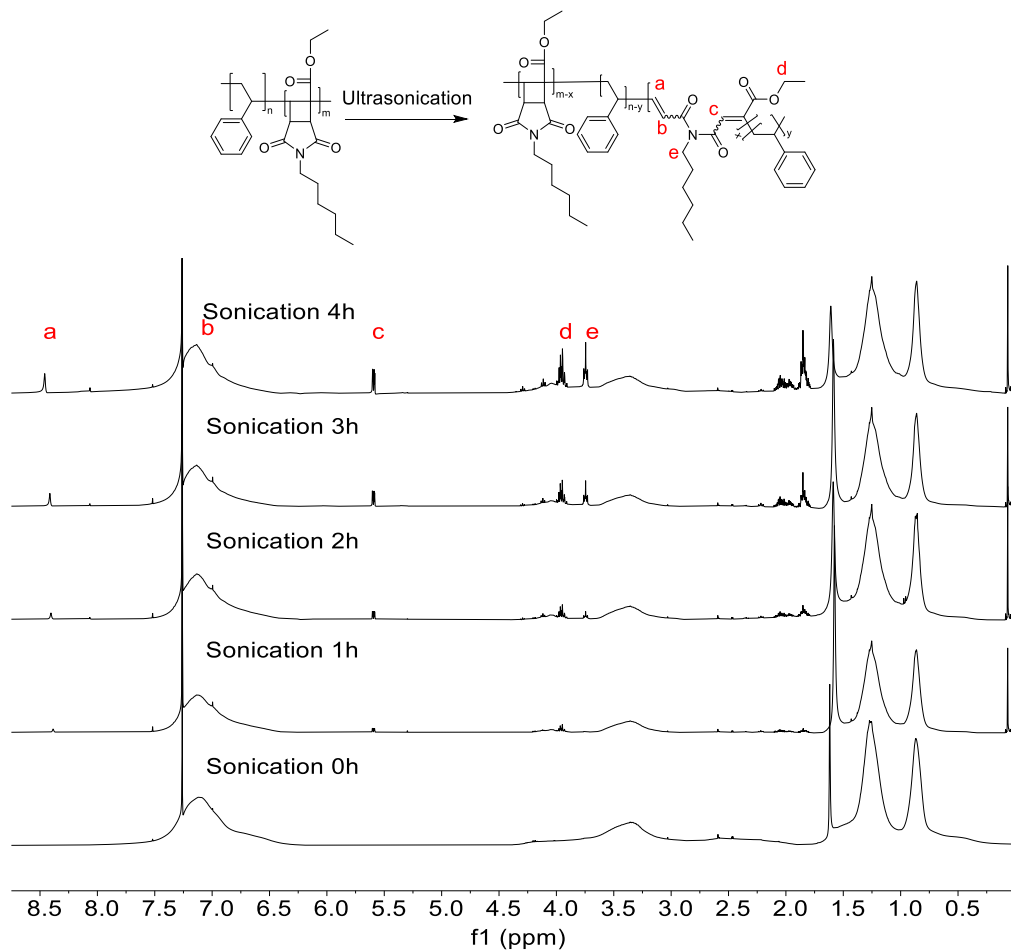


Fig. S44 ^1H NMR spectra (400 MHz, Chloroform-*d*) of $\text{PS}_{50}\text{-}co\text{-}\text{PHCBI}_{50}$ after sonication for the time indicated (magnified portions of the spectra are shown in Fig. 4 of the main manuscript).

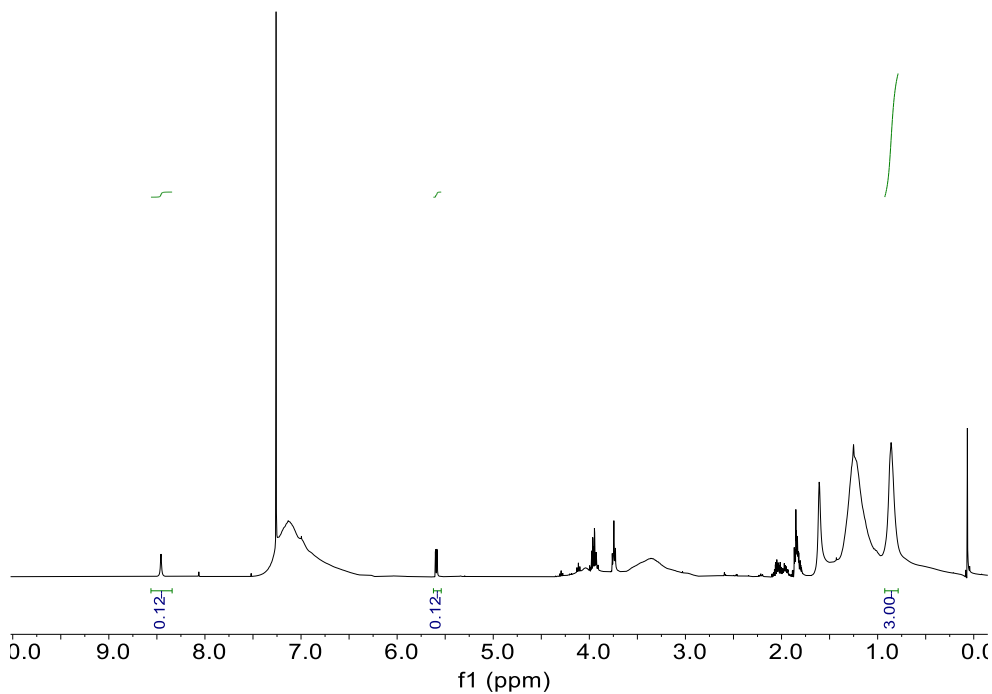


Fig. S45 ^1H NMR spectrum (400 MHz, Chloroform-*d*) of PS₅₀-*co*-PHCBI₅₀ after sonication for 240 min.

The peak at 0.8 ppm is assigned to the -CH₃ in *N*-hexyl, while the peaks at 5.60 ppm and 8.46 ppm are assigned to the alkene peaks formed upon the cyclobutane ring-opening. If all of the cyclobutane rings would have opened, the integrals of both these peaks at 5.60 ppm and 8.46 ppm should be 1. Therefore, based on ^1H NMR measurements, the fraction of ring-opened cyclobutane is $\frac{0.12}{1} \times 100\% = 12\%$.

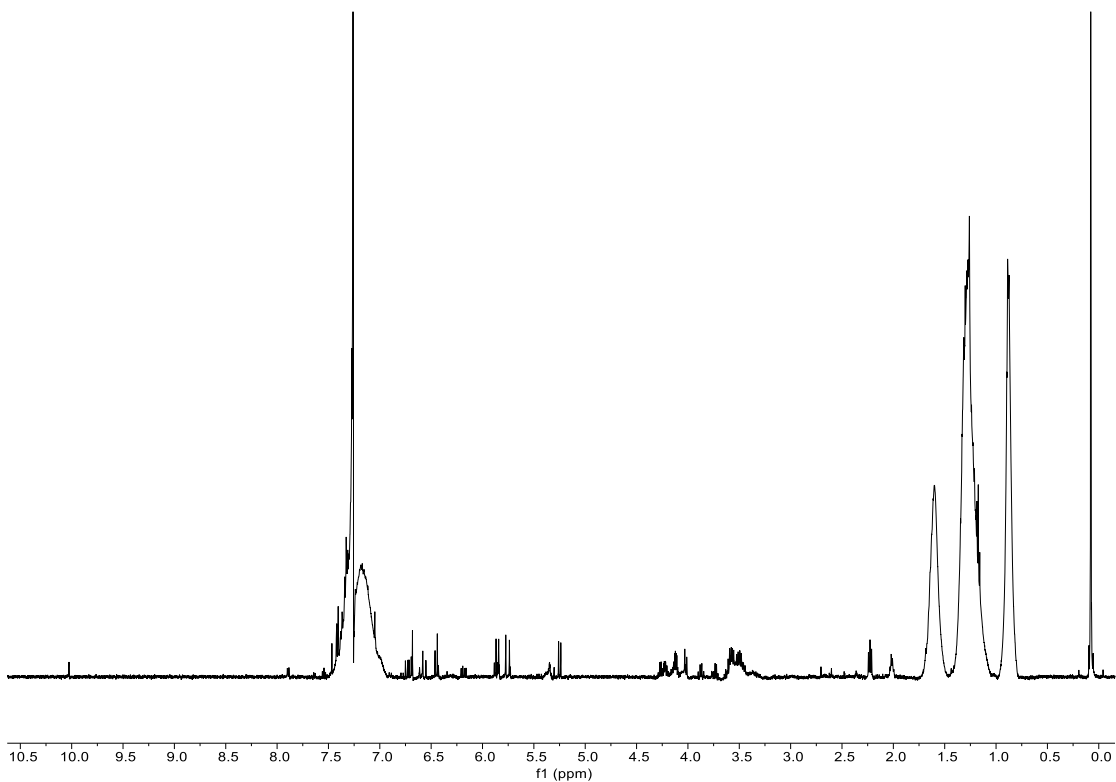


Fig. S46 ^1H NMR spectrum (400 MHz, CDCl_3) of $\text{PS}_{50}\text{-co-PHCBI}_{50}$ after cryo-milling for 60 min.
(The alkene peaks are too messy to quantify the amount of cyclobutane ring-opening.)

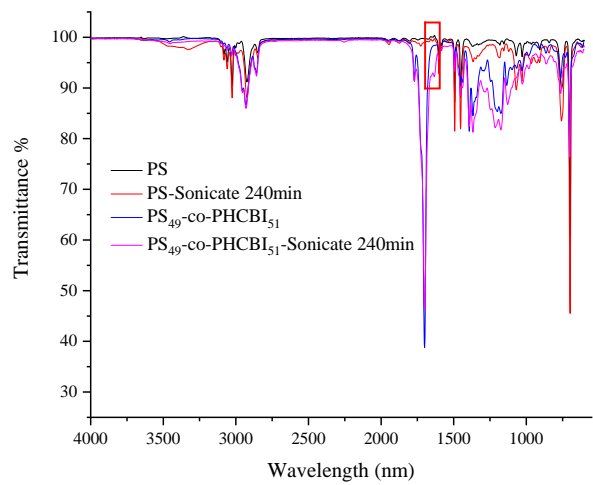


Fig. S47 IR spectra of PS and $\text{PS}_{49}\text{-co-PHCBI}_{51}$ before and after sonication (4 mg mL^{-1} in THF). The new signals in the red boxes of the IR spectra indicate carbon-carbon double bond formation associated with cyclobutane ring opening.

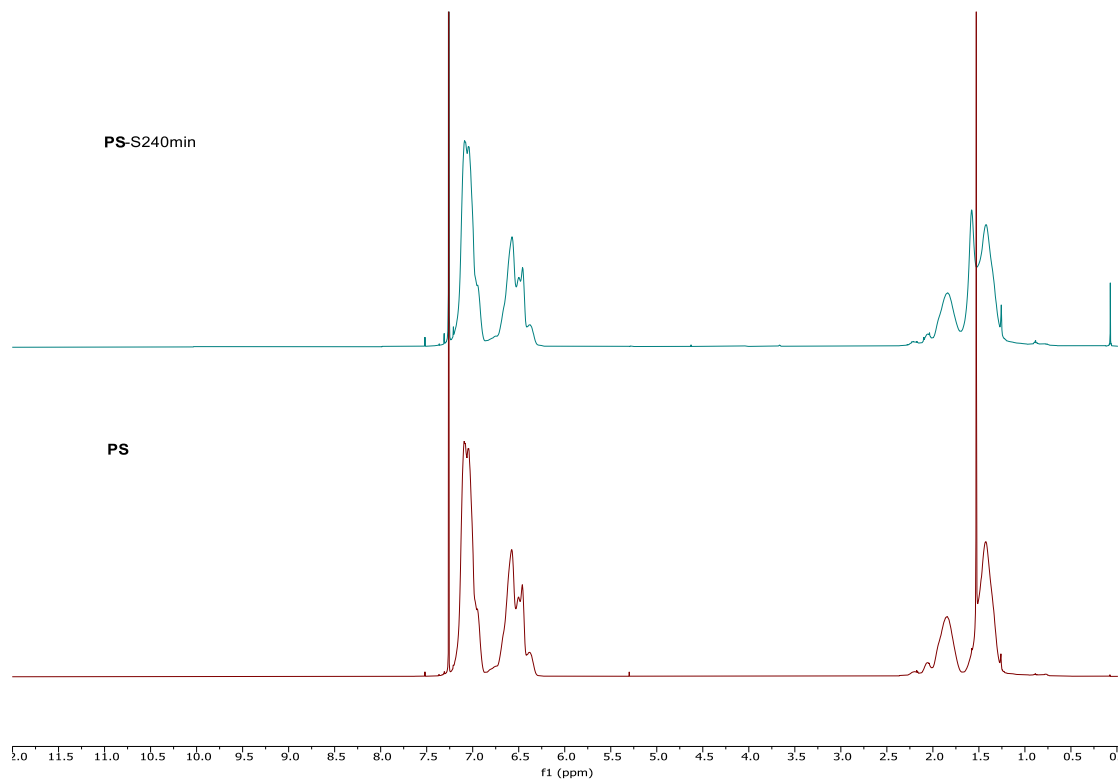


Fig. S48 ^1H NMR spectrum (400 MHz, Chloroform-*d*) of PS after sonication for 240 min (full spectrum). There was no change observed after sonication for 240min.

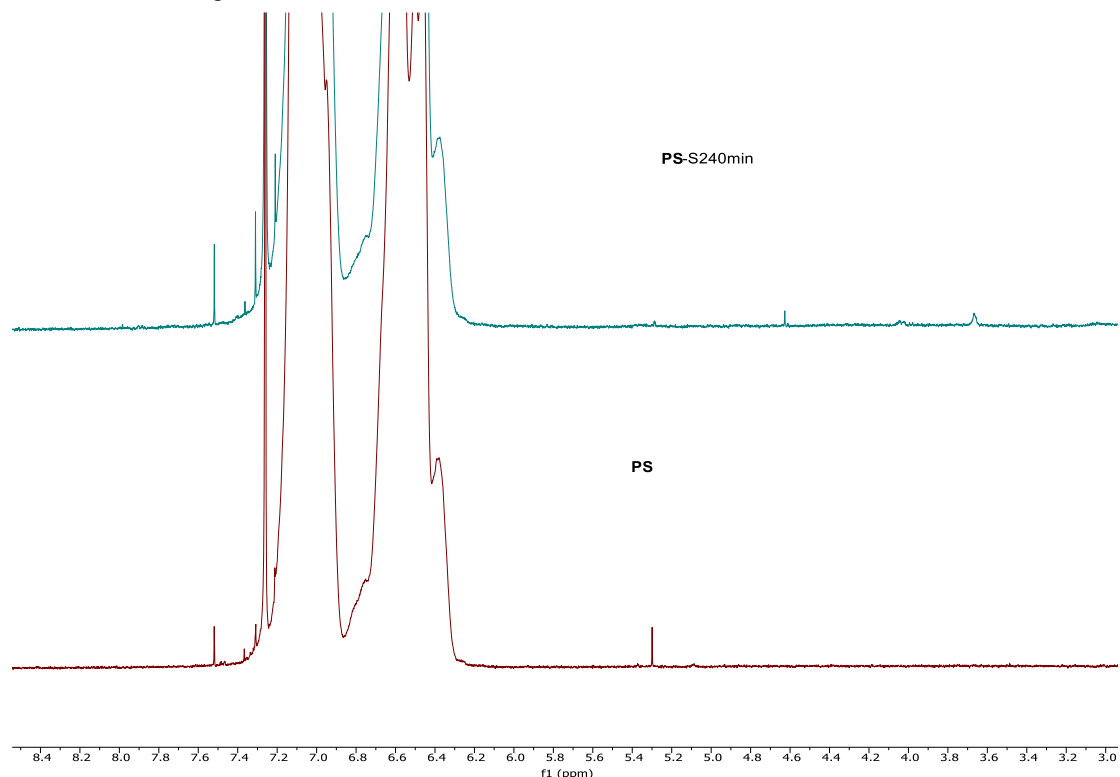


Fig. S49 ^1H NMR spectrum (400 MHz, Chloroform-*d*) of PS after sonication for 240 min (zoomed in spectrum). There was no change observed after sonication for 240min.

Ultrasonication of polymers followed by NaOH solution treatment

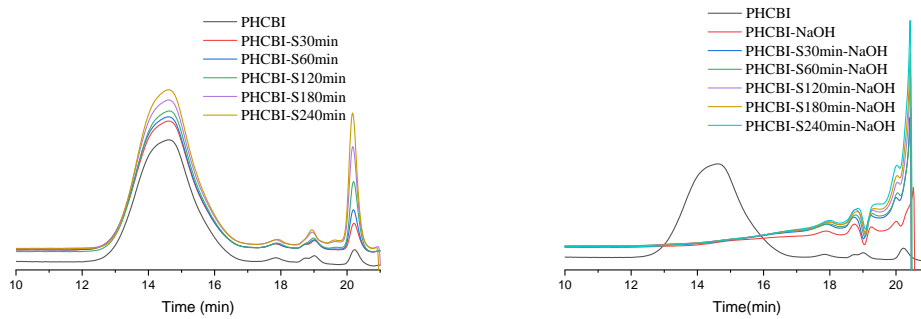


Fig. S50 SEC traces of PHCBI after sonication (left) and sonication-hydrolysis (right) (differential refractive index (dRI) signal). (After the NaOH solution addition, the mixture became dark blue and the polymers precipitated out from THF. This seems most likely because the formation of carboxylate salts. Therefore, there is no signal in SEC after NaOH treatment).

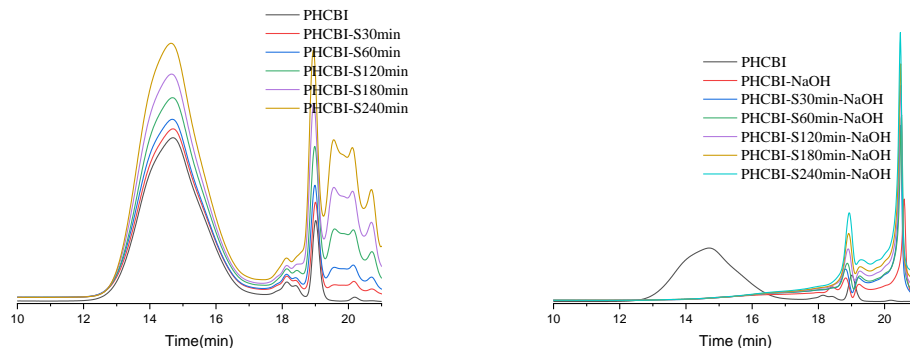


Fig. S51 SEC traces of PHCBI after sonication (left) and sonication-hydrolysis (right) (UV signal). (After the NaOH solution addition, the mixture became dark blue and the polymers precipitated out from THF. This seems most likely because the formation of carboxylate salts. Therefore, there is no signal in SEC after NaOH treatment).

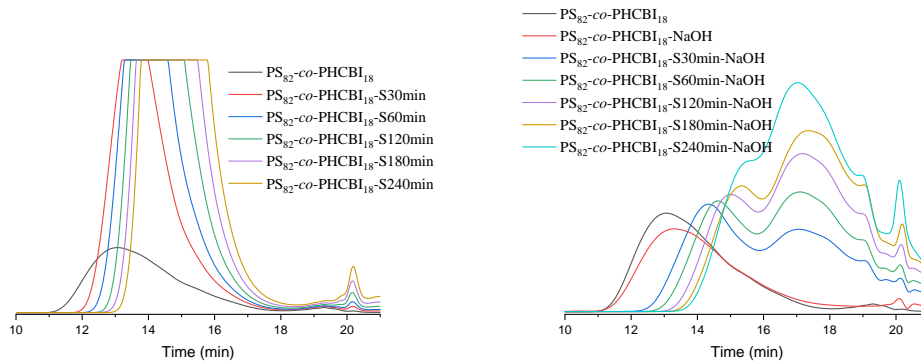


Fig. S52 SEC traces of PS₈₂-co-PHCBI₁₈ after sonication (left) and sonication-hydrolysis (right) (UV signal).

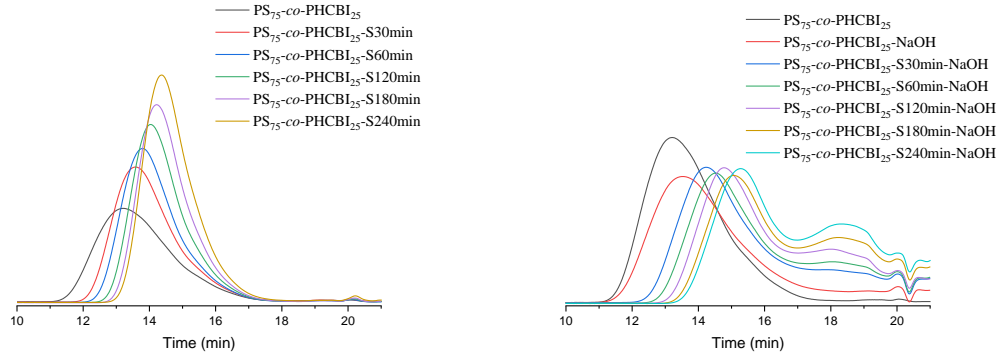


Fig. S53 SEC traces of PS₇₅-co-PHCBI₂₅ after sonication (left) and sonication-hydrolysis (right) (dRI signal).

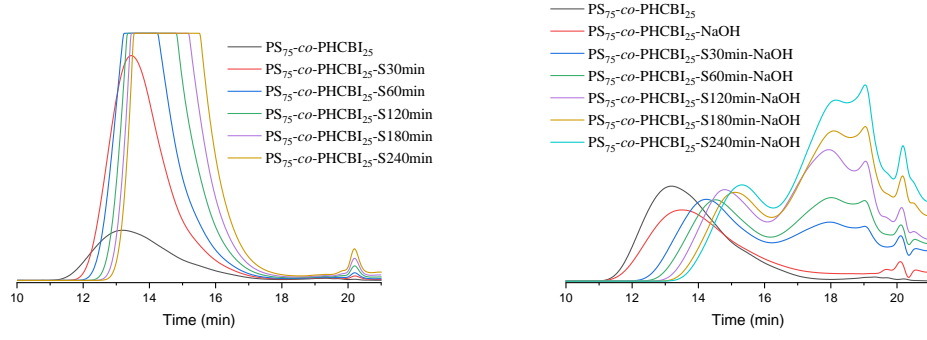


Fig. S54 SEC traces of PS₇₅-co-PHCBI₂₅ after sonication (left) and sonication-hydrolysis (right) (UV signal).

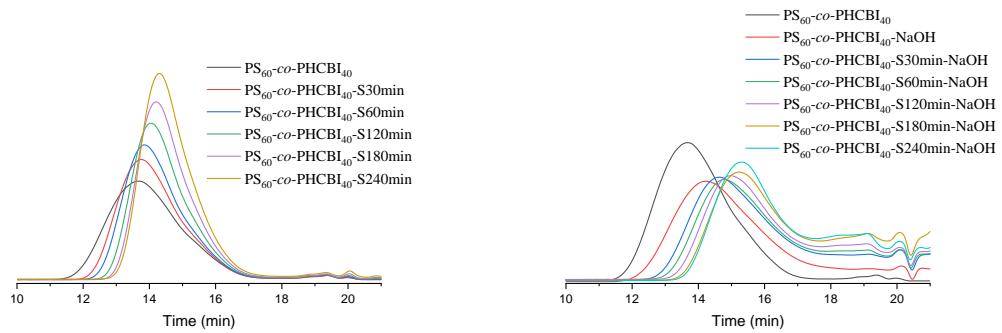


Fig. S55 SEC traces of PS₆₀-co-PHCBI₄₀ after sonication (left) and sonication-hydrolysis (right) (dRI signal).

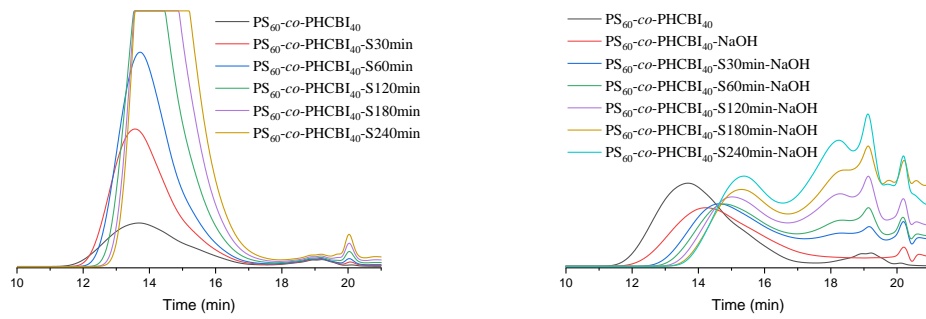


Fig. S56 SEC traces of $\text{PS}_{60}\text{-co-PHCBI}_{40}$ after sonication (left) and sonication-hydrolysis (right) (UV signal).

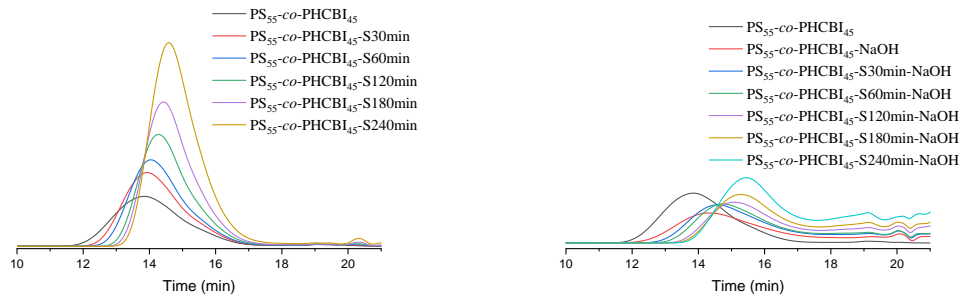


Fig. S57 SEC traces of $\text{PS}_{55}\text{-co-PHCBI}_{45}$ after sonication (left) and sonication-hydrolysis (right) (dRI signal).

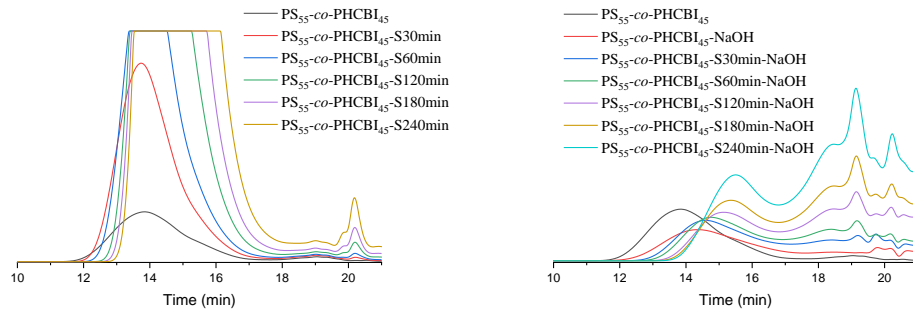


Fig. S58 SEC traces of $\text{PS}_{55}\text{-co-PHCBI}_{45}$ after sonication (left) and sonication-hydrolysis (right) (UV signal).

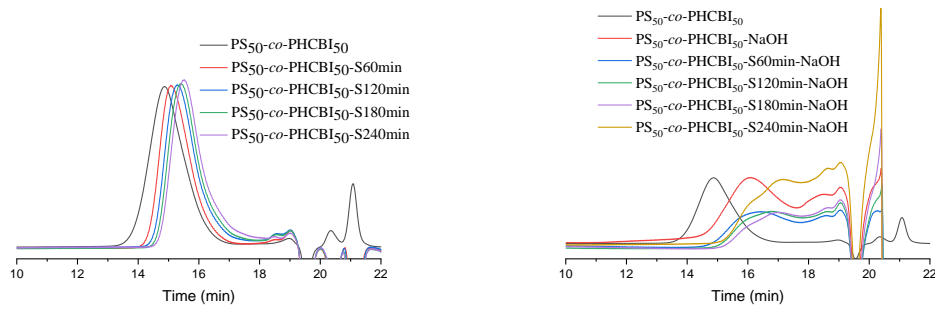


Fig. S59 SEC traces of PS₅₀-co-PHCBI₅₀ after sonication (left) and sonication-hydrolysis (right) (dRI signal).

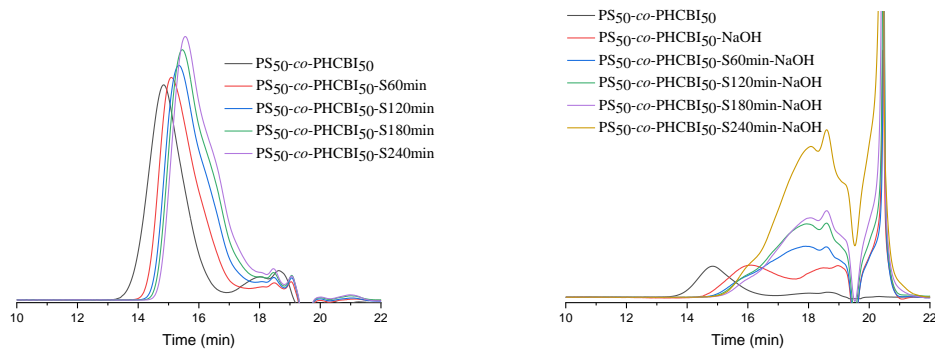


Fig. S60 SEC traces of PS₅₀-co-PHCB₅₀ after sonication (left) and sonication-hydrolysis (right) (UV signal).

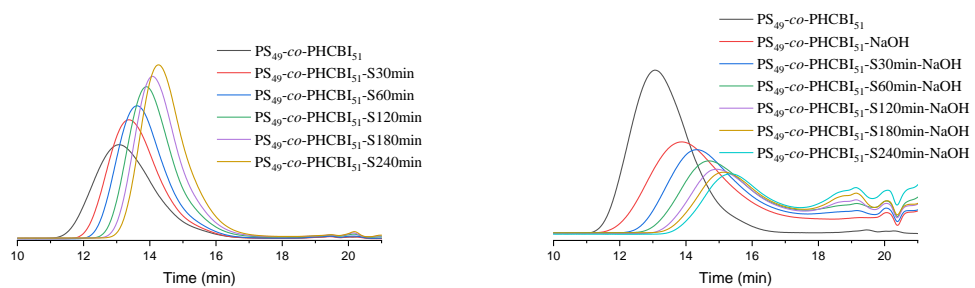


Fig. S61 SEC traces of PS₄₉-co-PHCBI₅₁ after sonication (left) and sonication-hydrolysis (right) (dRI signal).

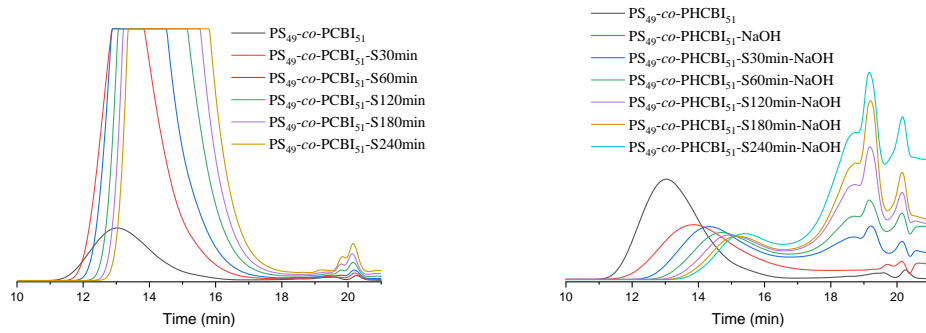


Fig. S62 SEC traces of $\text{PS}_{49}\text{-co-PHCBI}_{51}$ after sonication (left) and sonication-hydrolysis (right) (UV signal).

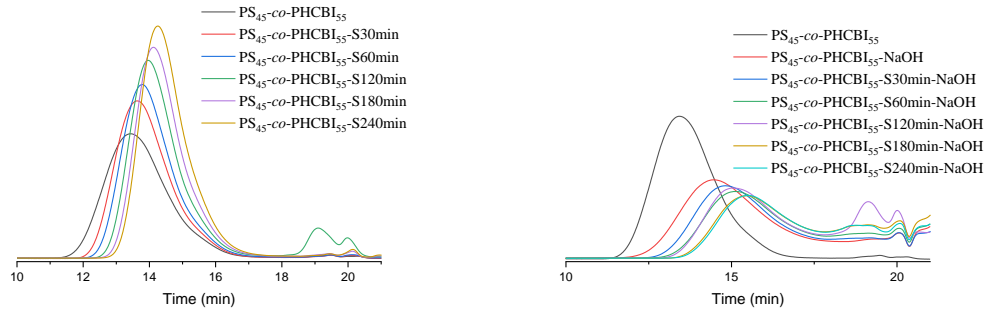


Fig. S63 SEC traces of $\text{PS}_{45}\text{-co-PHCBI}_{55}$ after sonication (left) and sonication-hydrolysis (right) (dRI signal).

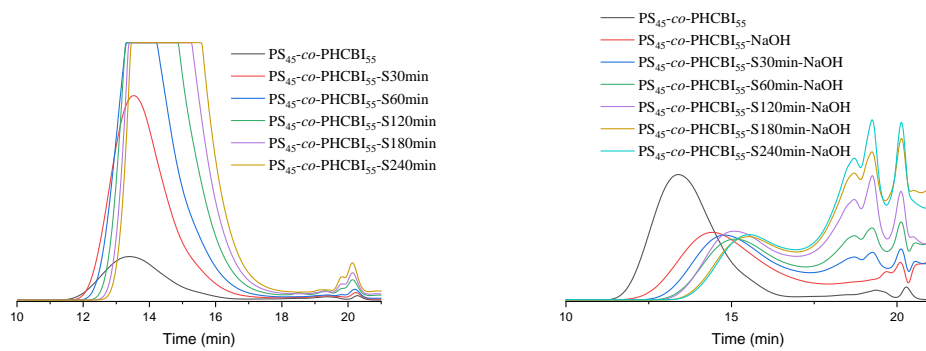


Fig. S64 SEC traces of $\text{PS}_{45}\text{-co-PHCBI}_{55}$ after sonication (left) and sonication-hydrolysis (right) (UV signal).

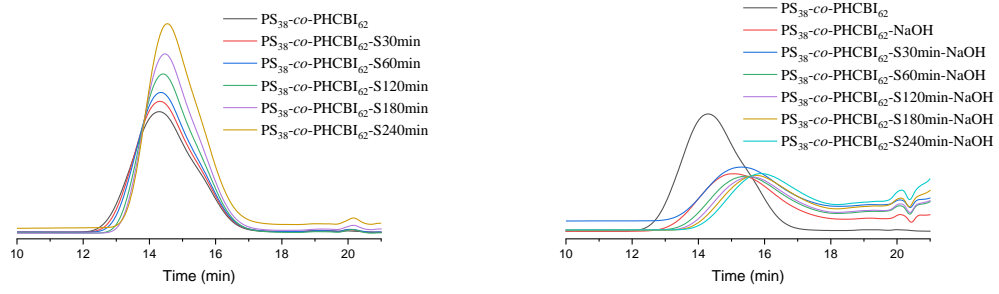


Fig. S65 SEC traces of PS₃₈-co-PHCBI₆₂ after sonication (left) and sonication-hydrolysis (right) (dRI signal).

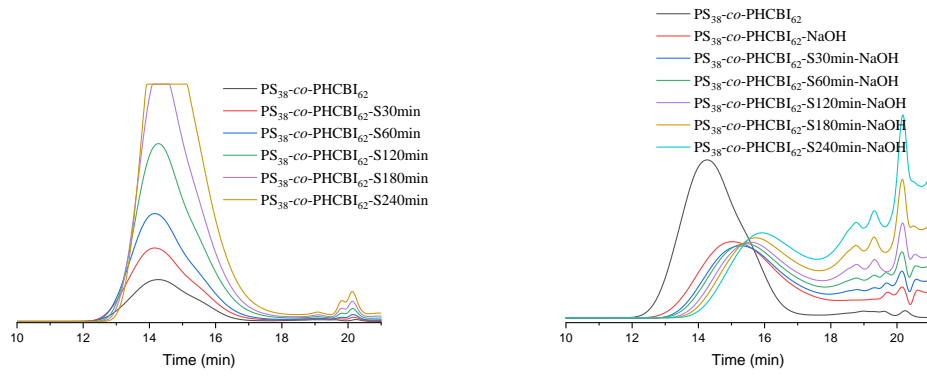


Fig. S66 SEC traces of PS₃₈-co-PHCBI₆₂ after sonication (left) and sonication-hydrolysis (right) (UV signal).

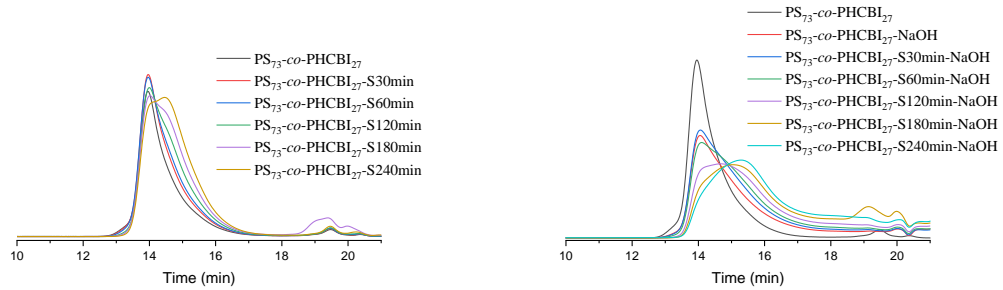


Fig. S67 SEC traces of PS₇₃-co-PHCBI₂₇ after sonication (left) and sonication-hydrolysis (right) (dRI signal).

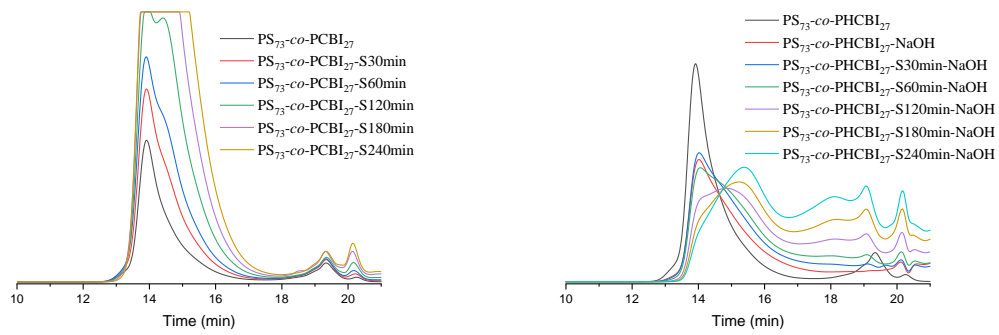


Fig. S68 SEC traces of $\text{PS}_{73}\text{-co-PHCBI}_{27}$ after sonication (left) and sonication-hydrolysis (right) (UV signal).

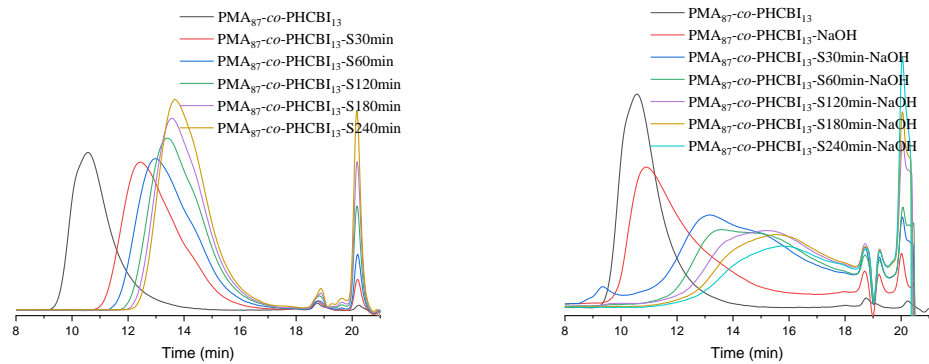


Fig. S69 SEC traces of $\text{PMA}_{87}\text{-co-PHCBI}_{13}$ after sonication (left) and sonication-hydrolysis (right) (dRI signal).

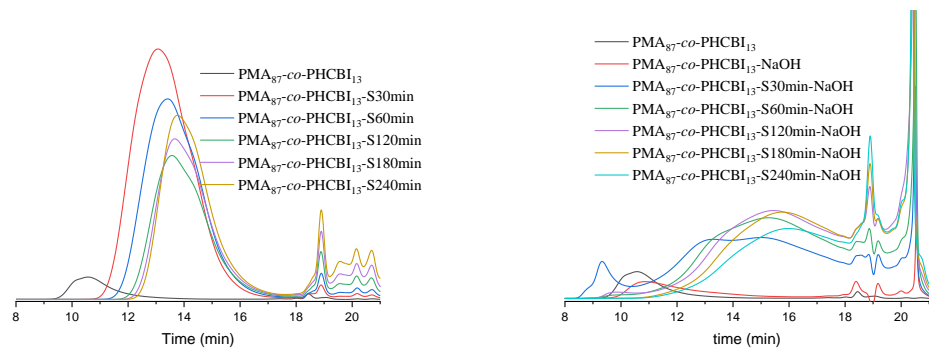


Fig. S70 SEC traces of $\text{PMA}_{87}\text{-co-PHCBI}_{13}$ after sonication (left) and sonication-hydrolysis (right) (UV signal).

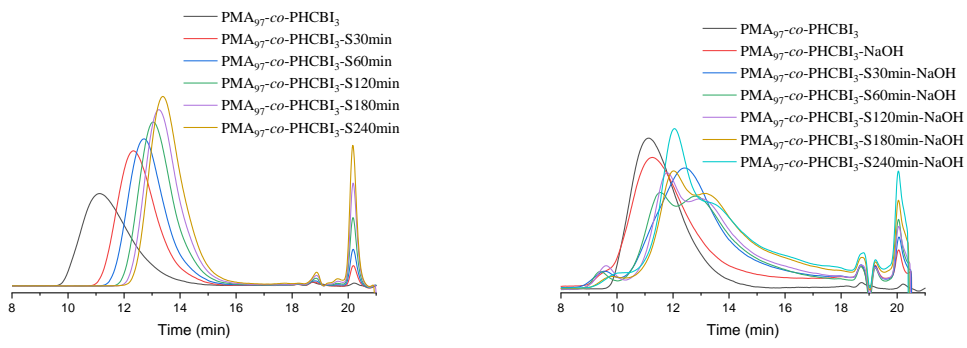


Fig. S71 SEC traces of PMA₉₇-co-PHCBI₃ after sonication (left) and sonication-hydrolysis (right) (dRI signal).

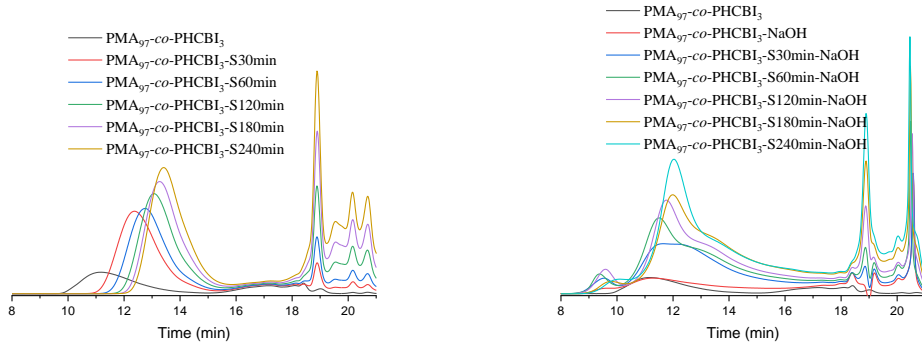


Fig. S72 SEC traces of PMA₉₇-co-PHCBI₃ after sonication (left) and sonication-hydrolysis (right) (UV signal).

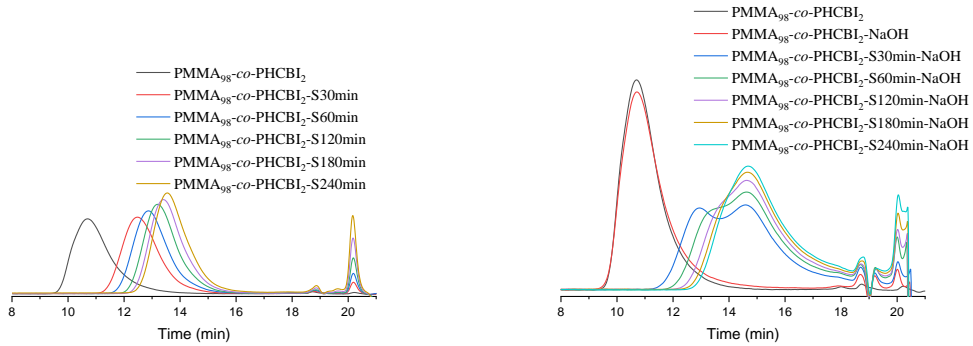


Fig. S73 SEC traces of PMMA₉₈-co-PHCBI₂ after sonication (left) and sonication-hydrolysis (right) (dRI signal).

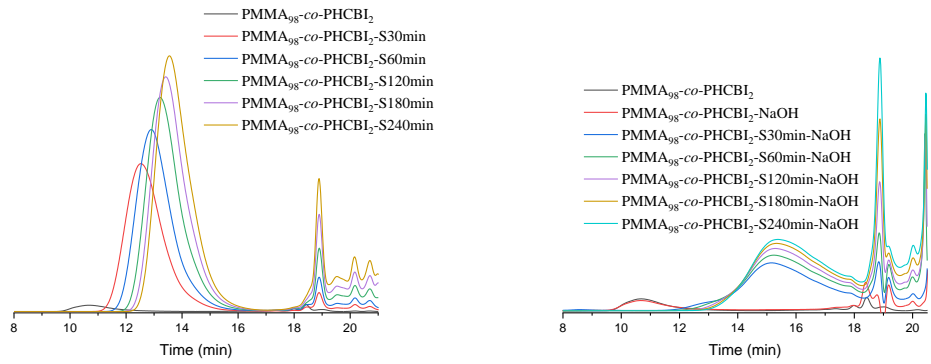


Fig. S74 SEC traces of PMMA₉₈-co-PHCBI₂ after sonication (left) and sonication-hydrolysis (right) (UV signal).

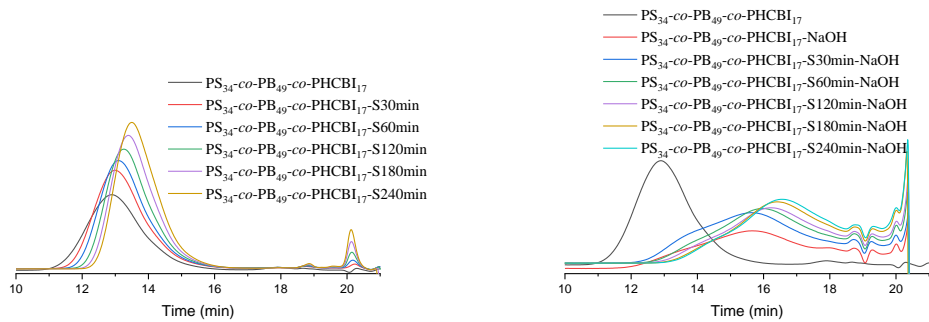


Fig. S75 SEC traces of PS₃₄-co-PB₄₉-co-PHCBI₁₇ after sonication (left) and sonication-hydrolysis (right) (dRI signal).

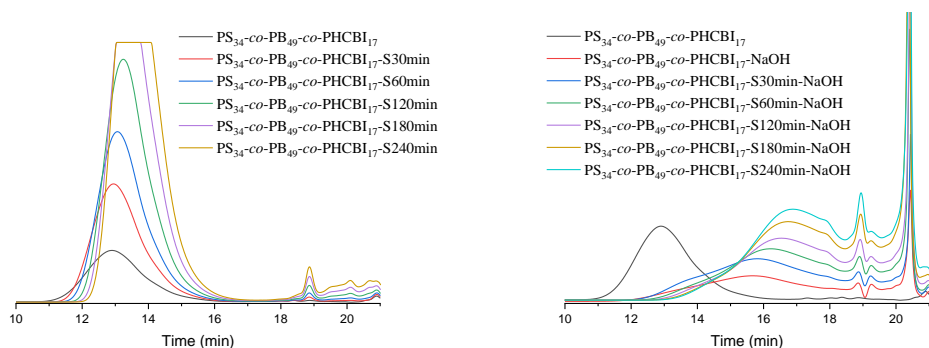


Fig. S76 SEC traces of PS₃₄-co-PB₄₉-co-PHCBI₁₇ after sonication (left) and sonication-hydrolysis (right) (UV signal).

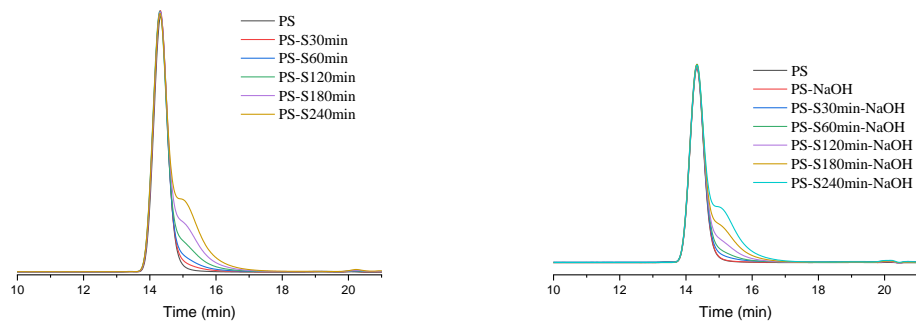


Fig. S77 SEC traces of PS (commercially available polystyrene, 50 kg mol⁻¹) after sonication (left) and sonication-hydrolysis (right) (dRI signal).

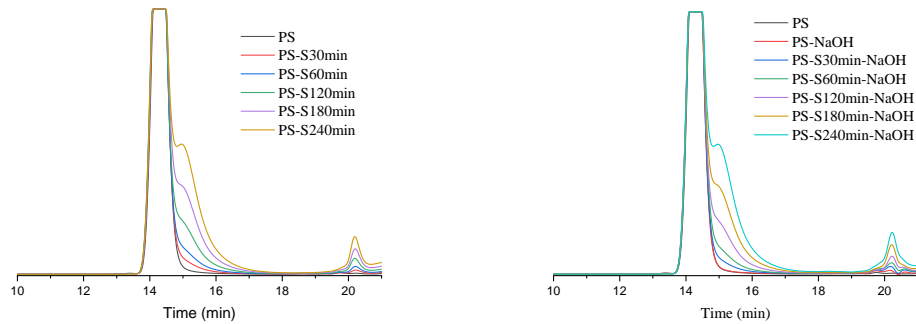


Fig. S78 SEC traces of PS (commercially available polystyrene, 50 kg mol⁻¹) after sonication (left) and sonication-hydrolysis (right) (UV signal).

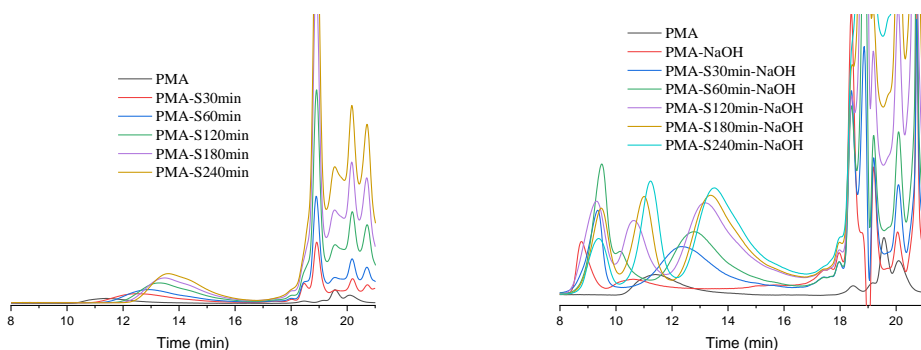


Fig. S79 SEC traces of PMA after sonication (left) and sonication-hydrolysis (right) (UV signal).

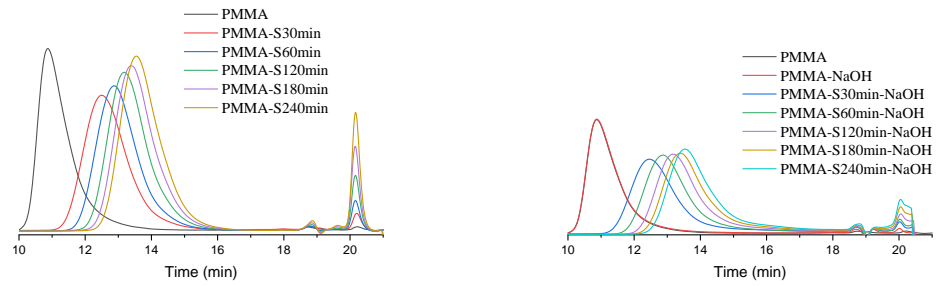


Fig. S80 SEC traces of PMMA after sonication (left) and sonication-hydrolysis (right) (dRI signal).

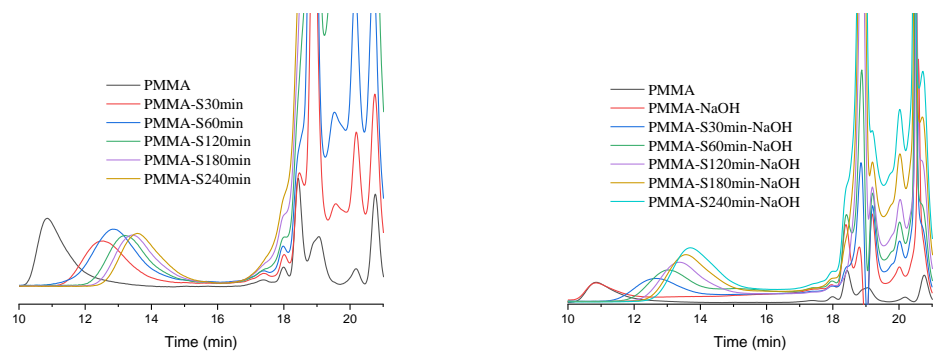


Fig. S81 SEC traces of PMMA after sonication (left) and sonication-hydrolysis (right) (UV signal).

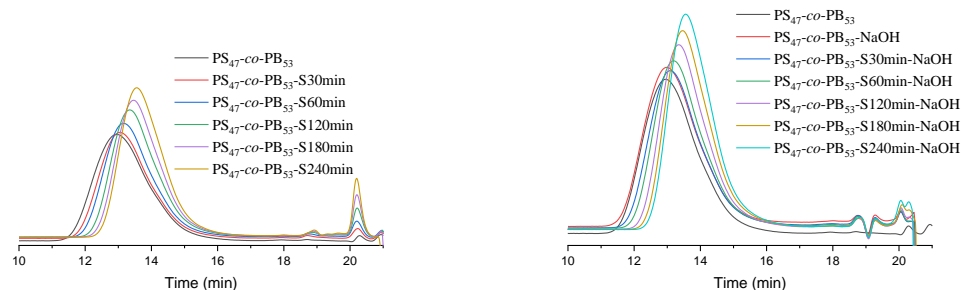


Fig. S82 SEC traces of PS₄₇-co-PB₅₃ after sonication (left) and sonication-hydrolysis (right) (dRI signal).

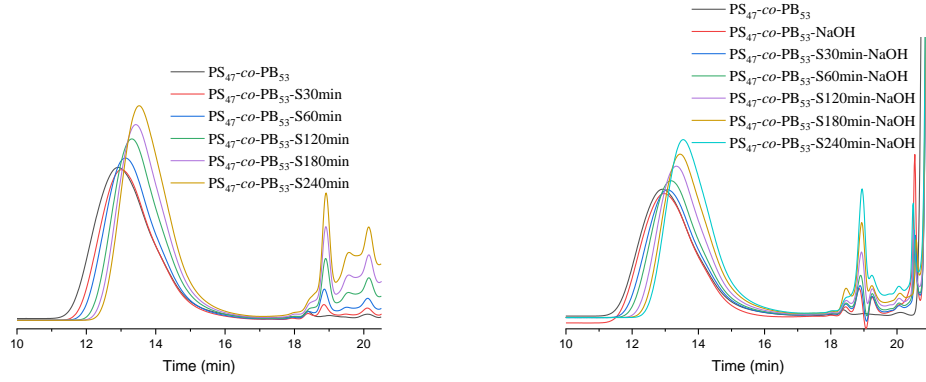


Fig. S83 SEC traces of PS₄₇-co-PB₅₃ after sonication (left) and sonication-hydrolysis (right) (UV signal).

Treatment of polymers with NaOH solution followed by ultrasonication

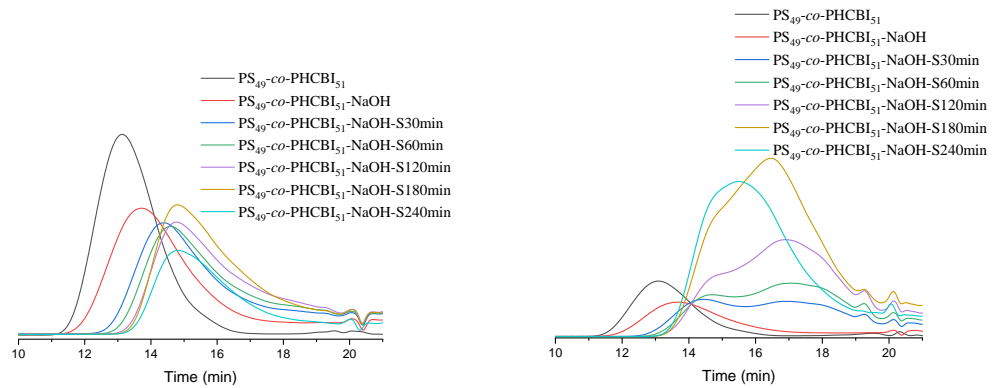


Fig. S84 SEC traces of PS₄₉-co-PHCBI₅₁ after treatment with NaOH, followed by ultrasonication (left: dRI signal; right: UV signal).

Cryo-milling of polymers followed by treatment with NaOH solution

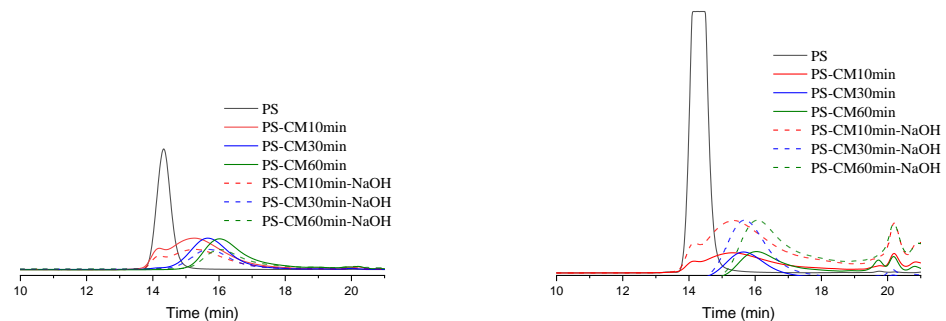


Fig. S85 SEC traces of PS after cryo-milling and cryo-milling-hydrolysis (left: dRI signal; right: UV signal).

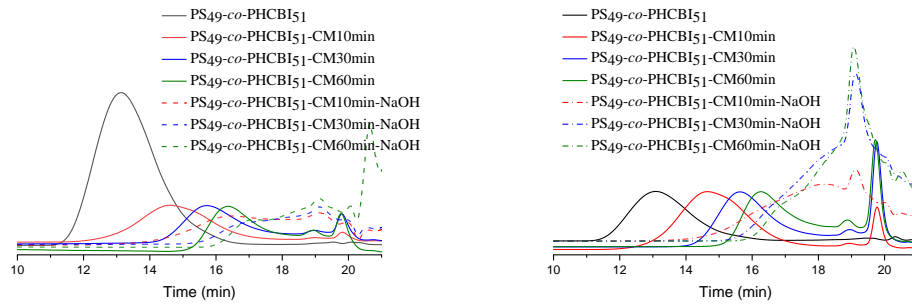


Fig. S86 SEC traces of PS₄₉-co-PHCBI₅₁ after cryo-milling and cryo-milling-hydrolysis (left: dRI signal; right: UV signal).

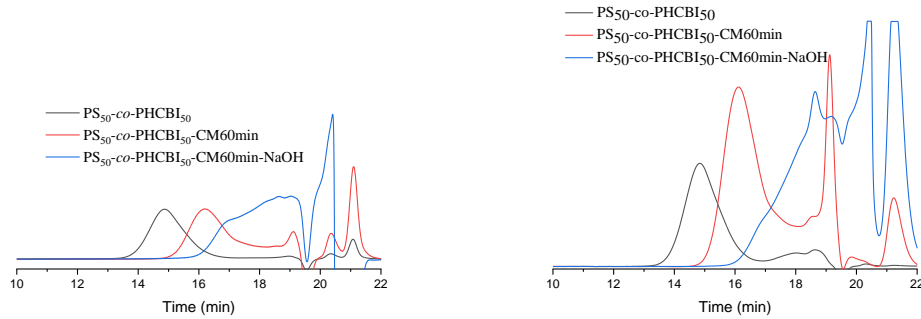


Fig. S87 SEC traces of PS₅₀-co-PHCBI₅₀ after cryo-milling and cryo-milling-hydrolysis (left: dRI signal; right: UV signal).

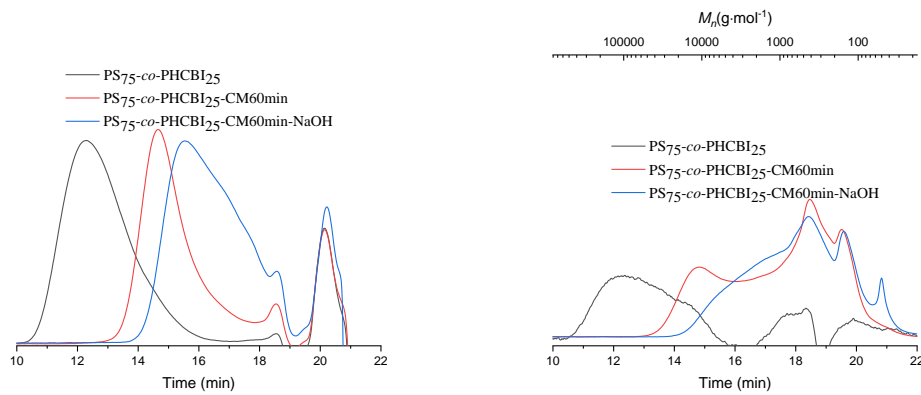


Fig. S88 SEC traces of PS₇₅-co-PHCBI₂₅ after cryo-milling and cryo-milling-hydrolysis (left: dRI signal; right: UV signal).

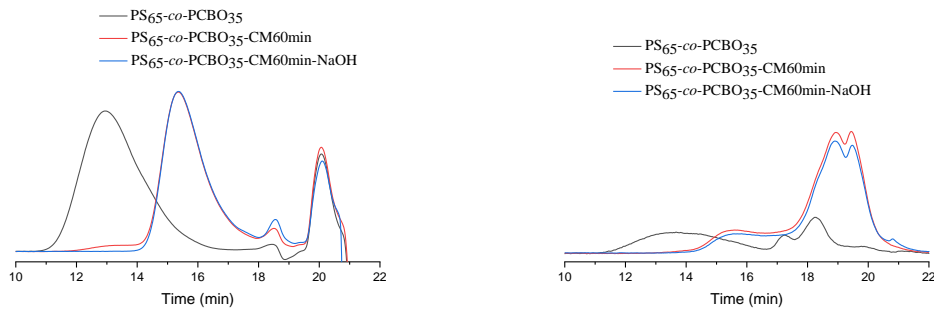


Fig. S89 SEC traces of PS₆₅-co-PCBO₃₅ after cryo-milling and cryo-milling-hydrolysis (left: dRI signal; right: UV signal).

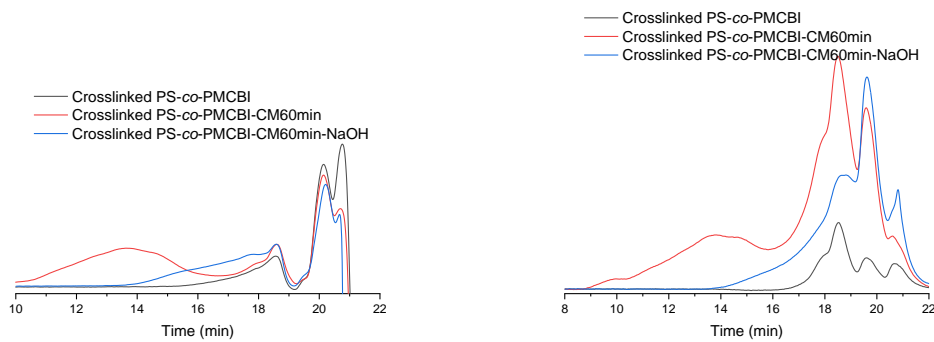


Fig. S90 SEC traces of (PS-co-PMCB)-l-PDCBI, i.e. cross-linked PS-co-PMCB, after cryo-milling and cryo-milling-hydrolysis (left: dRI signal; right: UV signal). The SEC trace (black) of cross-linked PS-co-PHCBI originates from the extractable sol fraction of the material (i.e. residual monomers and polymer chains that were not linked into the polymer network). After cryo-milling, the copolymer was slightly soluble in THF (red trace). After the hydrolysis step, the polymer was soluble in THF (blue trace).

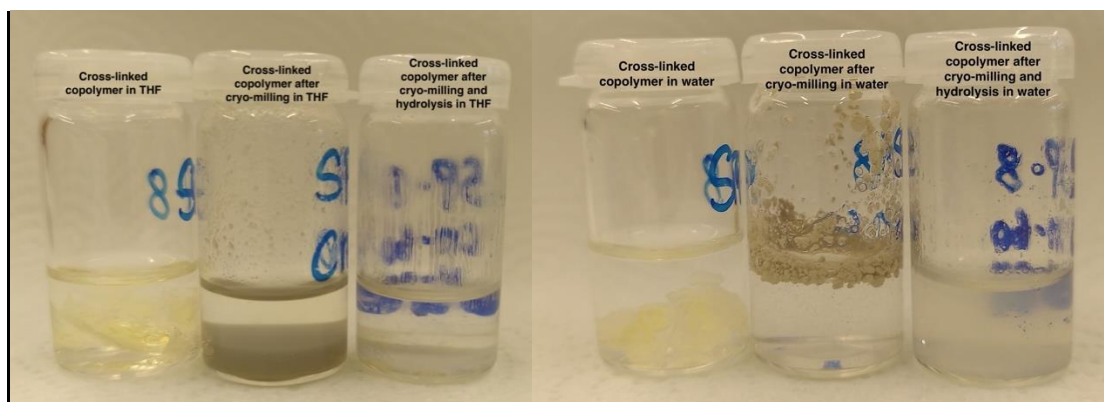


Fig. S91 Photographs of (PS-co-PMCB)-l-PDCBI (i.e. cross-linked PS-co-PMCB), (PS-co-PMCB)-l-PDCBI after cryo-milling and (PS-co-PMCB)-l-PDCBI after cryo-milling-hydrolysis (left in THF, right in water). The cross-linked copolymer was neither soluble in THF nor in water. After cryo-milling, the copolymer was still not soluble in THF and water (The grey color of the copolymers is from the stainless

steel end-caps and grinding cylinder of the cyro-mill). After cryo-milling and hydrolysis the copolymer was well-soluble in THF and partly soluble in water.

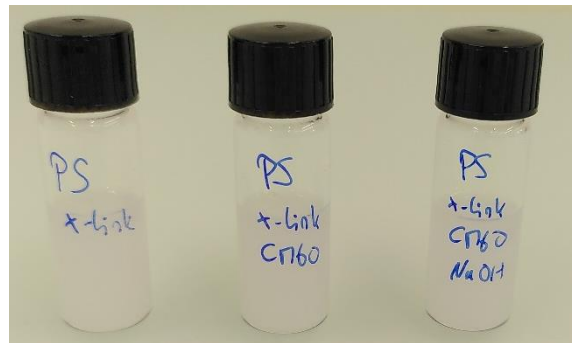


Fig. S92 Photographs of cross-linked PS, cross-linked PS after cryo-milling and cross-linked PS after cryo-milling-hydrolysis in THF. The cross-linked PS was not soluble in THF and did not become soluble in THF after cryo-milling and hydrolysis.

Treatment of polymers with different mechanical methods and hydrolysis

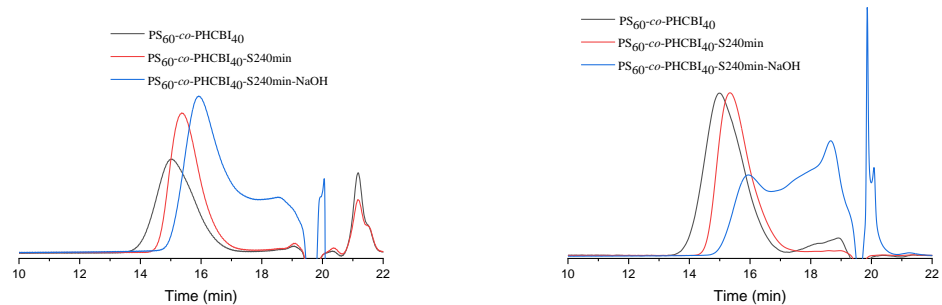


Fig. S93 SEC traces of PS₆₀-co-PHCBI₄₀ after sonication-hydrolysis (left: dRI signal; right: UV signal).

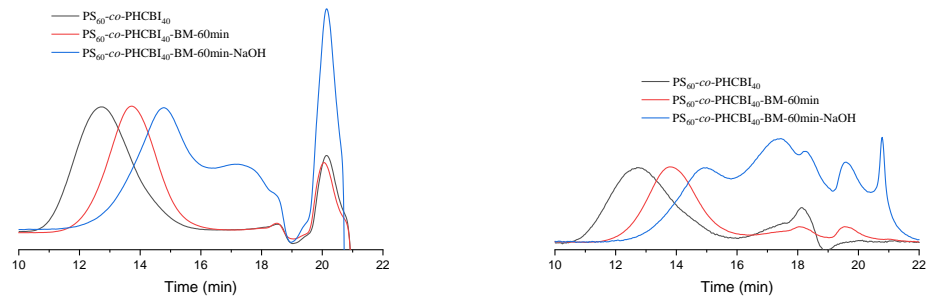


Fig. S94 SEC traces of PS₆₀-co-PHCBI₄₀ after ball-milling-hydrolysis (left: dRI signal; right: UV signal).

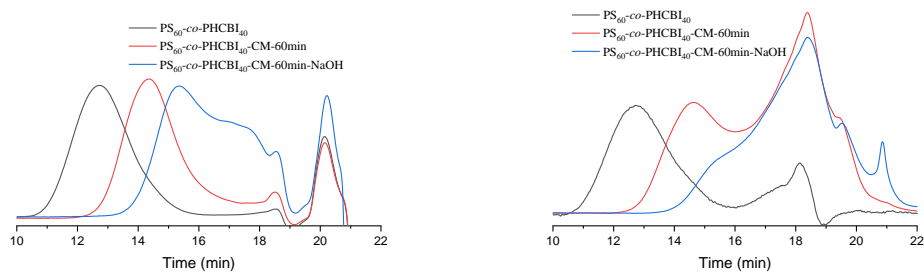


Fig. S95 SEC traces of $\text{PS}_{60}\text{-co-PHCBI}_{40}$ after cryo-milling-hydrolysis (left: dRI signal; right: UV signal).

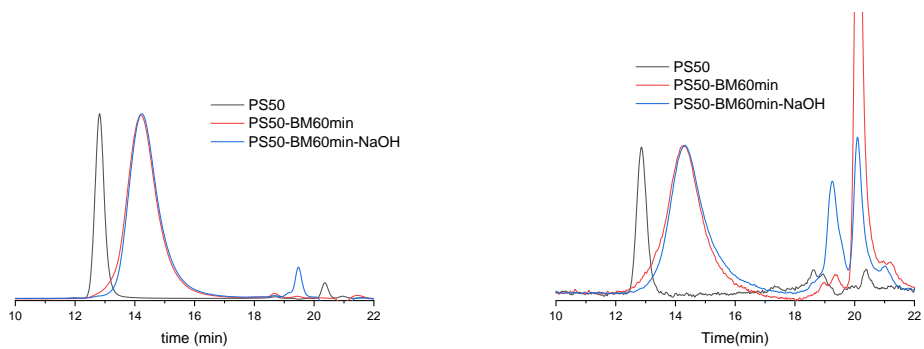


Fig. S96 SEC traces of PS after ball-milling-hydrolysis (left: dRI signal; right: UV signal).

Ball-milling of dry polymers with solid NaOH

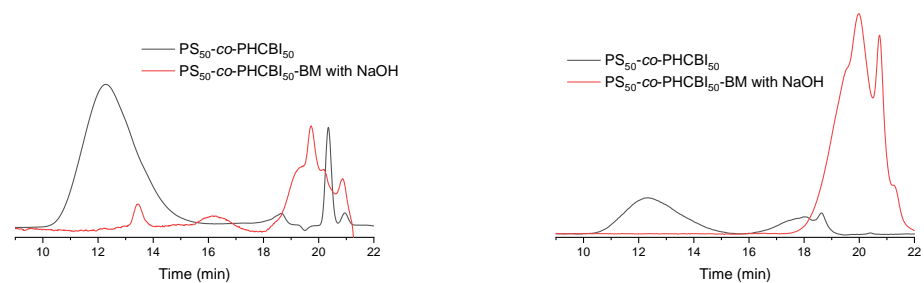


Fig. S97 SEC traces of $\text{PS}_{50}\text{-co-PHCBI}_{50}$ after dry ball-milling (60 min) in the presence of solid NaOH (left: dRI signal; right: UV signal).

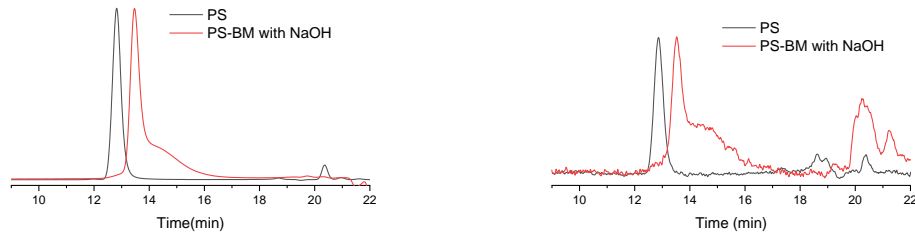


Fig. S98 SEC traces of PS after dry ball-milling (60 min) in the presence of solid NaOH (left: dRI signal; right: UV signal).

Ultrasonication of polymer followed by treatment with NaOH solutions of different concentrations

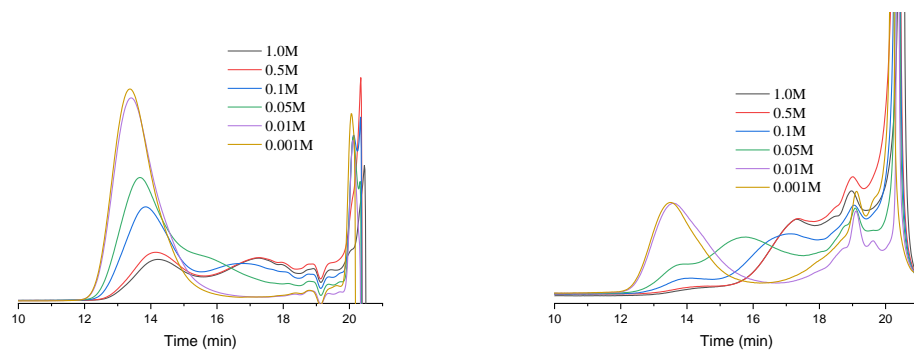


Fig. S99 SEC traces of $\text{PS}_{49}\text{-co-PHCBI}_{51}$ after sonication for 240 min and hydrolysis with NaOH solutions of different concentrations (left dRI signal, right UV signal). The hydrolysis efficiency increased with increasing NaOH concentration.

Chromatographic isolation and characterization of degradation products of $\text{PS}_{50}\text{-co-PHCBI}_{50}$

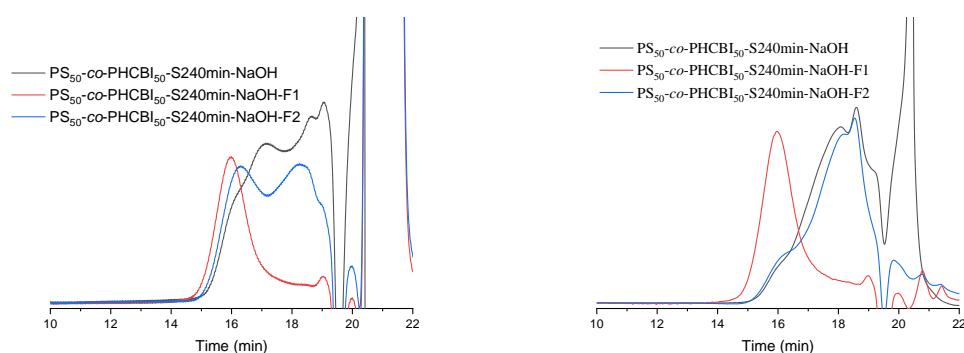


Fig. S100 SEC traces of $\text{PS}_{50}\text{-co-PHCBI}_{50}$ after sonication for 240 min and hydrolysis with NaOH, and of fractions obtained by flash silica chromatography (left dRI signal, right UV signal).

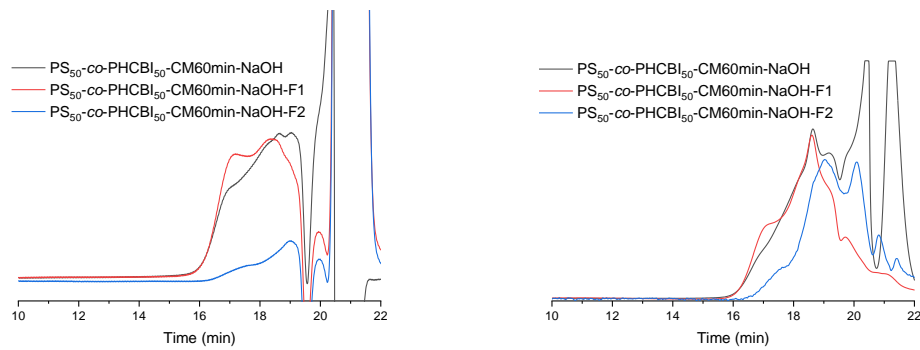


Fig. S101 SEC traces of $\text{PS}_{50}\text{-co-PHCBI}_{50}$ after cryo-milling and hydrolysis with NaOH, and of fractions obtained by flash silica chromatography (left dRI signal, right UV signal).

Characterization of the degradation products

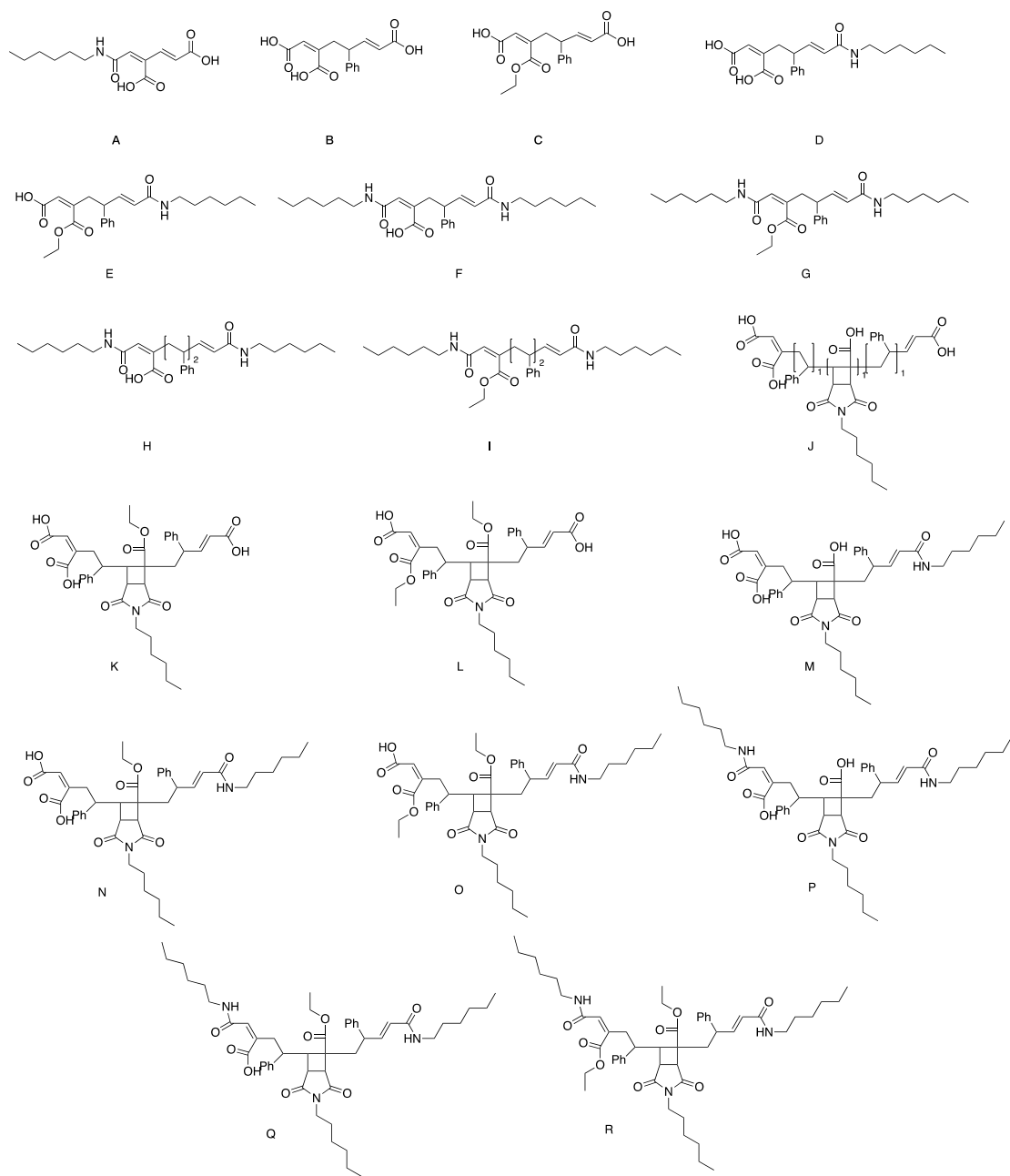


Fig. S102 List of expected degradation products.

LC-MS:

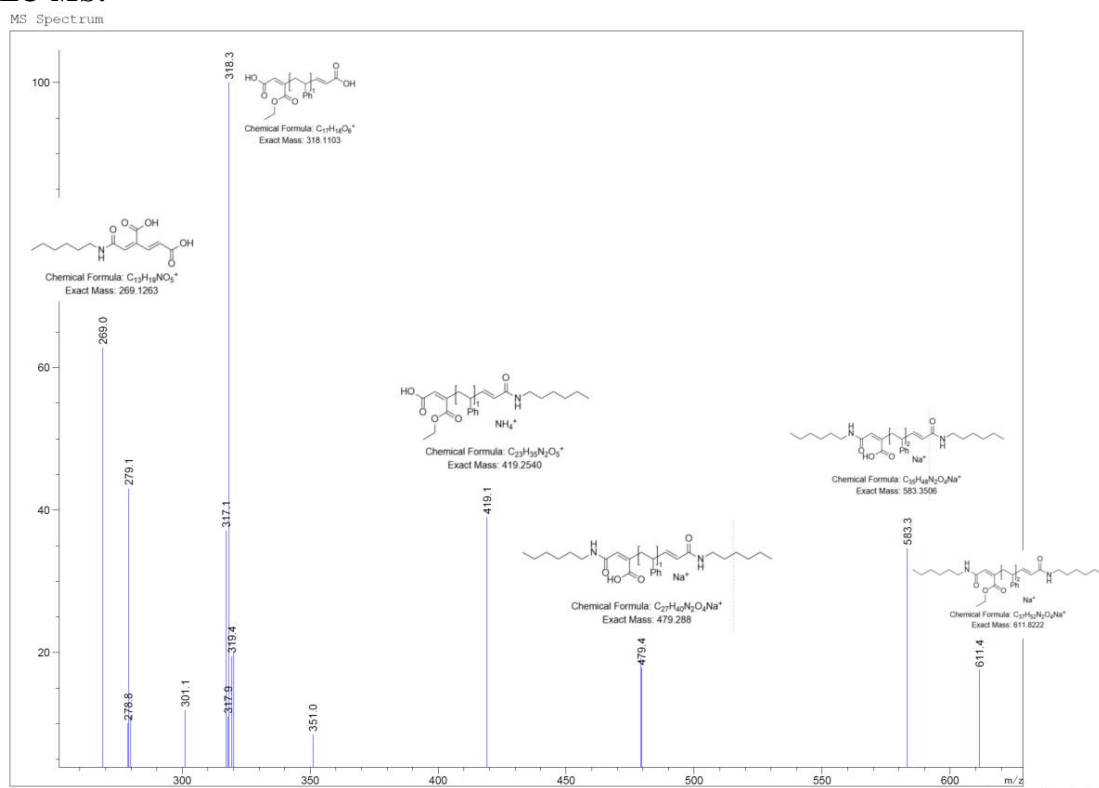


Fig. S103 ESI-MS analysis of PS₅₀-co-PHCBI₅₀ after sonication (240 min) and hydrolysis with NaOH solution overnight at room temperature (This figure was also showed as Fig. 5f in manuscript).

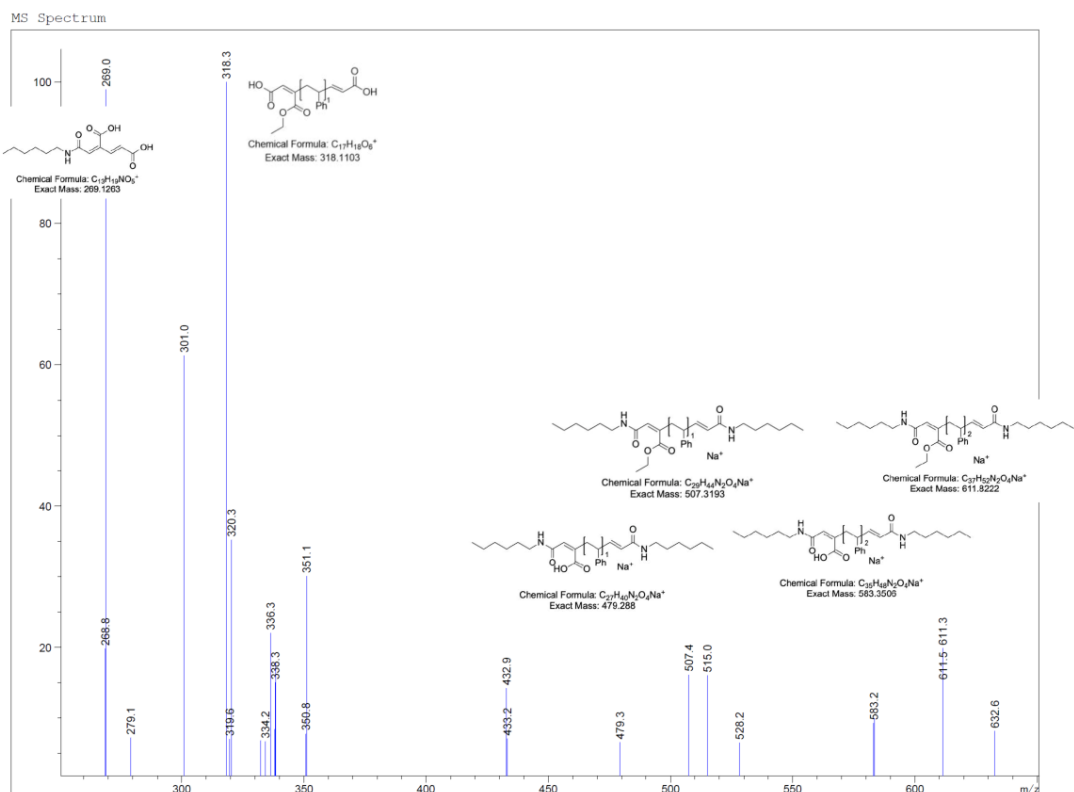


Fig. S104 ESI-MS of PS₅₀-co-PHCBI₅₀ after cryo-milling (60 min) and hydrolysis with NaOH solution overnight at room temperature.

UPLC-QToF:

The waters_connect software platform with UNIFIT™ was used to process the MS data. Fig. S105 and Fig. S106 show the base peak intensity chromatograms (BPI) in ESI⁺ and ESI⁻ mode for the Solvent, Blank Matrix, PS₄₉-co-PHCBI₅₁, PS₄₉-co-PHCBI₅₁-cryo-milling-hydrolysis and PS₄₉-co-PHCBI₅₁-sonication-hydrolysis. The BPI full scan chromatograms give an indication of the abundance of compounds detected in the samples. It is obvious that the blank matrix sample already shows numerous peaks. Nevertheless, some potential unique peaks and differences between the samples can already be observed by visual inspection, such as peaks at retention time at 8.14 and 9.55 min in ESI⁺ mode (Fig. S105) and at retention time at 4.12 and 7.94 min in ESI⁻ mode (Fig. S106). A precise evaluation of eluting *m/z*-RT pairs with their corresponding intensities was carried out with the UNIFIT™ software. Data was processed in two steps: 1) a three-dimensional (3D) peak detection, which is based on the calculation of peak volumes the detection of all ion clusters in a given retention time range, and 2) a screening step, where the software matches the retention time, *m/z* (± 5 ppm) and intensity pairs (3D peak picking) of detected peaks (features) automatically against library containing 18 target compounds. For most compounds several isomeric species were observed in the accurate extracted ion chromatogram (XIC). Initially, only the up to 4 most intense chromatographic peaks were evaluated. A total of 17 target compounds were identified using this approach from data acquired in either ESI⁺ or ESI⁻ mode. The detailed MS information of these compounds is summarized in Table S2 for sample PS₄₉-co-PHCBI₅₁-cryo-milling-hydrolysis and in Table S3 for sample PS₄₉-co-PHCBI₅₁-sonication-hydrolysis. The compounds listed as identified in the Table S2 and S3 can be confirmed with high confidence based on mass accuracy (± 5 ppm) and the fit of the experimental isotope data to the theoretical isotope distribution (i-FIT). For all identified compounds, the isotope fit criteria defined as the deviation of the isotope match intensity in percent was less than 25 %. The mass accuracy was calculated as the mean value (ppm) of the five replicated measurements. Additional target compounds not identified in Table S2 and Table S3 could not be confirmed with sufficient level of confidence and were therefore not considered for evaluation or were not detectable. If two adducts are mentioned in the adduct column, both adducts could be detected. The adduct that is mentioned the first is the more abundant ion and was used for the confirmation purposes and accurate mass determination. All confirmed compounds in PS₄₉-co-PHCBI₅₁-cryo-milling-hydrolysis and PS₄₉-co-PHCBI₅₁-sonication-hydrolysis were not detected in the reference samples (solvent, blank matrix sample, non-degraded PS₄₉-co-PHCBI₅₁).

As an example, Compound I in ESI⁺ mode is selected here. This compound has two isomers (at RT=7.95 min and RT=8.05 min). Fig. S101 shows a comparative XIC of this compound (*m/z* 589.400) for all five samples analyzed. While no signals can be observed in the solvent, blank matrix and PS₄₉-co-PHCBI₅₁ samples, two species of Compound I can be observed in PS₄₉-co-PHCBI₅₁-cryo-milling-hydrolysis and PS₄₉-co-PHCBI₅₁-sonication-hydrolysis. The corresponding low and high energy

(fragmented) mass spectra of the peaks at retention time 7.95 and 8.05 min are shown in Fig. S108 and S109 with their accurate molecular ion and product ion information, respectively. Compound I isomers were confirmed using the accurate mass information of the protonated precursor ions and compound structure (and elemental composition) was supported by the analysis of the fragment ions and their corresponding mass accuracies. The fragment match functionality of UNIFIT™ was used to match the m/z values of theoretical sub-structures to measured fragment ions in the high energy spectrum function (Fig. S108, S109).

The chromatograms of the target compounds with $m/z > 673$ became very complex due to the presence of numerous isomeric species. Further investigation using fragment ion data is necessary to elucidate the chemical structure of these compounds. The intensity distribution of the observed isomeric species was partly different depending on the sample PS₄₉-co-PHCBI₅₁-cryo-milling-hydrolysis or PS₄₉-co-PHCBI₅₁-sonication-hydrolysis. Some isomeric species could only be partially detected in one or the other sample (e.g. compound 373 or 811). The exact elucidation of the structure is subject of further evaluations.

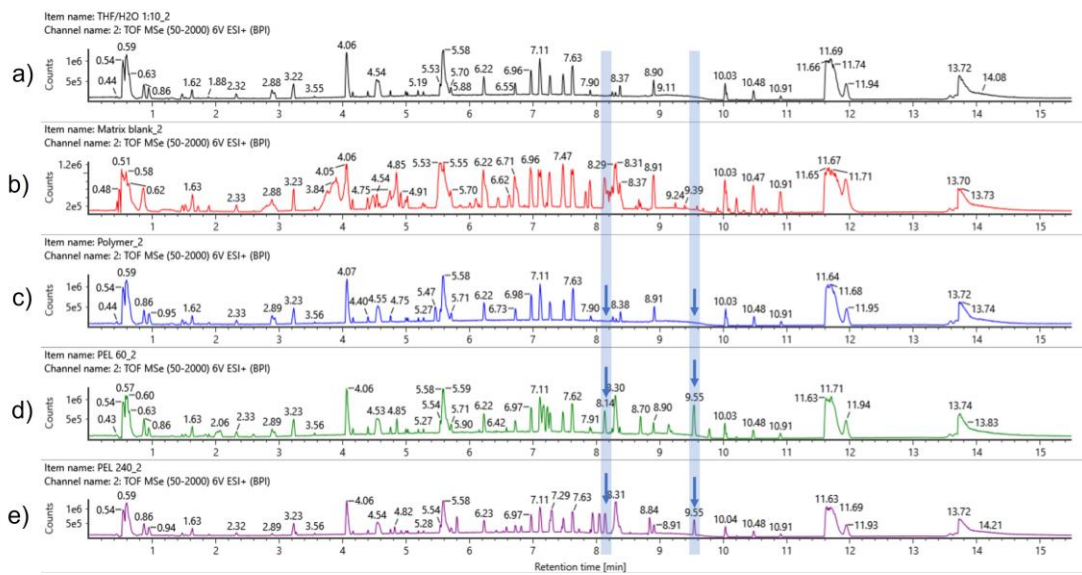


Fig. S105 BPI Chromatograms ESI⁺ mode (a) Solvent (b) Blank Matrix (c) PS₄₉-co-PHCBI₅₁ (d) PS₄₉-co-PHCBI₅₁-cryo-milling-hydrolysis (e) PS₄₉-co-PHCBI₅₁-sonication-hydrolysis. Blue bars with blue arrows indicate a selection of potential target peaks and also possible differences between the samples. Item name THF/H₂O 1:10_2 corresponds to sample solvent; Item name Matrix blank_2 corresponds to blank matrix sample; Item name Polymer_2 corresponds to PS₄₉-co-PHCBI₅₁; Item name PEL 60_2 corresponds to PS₄₉-co-PHCBI₅₁-cryo-milling-hydrolysis; Item name PEL 240_2 corresponds to PS₄₉-co-PHCBI₅₁-sonication-hydrolysis.

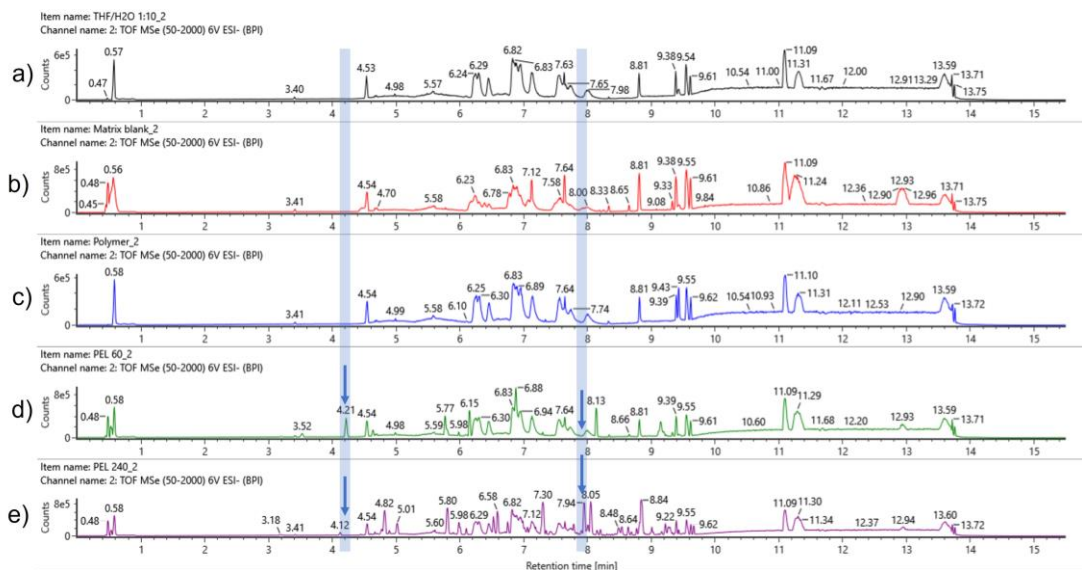


Fig. S106 BPI Chromatograms ESI⁻ mode (a) Solvent (b) Blank Matrix (c) PS₄₉-co-PHCBI₅₁ (d) PS₄₉-co-PHCBI₅₁-cryomilling-hydrolysis (e) PS₄₉-co-PHCBI₅₁-sonication-hydrolysis. Blue bars with blue arrows indicate a selection of potential target peaks and also possible differences between the samples. Item name THF/H₂O 1:10_2 corresponds to sample solvent; Item name Matrix blank_2 corresponds to blank matrix sample; Item name Polymer_2 corresponds to PS₄₉-co-PHCBI₅₁; Item name PEL 60_2 corresponds to PS₄₉-co-PHCBI₅₁-cryo-milling-hydrolysis; Item name PEL 240_2 corresponds to PS₄₉-co-PHCBI₅₁-sonication-hydrolysis.

Table S2 Identification of expected targets in PS₄₉-co-PHCBI₅₁-cryo-milling-hydrolysis, ESI⁻ and ESI⁺ mode. (Compound names correspond to the letter code shown in Fig. S102.)

Compound name	Formula	t _R (min)	Adduct	Theoretical mass (<i>m/z</i>)	Experimental mass (<i>m/z</i>)	Mass accuracy (ppm)
A	C ₁₃ H ₁₉ NO ₅	3.56	[M-H] ⁻	268.1191	268.1189	-0.8
B	C ₁₅ H ₁₄ O ₆	2.66	[M-H] ⁻	289.0718	289.0713	-1.7
C	C ₁₇ H ₁₈ O ₆	4.19	[M-H] ⁻	317.1031	317.1029	-0.6
D	C ₂₁ H ₂₇ NO ₅	4.60	[M-H] ⁻	372.1817	372.1816	-0.2
		4.60	[M+H] ⁺	374.1962	374.1962	±0.0
E	C ₂₃ H ₃₁ NO ₅	5.80	[M-H] ⁻	400.2130	400.2129	-0.2
		5.80	[M+H] ⁺ , [M+Na] ⁺	402.2275	402.2270	-1.2
E	C ₂₃ H ₃₁ NO ₅	5.99	[M-H] ⁻ , [M-H+HCOO] ⁻	400.2130	400.2125	-1.2
		5.99	[M+H] ⁺ , [M+Na] ⁺	424.2094	402.2271	-0.9
G	C ₂₉ H ₄₄ N ₂ O ₄	7.30	[M-H+HCOO] ⁻	529.3283	529.3284	+0.1
		7.30	[M+H] ⁺ , [M+Na] ⁺	485.3374	485.3379	+1.1
I	C ₃₇ H ₅₂ N ₂ O ₄	7.94	[M-H+HCOO] ⁻	633.3909	633.3904	-0.8
		7.94	[M+H] ⁺ , [M+Na] ⁺	589.4000	589.3997	-0.4
I	C ₃₇ H ₅₂ N ₂ O ₄	8.05	[M-H+HCOO] ⁻	633.3909	633.3900	-1.4
		8.05	[M+H] ⁺ , [M+Na] ⁺	589.4000	589.3986	-2.3
K	C ₃₈ H ₄₃ NO ₁₀	6.00	[M-H] ⁻	672.2814	672.2805	-1.3
L	C ₄₀ H ₄₇ NO ₁₀	6.86	[M-H] ⁻	700.3127	700.3120	-1.1
		6.86	[M+H] ⁺ , [M+Na] ⁺	702.3273	702.3257	-2.2
L	C ₄₀ H ₄₇ NO ₁₀	7.01	[M-H] ⁻	700.3127	700.3117	-1.4
N	C ₄₄ H ₅₆ N ₂ O ₉	7.18	[M-H] ⁻	755.3913	755.3893	-2.7
		7.18	[M+H] ⁺ , [M+Na] ⁺	757.4059	757.4044	-2.0
N	C ₄₄ H ₅₆ N ₂ O ₉	7.38	[M-H] ⁻	755.3913	755.3893	-2.7
		7.38	[M+H] ⁺ , [M+Na] ⁺	757.4059	757.4034	-3.3
O	C ₄₆ H ₆₀ N ₂ O ₉	8.01	[M+H] ⁺	785.4372	785.4348	-3.1
O	C ₄₆ H ₆₀ N ₂ O ₉	8.17	[M-H] ⁻	783.4226	783.4205	-2.6
		8.17	[M+H] ⁺ , [M+Na] ⁺	785.4372	785.4351	-2.7
P	C ₄₈ H ₆₅ N ₃ O ₈	8.85	[M+H] ⁺	812.4844	812.4828	-2.0
P	C ₄₈ H ₆₅ N ₃ O ₈	9.08	[M+H] ⁺	812.4844	812.4830	-1.7
Q	C ₅₀ H ₆₉ N ₃ O ₈	8.53	[M+Na] ⁺ , [M+H] ⁺	862.4977	862.4958	-2.2
R	C ₅₂ H ₇₃ N ₃ O ₈	9.14	[M-H+HCOO] ⁻	912.5380	912.5378	-0.2
		9.14	[M+H] ⁺	868.5470	868.5474	+0.4

Table S3 Identification of expected targets in PS₄₉-co-PHCBI₅₁-sonication-hydrolysis, ESI⁻ and ESI⁺ mode. (Compound names correspond to the letter code shown in Fig. S102.)

Compound name	Formula	t _R (min)	Adduct	Theoretical mass (m/z)	Experimental mass (m/z)	Mass accuracy (ppm)
A	C ₁₃ H ₁₉ NO ₅	3.56	[M-H] ⁻	268.1191	268.1187	-1.8
B	C ₁₅ H ₁₄ O ₆	2.66	[M-H] ⁻	289.0718	289.0715	-0.2
D	C ₂₁ H ₂₇ NO ₅	4.82	[M-H] ⁻ , [M-H+HCOO] ⁻	372.1817	372.1815	-0.4
		4.82	[M+H] ⁺ , [M+Na] ⁺	374.1962	374.1968	+1.2
E	C ₂₃ H ₃₁ NO ₅	5.80	[M-H] ⁻	400.2130	400.2131	+0.2
		5.80	[M+H] ⁺ , [M+Na] ⁺	402.2275	402.2280	+1.2
E	C ₂₃ H ₃₁ NO ₅	5.99	[M-H] ⁻ , [M-H+HCOO] ⁻	400.2130	400.2129	-0.2
		5.99	[M+Na] ⁺ , [M+H] ⁺	424.2094	424.2094	-1.6
F	C ₂₇ H ₄₀ N ₂ O ₄	6.53	[M-H] ⁻ , [M-H+HCOO] ⁻	455.2915	455.2917	+0.4
		6.53	[M+H] ⁺ , [M+Na] ⁺	457.3061	457.3062	+0.2
G	C ₂₉ H ₄₄ N ₂ O ₄	7.30	[M-H] ⁻ , [M-H+HCOO] ⁻	529.3283	529.3284	+0.2
		7.30	[M+H] ⁺ , [M+Na] ⁺	485.3374	485.2277	+0.6
H	C ₃₅ H ₄₈ N ₂ O ₄	7.18	[M-H] ⁻	559.3541	559.3545	+0.6
		7.18	[M+H] ⁺ , [M+Na] ⁺	561.3687	561.3681	-1.1
H	C ₃₅ H ₄₈ N ₂ O ₄	7.35	[M-H] ⁻	559.3541	559.3537	-0.7
		7.35	[M+H] ⁺ , [M+Na] ⁺	561.3687	561.3688	+0.2
I	C ₃₇ H ₅₂ N ₂ O ₄	7.94	[M-H+HCOO] ⁻	633.3911	633.3912	+0.3
		7.94	[M+H] ⁺ , [M+Na] ⁺	589.4000	589.4005	+0.9
I	C ₃₇ H ₅₂ N ₂ O ₄	8.05	[M-H+HCOO] ⁻	633.3909	633.3912	+0.5
		8.05	[M+H] ⁺ , [M+Na] ⁺	589.4000	589.4002	+0.4
K	C ₃₈ H ₄₃ NO ₁₀	5.87	[M+H] ⁺ , [M+Na] ⁺	674.2960	674.2948	-1.7
K	C ₃₈ H ₄₃ NO ₁₀	6.00	[M-H] ⁻	672.2814	672.2801	-1.9
		6.00	[M+H] ⁺	674.2960	674.2955	-0.7
L	C ₄₀ H ₄₇ NO ₁₀	6.86	[M-H] ⁻	700.3127	700.3122	-0.7
		6.86	[M+H] ⁺ , [M+Na] ⁺	702.3273	702.3264	-1.2
L	C ₄₀ H ₄₇ NO ₁₀	7.01	[M-H] ⁻	700.3127	700.3125	-0.3
		7.01	[M+H] ⁺ , [M+Na] ⁺	702.3273	702.3268	-0.6
M	C ₄₂ H ₅₂ N ₂ O ₉	6.61	[M-H] ⁻	727.3600	727.3594	-0.7
		6.61	[M+H] ⁺ , [M+Na] ⁺	729.3746	729.3734	-1.6
M	C ₄₂ H ₅₂ N ₂ O ₉	6.76	[M-H] ⁻	727.3600	727.3596	-0.6
		6.76	[M+H] ⁺ , [M+Na] ⁺	729.3746	729.3736	-1.3
N	C ₄₄ H ₅₆ N ₂ O ₉	7.18	[M-H] ⁻	755.3913	755.3910	-0.4
		7.18	[M+H] ⁺ , [M+Na] ⁺	757.4059	757.4054	-0.6
N	C ₄₄ H ₅₆ N ₂ O ₉	7.38	[M-H] ⁻	755.3913	755.3909	-0.6
		7.38	[M+H] ⁺ , [M+Na] ⁺	757.4059	757.4046	-1.7
O	C ₄₆ H ₆₀ N ₂ O ₉	7.90	[M-H] ⁻	783.4226	783.4227	+0.1
		7.90	[M+H] ⁺ , [M+Na] ⁺	785.4372	785.4367	-0.6
O	C ₄₆ H ₆₀ N ₂ O ₉	8.01	[M-H] ⁻	783.4226	783.4225	-0.1
		8.01	[M+H] ⁺ , [M+Na] ⁺	785.4372	785.4370	-0.2
O	C ₄₆ H ₆₀ N ₂ O ₉	8.17	[M-H] ⁻	783.4226	783.4230	+0.5
		8.17	[M+H] ⁺ , [M+Na] ⁺	785.4372	785.4361	-1.4
P	C ₄₈ H ₆₅ N ₃ O ₈	7.80	[M-H] ⁻	810.4699	810.4693	-0.8
		7.80	[M+H] ⁺	812.4844	812.4831	-1.6
P	C ₄₈ H ₆₅ N ₃ O ₈	8.15	[M-H] ⁻	810.4699	810.4703	+0.5
		8.15	[M+H] ⁺ , [M+Na] ⁺	812.4844	812.4823	-2.5
Q	C ₅₀ H ₆₉ N ₃ O ₈	8.20	[M-H] ⁻	838.5012	838.5017	+0.6
		8.20	[M+H] ⁺	840.5157	840.5151	-0.8
Q	C ₅₀ H ₆₉ N ₃ O ₈	8.53	[M-H] ⁻	838.5012	838.5013	+0.1
		8.53	[M+H] ⁺ , [M+Na] ⁺	840.5157	840.5149	-0.9
R	C ₅₂ H ₇₃ N ₃ O ₈	8.84	[M-H+HCOO] ⁻	912.5380	912.5378	-0.2
		8.84	[M+Na] ⁺	890.5290	890.5285	-0.6
R	C ₅₂ H ₇₃ N ₃ O ₈	9.14	[M+H] ⁺ , [M+Na] ⁺	868.5470	868.5486	+1.9

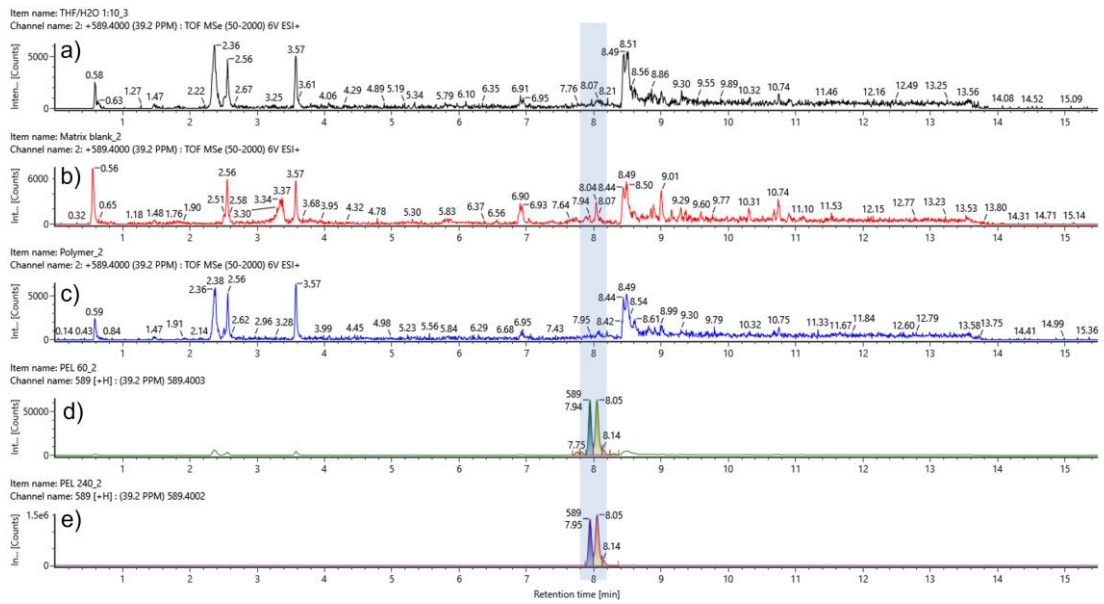


Fig. S107 XIC m/z 589.4000 of Compound I; ESI+ mode; (a) Solvent (b) Blank Matrix (c) PS₄₉-co-PHCBI₅₁; observed two isomers at RT=7.95 and RT=8.05 min in (d) PS₄₉-co-PHCBI₅₁-cryo-milling-hydrolysis and (e) PS₄₉-co-PHCBI₅₁-sonication-hydrolysis. The y-achsis (Intensity [counts]) is not linked. Item name THF/H₂O 1:10_3 corresponds to sample solvent; Item name Matrix blank_2 corresponds to blank matrix sample; Item name Polymer_2 corresponds to PS₄₉-co-PHCBI₅₁; Item name PEL 60_2 corresponds to PS₄₉-co-PHCBI₅₁-cryo-milling-hydrolysis; Item name PEL 240_2 corresponds to PS₄₉-co-PHCBI₅₁-sonication-hydrolysis.

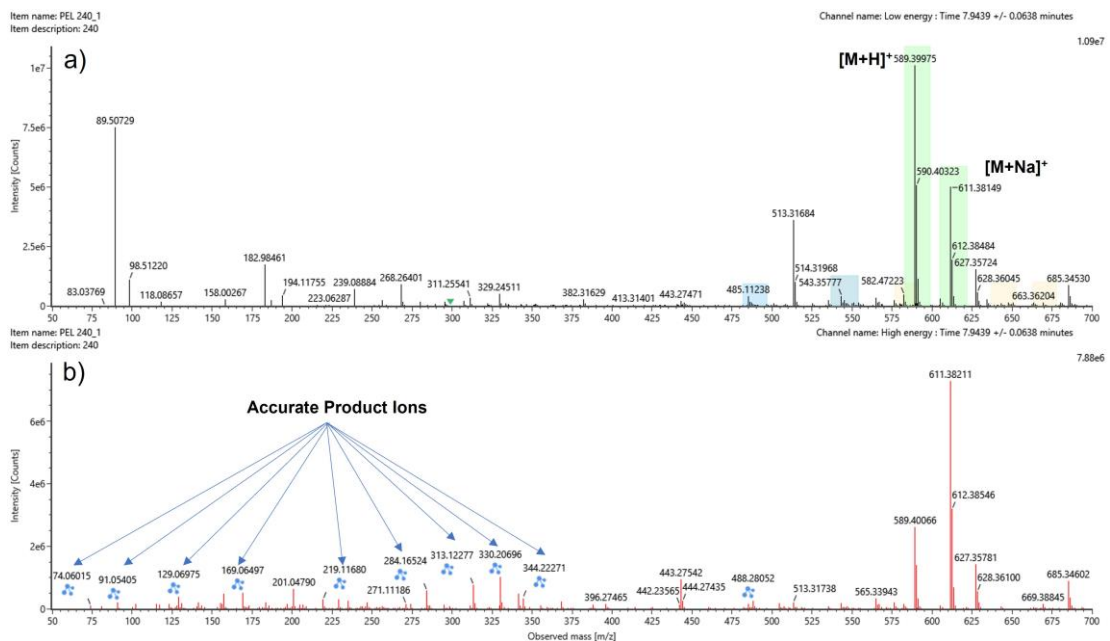


Fig. S108 (a) Low and (b) high energy mass spectra of Compound I at RT=7.95 min; PS₄₉-co-PHCBI₅₁-sonication-hydrolysis. Item name PEL 240_1 corresponds to PS₄₉-co-PHCBI₅₁-sonication-hydrolysis. Blue icons indicate matched product ions in the high-energy spectrum.

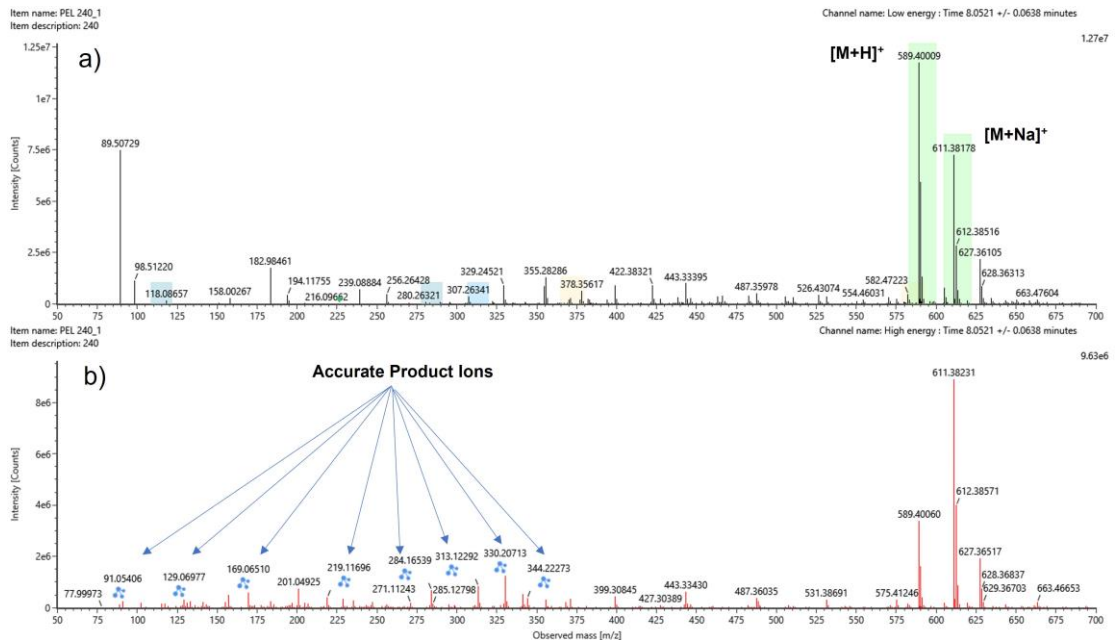


Fig. S109 (a) Low and (b) high energy mass spectra of Compound I at RT=8.05 min; PS₄₉-co-PHCBI₅₁-sonication-hydrolysis. Item name PEL 240_1 corresponds to PS₄₉-co-PHCBI₅₁-sonication-hydrolysis. Blue icons indicate matched product ions in the high-energy spectrum.

CoGEF Calculation

In order to shed some further light onto the degradation mechanism of PS-*co*-PCBI copolymers under influence of mechanical stress, a detailed computational study was carried out using the constrained geometries simulate external force (CoGEF) method¹⁰⁻¹² as well as unrestrained DFT calculations similar to previous reports¹³⁻¹⁷. The CoGEF method yields bond ruptures (chemical transitions) under the influence of strain applied to the chain model. These can be different from "relaxed" TS that occur in unconstrained systems. However, these bond rupture points represent "transition states" (though strained ones) that formally meet the criteria for a TS, namely the first derivative of the energy with respect to the nuclear coordinates vanishes (becomes zero), and the energy along this intrinsic reaction coordinate (IRC) is a maximum. As TS in constrained and relaxed calculations can differ, the "true" and fully relaxed transition states (in the traditional sense of a TS) for the models under consideration were located by DFT calculations.

The CoGEF method was employed on models containing a central MCBI unit, flanked on each side by single styrene moieties, and terminated on both ends by methyl groups to be used as pulling positions. For computational efficiency, MCBI and not HCBI was applied in the *in-silico* models. As the individual degradation pathway may depend on the specific stereochemical arrangement of the chain models on both side of the MCBI unit, four different diastereomeric models **cis/trans-1/2** were analyzed (Fig. S110a). Here *cis*- and *trans*-descriptors refer to the relative arrangement of the styrene units (propagating chains) on the central cyclobutene ring, and the numbering 1 and 2 refers

to the orientation of the five-membered cycloimide ring. In each case, CoGEF analysis was started from fully density functional theory (DFT) optimized molecular geometries (B3LYP/6-31G(d)) with end-to-end separations d between $d \approx 4.5$ (*cis*) and $d \approx 5.5$ Å (*trans*).

The mechanical stress (pulling force) was simulated by constraining and gradually increasing the end-to-end distance between the terminal methyl groups in steps of 0.05 Å at the same level of theory (Fig. S110b), whilst optimizing all other internal coordinates at each point. With increasing stress, some low-barrier and low-force initial conformational changes between $d \approx 5.8$ Å led to extended molecular models. Notably, with increasing mechanical stress in particular the cyclobutane C-C-bond located in the polymer chain underwent significant elongation. Thus, it became apparent at an early stage of the analysis that diradical species had to be expected along the degradation pathway, and all simulations after the last conformational transitions ($d \approx 8.5$ Å) were continued on an unrestricted open-shell level of theory (UB3LYP/6-31G(d)). The DFT calculations with an unrestricted UB3LYP functional may yield heterolytic or homolytic bond ruptures, while a restricted (closed shell) RB3LYP DFT calculation can only yield heterolytic bond cleavage and will never locate radical or diradical transition states as it forces electrons always to be paired.

All models examined – with exception of *trans*-2, which underwent a C-C-chain break event and the loss of a styrene unit – displayed the formation of a diradical species through rupture of the cyclobutane ring upon increasing stress (transition state TS1 in Figs. S110 and S111). Note that the energies plotted in Fig. S110 do not visualize real “transitions states”, but only show the gradually increasing electronic energy of the systems upon action of the pulling constraint. Bond breakage is characterized by a gradual and continuous increase of the corresponding C-C separation from an equilibrium bond length of ≈ 1.59 Å to ≈ 2.0 Å without a sharp energy step (Fig. S110b, grey shaded area) during formation of the singlet diradical species (the reverse process would be an essentially barrier-free diradical recombination process with a very early transition state, hence the missing distinct energy jumps).

Increasing the end-to-end pulling force even further absorbs energy by radical separation ($d_{C-C} > 3.0$ Å) and elongation of the second cyclobutane C-C-bond, the transition between both bond elongation regimes is marked by a characteristic kink in the energy plots (Fig. S110b, end of grey shaded area). As the effective force acting on the polymer models corresponds to the first derivative $\partial E / \partial d$ of the DFT self-consistent field (SCF) electronic energy E with respect to end-to-end distance d , Fig. 110c displays a maximum at the point where diradical formation along transition TS1 (Fig. S111) is observed.

Two different reaction pathways are conceivable in the further course of the chain degradation profile: *cis*-1 and *trans*-1 both undergo direct cleavage of the second C-C bond and ring opening along TS2 (Fig. S111), accompanied by formation of two double bonds. Molecular geometries before and after rearrangement, as well as inherent strain energies of the species involved are visualized in Fig. S112, and some characteristic

parameters are listed in Table S4. A “true” transition state TS2[†] for the final cyclobutane ring opening of *cis*-1 is shown in Fig. S113. In contrast, *cis*-2 displays a rearrangement and radical recombination via the carbonyl group of the ethyl ester, furnishing a cyclic ketene acetal derivative (TS3 in Fig. S111). This formal cyclobutane → pyran ring expansion releases strain, and in the case of *cis*-2 was preferred due to a favorable orientation of the ester group. Though in principle this 3,4-dihydro-2*H*-pyran intermediate could be imagined to transform via a hetero retro-Diels Alder reaction (TS4 in Fig. S111) into the same cyclobutane degradation product as before, this was not observed here. Due to the unfavorable direction of the pulling vector (see Figs. S111 and S112) relative to a putative Diels-Alder transition state, a final C-C chain break (loss of a terminal methyl group) is observed in the case of *cis*-2 at high energies and forces (Fig. S110b,c; rightmost points of the blue curves marked by an asterisk). A ring opening of the cyclobutane units through a concerted [2π+2π] cycloreversion process (TS5) was not observed in any case.

In summary, the CoGEF analysis of the PS_x-co-PMCBI_y polymer models reveal that all rearrangements did proceed via initial diradical formation. Though in principle, conrotatory thermally allowed [2+2]-cycloreversions (TS5 in Fig. S111) or strain-induced disrotatory (thermally forbidden) ring openings are conceivable,¹⁸⁻¹⁹ the corresponding processes were not observed here.

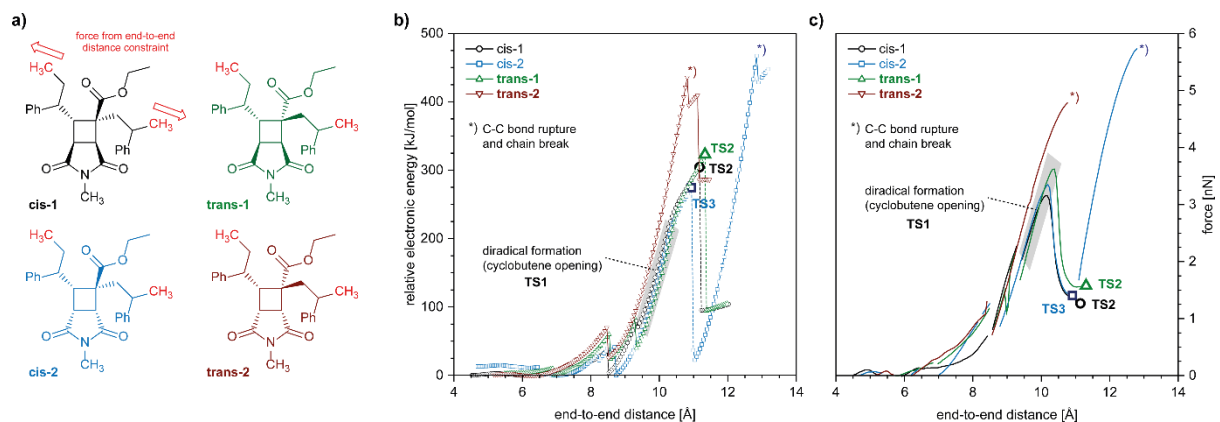


Fig. S110 (a) Different diastereomeric PS-*co*-PMCB1 polymer models used for the CoGEF analysis of the degradation mechanism. (b) CoGEF energy profiles (DFT UB3LYP/6-31G(d)) as a function of the constrained end-to-end distances between terminal methyl groups. Characteristic reaction transitions (TS1-3) are marked by bold symbols, and characteristics of the corresponding molecular geometries are listed in Table S4; points marked by asterisks correspond to chain break events through C-C bond rupture. (c) Plot of the effective forces originating from chain elongation constraints (first derivative $\partial E / \partial d$ of plot b); curve segments of negative forces (strain releasing conformational transitions and reaction events) are not plotted for clarity (gaps in curves).

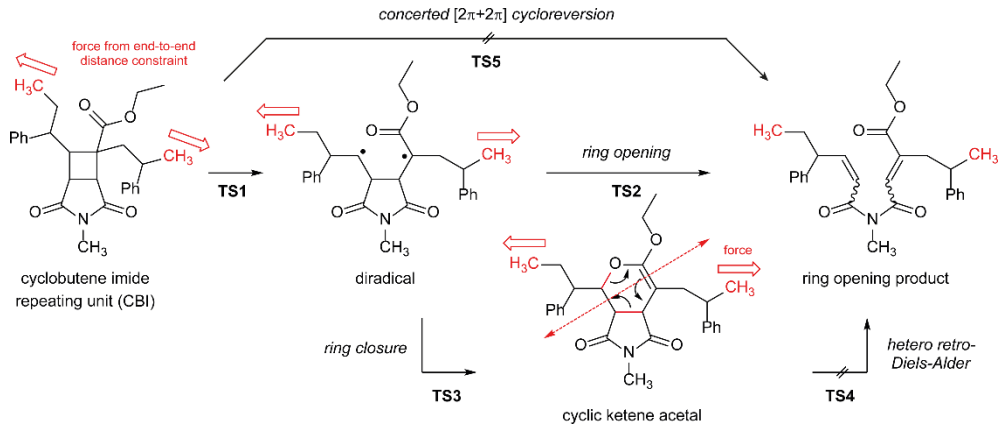


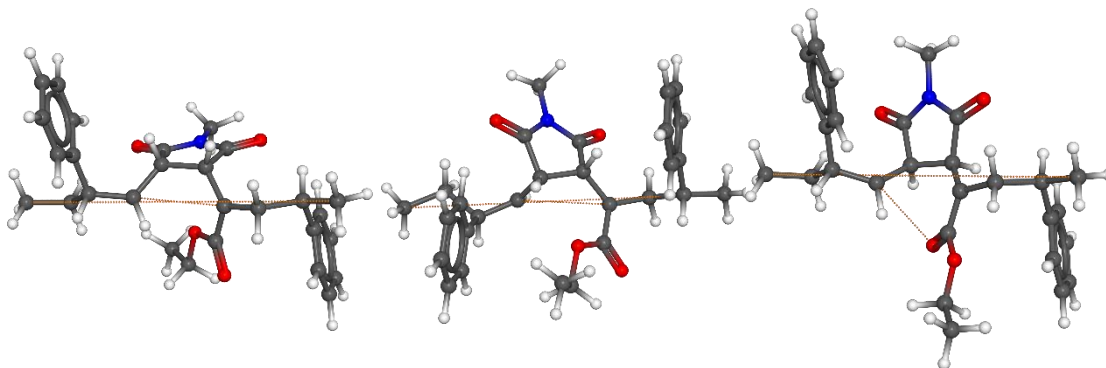
Fig. S111 Reaction and conceivable degradation pathways (labelled TS1-5) emerging from the CoGEF analysis of PS-*co*-PMCBI polymer models (Fig. S110). In the lower formula, the misalignment of the vector of strain with the force direction required to initiate retro-Diels-Alder ring opening (dashed arrow) is indicated.

Table S4. Characteristics of the CoGEF analysis on the degradation mechanism of different diastereomeric of PS-*co*-PMCBI polymer models, c.f. Figs. S110 and S111 (reaction pathways TS1-3), molecular structures are plotted in Fig. S112.

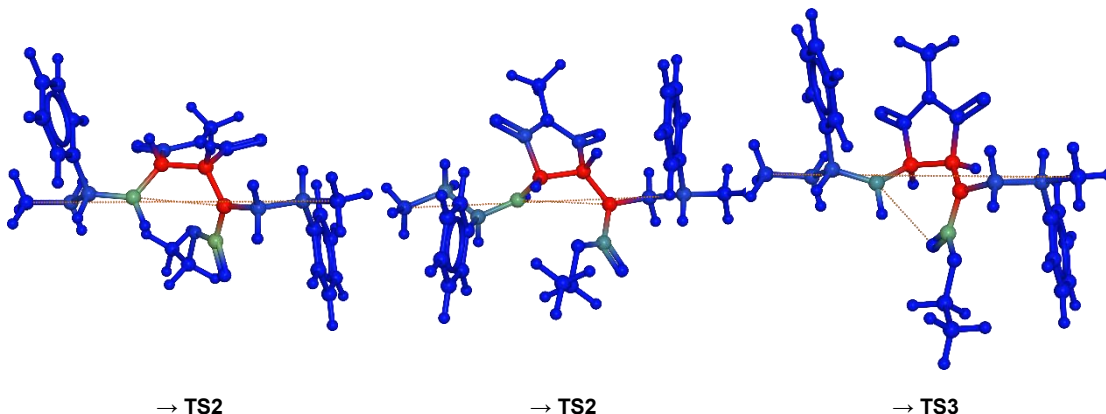
config. ^[a]	d ^[b] [Å]	d _{C-C} ^[c] [Å]	F _{max} [nN]	d ^[b] [Å]	d _{C-C} ^[c] [Å]	ΔE _{max} [kJ/mol]	remark ^[d]
cis-1	10.176	1.955	3.2	11.176	3.173	304.2	→TS2
cis-2	10.243	1.949	3.3	10.943	2.953	274.3	→TS3
trans-1	10.383	1.963	3.6	11.333	3.270	322.7	→TS2
trans-2	10.765	1.779	4.8	10.815	[e]	435.6	[e]

[a] initial configuration cf. Fig. S1a. [b] end-to-end (methyl-methyl) distance at F_{max} or ΔE_{max}. [c] C-C distance between radical positions at F_{max} or ΔE_{max}. [d] reaction transition c.f. Fig. S111. [e] chain break.

a) molecular structures (diradicals) before cyclobutane rearrangement (cleavage of the second C-C-bond):



b) relative distribution of strain energy:



c) final products of cyclobutane rearrangement:

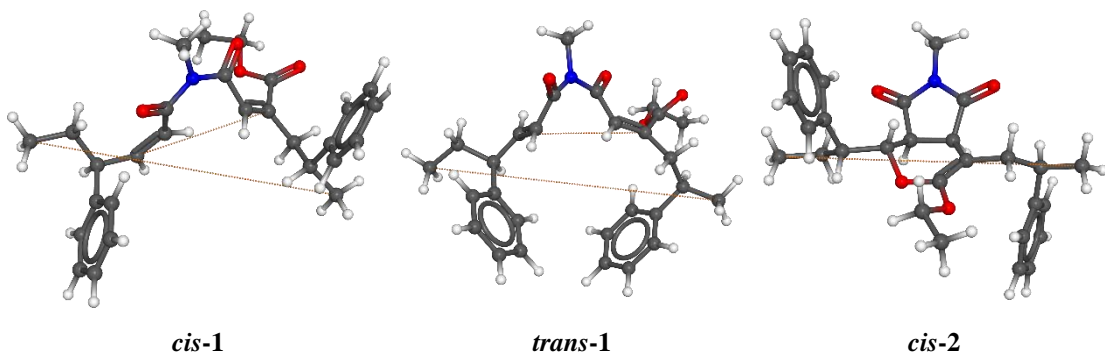


Fig. S112 Molecular structures of PS-*co*-PMcB1 polymer models obtained from CoGEF analysis. (a) Molecular structures of the diradicals before rearrangement at the points labelled TS2/3 in Fig. S110c. The dashed orange lines display the strain vector from constrained end-to-end distances, and relevant C···C or C···O vectors for the observed rearrangements. (b) Relative strain-energy mapped onto atomic positions of structures shown in the top row (blue: low strain, red: high strain). (c) Molecular structures of final CoGEF reaction products. Note that the rearrangement of both models *cis*-1 and *trans*-1 (left and center column) proceeds via pathway TS2 (cf. Fig. S111), whereas for *cis*-2 the formation of a pyran ring (right column, TS3) was computed.

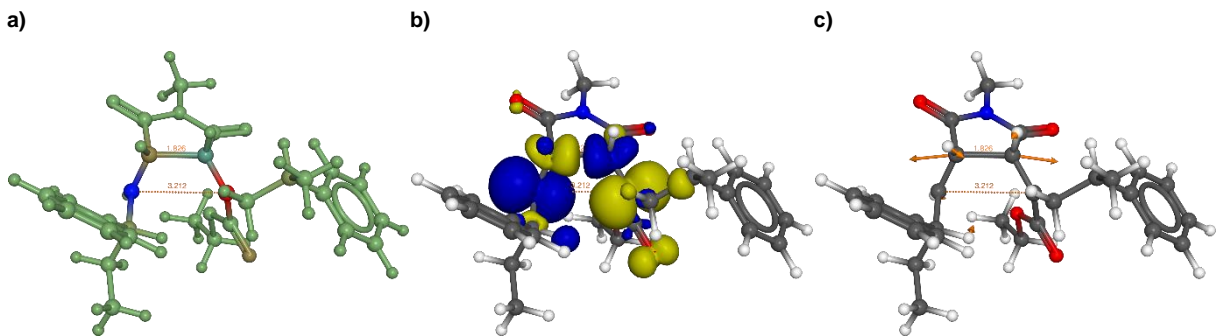


Fig. S113 True transition state computed for the model *cis*-**1** and the cyclobutane ring opening TS2^\ddagger process c.f. Fig. S111. The molecular model was obtained from a separate unconstrained DFT simulation (UB3LYP/6-31G(d)). (a) Molecular model with Mulliken spin densities mapped onto atomic positions of this singlet diradical species. The blue and red carbon atoms correspond to the two radical positions that emerged from the first (completed) C-C-bond rupture with a C-C separation of 3.212 Å. The second cyclobutane bond is elongated to 1.826 Å in this transition state, indicating imminent bond rupture to complete the cyclobutane ring opening. (b) Iso-contour plot of the spin density (difference of electron density for α and β electrons plotted as blue and yellow surfaces) for the transitions state TS2^\ddagger . (c) Atomic displacement vectors (scaled by a factor 2.5 for visualization) corresponding to the single negative (imaginary) vibrational eigenvalue of the transition state ($\tilde{\nu} = -601.7 \text{ cm}^{-1}$). The large orange vectors associated with the single C-C-bond indicate bond rupture along the intrinsic reaction coordinate (IRC) of this transition state.

The above considerations on the degradation mechanism are further supported by the “true” relaxed electronic transition states identified from unrestrained DFT calculations (Figs. S113-S116). In contrast to the above CoGEF-derived strain-induced transition states of debonding (labeled TS1-5), these relaxed TS (labeled TS1-5^\ddagger) were computed without additional constraints applied to the polymer chain. Thus, TS1-5^\ddagger represent the “natural” intrinsic reaction pathways that are plausible for the corresponding molecular models, and these models have been included here for the sake of completeness of the computational study. In combination with the energy profiles along the various intrinsic reaction coordinates shown in Figs. S114-S116, these TS yield a concise picture of possible reaction pathways that additionally supports the CoGEF analysis described above. The stepwise process (TS1^\ddagger and TS2^\ddagger) involving successive bond breakage (first C1 C2 and then C3 C4) and a diradical type intermediate is the most favorable mechanism (Fig. S116), while the concerted ring opening through [2+2] cycloreversion (TS5^\ddagger) is disfavored.

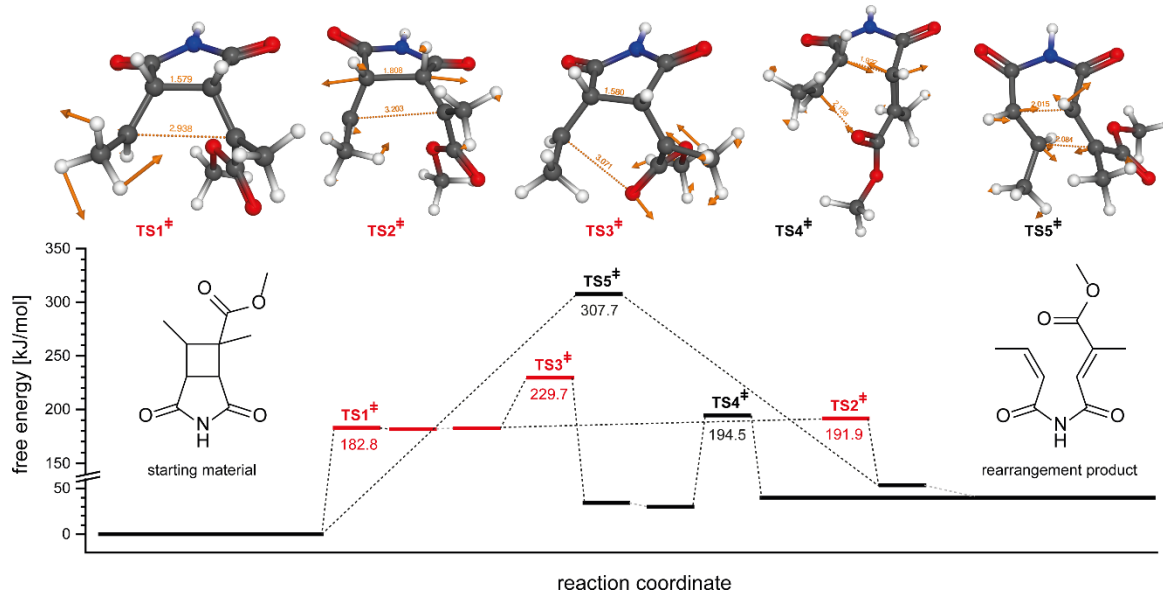


Fig. S114 True transition states and free energy profile computed for a simplified molecular model as shown and the processes TS1-5 cf. Fig. S111 (DFT UB3LYP/6-31G(d), including thermal vibrational corrections for $T=298.15$ K). The dashed lines connect the transition states with forward and reverse reaction products identified from intrinsic reaction coordinate (IRC) analysis following the corresponding eigenvectors in forward and reverse direction, free energies of activation (ΔG^\ddagger) are given in [kJ/mol]. Molecular models of the transition states $TS1-5^\ddagger$ are plotted with atomic displacement vectors (scaled by a factor 2.5 for visualization) corresponding to the single negative (imaginary) vibrational eigenvalue of each TS; these vectors define the IRC for each process. Note that for $TS1^\ddagger$ this seems to imply a methyl rotation, but in fact is the process of diradical formation that in reverse corresponds to the TS of radical recombination with a very shallow barrier of activation ($\Delta G^\ddagger=1.0$ kJ/mol, $\tilde{\nu} = -89.3$ cm $^{-1}$). Red labels correspond to singlet diradical species, closed-shell TS are labeled in black.

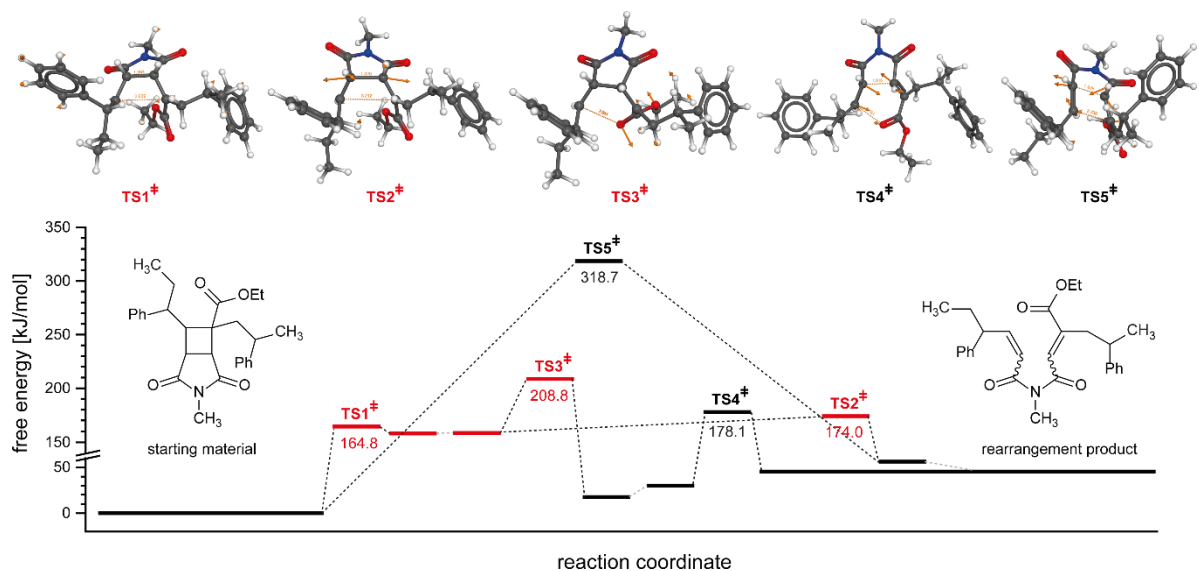


Fig. S115 True transition states and free energy profile computed for the polymer model *cis*-1 and the processes TS1-5 cf. Fig. S111 (DFT UB3LYP/6-31G(d), including thermal vibrational corrections for $T=298.15$ K). The dashed lines connect the transition states with forward and reverse reaction products

identified from intrinsic reaction coordinate (IRC) analysis following the corresponding eigenvectors in forward and reverse direction, free energies of activation (ΔG^\ddagger) are given in [kJ/mol]. Molecular models of the transition states TS1-5[‡] are plotted with atomic displacement vectors (scaled by a factor 2.5 for visualization) corresponding to the single negative (imaginary) vibrational eigenvalue of each TS; these vectors define the IRC for each process. Red labels correspond to singlet diradical species, closed-shell TS are labeled in black.

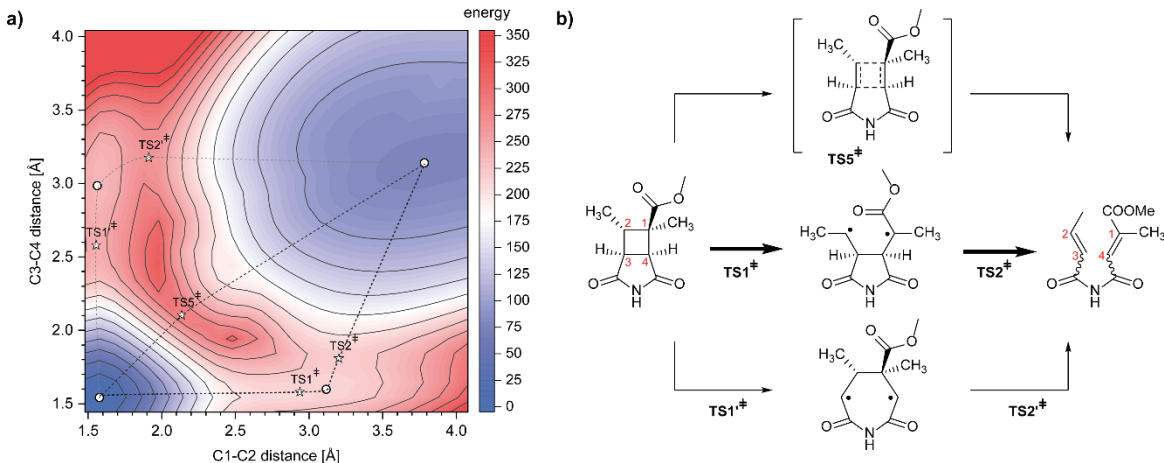


Fig. S116 (a) Adiabatic potential energy surface (PES, DFT UB3LYP/6-31G(d)) electronic energies of the simplified molecular model plotted as a 2D-function of the cyclobutane C1-C2 and C3-C4 separations. (b) Reaction scheme with plausible transition pathways for the cyclobutane ring opening. The transition states are marked in plot a) by asterisks, the corresponding intrinsic reaction coordinates (IRC) are indicated by dashed lines connecting the transition states with the relaxed molecular geometries of the starting material and the product (solid circles), respectively. The concerted ring opening through [2+2] cycloreversion (TS5[‡]) is disfavored over the stepwise process (TS1[‡] and TS2[‡]) involving successive bond breakage (first C1-C2 and then C3-C4) and a diradical type intermediate. The latter is located at a broad high energy plateau of the PES, with very shallow forward and reversion energy barriers of reaction. On the potential energy surface, the process with the reverse order of bond cleavage (first C3-C4 and then C1-C2, TS1[‡] and TS2[‡]) can be identified, but was not observed in the CoGEF analysis of the polymer models (mismatching mode of stress excerpted from external forces).

Computational Methods

Quantum chemical DFT calculations were carried out using the *Gaussian09* program package²⁰ Unless stated otherwise, calculations were carried out at the unrestricted UB3LYP/6-31G(d) level of theory. All optimized stationary molecular structures were verified by vibrational analysis, and all transition states (TS, first order saddle points) are characterized by exactly one negative (imaginary) vibrational mode. Transition states were located using the quadratic synchronous transit method (QST3) as implemented in Gaussian,²¹⁻²² and all TS were additionally confirmed by visual inspection of the imaginary vibrational mode as well as by intrinsic reaction coordinate (IRC) calculations. Energies reported here are given relative to the most stable conformers of the reactants, all energies were calculated using the harmonic oscillator

approximation. Enthalpies (ΔH) and free energies (ΔG) including zero-point correction, temperature correction, and vibrational energy were computed for standard conditions ($T = 298.15$ K, $P = 1.0$ atm) using unscaled vibrational frequencies. Plots and atomic coordinates of all molecular structures are given in the Tables below.

CoGEF Analysis

For all structures along the stretching trajectory of the mechanophores, the total SCF electronic energy $E_{total}(d)$ (DFT UB3LYP/6-31G(d)) was computed as a function of an end-to-end constraint d applied to each molecular geometry:

$$E_{total}(d) = E_{SCF}(d) - E_{SCF}(d_0),$$

where d_0 was the equilibrium end-to-end distance of a fully optimized structure of the mechanophore unit, and $E(d_0)$ was the corresponding global minimum SCF energy. The distance constraint d was increased in steps of 0.05 Å. At each step, a full SCF geometry optimization of all other internal coordinates was carried out. Relative electronic energies (in [kJ mol⁻¹]) were then plotted as a function of the end-to-end distance (in [Å]); the resulting forces (in [nN]) were computed from the partial derivative $\partial E_{total}/\partial d$.

As DFT calculations do not yield split terms of energy on bond length or angle deformations,²³ an *ad hoc* chosen geometry-based mapping of strain-energies onto atomic positions was used. For this, classical harmonic potentials were assumed for both types of deformations:

$$E_{bonds}(d) = \frac{1}{2} K_{bonds} \sum_{bonds} (r - r_0)^2 = \frac{1}{2} K_{bonds} \sum_{bonds} \Delta r^2$$

$$E_{angles}(d) = \frac{1}{2} K_{angles} \sum_{angles} (\alpha - \alpha_0)^2 = \frac{1}{2} K_{angles} \sum_{angles} \Delta \alpha^2$$

where $\Delta r = r - r_0$ and $\Delta \alpha = \alpha - \alpha_0$ are the deformations of all distance and angle parameters relative to the equilibrium (energy minimum) molecular geometry, respectively. Setting

$$E_{total}(d) = E_{bonds}(d) + E_{angles}(d),$$

and choosing the “force constants” K_{bonds} and K_{angles} from:

$$K_{bonds} = E_{total}(d) / \sum_{bonds} (r - r_0)^2$$

$$K_{angles} = E_{total}(d) / \sum_{angles} (\alpha - \alpha_0)^2$$

implies that:

$$E_{bonds}(d) = E_{angles}(d) = \frac{1}{2}E_{total}(d).$$

Note that this ensures an “equipartition” of bond length and angle deformation energies irrespective of the different orders of magnitude of the Δr and $\Delta\alpha$ terms, which is kind of intuitive: higher strain set on bonds will induce angle deformations, and vice versa, until all contributions are equally distributed. With these purely empirical “force constants” K_{bonds} and K_{angles} , individual deformations Δr and $\Delta\alpha$ can now be mapped onto individual atomic positions i :

$$E_i(d) = \frac{1}{4}K_{bonds} \sum \Delta d^2 + \frac{1}{2}K_{angles} \sum \Delta\alpha^2$$

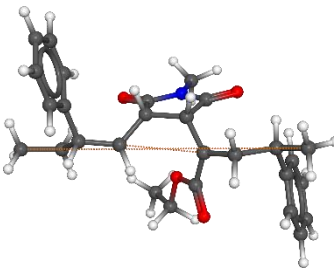
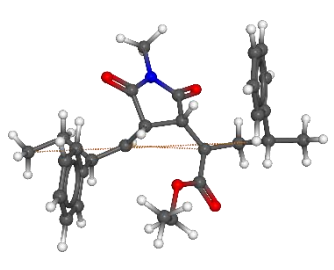
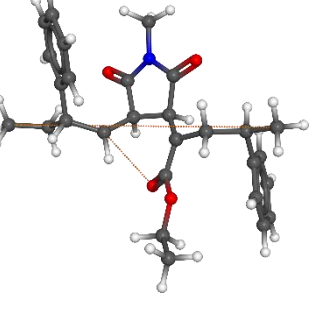
where the sums now run only over all bonds and angles a specific atom is associated with. Note that an additional pre-factor $\frac{1}{2}$ is required on distance violations due to two atoms being involved in each bond, whereas angle deformations are associated with a single central atom only. This definition implies that the total electronic energy of each molecular geometry is also simply the sum of all atomic contributions:

$$E_{total}(d) = \sum_{atoms} E_i(d)$$

Atomic deformation energies were then mapped onto the individual atoms using a 16-color code ranging from blue (low strain) to red (highest strain).

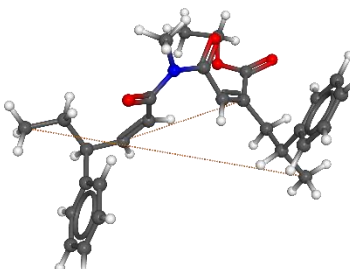
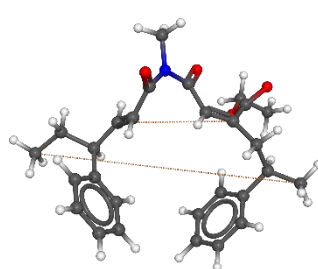
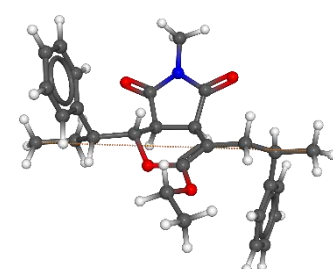
The following tables provide structure plots and atomic coordinates for all characteristic molecular geometries identified from CoGEF analysis (Tables S5a-b) of the polymer models, including all relaxed transition states computed (Tables S6a-e and S7a-e).

Table S5a Molecular structures and atomic coordinates (in Å) obtained from the CoGEF analysis of the polymer models just before final rupture of the cyclobutane ring is observed. The dotted orange lines in the structure plots connect the characteristics radical positions involved in the rearrangements, respectively, as well as the terminal methyl groups of the models that were used as constrained “pulling points” in the CoGEF analysis.

<i>cis</i> -1	<i>trans</i> -1	<i>cis</i> -2
 C -3.62998551 -2.03536362 4.20713178 C -2.48878428 -1.47143883 3.30645048 C -2.87416735 -1.18774081 1.78958815 C -3.49165018 -2.40915580 1.10308042 C -4.68839634 -2.25601796 0.38932093 C -2.90103503 -3.68108892 1.15132467 C -5.28656112 -3.33996770 -0.25570795 C -3.49737801 -4.76550075 0.50455202 C -4.69165850 -4.60064019 -0.19986256 C -1.80459176 -0.51903200 0.93572908 C -0.06427636 1.01557473 -1.22916194 C -0.83743716 -1.22951599 0.04611959 C -0.05821707 -0.49413906 -1.10080038 C 0.26076866 -1.99518564 0.83996188 C 1.36846645 -0.17557297 -0.99216709 O 0.13827269 -2.64601679 1.85948620 O 2.29130572 -0.91889299 -1.76449589 N 1.45349250 -1.86111013 0.15746991 C 2.68812886 -2.49337745 0.60470941 C 0.06333983 1.85109302 -0.07028813 O -0.09161092 3.06758623 -0.00720526 O 0.40653418 1.10834345 1.06100326 C 0.65770703 1.89063560 2.24514542 C 1.18914305 0.95601625 3.31670739 C -0.00720494 1.69213418 -2.58770455 C 1.42453298 1.92771389 -3.24782116 C 2.35600324 2.75285768 -2.36869311 C 2.09053831 4.09966621 -2.08029091 C 3.53379648 2.18871133 -1.86011926 C 4.42393460 2.94679826 -1.09528705 C 2.97536250 4.85988782 -3.17120458 C 4.14959246 4.28693709 -0.82321816 C 1.34974467 5.55824477 -4.68080686 H -3.25390135 -2.14214850 5.22993900 H -4.49600316 -1.36327325 4.23054866 H -3.96870084 -3.01576510 3.86005572 H -1.63501986 -2.15143197 3.32088608 H -2.13766428 -0.52129200 3.72784396 H -3.66784019 -0.42841331 1.85009293 H -5.16003491 -2.27680319 0.34067743 H -1.96985787 -3.82132266 1.69123454 H -6.21667100 -3.19740078 -0.79959316 H -3.02709308 -5.74415585 0.55626504 H -5.15431648 -5.44744338 -0.69953979 H -1.83153301 0.55991314 0.88533108 H -1.39616890 -0.23119947 -0.46462869 H -0.44693431 -0.88706251 -2.04965839 H 2.47876728 -3.52001206 0.91176283 H 3.38871022 -2.47366647 -0.23044590 H 3.11066599 -1.94751702 1.45375911 H 1.37429865 2.67885136 1.99491231 H -0.26969611 2.38552158 2.55521376 H 2.13320975 0.49873408 3.00201589 H 1.37160877 1.51406935 4.24183336 H 0.47560319 0.15331704 3.53091835 H -0.59271898 1.10882723 -3.31267824 H -0.49266271 2.66973283 -2.48144963	 C -5.66610914 -1.48106696 0.72636013 C -4.11809981 -1.70520182 0.65070941 C -3.17799967 -0.43955747 0.93772655 C -3.56779152 0.73371576 0.04718515 C -4.07099740 1.90485135 0.62982186 C -3.50942658 0.65824934 -1.35385110 C -4.50185371 2.97545559 -0.15626692 C -3.93409383 1.73063787 -2.14115715 C -4.43365679 2.89165175 -1.54737666 C -1.69452744 -0.77710926 0.98293464 C 1.42168841 0.15735929 1.30249171 C -0.70121950 -0.61959299 -0.12461457 C 0.79929580 -0.74691559 0.27484897 C -0.88302700 -1.94244075 -0.94677613 C 0.93130240 -2.28057457 0.46498262 O -1.70020230 -2.17426588 -0.81660688 O 1.71895200 -2.92056244 1.12626441 N 0.00883123 -2.86196121 -0.41293177 C 0.02720315 -4.27526830 -0.75519814 C 0.88394914 1.45902632 1.67687656 O 1.27031207 2.08684895 2.65919004 O -0.00929340 1.98542494 0.77965737 C -0.57112561 3.27359425 1.09886087 C -0.78966964 4.03043371 -0.19976950 C 2.86133913 -0.06887138 1.76009270 C 3.99424110 0.75513648 1.00129962 C 4.04455781 0.37769556 -0.47182845 C 4.45309628 -0.90198136 -0.88330018 C 3.66845753 1.29714514 -1.46094863 C 3.70032220 0.95653112 -2.81558165 C 4.48784878 -1.24640992 -2.23462067 C 4.11151934 -0.31742437 -3.20803029 C 5.42351625 0.66130323 1.65392632 H -6.16857665 -2.43793727 0.55151550 H -5.97067935 -1.10812961 1.71114523 H -6.00327905 -0.76760858 -0.03069413 H -3.86181930 -2.09180276 -0.34063336 H -3.83812640 -2.48381737 1.37214452 H -3.42091038 -0.15526831 1.97499918 H -4.13524080 -1.97652527 1.71361672 H -3.13488973 -0.24424782 -1.83281012 H -4.89328842 3.87088240 3.01935742 H -3.87993971 1.65319273 -3.22401691 H -4.76974691 3.72135559 -2.16353684 H -1.41400851 -1.47022517 1.77582929 H -0.91525507 -0.24498734 -0.74910932 H 1.39453259 -0.63060260 -0.65764139 H -0.82727294 -4.47014784 -1.40448922 H 0.95410658 -4.53099646 -1.27731189 H -0.03980246 -4.87741272 0.15490369 H -1.51916011 3.10924343 1.62606229 H 0.10997394 3.79825186 1.77173291 H -1.46273171 3.48551485 -0.86824418 H -1.23673381 5.00882040 0.0111085 H 0.16230134 4.19250032 -0.71688050 H 2.90229280 0.25168242 2.80791833 H 3.10140585 -1.13351044 1.72017623	 C -2.02286231 -3.56894401 4.29564735 C -1.05432592 -2.77558775 3.35994076 C -1.70449440 -1.92443715 2.19164641 C -2.45500228 -2.73064458 1.12083334 C -3.32564427 -2.03089088 0.26851293 C -2.33413027 -4.11535161 0.95159338 C -4.05851945 -2.69087775 -0.71611913 C -3.07233688 -4.78111426 -0.03107970 C -3.93665449 -4.07403134 -0.86765612 C -0.74387582 -0.91968645 1.56744723 C 0.71943036 1.10557311 -0.42088754 C 0.75088826 -0.25328684 -0.44333481 C 0.50311006 -1.20248904 0.75910101 C 0.43424819 -1.14345547 -1.65709625 C 0.56401904 -2.60006546 0.14357864 O 0.30877439 -0.81020933 -2.81804075 O 0.72485452 -3.66065039 0.71603433 N 0.41724480 -2.46833048 -1.22695819 C 0.32580163 -3.60924693 -2.12638042 C 0.18328015 1.81717576 0.82999167 C 0.79458221 1.40860988 1.82847333 O 0.46577565 3.02296171 0.84526283 C 0.30950452 3.79828870 2.04536376 C -1.16389395 5.04476245 1.89730314 C -0.15317411 1.91362149 -1.69807955 C 1.14085450 2.39299178 -2.49418769 C 2.19871605 3.02506824 -1.60083000 C 1.97841997 4.24694141 -0.94568248 C 3.44849167 2.41173198 -1.43982558 C 4.44455690 2.98796434 -0.64783377 C 2.96950526 4.82832194 -0.15510554 C 4.20820643 4.20045211 -0.00157921 C 0.81436350 3.34319202 -3.69926523 H -1.43322770 -4.07389201 5.06778770 H -2.73188137 -2.89684524 4.79291471 H -2.59757900 -4.32368496 3.75135121 H -0.31588931 -3.45182512 2.91960578 H -0.48790546 -2.07136331 3.98200815 H -2.46407286 -1.29837487 2.68152380 H -3.42227598 -0.95325662 0.38054975 H -1.65248414 -4.68242651 1.57446687 H -4.72599111 -2.12638343 -1.36182689 H -2.96899518 -5.85790327 -0.13846591 H -4.51077751 -4.59478195 -1.62937058 H -0.73815554 0.05974371 2.02155560 H 1.84711185 -0.09459560 -0.54103912 H 1.33704110 -1.12605572 1.47831534 H 0.30830135 -3.22444129 -3.14631898 H 1.18777064 -4.26547648 -1.97979675 H -0.58869135 -4.17139088 -1.92020551 H -0.61605329 3.19799063 2.90874490 H 0.75022679 4.04313694 2.17743975 H -2.21784528 4.78194591 1.75865037 H -1.07854577 5.66637986 2.79561751 H -0.84445339 5.64073773 1.03581981 H -0.73817062 1.32652464 -2.41315131 H -0.73980367 2.79493962 -1.42688511

H	1.87393446	0.93577351	-3.35352742	H	3.69120744	1.80703367	1.06716734	H	1.57461448	1.48190434	-2.92169765
H	1.17474510	4.55930558	-2.44202790	H	4.74143397	-1.64031391	-0.13896900	H	1.01907309	4.74634131	-1.04989221
H	3.74828216	1.14287199	-2.06049550	H	3.34469299	2.29238306	-1.16448474	H	3.64813095	1.47249492	-1.95241888
H	5.33363135	2.48763488	-0.71517077	H	3.40444545	1.68885870	-3.56257420	H	5.40484914	2.48975702	-0.54070617
H	2.74473108	5.90052944	-1.10337557	H	4.81030306	-2.24235790	-2.52815489	H	2.77642995	5.57772939	0.33947926
H	4.84116512	4.88015364	-0.23001816	H	4.13908869	-0.58509472	-4.26097830	H	4.98000285	4.65405535	0.61456520
H	0.90959144	3.56136470	-4.65772705	H	5.80475810	-0.36564553	1.64821843	H	0.37234488	4.28592419	-3.35820065
H	2.35904567	2.63826217	-5.09569867	H	6.11983418	1.28953798	1.09013634	H	1.73526267	3.57334565	-4.24374946
H	0.74503932	1.93710760	-5.35311588	H	5.39475695	1.01022365	2.69195319	H	0.10993433	2.86515100	-4.38962221

Table S5b Molecular structures and atomic coordinates (in [Å]) obtained from the CoGEF analysis of the polymer models after final rupture of the cyclobutane ring.

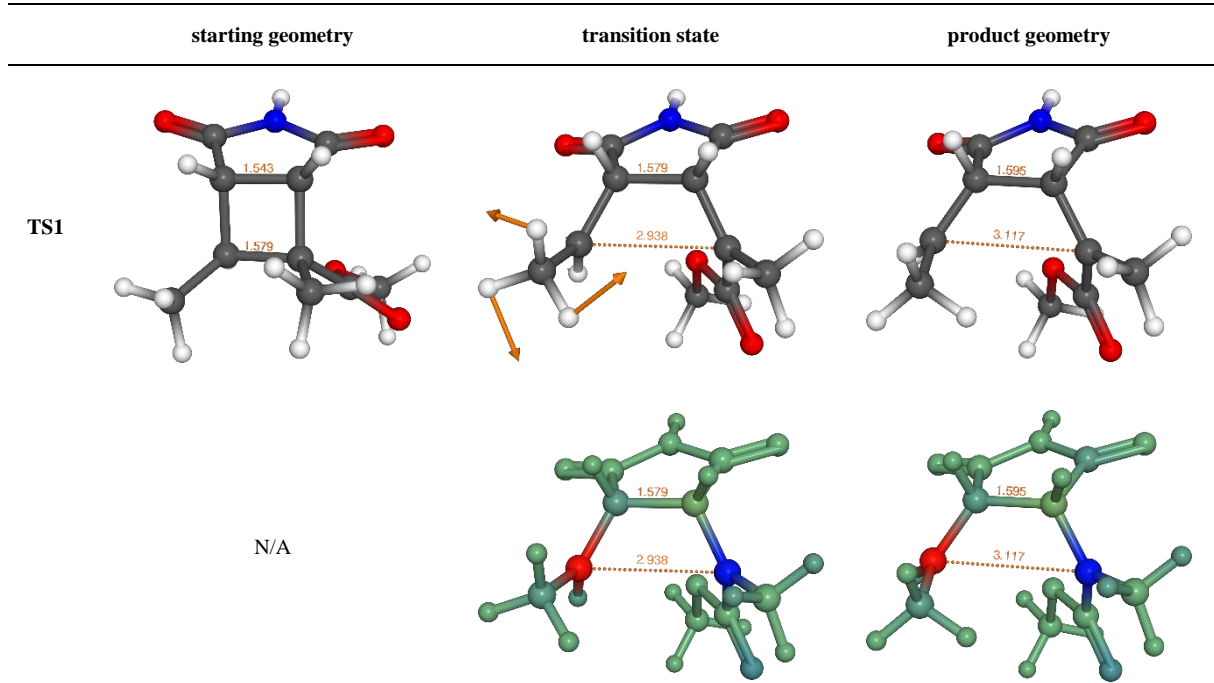
<i>cis</i> -1	<i>trans</i> -1	<i>cis</i> -2
  		

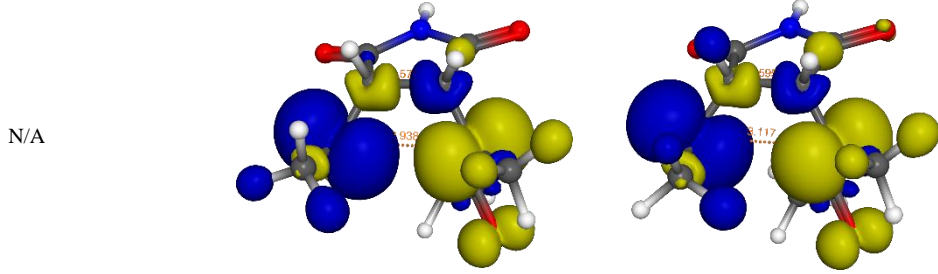
C	-3.46312702	-4.09883619	3.66577900	C	-6.10878026	0.41192019	-1.19356954	C	-1.18827946	-3.39773350	4.22860164
C	-2.51063924	-3.09934134	2.99618757	C	-5.06214322	-0.48191326	-0.51254554	C	-0.44408510	-2.66459640	3.0264782
C	-3.14200251	-2.42381420	1.75510708	C	-3.57669586	-0.12858115	-0.82464259	C	-1.31074449	-1.66652970	2.20632829
C	-3.39043750	-3.38429774	0.58600420	C	-3.18390960	-0.20189400	-2.29443856	C	-2.62371310	-2.30616419	1.75694473
C	-4.69556173	-3.63652668	0.14499681	C	-2.21179454	0.67005330	-2.79024616	C	-3.84672361	-1.72218873	2.11202666
C	-2.32534165	-4.02480485	-0.06635888	C	-3.71954658	-1.16586005	-3.16956153	C	-2.64776774	-3.47411911	0.97738857
C	-4.93945215	-4.51085074	-0.91653880	C	-1.78888810	0.60461866	-4.11718719	C	-5.06024151	-2.27947557	1.70319503
C	-2.56842820	-4.89096587	-1.12523242	C	-3.30227945	-1.21617170	-4.05113345	C	-3.85898462	-4.03312065	0.56774117
C	-3.87476945	-5.14566452	-1.55542733	C	-2.33625589	-0.34652441	-4.98030694	C	-5.07041104	-3.43866487	0.92771885
C	-2.48227202	-1.15019296	1.24217343	C	-2.69549598	-0.97564087	0.07672825	C	-0.67361018	-0.88558237	0.95781747
C	0.72144761	2.46628732	-0.36894625	C	2.00494578	-0.48009811	1.39868893	C	0.36474928	1.11676131	-0.80633879
C	-1.21793998	-0.69356860	1.13032844	C	-1.91571803	-0.03091221	-0.29364615	C	1.08703587	-0.22534381	-0.80024311
C	0.86333498	1.17249749	-0.03217672	C	0.86621233	-1.15026501	4.11312224	C	0.71447793	-1.23141482	0.35219793
C	0.04319155	-1.39209450	1.46702434	C	-1.39855423	-2.99664451	0.68271900	C	0.92224254	-1.04779188	-2.08235648
C	1.44270230	0.72522319	1.26798198	C	-0.07560722	-1.52038812	2.23365691	C	0.71220697	-2.59149779	-0.34638300
O	0.12796144	-2.60048516	1.65654184	O	-1.46118415	-4.19176948	0.44515965	O	0.9776446	-0.66398781	-3.23317056
O	0.23031093	1.42500024	1.88834952	O	0.05944393	-1.20192788	3.37724908	O	0.65641499	-3.69797867	0.16084320
N	1.19789716	-0.60428424	1.67763697	N	-1.01410652	-2.53492851	1.96791512	N	0.75344148	-2.38507604	-1.71637625
C	2.24864526	-1.26084678	2.47463400	C	-1.36267180	-3.40703710	3.10154784	C	0.68377472	-3.47719348	-2.67547466
C	0.98233319	3.57036071	0.62362154	C	2.32518917	0.06149951	2.77296812	C	-0.35361832	1.39636444	0.30250490
O	0.173818273	4.49263542	0.39305957	O	3.13849125	-0.46327386	0.50267031	O	-0.61458626	0.51175003	1.32409088
O	0.22898624	3.45755715	1.72786555	O	1.71030423	2.13427201	3.01404826	O	-0.85244185	2.62881416	0.56000029
C	0.51255588	4.41056098	2.78213396	C	1.88040144	1.78433314	4.34636316	C	-2.19236349	2.70739051	1.09055559
C	-0.44933812	4.12801971	3.91975278	C	3.14563397	2.62147313	4.45639365	C	-2.56312843	4.17733576	1.15810300
C	0.35934264	2.96758467	-1.75230810	C	3.17049183	-0.40709085	0.43715259	C	0.45088040	2.10669539	-1.98715449
C	0.80058968	2.12344098	-2.96628216	C	3.75680323	0.10232771	0.16401968	C	1.84927665	2.58087369	-2.52174930
C	2.29006774	1.79383239	-3.00765404	C	2.86693322	1.79602503	-0.79549642	C	2.79056190	3.07442636	-1.43150521
C	3.26811431	2.62816163	-2.44664659	C	3.03160612	1.72693064	-2.18625845	C	2.35171810	3.88553034	-0.37402233
C	2.70992322	0.63740691	-3.68105125	C	1.82435825	2.58785077	-0.29167837	C	1.4549166	2.75129082	-1.48978950
C	4.06320646	0.32358205	-3.80434902	C	0.97832723	3.29380932	-1.14832246	C	5.05492483	3.22578156	-0.53455833
C	4.62386407	2.31506821	-2.56846983	C	2.18846663	2.43269564	-3.04650252	C	3.24806747	4.36095838	0.58445876
C	5.02771554	1.16582735	-3.24848673	C	1.15881411	3.22181092	-2.53113744	C	4.60362892	4.03597352	0.50807442
C	0.38317040	2.85630197	-4.26180043	C	5.22748392	0.00996962	-0.28997217	C	1.74096188	3.66548275	-3.66908121
H	-2.99220838	-4.54597061	4.54833252	H	-7.11863051	0.11273254	-0.89246157	H	-0.46817487	-4.01348121	4.77669102
H	-4.39198179	-3.61463728	3.99411254	H	-5.97344161	1.46372193	-0.91346723	H	-1.63340387	-2.68306878	4.93111245
H	-3.73457963	-4.91220829	2.98386075	H	-6.04702169	0.34732221	-2.28451047	H	-1.98378362	-4.04560724	3.85061282
H	-1.57749398	-3.59164137	2.72193966	H	-5.24064570	-1.53247391	-0.77282527	H	-0.00927433	-3.42016224	2.39261005
H	-2.24652835	-2.31195566	3.71495026	H	-5.19468501	-0.42211938	0.57578441	H	0.40040887	-2.10250101	3.47471319
H	-4.13799558	-2.08758803	2.07751128	H	-3.43282321	0.91594541	-0.50741017	H	-1.57907581	-0.84399204	2.88013384
H	-5.53185457	-3.14737582	0.64025937	H	-1.76931789	1.40803570	-2.12466540	H	-3.84916930	-0.82043856	2.72069016
H	-1.30878887	-3.8306816	0.26287314	H	-4.47028285	-1.86701673	-2.81610903	H	-1.71411590	-3.95097159	0.69230098
H	-5.96066734	-4.69478177	-1.24059296	H	-1.02834981	0.29505621	-4.47187001	H	-5.99573120	-1.80824952	1.99408313
H	-1.73270593	-5.39006321	-1.61767488	H	-3.73410411	-1.97824786	-5.16251687	H	-3.85560654	-4.93919128	-0.03314014
H	-4.05995878	-5.82771462	-2.38117638	H	-2.01190965	-0.39856271	-6.01619231	H	-6.01234212	-3.87688240	0.60859403
H	-3.22600209	-0.43225925	0.89285517	H	-2.79873225	-0.76202294	1.14082065	H	-1.39863322	-0.95984509	0.13678413
H	-1.11661897	0.33080336	0.78874233	H	-1.83403594	-2.30242357	-1.33493476	H	2.17119871	-0.03376965	-0.73593073
H	0.68282105	0.39918378	-0.77401076	H	0.71752446	-1.57989271	0.15537008	H	1.46366701	-1.23401816	1.14868268
H	2.61596963	-2.14044775	1.94148379	H	-2.29880309	-3.91871110	2.87774928	H	0.82572162	-3.05061992	-3.66885644
H	3.04769634	-0.54110720	2.63458776	H	-0.58458100	-4.15186469	3.27052429	H	1.46328391	-4.21217015	-2.45880106
H	1.84536415	-1.38655408	3.43711588	H	-1.46864925	-2.78472330	3.98883604	H	-0.29007169	-3.97136864	-2.61551901

H	1.55661099	4.27996522	3.08252229	H	0.98357458	2.38954554	4.49836998	H	-2.87447072	2.15382743	0.43132950
H	0.39804647	5.42289065	2.38246514	H	1.88166554	0.95802237	5.06031418	H	-2.22149989	2.24301905	2.08069573
H	-0.31965976	3.10769345	4.29386089	H	3.15129213	3.42425309	3.71109850	H	-2.54081933	4.63282191	0.16292074
H	-0.26215086	4.82451962	4.74426970	H	3.20034458	3.07980327	5.45082733	H	-3.57208771	4.29106889	1.56943714
H	-1.48819838	4.24978269	3.59591639	H	4.03330796	1.99881199	4.31649792	H	-1.86407457	4.72079934	1.80188883
H	-0.73308264	3.09352691	-1.80163039	H	3.96402231	-1.01304291	0.89859763	H	-0.05640942	1.65165107	-2.84692014
H	0.76882000	3.97945682	-1.84527312	H	2.90521670	-0.88699749	-0.51133559	H	-0.14230757	2.98190647	-1.70622083
H	0.25247970	1.17081327	-2.94352309	H	3.76055954	1.55661843	1.11656787	H	2.31707066	1.70190820	-2.98301496
H	2.98229391	3.51430367	-1.88923067	H	3.82980414	1.12316437	-2.60922453	H	1.29851374	4.13436598	-0.28294452
H	1.96395726	-0.02609319	-4.11538215	H	1.67205759	2.64314721	0.78301690	H	4.51518683	2.12081871	-2.30068531
H	4.36273766	-0.58016826	-4.32898792	H	0.18376353	3.90908252	-0.73325890	H	6.10687780	2.95966381	-0.60418274
H	5.36475909	2.97142193	-2.11958723	H	2.34278391	2.37062914	-4.12086358	H	2.88354454	4.98426583	1.39736792
H	6.08347519	0.92387397	-3.33749777	H	0.51004579	3.78236713	-3.19939411	H	5.29972734	4.40612229	1.25633512
H	0.90923726	3.81394820	-4.34863173	H	5.33870136	0.25412513	-1.16871343	H	1.30502110	4.59567417	-3.28702642
H	0.63152784	2.25774199	-5.14379190	H	5.63601312	1.88431473	-0.54131371	H	2.73882908	3.88783461	-4.05823681
H	-0.69564818	3.05484945	-4.27499107	H	5.83605983	0.46928995	0.51233300	H	1.11604130	3.29714827	-4.49070388

Transition States

Table S6a Molecular structure plots of the truncated polymer models (MCBI unit only), computed energies (excerpts from the *Gaussian* output) and atomic coordinates (in [Å]) for the intrinsic reaction coordinate **TS1** (starting geometry, transition state, and final product geometry). The dotted orange lines indicate characteristic intramolecular atom-atom distances. For the transition state, the orange vectors visualize the eigenvector associated with the vibrational mode of negative (imaginary) frequency (atomic displacement vectors are scaled by a factor of 2.5 for clarity). For the singlet diradical species involved in this process, the models displayed in the second row show the Mulliken spin densities mapped on atomic positions in color coded form (blue and red: high negative and positive spin density; N/A: closed-shell non-radical species). The models displayed in the third row show the 3D-spin SCF density iso-contour surfaces of the diradicals (blue and yellow lobes of excess α - and β -electron density).

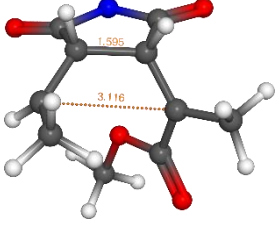
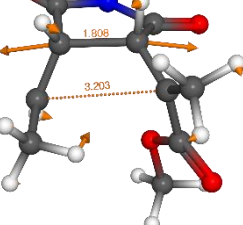
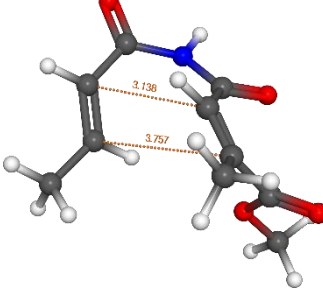
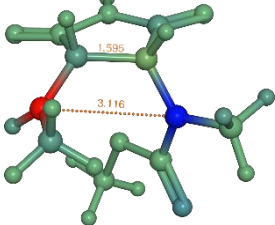
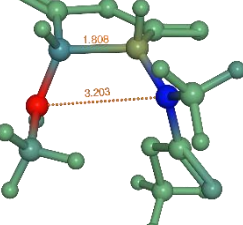
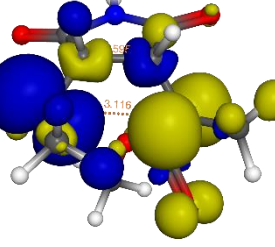
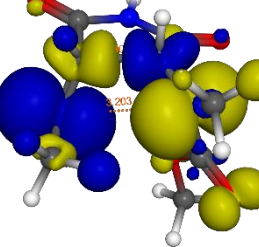




SCF Energy: E(UB3LYP) = -744.556822101 A.U.	SCF Energy: E(UB3LYP) = -744.477190461 A.U.	SCF Energy: E(UB3LYP) = -744.477572195 A.U.
Zero-point correction= 0.226808	Zero-point correction= 0.220137	Zero-point correction= 0.220280
Thermal correction to Energy= 0.241364	Thermal correction to Energy= 0.236068	Thermal correction to Energy= 0.236808
Thermal correction to Enthalpy= 0.242308	Thermal correction to Enthalpy= 0.237012	Thermal correction to Enthalpy= 0.237752
Thermal correction to Gibbs Free Energy= 0.185067	Thermal correction to Gibbs Free Energy= 0.175075	Thermal correction to Gibbs Free Energy= 0.175058
Sum of electronic and zero-point Energies= -744.330014	Sum of electronic and zero-point Energies= -744.257053	Sum of electronic and zero-point Energies= -744.257292
Sum of electronic and thermal Energies= -744.315458	Sum of electronic and thermal Energies= -744.241123	Sum of electronic and thermal Energies= -744.240764
Sum of electronic and thermal Enthalpies= -744.314514	Sum of electronic and thermal Enthalpies= -744.240179	Sum of electronic and thermal Enthalpies= -744.239820
Sum of electronic and thermal Free Energies= -744.317555	Sum of electronic and thermal Free Energies= -744.302116	Sum of electronic and thermal Free Energies= -744.302515
Imaginary frequency: -89.2919 cm ⁻¹		

C -2.6750015 -0.3992042 1.56261535	C -2.88829507 -0.86908084 1.81291420	C -2.62177399 -0.52231235 1.81744771
C -1.31445172 -0.35160112 0.88161487	C -1.42882878 -0.78119775 1.51546771	C -1.21473525 -0.98316997 1.67234563
C -1.02994820 0.73503319 -0.22843073	C -0.92149507 1.00792115 -0.75962284	C -0.79372929 0.97242406 -0.74279598
C -0.98042585 -1.48219100 -0.15351401	C -0.81093090 -1.38340091 0.29450521	C -0.68700937 -1.44737412 0.36349128
C -0.42891187 -0.41773350 -1.12464851	C -0.67674079 -0.46397667 -0.98217990	C -0.73641016 -0.49667553 -0.91632389
C 0.19870524 -2.36113507 0.22548276	C 0.61147495 -1.92018273 0.51616109	C 0.77341700 -1.90141038 0.43725770
C 1.08439354 -0.62678393 -1.11539906	C 0.73928292 -0.76348273 1.52190975	C 0.62926094 -0.75524768 -1.60346641
O 0.21227551 -3.35704476 0.91524314	O 1.03542807 -2.51249965 1.48246831	O 1.32613380 -2.46661424 1.35384876
O 0.19322242 0.03581287 -1.67263480	O 1.23636473 -0.33086336 -2.53719811	O 0.98796026 -0.31884184 -2.67401990
N 1.32565989 -1.77149172 -0.35652516	N 1.34301700 -1.64379699 -0.63684120	N 1.37162521 -1.58308232 -0.77885662
H 2.26148766 -2.13070642 -0.20711696	H 2.31476441 -1.91502696 -0.73290897	H 2.33913106 -1.80996636 -0.97818342
C -0.05161924 1.84834986 0.13489174	C -0.05777947 1.82663976 0.08292947	C -0.16940842 1.79513237 0.14606857
O -0.12103706 2.98956256 -0.26558868	O -0.21415984 3.02103928 0.29192478	O -0.34128629 2.98820723 0.35135553
O 0.93326803 1.40530672 0.94762059	O 0.97113304 1.11336755 0.62545999	O 0.82833253 1.08119107 0.74343908
C 1.98476661 2.34986725 1.21716848	C 1.87809490 1.86748340 1.44366576	C 1.66622774 1.82486769 1.64067127
H 2.65948961 1.84547697 1.90921143	H 2.61457204 1.14798968 1.80253956	H 2.37872415 1.10277248 2.04041988
C -2.27171896 1.34116062 -0.88362663	C -2.04538765 1.67653438 -1.47631129	C -1.99095887 1.64967819 -1.60620001
H -1.97826772 1.95622892 -1.73830451	H -1.87864421 1.64308426 -2.56424655	H -1.67008330 1.61658864 -2.65935669
H -0.53422154 -0.30509194 1.64508533	H -0.77915026 -0.26554983 2.21471765	H -0.52202489 -0.90967972 2.50276105
H -1.83989166 -2.07578602 -0.47142890	H -1.40568599 -2.26044127 -0.00193552	H -1.25451156 -2.34451077 0.05637059
H -0.78167230 -0.40231263 -2.15971145	H -1.37693025 -0.79767774 -1.75503059	H -1.49510831 -0.86911323 -1.61238294
H 2.50323449 2.60298815 0.28929782	H 2.36044602 2.65308354 0.85592980	H 2.18542629 2.62428913 1.10508784
H 1.57676348 3.25841609 1.66607756	H 1.34810966 2.32677422 2.28232431	H 1.07144184 2.26577915 2.44499786
H -2.95403323 0.55949921 -1.23320922	H -2.99811542 1.15896892 -1.29295753	H -2.96350200 1.14031069 -1.55982541
H -2.81402739 1.98442964 -0.18383764	H -2.13748871 2.71977309 -1.17004018	H -2.11451162 2.69427802 -1.31509553
H -3.49860826 -0.46801356 0.84410881	H -3.40121965 -1.57336503 1.14728057	H -3.32991201 -1.19058324 1.30451930
H -2.73020267 -1.27546977 2.21867176	H -3.06746039 -1.19519376 2.84760863	H -2.91940179 -0.45397598 2.86852813
H -2.83906188 0.49123817 2.18082622	H -3.39528301 0.10488227 1.71124342	H -2.77276064 0.47930817 1.37317517

Table S6b Molecular structure plots, computed energies (excerpts from the *Gaussian* output) and atomic coordinates (in Å) for the intrinsic reaction coordinate **TS2** (for details, see also Table S6a).

	starting geometry	transition state	product geometry
TS2			
			N/A
			N/A
<hr/>			
SCF Energy: E(UB3LYP) = -744.477545170 A.U. Zero-point correction= 0.220339 Thermal correction to Energy= 0.236800 Thermal correction to Enthalpy= 0.237744 Thermal correction to Gibbs Free Energy= 0.175258 Sum of electronic and zero-point Energies= -744.257206 Sum of electronic and thermal Energies= -744.240745 Sum of electronic and thermal Enthalpies= -744.239801 Sum of electronic and thermal Free Energies= -744.302287			
SCF Energy: E(UB3LYP) = -744.474679180 A.U. Zero-point correction= 0.219792 Thermal correction to Energy= 0.235632 Thermal correction to Enthalpy= 0.236576 Thermal correction to Gibbs Free Energy= 0.176007 Sum of electronic and zero-point Energies= -744.254887 Sum of electronic and thermal Energies= -744.239047 Sum of electronic and thermal Enthalpies= -744.238103 Sum of electronic and thermal Free Energies= -744.298672			
SCF Energy: E(UB3LYP) = -744.528225548 A.U. Zero-point correction= 0.222608 Thermal correction to Energy= 0.239321 Thermal correction to Enthalpy= 0.240265 Thermal correction to Gibbs Free Energy= 0.176792 Sum of electronic and zero-point Energies= -744.305618 Sum of electronic and thermal Energies= -744.288905 Sum of electronic and thermal Enthalpies= -744.287960 Sum of electronic and thermal Free Energies= -744.351434			
Imaginary frequency: -552.5044 cm ⁻¹			
<hr/>			
H -3.09080623 -0.82776209 2.56485946 C -2.72248358 -0.79247795 1.53498217 H -3.38018960 -1.42145518 0.91554696 C -1.29874988 -1.21235992 1.44373251 C -0.95553089 0.3296250 -0.68914306 C -0.66358717 -1.49884557 0.13168149 C -0.65395532 -0.39716433 -1.02187977 C 0.80241295 -1.92252836 0.25809289 C 0.76488614 -0.53502967 -1.63198931 O 1.30710420 -2.58486095 1.13656493 O 1.18306083 0.03878066 -2.61235387 N 1.47486637 -1.43915100 -0.86090777 H 2.46093888 -1.61637948 -1.01428919 C -0.23868668 1.75699674 0.35259802 O -0.46128232 2.91171050 0.68741350 O 0.73395261 0.99615749 0.93367235 C 1.48152257 1.64142448 1.97523437 H 2.18426251 0.89066256 2.33770355 C -1.91596687 1.79229130 -1.54287473 H -1.50450069 1.91129250 -2.55777429 H -2.86574897 0.24308060 1.17371896 H -0.67340714 -1.2442895 2.32845198 H -1.1718933 -2.36443414 -0.32503513 H -1.34797912 -0.69785913 -1.81355283			
H -2.31776088 -0.41086478 2.88022251 C -2.23801948 -0.55589653 1.79983854 H -3.14656742 -1.05298282 1.43536036 C -1.00395423 -1.26106805 1.39495801 C -0.91439376 1.12145067 -0.74376200 C -0.80126708 -1.58911582 0.01928418 C -0.38884743 -0.18343539 -0.04006803 C 0.42003250 -2.46770641 -0.23245534 C 1.12853345 -0.38044482 -1.12170533 O 0.51188566 -3.65329214 0.00214290 O 0.19348361 0.40995385 -0.55492076 N 1.44321117 -1.68238159 -0.74048320 H 2.37210493 -2.05919229 -0.89249488 C -0.32144893 1.96574545 0.28794784 O -0.58628806 3.14215898 0.48205533 O 0.57151968 1.27349265 1.05967885 C 1.24085350 2.05180998 2.06101052 H 1.90331132 1.35790044 2.58022970 C -0.04396663 1.69898313 -1.54680045 C -1.67558249 2.13631607 -2.48748168 H -2.23324268 0.44816763 1.31709098 H -0.15547047 -1.27397276 2.07242403 H -1.69915567 -1.97944470 -0.46604662 H -0.79984290 -0.55049733 1.98766092			
H -2.50177039 -1.57803520 3.11401372 C -2.65879049 -1.44584230 2.03540232 H -3.42285241 -2.15693161 1.70705166 C -1.37289704 -1.61750234 1.28811514 C -0.73332403 1.42159746 -0.82523013 C -1.16041525 -2.54419590 0.34232111 C -0.36818310 0.15054927 -1.05640868 C 0.14386538 -2.82286294 -0.30275975 C 0.96740339 -0.40193783 -0.69696584 O 0.46614257 -3.95961665 -0.61005640 O 1.98209880 0.27892169 -0.68478811 N 1.07462309 -1.78029800 -0.47967512 H 2.02622282 -2.11912624 -0.58991656 C 0.12641179 2.37415910 -0.04043793 O 0.41570944 3.48376804 -0.43172683 O 0.45814751 1.88109674 1.16947503 C 1.37514381 2.69134724 1.92721141 H 1.48571541 2.18664696 2.88716118 C -1.99755070 2.02743895 -1.36979120 H -1.75019047 2.91800370 -1.95842532 H -3.04768276 -0.42756971 1.90101228 H -0.57072068 -0.93360497 1.56016763 H -1.92791148 -3.27458885 0.09661026 H -1.03734520 -0.50004743 -1.61279898			

H 2.01401864	2.51123246	1.58108106	H 1.81796816	2.85524629	1.59574171	H 2.33539602	2.74430968	1.40805449
H 0.81679592	1.96776348	2.77943935	H 0.51996785	2.49094801	2.75619693	H 0.97686124	3.69987436	2.06178463
H -2.86802456	1.25506628	-1.65236734	H -2.77778182	0.92985886	-1.81815887	H -2.54332128	1.32040029	-2.00022153
H -2.10434007	2.78452324	-1.12895494	H -2.54621893	2.49896932	-0.99808293	H -2.66035814	2.35878283	-0.55973788

Table S6c Molecular structure plots, computed energies (excerpts from the *Gaussian* output) and atomic coordinates (in [Å]) for the intrinsic reaction coordinate **TS3** (for details, see also Table S6a).

	starting geometry	transition state	product geometry
TS3			
			N/A
			N/A
<p>SCF Energy: E(UB3LYP) = -744.477587781 A.U.</p> <p>Zero-point correction= 0.220296</p> <p>Thermal correction to Energy= 0.236815</p> <p>Thermal correction to Enthalpy= 0.237759</p> <p>Thermal correction to Gibbs Free Energy= 0.175068</p> <p>Sum of electronic and zero-point Energies= -744.257291</p> <p>Sum of electronic and thermal Energies= -744.240773</p> <p>Sum of electronic and thermal Enthalpies= -744.239829</p> <p>Sum of electronic and thermal Free Energies= -744.302520</p> <p>SCF Energy: E(UB3LYP) = -744.460255895 A.U.</p> <p>Zero-point correction= 0.219794</p> <p>Thermal correction to Energy= 0.235629</p> <p>Thermal correction to Enthalpy= 0.236574</p> <p>Thermal correction to Gibbs Free Energy= 0.175978</p> <p>Sum of electronic and zero-point Energies= -744.240462</p> <p>Sum of electronic and thermal Energies= -744.224626</p> <p>Sum of electronic and thermal Enthalpies= -744.223682</p> <p>Sum of electronic and thermal Free Energies= -744.284278</p> <p>SCF Energy: E(UB3LYP) = -744.545276483 A.U.</p> <p>Zero-point correction= 0.227754</p> <p>Thermal correction to Energy= 0.242019</p> <p>Thermal correction to Enthalpy= 0.242963</p> <p>Thermal correction to Gibbs Free Energy= 0.186649</p> <p>Sum of electronic and zero-point Energies= -744.317522</p> <p>Sum of electronic and thermal Energies= -744.303257</p> <p>Sum of electronic and thermal Enthalpies= -744.302313</p> <p>Sum of electronic and thermal Free Energies= -744.358627</p> <p>Imaginary frequency: -68.2630 cm-1</p>			
<p>H -3.38300421 -1.65520372 1.63514572</p> <p>C -2.56637427 -0.93070245 1.71241287</p> <p>H -2.85592108 -0.16736748 2.45076612</p> <p>C -2.23289698 -0.33263570 0.39193959</p> <p>C 0.74440292 -0.41654044 1.31572218</p> <p>C -1.36679947 0.86971952 0.28729636</p> <p>C 0.09678015 0.87651375 0.92188568</p> <p>C -1.15121121 1.32246407 -1.15937761</p> <p>C 0.94251358 1.61760444 -0.14577695</p> <p>O -1.94284365 1.27522651 -2.07385781</p> <p>O 2.10353871 1.94371819 -0.04170358</p> <p>N 0.13363727 1.85108222 -1.24464893</p> <p>H 0.49927305 2.24023495 -2.10612799</p> <p>C 0.88843071 -1.52816335 0.38455063</p> <p>H -3.55651826 -1.38562298 1.95363775</p> <p>C -2.63750845 -0.78992308 1.95550104</p> <p>H -2.74804733 0.00739611 2.70467885</p> <p>C -2.33570432 -0.25019897 0.60179471</p> <p>C 0.72581418 -0.48054043 1.19631156</p> <p>C -1.40878165 0.89989524 0.41988056</p> <p>C 0.05256216 0.85174375 1.01776546</p> <p>C -1.19718279 1.28903145 -1.04777386</p> <p>C 0.87393071 1.67690184 -0.00847877</p> <p>O -1.98728985 1.21435584 -1.96123517</p> <p>O 1.99587925 2.11051658 0.13198153</p> <p>N 0.09883675 1.79404999 -1.15341318</p> <p>H 0.45546695 2.19114759 -2.01155942</p> <p>C 0.59782584 -1.54922484 0.16047394</p> <p>H -2.28978943 -2.72469879 0.89722387</p> <p>C -2.07510968 -1.70109296 1.21966263</p> <p>H -2.98432813 -1.28621780 1.66859020</p> <p>C -1.64549094 -0.85764314 0.02077584</p> <p>C 1.02124662 -0.36721353 0.83055576</p> <p>C -1.31421485 0.59456705 0.37349390</p> <p>C 0.06529633 0.79451700 1.04314508</p> <p>C -1.29140088 1.49142236 -0.87212945</p> <p>C 0.63245672 2.04818455 0.34793035</p> <p>O -2.10071143 1.51372374 -1.77383374</p> <p>O 1.61236766 2.69142492 0.65178543</p> <p>N -0.17829905 2.30972183 -0.75788325</p> <p>H 0.04360021 3.03061657 -1.43522282</p> <p>C 0.68562169 -1.34494964 -0.03194679</p>			

O	1.38082444	-2.61404749	0.65559041	O	-0.22653776	-2.44021285	0.16833997	O	-0.52302285	-1.46136794	-0.65769563
O	0.40445868	-1.22761709	-0.85542796	O	1.55369286	-1.43243804	-0.79100356	O	1.56579312	-2.30086809	-0.40954279
C	0.50436750	-2.27819509	-1.82818420	C	1.53957908	-2.44626459	-1.81563090	C	1.04985858	-3.60840665	-0.68410847
H	0.05208191	-1.87850357	-2.73624904	H	2.36694069	-2.19842848	-2.48071126	H	1.92504991	-4.22152104	-0.90552863
C	1.39284250	-0.52928077	2.65519587	C	1.89495333	-0.56395058	2.13125958	C	2.34115321	-0.33291122	1.55264358
H	2.26361396	0.14322228	2.71019820	H	2.76052622	-0.01790309	1.72270633	H	2.94033822	0.53612341	1.25588887
H	-1.70108069	-1.46270822	2.15012835	H	-1.82702685	-1.45172550	2.30703862	H	-1.29444819	-1.73431590	1.98565996
H	-2.55458111	-0.80816418	-0.52743701	H	-2.6788024	-0.77356374	-0.28322701	H	-2.43427810	-0.85368496	-0.73596744
H	-1.87980321	1.71447065	0.78215897	H	-1.86159433	1.79749187	0.88244328	H	-2.11474683	0.98580459	1.01418822
H	0.10209552	1.52269825	1.80579036	H	0.10614749	1.38372073	1.97363488	H	-0.01407494	1.01644328	2.11483747
H	1.55151428	-2.54099609	-2.00117036	H	1.68145640	-2.16312710	-1.37446108	H	0.52720463	-4.01919535	0.18857918
H	-0.03262091	-3.16793764	-1.48884917	H	0.58982746	-2.42932583	-2.35628056	H	0.37412887	-3.60017585	-1.54275258
H	0.70983974	-0.22260180	3.45920188	H	1.65550974	-0.10407688	3.09830359	H	2.18930794	-0.25230691	2.63900774
H	1.73387291	-1.54997460	2.83740815	H	2.20217797	-1.59979895	2.30862067	H	2.91930997	-1.23722291	1.35206475

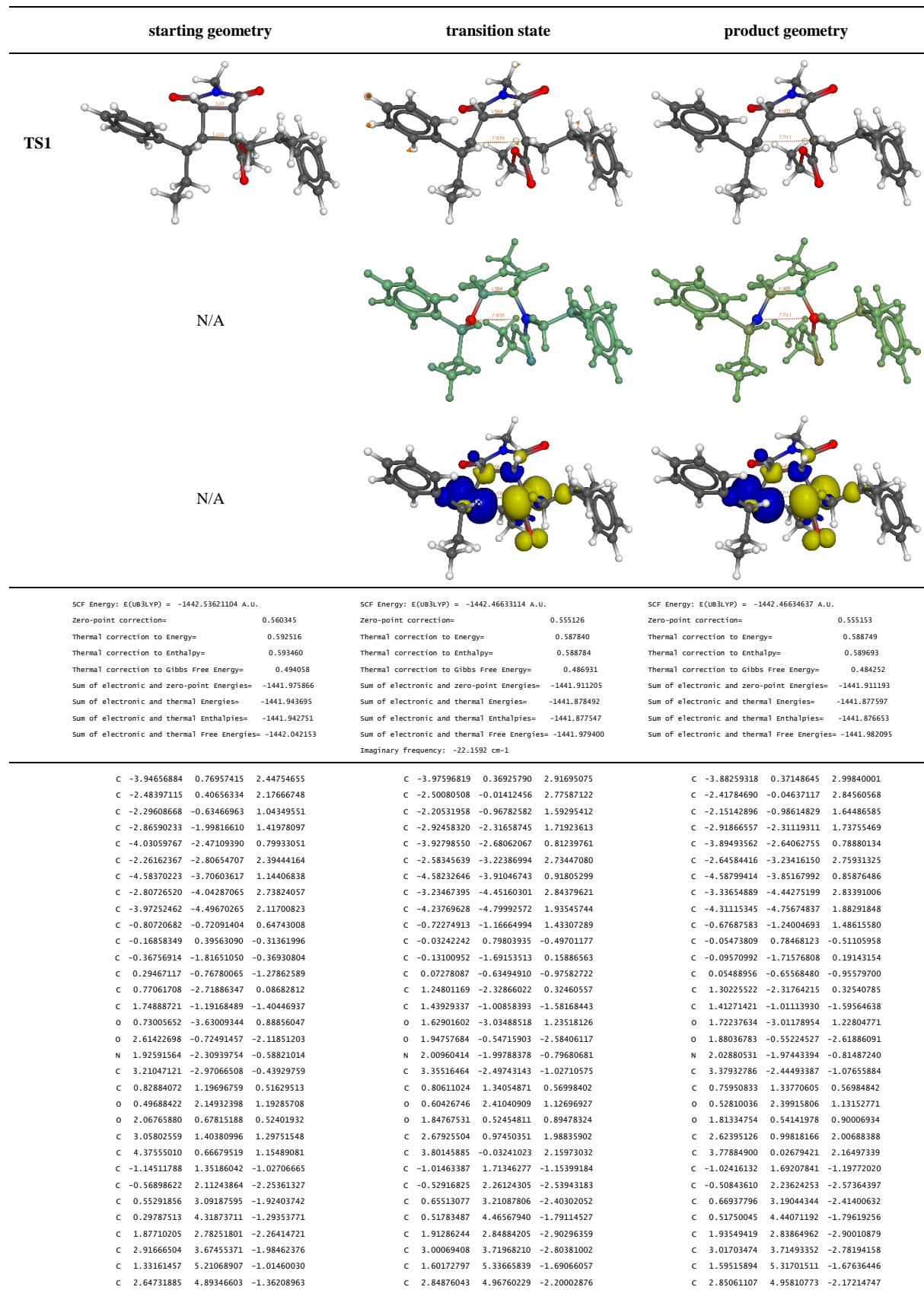
Table S6d Molecular structure plots, computed energies (excerpts from the Gaussian output) and atomic coordinates (in Å) for the intrinsic reaction coordinate **TS4** (for details, see also Table S6a).

starting geometry	transition state	product geometry
<p>TS4</p>		
<p>SCF Energy: E(UB3LYP) = -744.546606022 A.U. Zero-point correction= 0.227569 Thermal correction to Energy= 0.241914 Thermal correction to Enthalpy= 0.242858 Thermal correction to Gibbs Free Energy= 0.186286 Sum of electronic and zero-point Energies= -744.319037 Sum of electronic and thermal Energies= -744.304692 Sum of electronic and thermal Enthalpies= -744.303748 Sum of electronic and thermal Free Energies= -744.360320</p>	<p>SCF Energy: E(UB3LYP) = -744.477243700 A.U. Zero-point correction= 0.222172 Thermal correction to Energy= 0.237437 Thermal correction to Enthalpy= 0.238381 Thermal correction to Gibbs Free Energy= 0.179556 Sum of electronic and zero-point Energies= -744.255072 Sum of electronic and thermal Energies= -744.239807 Sum of electronic and thermal Enthalpies= -744.238862 Sum of electronic and thermal Free Energies= -744.297688</p>	<p>SCF Energy: E(UB3LYP) = -744.532820836 A.U. Zero-point correction= 0.222883 Thermal correction to Energy= 0.239647 Thermal correction to Enthalpy= 0.240591 Thermal correction to Gibbs Free Energy= 0.176320 Sum of electronic and zero-point Energies= -744.309938 Sum of electronic and thermal Energies= -744.293174 Sum of electronic and thermal Enthalpies= -744.292230 Sum of electronic and thermal Free Energies= -744.356501</p>
<p>Imaginary frequency: -501.0658 cm⁻¹</p>		
<p>H -0.71657758 -1.02485979 -3.22988118 C -1.47394675 -0.93591547 -2.44394449 H -1.85265108 -1.93459649 -2.21353985 C -0.86883067 -0.30046542 -1.20382226 C 0.83479421 1.16575031 0.47872982 C 0.94874195 -0.33736354 -0.57791757 C 0.28231248 -1.12192278 -0.57679039 C 0.35865887 -0.97016682 1.85271110 C -0.27986821 -2.38253582 0.08327957 O 0.42059482 -0.58405867 2.99851784 O -0.71966932 -3.37741325 -0.45404918 N -0.25090945 -2.16201054 1.45466702 H -0.64181906 -2.81998228 2.11963540 C 0.26375610 1.69889764 -0.61623112 O -0.37940320 0.98925827 -1.59155828 O 0.33747525 0.01911651 -0.90420657 C -0.84329666 3.63477585 -1.43355106 H -0.59895549 4.69358802 -1.53423214 C 1.52450966 2.00773872 1.51998137 H 2.61097521 1.83035696 1.51155630 H -2.29330499 -0.31708570 -2.82232548 H -1.63945430 -0.14411102 -0.43254519 H 2.01848799 -0.60700096 0.61570701 H 0.98697894 -1.39857448 -1.36639990 H -1.68875351 3.51818321 -0.74393409 H -1.10748619 3.21988635 -2.40951959 H 1.17105114 1.75772575 2.52527028 H 1.35687390 3.07048624 1.33436961</p>	<p>H -0.37882307 -1.46987461 -3.24083547 C -1.32727703 -0.9560093 -2.87890292 H -2.10298367 -1.82559814 -3.02625147 C -1.24220079 -0.69823695 -1.43230834 C 0.75450483 0.98317172 0.35269021 C 0.10986661 -0.36638097 0.05443803 C -0.42083908 -1.39891873 -0.52816186 C 1.44448001 -1.24628276 1.24421687 C -0.85968627 -1.75773542 0.86963388 O 2.52442576 -1.35093760 1.78041350 O -1.98904852 -1.96030387 1.26269700 N 0.27964451 -1.87796616 1.67662287 H 0.23292333 -2.31904172 2.58858617 C 0.16843197 -0.66220482 -0.73393332 O -0.10542151 1.07100294 -1.81567152 O -0.23750397 2.94395677 -0.51290515 C -0.88201803 3.59374795 -1.61085664 H -1.08202668 4.61119406 -1.27113156 C 0.68347035 1.54070663 1.75315698 H 1.47237033 1.12775314 2.38841991 H -1.58816169 -0.19097248 -3.48854559 H -2.05990418 -0.11058753 -1.02398121 H 1.68447173 -0.52756360 -0.84737263 H 0.14176819 -2.22107148 -0.97684895 H -1.82074531 3.09497315 -1.87197510 H -0.23546668 3.61007117 -2.49388241 H -0.28275440 1.33836144 2.24074306 H 0.80191929 2.62663196 1.72679847</p>	<p>H -1.69607311 -1.22805918 -3.11381838 C -2.51937639 -1.71434570 -2.58164710 H -2.80793814 -2.61620371 -3.13802800 C -2.15616391 -2.06155460 -1.17364591 C 0.43186705 1.15004084 0.27319072 C 1.32171601 0.14603764 0.18285341 C -0.96929945 -1.81821234 -0.59955630 C 1.50851397 -0.96818527 1.15815253 C -0.72255901 -2.25267054 0.79436747 O 2.56428084 -1.06084936 1.76148078 O -1.48391820 -2.97636054 1.41861132 N 0.48325773 -1.87593578 1.42376208 H 0.67097602 -2.43865922 2.24970116 C 0.57853858 2.23119458 -0.76112155 O 1.38464400 2.22675028 -1.67019726 O -0.31427459 3.22588539 -0.56813188 C -0.24442512 4.30552580 -1.51463004 H -1.01873184 5.01023894 -2.10903400 C -0.65721509 1.28446213 1.30362048 H -0.61652192 0.48332292 2.04371905 H -3.39133397 -1.04692259 -2.60402523 H -2.91453048 -2.55612218 -0.56801920 H 2.09617235 0.21670697 -0.57690936 H -0.17383781 -1.32923294 -1.15057733 H -0.43068808 3.93883265 -2.52746479 H 0.74135094 4.77665412 -1.48367586 H -1.64510757 1.26756639 0.82869979 H -0.57534899 2.24465324 1.82318101</p>

Table S6e Molecular structure plots, computed energies (excerpts from the *Gaussian* output) and atomic coordinates (in Å) for the intrinsic reaction coordinate **TS5** (for details, see also Table S6a).

	starting geometry	transition state	product geometry
TS5	<p>Detailed description: A ball-and-stick model of a molecule in its starting geometry. Atoms are represented by spheres and connected by lines. Several bond lengths are labeled in orange: 1.543, 1.579, and 1.575 Å.</p>	<p>Detailed description: A ball-and-stick model of the transition state. It shows the molecule in a partially broken and partially formed state. Bond lengths are labeled: 2.015, 2.064, and 3.142 Å.</p>	<p>Detailed description: A ball-and-stick model of the product molecule. Bond lengths are labeled: 3.788 Å.</p>
	SCF Energy: E(UB3LYP) = -744.556829396 A.U. Zero-point correction= 0.226822 Thermal correction to Energy= 0.241366 Thermal correction to Enthalpy= 0.242310 Thermal correction to Gibbs Free Energy= 0.185168 Sum of electronic and zero-point Energies= -744.330007 Sum of electronic and thermal Energies= -744.315463 Sum of electronic and thermal Enthalpies= -744.314519 Sum of electronic and thermal Free Energies= -744.371661 Imaginary frequency: -752.4514 cm ⁻¹	SCF Energy: E(RB3LYP) = -744.434801047 A.U. Zero-point correction= 0.222042 Thermal correction to Energy= 0.237158 Thermal correction to Enthalpy= 0.238103 Thermal correction to Gibbs Free Energy= 0.180256 Sum of electronic and zero-point Energies= -744.212759 Sum of electronic and thermal Energies= -744.197643 Sum of electronic and thermal Enthalpies= -744.196698 Sum of electronic and thermal Free Energies= -744.254545	SCF Energy: E(UB3LYP) = -744.528241667 A.U. Zero-point correction= 0.222571 Thermal correction to Energy= 0.239314 Thermal correction to Enthalpy= 0.240258 Thermal correction to Gibbs Free Energy= 0.176551 Sum of electronic and zero-point Energies= -744.305671 Sum of electronic and thermal Energies= -744.288928 Sum of electronic and thermal Enthalpies= -744.287984 Sum of electronic and thermal Free Energies= -744.351691

Table S7a Molecular structure plots of the extended polymer models, computed energies (excerpts from the Gaussian output) and atomic coordinates (in [Å]) for the intrinsic reaction coordinate **TS1** (starting geometry, transition state, and final product geometry). For further explanations, see also Table S6a.



C	-1.72154570	2.79493737	-3.01714116	C	-1.71003372	2.91067974	-3.28418799	C	-1.67353092	2.88087524	-3.34690190
H	-4.02140855	1.50035381	3.26042596	H	-4.11965300	1.05563067	3.75869421	H	-4.00649038	1.04727699	3.85178238
H	-4.41657166	1.21260951	1.56028355	H	-4.34249011	0.87267118	2.01355984	H	-4.23923486	0.89860999	2.10466888
H	-4.53349198	-0.11074225	2.73058781	H	-4.60615023	-0.51006764	3.08767719	H	-4.53374624	-0.49478122	3.15669340
H	-2.02833511	0.00730338	3.09330448	H	-2.14928723	-0.48372027	3.70499643	H	-2.07500928	-0.53946477	3.76577627
H	-1.91674076	1.31127286	1.92794357	H	-1.89381277	0.88999104	2.63793979	H	-1.78904616	0.84439204	2.71982660
H	-2.86836600	-0.28695389	0.17425697	H	-2.59669017	-0.49128501	0.68036776	H	-2.51979036	-0.47544078	0.74155666
H	-4.51421190	-1.86076877	0.03920228	H	-4.20517277	-1.99030736	0.01818283	H	-4.12111116	-1.93738690	-0.01020072
H	-1.34726405	-2.47986145	2.88135163	H	-1.79579244	-2.97087680	3.43931651	H	-1.88161891	-3.00772713	3.49839248
H	-5.48958478	-4.04835761	0.65025747	H	-5.36030811	-4.17077440	0.20486362	H	-5.34386075	-4.08470288	0.11307589
H	-2.31563008	-4.65582572	3.48881006	H	-2.95541764	-5.14037193	3.63686335	H	-3.11061813	-5.14347674	3.63349330
H	-4.39642252	-5.46051655	2.38598646	H	-4.74337667	-5.75806429	2.01987581	H	-4.84756060	-5.70005312	1.94034745
H	-0.21833964	-0.79798477	1.56859948	H	-0.10094450	-1.18430871	3.2387557	H	-0.06581159	-1.34388830	2.37860907
H	-1.18284986	-2.41733919	-0.77997491	H	-0.77558873	-2.49647171	-0.23251718	H	-0.72309400	-2.53538263	-0.20064051
H	-0.11689704	-0.65386107	-2.28346407	H	-0.66522435	-0.77127043	-1.77264275	H	-0.70019758	-0.81782209	-1.73157149
H	3.06180569	-3.83835076	0.20465428	H	3.53151527	-3.31115919	-0.32285999	H	3.58642601	-3.26114972	-0.38370134
H	3.58556866	-3.28142520	-1.41812530	H	3.44402203	-2.85345006	-2.05621521	H	3.45352987	-2.78924170	-2.11066745
H	3.93662149	-2.28843308	0.01215907	H	4.08884528	-1.70186619	-0.86490413	H	4.10044975	-1.63649303	-0.92134741
H	3.11166609	2.42233062	0.90315250	H	3.05214337	1.97671225	1.75712330	H	2.96324243	2.01675460	1.79676087
H	2.71975113	1.45881291	2.33665334	H	2.05895836	1.05213384	2.88801439	H	1.99631964	1.03671038	2.90400785
H	4.65709979	0.58121056	0.10085208	H	4.43506270	-0.06723028	1.26700412	H	4.41619086	0.02961862	1.27417706
H	5.16389825	1.21305674	1.68429139	H	4.42862443	0.25524707	3.01074138	H	4.39303039	0.32037672	3.02341566
H	4.31315759	-0.33979155	1.58222708	H	3.40446732	-1.03582812	2.34313190	H	3.41562942	-0.99256655	2.32893118
H	-1.99815970	0.76589704	-1.39015913	H	-1.95632268	1.17108328	-1.32579184	H	-1.95914895	1.14505100	-1.38915495
H	-1.53381976	2.07155075	-0.30007659	H	-1.22581288	2.55476273	-0.48818123	H	-1.25496388	2.53570470	-0.54111685
H	-0.13856927	1.36610260	-2.93380489	H	-0.19095872	1.40210769	-3.13238181	H	-0.15467341	1.37595924	-3.15507260
H	-0.71747640	4.57980585	-1.00698815	H	-0.44327198	4.76775571	-1.38247418	H	-0.45049043	4.73503890	-1.39824884
H	2.10305568	1.82753654	-2.73265808	H	2.04337785	1.87053312	-3.35668692	H	2.07645310	1.86453934	-3.35959264
H	3.93520704	3.41467407	-2.26212784	H	3.96745177	3.41845016	-3.19962098	H	3.99034625	3.42188017	-3.16777961
H	1.11047763	6.15502361	-0.52381468	H	1.47288922	6.30370693	-1.21122459	H	1.45476926	6.28029843	-1.19261773
H	3.45289086	5.59166108	-1.14955418	H	3.69387920	5.64686133	-2.12275300	H	3.69087356	5.64152004	-2.08000128
H	-2.25277744	3.51812822	-2.38785817	H	-2.13172569	3.74876255	-2.71766253	H	-2.10871436	3.72119340	-2.79389202
H	-1.34393748	3.32952785	-3.89477031	H	-1.38783513	3.29455138	-4.25777753	H	-1.33019597	3.26072938	-4.31484286
H	-2.45429336	2.05346209	-3.35751877	H	-2.51376362	2.18358018	-3.45201074	H	-2.47240411	2.15196102	-3.52946901

Table S7b Molecular structure plots, computed energies (excerpts from the *Gaussian* output) and atomic coordinates (in Å) for the intrinsic reaction coordinate **TS2** (for details, see also Table S7a).

	starting geometry	transition state	product geometry
TS2			
			N/A
			N/A
	SCF Energy: E(UB3LYP) = -1442.46611609 A.U. Zero-point correction= 0.554673 Thermal correction to Energy= 0.588399 Thermal correction to Enthalpy= 0.589343 Thermal correction to Gibbs Free Energy= 0.484440 Sum of electronic and zero-point Energies= -1441.911443 Sum of electronic and thermal Energies= -1441.877717 Sum of electronic and thermal Enthalpies= -1441.876773 Sum of electronic and thermal Free Energies= -1441.981676		
	SCF Energy: E(UB3LYP) = -1442.46085342 A.U. Zero-point correction= 0.553786 Thermal correction to Energy= 0.586915 Thermal correction to Enthalpy= 0.587859 Thermal correction to Gibbs Free Energy= 0.484974 Sum of electronic and zero-point Energies= -1441.907067 Sum of electronic and thermal Energies= -1441.879398 Sum of electronic and thermal Enthalpies= -1441.872994 Sum of electronic and thermal Free Energies= -1441.975879		
	SCF Energy: E(UB3LYP) = -1442.50422099 A.U. Zero-point correction= 0.556227 Thermal correction to Energy= 0.590241 Thermal correction to Enthalpy= 0.591185 Thermal correction to Gibbs Free Energy= 0.483792 Sum of electronic and zero-point Energies= -1441.947994 Sum of electronic and thermal Energies= -1441.913980 Sum of electronic and thermal Enthalpies= -1441.913036 Sum of electronic and thermal Free Energies= -1442.020429		
	Imaginary frequency: -601.6774 cm ⁻¹		
	C -3.36496618 -0.06373346 3.99316726 C -2.02475330 -0.73806646 3.69181622 C -1.75466962 -0.97254439 2.18338908 C -2.78363373 -1.91217931 1.55141343 C -3.76027544 -1.42838846 0.67178230 C -2.77971831 -3.2835183 1.85115516 C -4.70904793 -2.28488920 0.10750508 C -3.72412711 -4.14236730 1.28934379 C -4.69338467 -3.64545912 0.41416001 C -0.34161008 -1.43286178 1.96553128 C -0.07262772 0.58233747 -0.34233398 C 0.16958710 -1.86927498 0.63680468 C 0.13624341 -0.88215761 -0.60727861 C 1.61823817 -2.34841270 0.69138030 C 1.47604047 -1.18358668 -1.31592730 O 2.15964776 -2.95079421 1.59585854 O 1.82556897 -0.77770996 -2.40660084 N 2.23117991 -2.02970501 -0.51691557 C 3.59230002 -2.40775852 -0.85455931 C 0.72802705 1.31460246 0.63511537 O 0.45147031 2.42471806 1.06675449 O 1.82603128 0.61654022 1.03927609 C 2.64923174 1.25918332 2.03941647 C 3.87283255 0.38907595 2.25867844 C -1.12313489 1.33050886 -1.10062521 C -0.67567896 1.77436879 -2.53524491 C 0.41116803 2.84174868 -2.50268815 C 0.16153427 4.1242003 -1.99194208		
	C -2.45492807 0.06462210 4.07011309 C -1.35906933 -0.89836508 3.60791175 C -1.33813098 -1.15020029 2.07926681 C -2.62162630 -1.80754237 1.57601648 C -3.59797573 -1.06269292 0.90224678 C -2.86245227 -3.17069682 1.80695124 C -4.78580626 -1.65924786 0.47223899 C -4.04660200 -3.76935687 1.37783057 C -5.01362299 -3.01482560 0.70904841 C -0.09453703 -1.85297537 1.64833579 C 0.05836412 0.49028690 0.13220990 C 0.175738907 -0.76537678 -0.78858097 C 1.35717464 -3.04744364 0.05323723 C 2.08614602 -0.99904159 0.86344434 O 1.44717883 -4.23002965 0.31737763 O 2.89800041 -0.22615653 -1.32876436 N 2.40306531 -2.29605707 -0.46337542 C 3.72966381 -2.86968134 -0.64760718 C 0.60639110 1.3555842 0.58965066 O 0.25986268 2.49369190 0.86642814 O 1.55482327 0.67928369 1.30690970 C 2.21363792 1.44044482 2.34100006 C 3.33890573 0.58719939 2.89631865 C -1.07015562 1.10666492 -1.30582244 C -0.63889946 1.64783407 -2.70830937 C 0.26033406 2.87350688 -2.60435158 C -0.26211764 4.14961036 -2.34987175		
	C -2.77676366 -1.97903238 4.17502154 C -1.50372846 -2.25136719 3.36922821 C -1.49834136 -1.58144767 1.96707934 C -2.62536033 -2.06112733 1.06518354 C -3.52017578 -1.14124310 0.50327189 C -2.80136389 -3.42178141 0.76970252 C -4.55942588 -1.56079622 -0.32973332 C -3.83802390 -3.84582007 -0.06212555 C -4.72157121 -2.91649334 -0.61532347 C -0.11810000 -1.67646863 1.35410735 C 0.67803830 1.77254004 0.27979646 C 0.20624879 -2.15437017 0.14487174 C 1.17540195 0.63138600 -0.22156071 C 1.59808775 -2.31617183 -0.34636523 C 2.41382211 -0.01724057 0.29852604 O 1.91014044 -3.30050567 -1.00090321 O 3.30518060 0.63357059 0.82719170 N 2.59046266 -1.39197386 0.04594872 C 3.97044202 -1.90140207 0.02030885 C 1.25073381 2.41568925 1.51482251 O 1.58690313 3.57980778 1.56292797 O 1.24877846 1.58111644 2.57401837 C 1.89218433 2.08962515 3.76754005 C 1.83424242 0.99688005 4.81758215 C -0.46536152 2.56722447 -0.31082466 C -1.14395479 2.04187403 -1.59040539 C -0.24503033 1.99645947 -2.82223006 C 0.61082474 3.05494275 -3.15772373		

C	1.68917358	2.56445644	-3.00583694	C	1.64745323	2.74305887	-2.75215958	C	-0.30893371	0.89752333	-3.69066043
C	2.68667161	3.54257745	-3.00733273	C	2.48761117	3.85412810	-2.65672714	C	0.45969827	0.85050555	-4.85480922
C	1.15481066	5.10241400	-1.99215097	C	0.57351314	5.26208189	-2.25711549	C	1.38187011	3.01208071	-4.31979865
C	2.42259369	4.81585143	-2.50331260	C	1.95345582	5.11938880	-2.41377886	C	1.30994725	1.90978808	-5.17338495
C	-1.90492427	2.22849762	-3.34397051	C	-1.88385405	1.88865725	-3.58012938	C	-2.40052414	2.88947076	-1.88482498
H	-3.48886583	0.08785623	5.07118175	H	-2.40642987	0.21300525	5.15448696	H	-2.72037483	-2.45237033	5.16146763
H	-3.43075232	0.91892024	3.51002797	H	-2.34427399	0.04650243	3.59395922	H	-2.92416730	-0.90283807	4.32912824
H	-4.20790539	-0.66712218	3.63997421	H	-3.45277335	-0.31530994	3.82770833	H	-3.66442205	-2.36753964	3.66541433
H	-1.96458876	-1.70113245	4.21609668	H	-1.46677166	-1.86239311	4.12243599	H	-1.35602281	-3.33260516	3.25470152
H	-1.20823187	-0.11848832	4.08596849	H	-0.37832196	-0.49752760	3.89742685	H	-0.63240303	-1.88266957	3.92689197
H	-1.87696399	0.00739513	1.68358669	H	-1.27992379	-0.15409836	1.57863601	H	-1.65445168	-0.50450792	2.14569400
H	-3.78277707	-0.36731259	0.43232995	H	-3.42843480	-0.00473773	0.71648365	H	-3.40499408	-0.08230483	0.72645057
H	-2.02529434	-3.67912015	2.52771195	H	-2.10922999	-3.76732796	2.31598656	H	-2.11878439	-4.15729601	1.18732676
H	-5.45914455	-1.88694123	-0.57117101	H	-5.53042754	-1.06296384	-0.04865557	H	-5.24259888	-0.82801103	-0.75117232
H	-3.70334012	-5.20117415	1.53451297	H	-4.21294694	-4.82728902	1.56326421	H	-3.95465666	-4.90439253	-0.27888271
H	-5.42875291	-4.31440436	-0.02469777	H	-5.93567704	-3.48180753	0.37353179	H	-5.52951443	-3.24754742	-1.26211826
H	0.35235444	-1.44450277	2.79990075	H	0.74758938	-1.86305661	2.33562172	H	0.67068527	-1.28461475	1.99510703
H	-0.41498871	-2.74644237	0.31008721	H	-0.75506113	-2.55548778	-0.22920234	H	-0.54005013	-2.60034553	-0.50563127
H	-0.64862061	-1.20031150	-1.30078596	H	0.15918962	-1.13394716	-1.73230409	H	0.73488551	0.19907713	-1.11243222
H	3.90928681	-3.16766961	-0.13964970	H	3.65922063	-3.77829283	-1.25103368	H	4.31868438	-2.00841747	-1.01137580
H	3.61864777	-2.80053767	-1.87345345	H	4.34519136	-2.12281962	-1.14871378	H	4.59591395	-1.19227639	0.55802739
H	4.25946180	-1.54231288	-0.79286070	H	4.16676828	-3.12791159	0.32108849	H	4.00440646	-2.88201361	0.49801344
H	2.90998041	2.26149813	1.68712364	H	2.58384532	2.37308670	1.90514004	H	2.92121124	2.35858226	3.51132101
H	2.05827849	1.37374291	2.95477958	H	1.47923313	1.70581525	3.10958869	H	1.37433703	2.99927653	4.08773922
H	4.46915088	0.31748520	1.34276479	H	4.05197995	0.32685671	2.10772134	H	2.36206989	0.10099144	4.47517051
H	4.50190461	0.82740352	3.04122351	H	3.87352443	1.13894945	3.67732119	H	2.31023949	1.34366582	5.74128667
H	3.58875876	-0.62227076	2.56590179	H	2.95527480	-0.33972484	3.33665442	H	0.79818255	0.72575947	5.04754356
H	-2.00798887	0.68858415	-1.21646536	H	-1.82409332	0.32294539	-1.47294884	H	-1.23874685	2.66666086	0.46659301
H	-1.41902364	2.21517090	-0.52879184	H	-1.54960813	1.91738561	-0.74863716	H	-0.09820336	3.59169358	-0.45804450
H	-0.25220373	0.89334371	-3.03187230	H	-0.05030681	0.85583964	-3.19164368	H	-1.48421560	1.01595346	-1.39133458
H	-0.81675549	4.36469100	-1.58320609	H	-1.33292297	4.28197848	-2.21844181	H	0.68526874	3.92262422	-2.50745558
H	1.90541362	1.56948100	-3.38412730	H	2.07868667	1.75977785	-2.91909747	H	-0.97006116	0.06673677	-3.45055105
H	3.67099053	3.30573378	-3.40380159	H	3.56091078	3.72660518	-2.77313234	H	0.39567858	-0.01532696	-5.50870253
H	0.93927214	6.08887123	-1.58953752	H	0.14543230	6.24173946	-2.05990384	H	2.04307358	3.84172866	-4.55612204
H	3.19710483	5.57858462	-2.50453245	H	2.60518432	5.98643702	-2.34263183	H	1.91343350	1.87594645	-6.07639971
H	-2.40717557	3.08048522	-2.87119353	H	-2.57450065	2.60198305	-3.11606940	H	-2.13099394	3.93445346	-2.07779578
H	-1.61088884	2.53361382	-4.35372141	H	-1.60307367	2.28587439	-4.56120036	H	-2.92377346	2.51172830	-2.76903824
H	-2.63653287	1.41615363	-3.43188249	H	-2.43457285	0.95297156	-3.73419595	H	-3.09783445	2.86980029	-1.03826030

Table S7c Molecular structure plots, computed energies (excerpts from the *Gaussian* output) and atomic coordinates (in Å) for the intrinsic reaction coordinate **TS3** (for details, see also Table S7a).

	starting geometry	transition state	product geometry
TS3			
			N/A
			N/A
SCF Energy: E(UB3LYP) = -1442.46610195 A.U. Zero-point correction= 0.554707 Thermal correction to Energy= 0.588366 Thermal correction to Enthalpy= 0.589310 Thermal correction to Gibbs Free Energy= 0.484209 Sum of electronic and zero-point Energies= -1441.911395 Sum of electronic and thermal Energies= -1441.877736 Sum of electronic and thermal Enthalpies= -1441.876792 Sum of electronic and thermal Free Energies= -1441.981893			
SCF Energy: E(UB3LYP) = -1442.44831941 A.U. Zero-point correction= 0.554227 Thermal correction to Energy= 0.587148 Thermal correction to Enthalpy= 0.588092 Thermal correction to Gibbs Free Energy= 0.485703 Sum of electronic and zero-point Energies= -1441.894093 Sum of electronic and thermal Energies= -1441.861171 Sum of electronic and thermal Enthalpies= -1441.860227 Sum of electronic and thermal Free Energies= -1441.962617			
SCF Energy: E(UB3LYP) = -1442.52908585 A.U. Zero-point correction= 0.561402 Thermal correction to Energy= 0.593279 Thermal correction to Enthalpy= 0.594223 Thermal correction to Gibbs Free Energy= 0.494186 Sum of electronic and zero-point Energies= -1441.967683 Sum of electronic and thermal Energies= -1441.935807 Sum of electronic and thermal Enthalpies= -1441.934862 Sum of electronic and thermal Free Energies= -1442.034900			
Imaginary Frequency: -64.2250 cm ⁻¹			
C -3.23905405 -0.22182948 4.11482186 C -1.83795947 -0.73539417 3.77650006 C -1.61286650 -0.13676944 2.27288404 C -2.54332618 -0.13604625 1.75633162 C -3.60116633 -0.183924315 0.88779908 C -2.36087959 -0.374109218 2.14983621 C -4.45688759 -0.84252463 0.42578652 C -3.21200403 -0.47579684 1.69060742 C -4.26453477 -0.16481717 0.82571917 C -0.16441667 -1.33854295 0.20888859 C -0.14845445 0.58474685 -0.38142961 C 0.33569818 -1.79245200 0.68162430 C 0.16976315 -0.86843098 -0.59836061 C 1.82143404 -2.14258277 0.69617402 C 1.50056489 -0.09072205 -1.35246113 O 2.44727835 -2.65364316 1.60229526 O 1.76988766 -0.71003864 -2.47465931 N 2.35672399 -1.82324215 -0.55049109 C 3.73203416 -2.10597107 -0.92884118 C 0.62319727 1.42135902 0.53388551 O 0.26979624 2.52264477 0.93058138 O 1.79025341 0.8533613 0.9207960 C 2.58919950 1.58594805 1.86485247 C 3.88144409 0.82176011 2.08538913 C -1.28250466 1.21423383 -1.12698495 C -0.91746463 1.64501458 -2.58888722			
C -3.53459410 -0.37316132 4.05936067 C -2.16419539 -1.00694004 3.80987092 C -1.82287739 -1.22278130 2.31374618 C -2.80221619 -0.17209771 1.62356058 C -3.76608952 -1.69381354 0.72663430 C -2.76730527 -3.55081264 1.88568180 C -4.67140126 -2.56121444 0.11005078 C -3.66799085 -4.42101637 1.27202455 C -4.62474301 -3.92881125 0.38057118 C -0.39450089 -1.65013208 2.15683208 C -0.03809821 0.51369933 -0.10259037 C 0.18895369 -1.97453344 0.82936351 C 0.07607029 -0.95543258 -0.38886291 C 1.67923760 -2.30489179 0.89062597 C 1.38315936 -1.24169572 -1.16293003 O 2.28116436 -2.85335630 1.78859336 O 1.64143682 -0.92838881 -2.30877319 N 2.25976109 -1.90218714 -0.31757460 C 3.63485227 -2.20184055 -0.68661832 C 0.86266069 1.15155232 0.90047604 O 0.68226988 1.09972975 2.10421696 O 1.89454719 1.80342255 0.33574014 C 2.79665888 2.48625033 1.24704139 C 3.94568660 3.03931481 0.42725151 C -1.04389549 1.34755122 -0.84772492 C -0.70320259 1.66702088 -2.34241798			
C -3.16165480 0.57706297 3.78052186 C -1.75741786 0.15010049 3.34240287 C -1.74641367 -0.71370580 2.05920050 C -2.51517879 -2.01808487 2.22565084 C -3.63839366 -2.29030717 1.43210531 C -2.12478237 -2.98078267 3.17047685 C -4.35086867 -3.48310178 1.57258797 C -2.8170187 -4.17483167 3.31210931 C -3.94812919 -4.43115345 2.51329073 C -0.29189646 -0.98958352 1.59364499 C -0.31103387 0.58587646 -0.77585938 C -0.17523833 -1.76861867 0.28209216 C -0.35861769 -0.92153911 -1.00473781 C 1.20944958 -2.40318044 0.15363443 C 0.79258873 -1.41250413 -1.90671246 O 1.81140104 -3.02357561 1.00611015 O 0.96236502 -1.19495559 -3.09099227 N 1.66094345 -2.18269183 -1.14183417 C 2.90638523 -2.72235150 -1.66468009 C 0.09216976 1.03974201 0.42649369 O 0.46555733 0.23398426 1.46926218 O 0.08158556 2.35353624 0.75266510 C 1.25013587 2.86832358 1.43147796 C 0.94750766 4.30030089 1.82918500 C -0.86399733 1.52729881 -1.82655770 C 0.03920986 1.88473201 -3.04338569			

C	0.08353403	2.79379034	-2.62423014	C	0.37112076	2.73485729	-2.50097951	C	1.32923059	2.58484681	-2.63760994
C	-0.25428551	4.07217477	-2.15572824	C	0.15716474	4.05446303	-2.07554076	C	1.33173235	3.89674959	-2.13880021
C	1.36882012	2.59559762	-3.14565868	C	1.58844150	2.42721030	-3.12183788	C	2.56186854	1.93169547	-2.77458241
C	2.28757552	3.64633266	-3.20632158	C	2.55873425	3.41070400	-3.32400276	C	3.75783083	2.56319259	-2.42402404
C	0.66034630	5.12255478	-2.21469733	C	1.12577855	5.03904983	-2.27040998	C	2.52348392	4.53379920	-1.79116250
C	1.93592963	4.91430474	-2.74412684	C	2.33132663	4.72134147	-2.90125163	C	3.74416004	3.86806811	-1.93093751
C	-2.20353633	1.97819526	-3.36718415	C	-1.99143951	2.05476556	-3.09477389	C	-0.77093603	2.71544353	-4.05678754
H	-3.32545313	-0.01017747	5.18636148	H	-3.70422842	-0.22578521	5.13189411	H	-3.11298669	1.20557576	4.67674291
H	-3.46234235	0.70645565	3.57443394	H	-3.61052516	0.60794111	3.57407539	H	-3.66062262	1.15824279	2.99510031
H	-4.01058501	-0.95406410	3.85435012	H	-4.34646278	-0.99957478	3.67453749	H	-3.79484697	-0.28661719	4.00942618
H	-1.62398483	-1.64429089	4.35475260	H	-2.09889813	-1.97100610	4.33205463	H	-1.26791650	-0.40333826	4.15570918
H	-1.09224922	0.0105009	4.08328850	H	-1.38175103	-0.36554091	4.23462339	H	-1.14488419	1.03857162	3.15986224
H	-1.88005710	-0.11601924	1.72038891	H	-1.92812627	-0.23718827	1.82026279	H	-2.24068769	-0.13512432	1.26753917
H	-3.76116036	-0.80924383	0.57558055	H	-3.81354617	-0.62730347	0.51574881	H	-3.96170210	-1.55482828	0.69849719
H	-1.53965840	-3.72220230	2.81746432	H	-2.02158291	-3.94124621	2.57468340	H	-1.26038055	-2.79928144	3.80423604
H	-5.27256107	-2.58854207	-0.24634770	H	-5.41180191	-2.16665777	-0.58129803	H	-5.22031045	-3.66863544	0.94725175
H	-3.05306379	-5.50343385	2.00730620	H	-3.62288010	-5.48526118	4.48917357	H	-2.50895582	-4.90653515	4.04806443
H	-4.92718392	-4.94769257	0.46676672	H	-5.32608749	-4.60645485	-0.09891758	H	-4.49903537	-5.36108922	2.62488418
H	0.56024582	-1.22274852	2.80854584	H	0.28533657	-1.54216823	2.99450177	H	0.23918560	-1.54820356	2.36893458
H	-0.18060562	-2.73113464	0.41752730	H	-0.29276341	-2.89003227	0.44252415	H	-0.89232367	-2.59698239	0.29944901
H	-0.61389964	-1.27859450	-1.24324533	H	-0.75878950	-1.23727825	-1.03748997	H	-1.29270357	-1.17111955	-1.52440594
H	4.14778162	-2.78394643	-0.18281290	H	4.11511992	-2.65545056	0.18107088	H	3.28804180	-3.43941906	-0.93699113
H	3.75282113	-2.56369479	-1.92052326	H	3.65888543	-2.89288983	-1.53431088	H	2.71899573	-3.20759022	-2.62530641
H	4.31685790	-1.81294111	-0.95503945	H	4.15147072	-2.8132761	-0.97017983	H	3.63753979	-1.92141021	-1.81103053
H	2.76275498	2.58681900	1.45861456	H	2.23659271	3.27617461	1.75804324	H	1.46438275	2.24871822	2.30738024
H	2.01680141	1.70005396	2.79195463	H	3.13155658	1.77271743	2.00595271	H	2.10229511	2.81823463	0.74311265
H	4.45529968	0.74991073	1.15527436	H	3.58312705	3.73169727	-0.33766358	H	0.08279093	4.34281767	2.49960289
H	4.49710691	1.34372807	2.82615224	H	4.64161405	2.7276185	1.08445335	H	1.81023786	4.73337068	2.34729746
H	3.68406320	-0.19181183	2.44803858	H	4.49325683	2.23284647	-0.07124972	H	0.73309631	4.90902476	0.94563735
H	-2.11249319	0.49638468	-1.19309339	H	-1.99801319	0.79830435	-0.84746098	H	-1.78468469	1.08063783	-2.23307836
H	-1.63482226	2.09033824	-0.57432147	H	-1.22577574	2.28734252	-0.31222274	H	-1.16341370	2.45784784	-1.33307275
H	-0.44251526	0.78349310	-3.07296472	H	-0.31622949	-0.74527969	-2.79059616	H	0.3485133	0.94697778	-3.53210975
H	-1.23966427	4.25254494	-1.73329012	H	-0.78006468	4.32358127	1.59305931	H	0.39198486	4.43096049	-2.02320752
H	1.65352207	1.60600735	-3.49134114	H	1.77837324	1.40468270	-3.43556411	H	2.57945027	0.91762710	-3.16553314
H	3.27912740	3.47017814	-3.61617057	H	3.49422091	3.15074379	-3.81326742	H	4.70134844	2.03589074	-2.54317042
H	0.37757769	6.10441434	-2.84368401	H	0.93620695	6.0561679	-1.93695497	H	2.50046233	5.55430292	-1.41608083
H	2.64900596	5.73340672	-2.79132379	H	3.08307512	5.48956110	-3.06404926	H	4.67331200	4.36491736	-1.66372381
H	-2.75475130	2.80291315	-2.90080546	H	-2.46674518	2.93977659	-2.65507255	H	-1.13487699	3.65333123	-3.61992388
H	-1.96639522	2.27450772	-4.39432732	H	-1.77298319	2.28187634	-4.14337757	H	-0.16219938	2.96911226	-4.93127888
H	-2.87233469	1.10989038	-3.40764019	H	-2.72047096	1.23593523	-3.06735950	H	-1.64543522	2.15225729	-4.40431247

Table S7d Molecular structure plots, computed energies (excerpts from the Gaussian output) and atomic coordinates (in Å) for the intrinsic reaction coordinate **TS4** (for details, see also Table S7a).

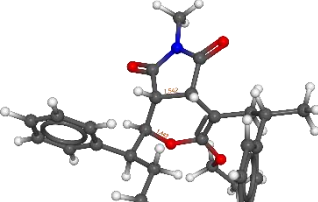
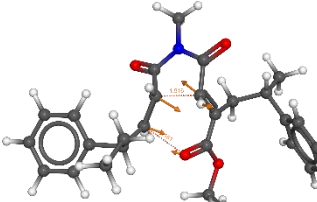
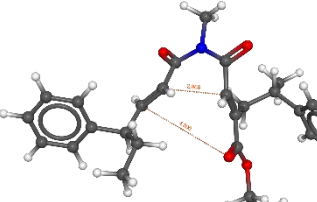
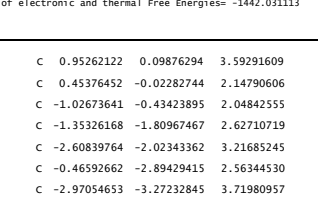
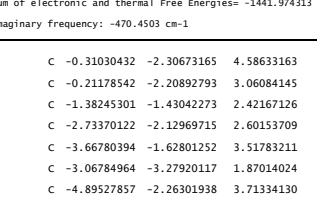
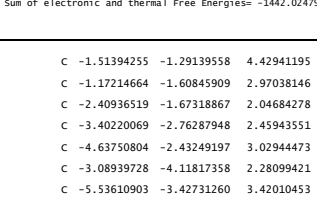
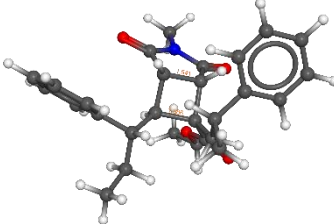
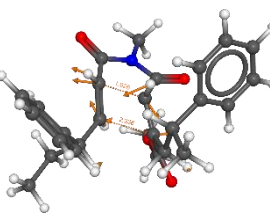
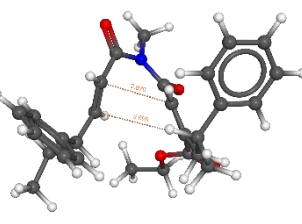
starting geometry	transition state	product geometry
 SCF Energy: E(UB3LYP) = -1442.52566438 A.U. Zero-point correction: 0.561362 Thermal correction to Energy= 0.593294 Thermal correction to Enthalpy= 0.594238 Thermal correction to Gibbs Free Energy= 0.494551 Sum of electronic and zero-point Energies= -1441.964303 Sum of electronic and thermal Energies= -1441.932371 Sum of electronic and thermal Enthalpies= -1441.931427 Sum of electronic and thermal Free Energies= -1442.031113 Imaginary frequency: -470.4503 cm^-1	 SCF Energy: E(UB3LYP) = -1442.46184547 A.U. Zero-point correction: 0.556161 Thermal correction to Energy= 0.588808 Thermal correction to Enthalpy= 0.589752 Thermal correction to Gibbs Free Energy= 0.487533 Sum of electronic and zero-point Energies= -1441.905685 Sum of electronic and thermal Energies= -1441.873038 Sum of electronic and thermal Enthalpies= -1441.872094 Sum of electronic and thermal Free Energies= -1441.974313	 SCF Energy: E(UB3LYP) = -1442.50989003 A.U. Zero-point correction= 0.557043 Thermal correction to Energy= 0.590891 Thermal correction to Enthalpy= 0.591835 Thermal correction to Gibbs Free Energy= 0.485093 Sum of electronic and zero-point Energies= -1441.952847 Sum of electronic and thermal Energies= -1441.918999 Sum of electronic and thermal Enthalpies= -1441.918055 Sum of electronic and thermal Free Energies= -1442.024797
 C 0.95262122 0.09876294 3.59291609 C 0.45376452 -0.02282744 2.14790606 C -1.02673641 -0.43423895 2.04842555 C -1.35326168 -1.80967467 2.62710719 C -2.60839764 -2.02343362 3.21685245 C -0.46592662 -2.89429415 2.56344530 C -2.97054653 -3.27232845 3.71980957 C -0.82238405 -4.14724205 3.06804479 C -2.07632089 -4.34193248 3.64666424 C -1.63699100 -0.31306821 0.62039121 C 0.12945626 0.90705355 -1.36062259	 C -0.31030432 -2.30673165 4.58633163 C -0.21178542 -2.20892793 3.06084145 C -1.38245301 -1.43024273 2.42167126 C -2.73370122 -2.12969715 2.60153709 C -3.66780394 -1.62801252 3.51783211 C -3.06784964 -3.27290117 1.87014024 C -4.89527857 -2.26301938 3.71334130 C -4.29555183 -3.91363501 2.06035094 C -5.21268799 -3.40993799 2.98466870 C -1.17983760 -1.10861405 0.95995415 C 0.78587923 0.59544169 -0.83227045	 C -1.51394255 -1.29139558 4.42941195 C -1.17214664 -1.60845909 2.97038146 C -2.40936519 -1.67318867 2.04684278 C -3.40220069 -2.76287948 2.45943551 C -4.63750804 -2.43249197 3.02944473 C -3.08939728 -4.11817358 2.28099421 C -5.53610903 -3.42731260 3.42010453 C -3.98385836 -5.11467199 2.67054776 C -5.21137206 -4.77232479 3.24207652 C -2.08458525 -1.82064325 0.57967082 C 0.96847368 0.85744865 -0.51547259

Table S7e Molecular structure plots, computed energies (excerpts from the *Gaussian* output) and atomic coordinates (in Å) for the intrinsic reaction coordinate **TS5** (for details, see also Table S7a).

starting geometry	transition state	product geometry
 TS5		
SCF Energy: E(RB3LYP) = -1442.53266895 A.U. Zero-point correction= 0.560010 Thermal correction to Energy= 0.592353 Thermal correction to Enthalpy= 0.593298 Thermal correction to Gibbs Free Energy= 0.492393 Sum of electronic and zero-point Energies= -1441.972659 Sum of electronic and thermal Energies= -1441.940316 Sum of electronic and thermal Enthalpies= -1441.939371 Sum of electronic and thermal Free Energies= -1442.040276	SCF Energy: E(RB3LYP) = -1442.40969779 A.U. Zero-point correction= 0.555684 Thermal correction to Energy= 0.588338 Thermal correction to Enthalpy= 0.589282 Thermal correction to Gibbs Free Energy= 0.488946 Sum of electronic and zero-point Energies= -1441.854014 Sum of electronic and thermal Energies= -1441.821360 Sum of electronic and thermal Enthalpies= -1441.820416 Sum of electronic and thermal Free Energies= -1441.920752	SCF Energy: E(RB3LYP) = -1442.50423811 A.U. Zero-point correction= 0.556099 Thermal correction to Energy= 0.590188 Thermal correction to Enthalpy= 0.591132 Thermal correction to Gibbs Free Energy= 0.483337 Sum of electronic and zero-point Energies= -1441.948139 Sum of electronic and thermal Energies= -1441.914050 Sum of electronic and thermal Enthalpies= -1441.913106 Sum of electronic and thermal Free Energies= -1442.020901
Imaginary frequency: -832.7201 cm ⁻¹		
C -1.67900692 0.24735834 1.48537846	C -1.30965714 0.07365637 2.19295660	C -1.20167731 -0.51894550 2.63715000
C -0.24278579 -0.01319821 0.98986900	C 0.01486630 -0.34854865 1.55679577	C -0.01321032 -1.07113231 1.88083028
C 0.50641807 1.07510857 0.11344491	C 0.33878230 1.21487757 -0.01216857	C 0.88977880 1.59763855 -0.51556105
O 0.03203881 -1.08490009 -0.12327507	C 0.20216487 -1.59821511 0.86847879	C -0.02412418 -1.98083657 0.89686610
C 1.02031771 -0.11069624 -0.79264056	C 0.70619588 -0.17317953 -0.30742014	C 1.13634365 0.28392479 -0.63449376
C 0.86154918 -2.27750122 0.31891087	C 1.45329477 -2.38081811 0.90506013	C 1.19551683 -2.56461937 0.28290138
C 2.39467817 -0.69487285 -0.49188792	C 2.18514118 -0.54628448 -0.41338727	C 2.37231225 -0.36843600 -0.11333859
O 0.49012392 -3.32490848 0.80666138	O 1.55369944 -0.53434559 1.29026490	O 1.22815284 -3.75436350 0.00545341
O 3.48288416 -0.20942606 -0.73065155	O 2.97093488 0.06234773 -1.11149431	O 3.43239790 0.23517342 -0.01138063
N 2.20492077 -1.94766472 0.08802756	N 2.51538291 -1.67269042 0.32275020	N 2.34347373 -1.75300252 0.12173742
C 3.31145036 -0.81262890 0.45751364	C 3.86279938 -2.25520630	C 3.6538281 -2.42098577 0.11397001
C 1.62352858 1.84655133 0.82745097	C 1.20691255 2.12676381 0.69520983	C 1.77874488 2.50445082 0.29278900
O 1.94776611 2.98922844 0.58175633	O 1.05382953 3.34275881 0.751414363	O 2.23966955 3.54008437 -0.13824015
O 2.24114258 1.09418562 1.76305330	O 2.25044084 1.51028772 1.36418020	O 1.91719498 2.08475085 1.56700551
C 3.42047730 1.68139979 2.36611847	C 3.21314894 2.39668604 1.96437891	C 2.85353687 2.84149599 2.37170470
C 3.97186696 0.68039877 3.36274584	C 4.37453350 1.55114449 2.45556498	C 2.91091804 2.18936418 3.73972195
C -0.37514716 2.10548235 -0.63275838	C -0.83540119 1.88675669 -0.70536960	C -0.25354585 2.33815266 -1.17357757
H 0.37649205 -0.24410097 1.86044261	H 0.88771354 0.05146395 2.06184183	H 0.93801525 -0.64041618 2.19099910
H -0.84803767 -1.39080585 -0.68678490	H -0.67866505 -2.15105434 0.58102953	H -0.94365549 -2.47008250 0.59042176
H 0.94310641 0.07020139 -1.86526037	H 0.13221505 -0.58515947 -1.13466845	H 0.47193819 -0.33495335 -1.22637862
H 4.13447337 1.90543586 1.56852460	H 3.53250967 3.13046814 2.12880168	H 3.82501050 2.82614271 1.86891370
H 3.13615357 2.62464582 2.84205476	H 2.73549373 2.94838405 2.78191431	H 2.51536049 3.88129995 2.42287486
C -3.03767566 1.75332841 3.08451116	C -2.25862177 0.47253095 4.56110385	C -1.98642921 0.11432114 5.01417615
C -1.65286450 2.15223260 2.66467845	C -1.07712868 -0.04563166 3.73503538	C -0.96133767 -0.64467109 4.16722984
H -2.96066225 4.46156697 3.91691303	H -2.02706553 0.41209210 5.63003450	H -1.75906802 0.01307852 6.08110297
H -3.54088460 2.26853111 2.25659972	H -2.47536641 1.52072727 4.32369469	H -1.98429180 1.18451215 4.77263412
H -3.68157533 0.92678408 3.40258257	H -3.16638405 -0.10990176 4.37797886	H -3.00086486 -0.26280741 4.84867533
H -1.15540753 0.77899610 3.52182540	H -0.86346161 -0.88883762 3.99883924	H -0.95603328 -1.70568209 4.44663100
H -1.02643795 2.11134487 2.38857539	H -0.17958521 0.53120827 3.99106805	H 0.046111434 -0.26648163 4.38642837
C -2.39830970 -1.04584864 1.85034501	C -2.55263347 -0.67819190 1.73564706	C -2.54758363 -1.07055045 2.19219811
C -3.59639287 -1.39291781 2.11186581	C -3.57059283 -0.00241003 1.04960200	C -3.45063481 -0.25503056 1.49826080
C -1.89713787 -1.91112924 2.83155231	C -2.74534300 -2.30882520 2.03045094	C -2.92312980 -2.39579017 2.46180601
C -4.27788022 -2.56633729 1.54153168	C -4.73405073 -0.66240023 4.68466388	C -4.69162890 -0.74217023 1.08275087
C -2.57202579 -3.08080331 3.16261058	C -3.90533659 -2.70220829 1.62897040	C -4.16167451 -2.88713150 2.04837611
C -3.76663208 -3.41853031 2.51979915	C -4.90331177 -2.01714857 0.93329241	C -5.051111475 -2.06175503 1.35698757
H -4.00524339 -0.73202652 0.45012401	C -3.45582465 -0.05160709 0.83267023	C -3.18071672 0.77759657 1.28666829
H -0.96462948 -1.67938233 3.33834881	H -1.98588780 -2.58909780 2.57887267	H -2.24015790 -3.05268727 2.99419078
H -5.20656119 -2.81220817 1.03291213	H -5.50774978 -0.11394364 0.11821392	H -5.37655884 -0.08895104 0.54846658
H -2.15981579 -3.74970889 3.91968930	H -4.02938035 -3.75559434 1.86517884	H -4.43156503 -3.91706179 2.26647363
H -4.29121905 -4.33462808 2.77752760	H -5.80703552 -2.53406089 0.62249942	H -6.01614495 -2.44477754 1.03646527
H -2.25447992 0.70488811 0.67525796	H -1.45620153 1.39808631 1.99127460	H -1.19846281 0.56185149 2.41822927
C -1.35791453 1.63622310 -1.73923189	C -1.51936197 1.15839646 -1.87987844	C -1.22099534 1.54479182 -2.07261888
C -0.72636607 1.38830391 -3.10815053	C -0.60029791 0.78763657 -0.04096452	C -0.58769128 0.94936019 -3.32636991
C 0.14245638 2.31387114 -3.70582846	C 0.51861083 1.55529170 -3.39316382	C 0.28925800 1.68391293 -4.13679635
C -1.07012119 0.24196488 -3.83984550	C -0.90381684 -0.33718861 3.82496628	C -0.93074832 -0.34839633 -3.73110975
C -0.55812196 0.01787798 -5.11899207	C -0.12364527 -0.68626713 -4.92842511	C -0.41268881 -0.90100395 -4.90351441
C 0.65754764 2.09396984 -4.98376026	C 1.30309625 2.1126241 -4.49583225	C 0.81050116 1.13564960 -5.30922140
C 0.31086128 0.94439868 -5.69593192	C 0.98537628 0.09419595 -5.26660884	C 0.46210684 -0.15912023 -5.69778421
C -2.48805440 2.68120592 -1.88382149	C -2.69081827 2.02004584 -2.40068383	C -2.41260259 2.44705029 -2.46049951
H -1.83329003 0.69574347 -1.43462222	H -1.96128529 0.22431176 -1.50138489	H -1.62453470 0.71289507 -1.47856640
H 0.42509163 3.21753690 -3.17244272	H 0.79379365 2.42091561 -2.79877196	H 0.57662837 2.69311003 -3.85372040
H -1.74920041 -0.4862655 -3.40012225	H -1.76778138 -0.94755507 -3.56642158	H -1.61372629 -0.93408941 -3.11834079
H -0.83790977 -0.88127656 -5.66189736	H -0.37961333 -1.55907436 -5.51857755	H -0.69056878 -1.91132663 -5.19225863
H 1.33329500 2.82343066 -5.42248314	H 2.17162273 1.81563104 -4.74333141	H 1.49344685 1.72197579 -5.91845280

H	0.71511542	0.77259014	-6.68977656	H	1.60029575	-0.17330832	-6.12381165	H	0.87115369	-0.58625247	-6.60938853
H	-2.07925487	3.66454889	-2.14361999	H	-2.32254932	2.97240449	-2.79922286	H	-2.07433922	3.31277701	-3.04177149
H	-3.18987259	2.39161368	-2.67224208	H	-3.22873251	1.50642636	-3.20443195	H	-3.13294875	1.89534747	-3.07292131
H	-3.04780010	2.78725328	-0.94597162	H	-3.40492716	2.24229862	-1.59822115	H	-2.93295703	2.81905725	-1.56947572
H	-0.95457425	2.64215133	0.12827473	H	-1.62530243	2.13422428	0.02278948	H	-0.84457505	2.81618035	-0.37690351
H	0.30010354	2.85723863	-1.04902657	H	-0.48478079	2.86995686	-1.04197653	H	0.18688401	3.17954833	-1.72481966
H	2.89590888	-3.78461398	0.72659877	H	3.86948909	-3.14818458	0.83286755	H	3.48065325	-3.49367898	0.16450829
H	4.00146562	-2.90840691	-0.38427616	H	4.13578526	-2.42909840	-0.78365761	H	4.19601170	-2.17312891	-0.80183841
H	3.85665852	-2.39440472	1.31001056	H	4.57589519	-1.50627819	0.66881068	H	4.24888498	-2.08263337	0.96618781
H	4.25961365	-0.25000528	2.86275235	H	4.84449352	1.02097273	1.62070877	H	3.25600062	1.15334920	3.66181426
H	4.86077558	1.09587974	3.84975359	H	5.12950112	2.19023709	2.92692684	H	3.60920830	2.73615841	4.38273488
H	3.23363057	0.44649648	4.13686196	H	4.04367420	0.81278968	3.19448112	H	1.92690700	2.19499287	4.22089277

NMR spectra

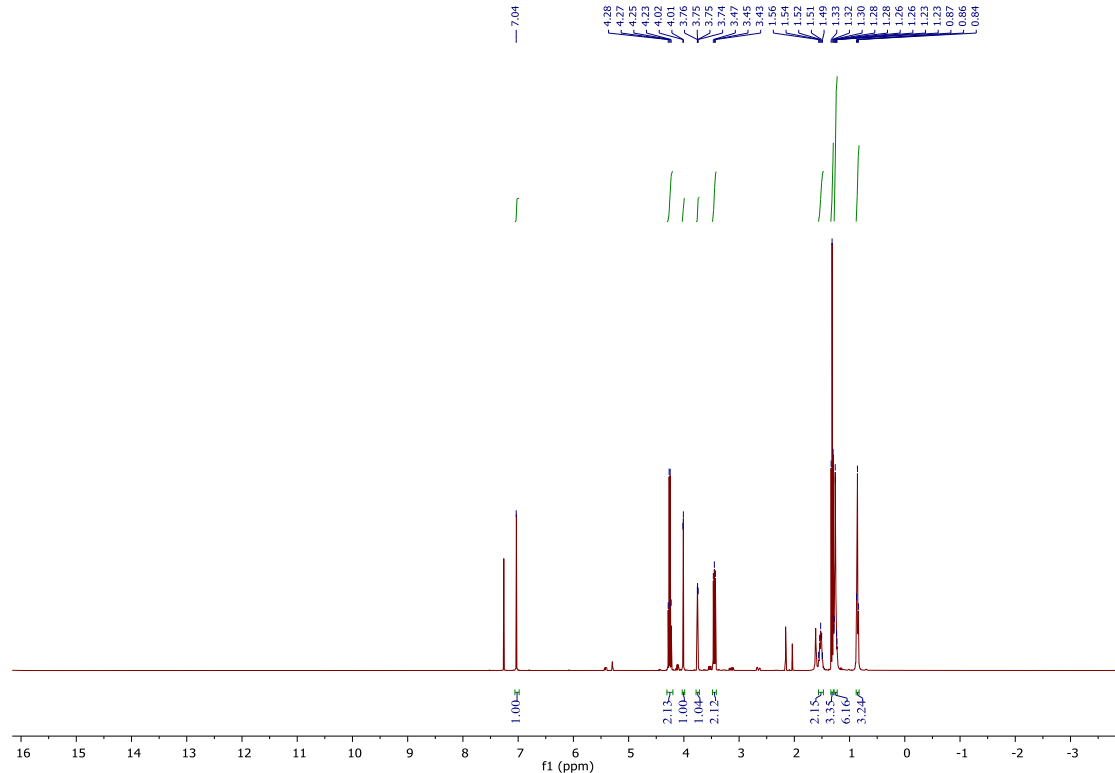


Fig. S117 ^1H NMR spectrum (400 MHz, CDCl_3) of HCBI.

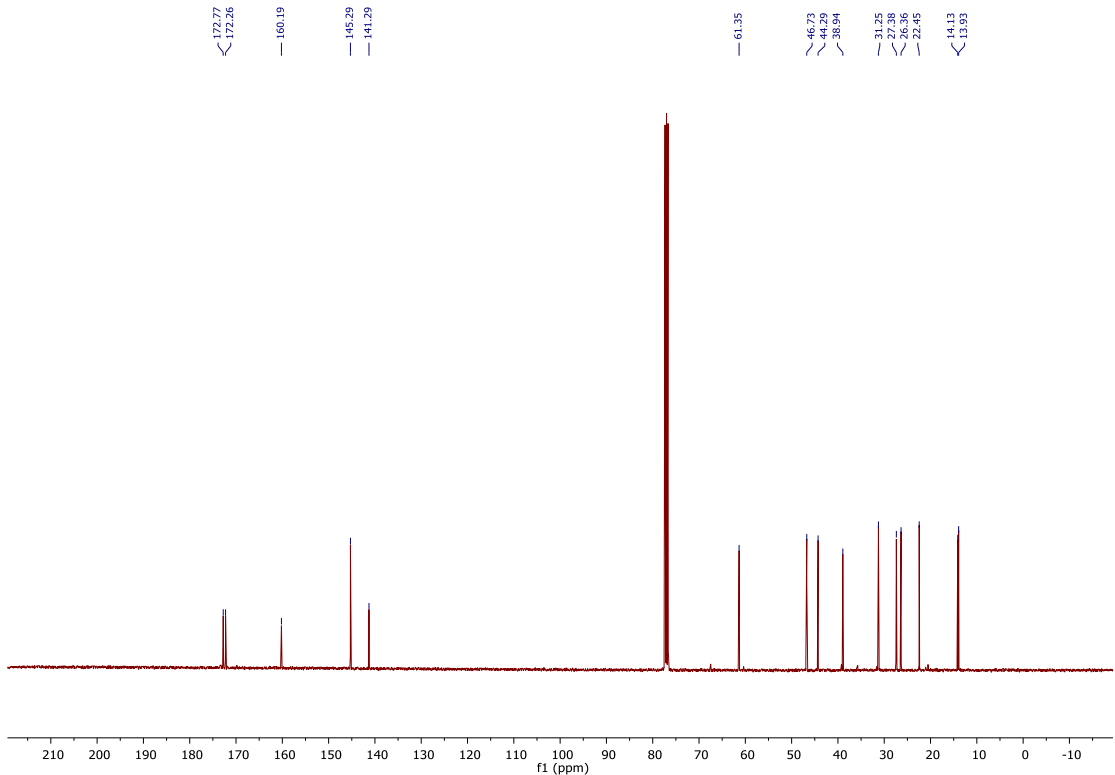


Fig. S118 ¹³C NMR spectrum (101 MHz, CDCl₃) of HCBI.

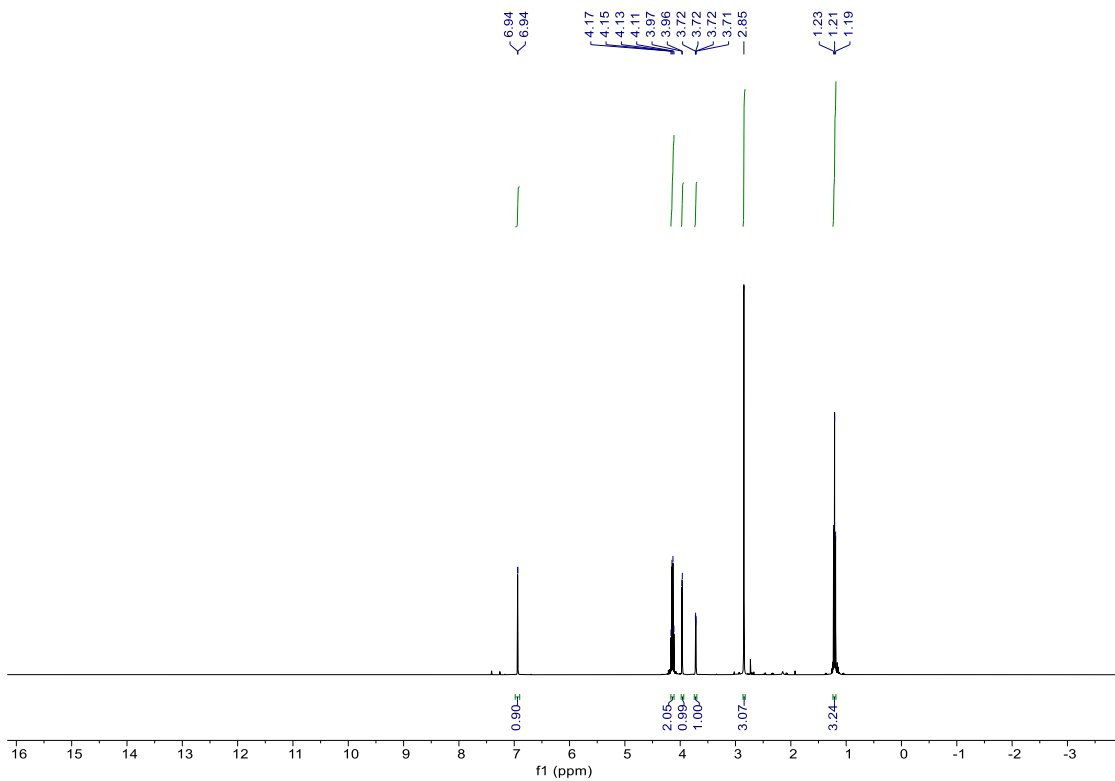


Fig. S119 ¹H NMR spectrum (400 MHz, CDCl₃) of MCBI.

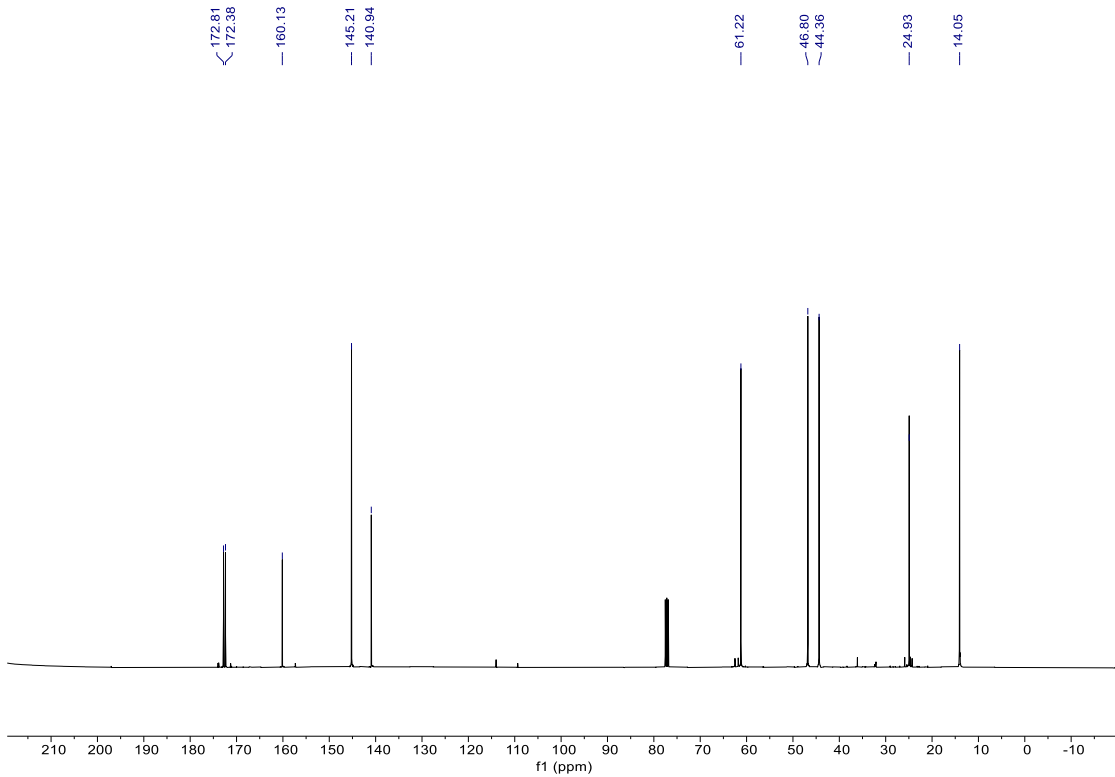


Fig. S120 ¹³C NMR spectrum (101 MHz, CDCl₃) of MCBI.

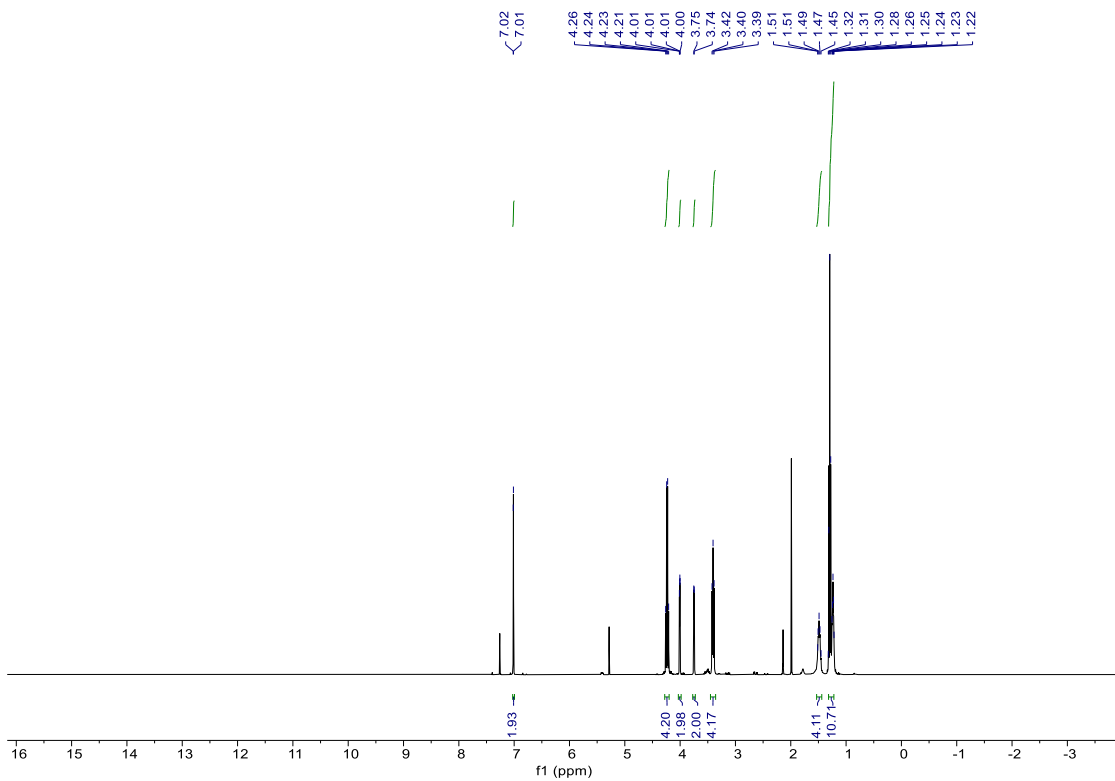


Fig. S121 ¹H NMR spectrum (400 MHz, CDCl₃) of DCBI.

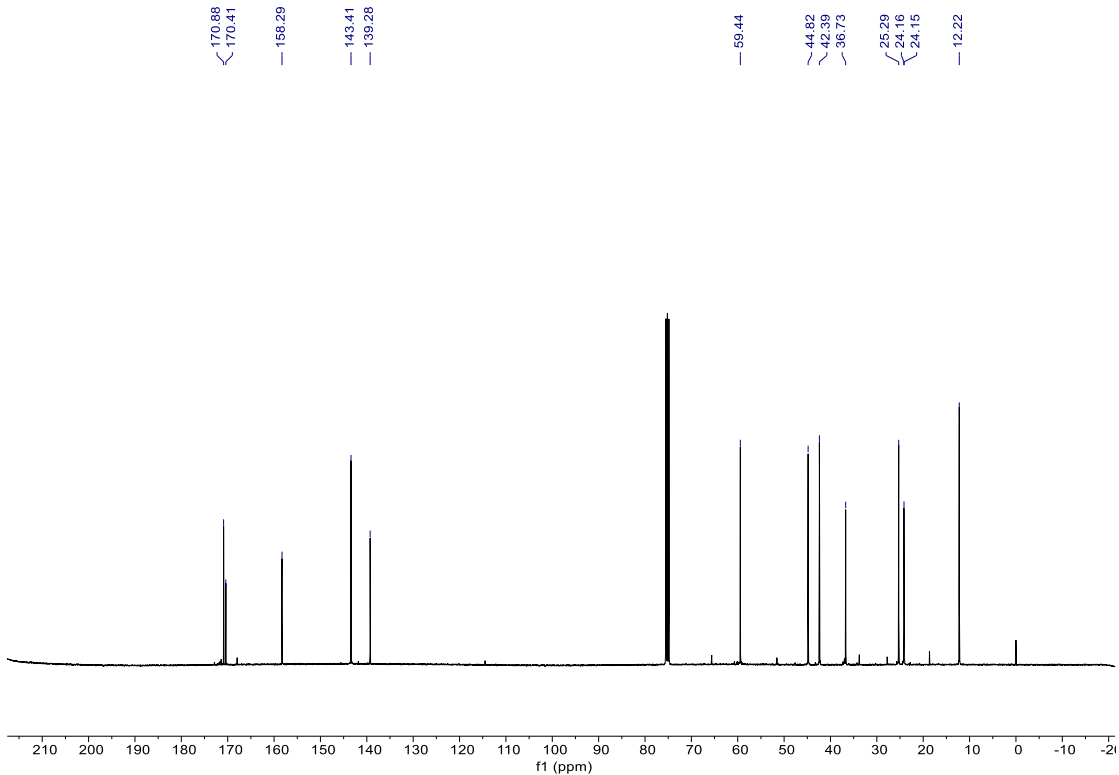


Fig. S122 ¹³C NMR spectrum (101 MHz, CDCl₃) of DCBI.

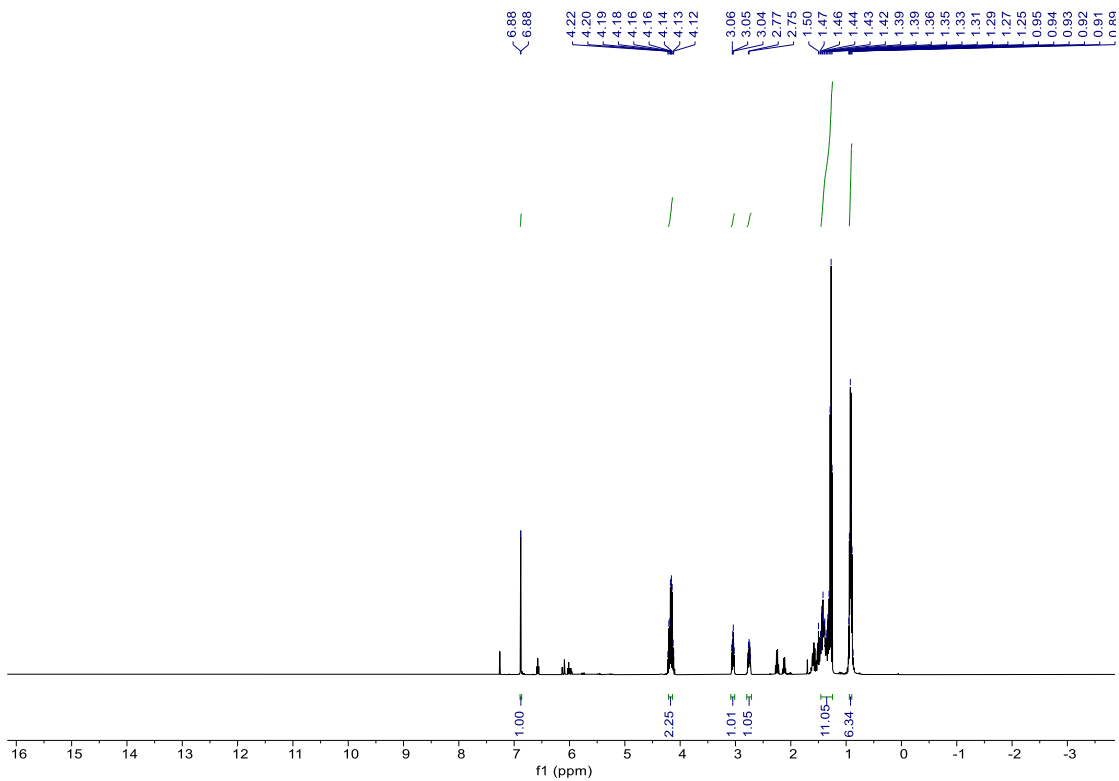


Fig. S123 ¹H NMR spectrum (400 MHz, CDCl₃) of CBO.

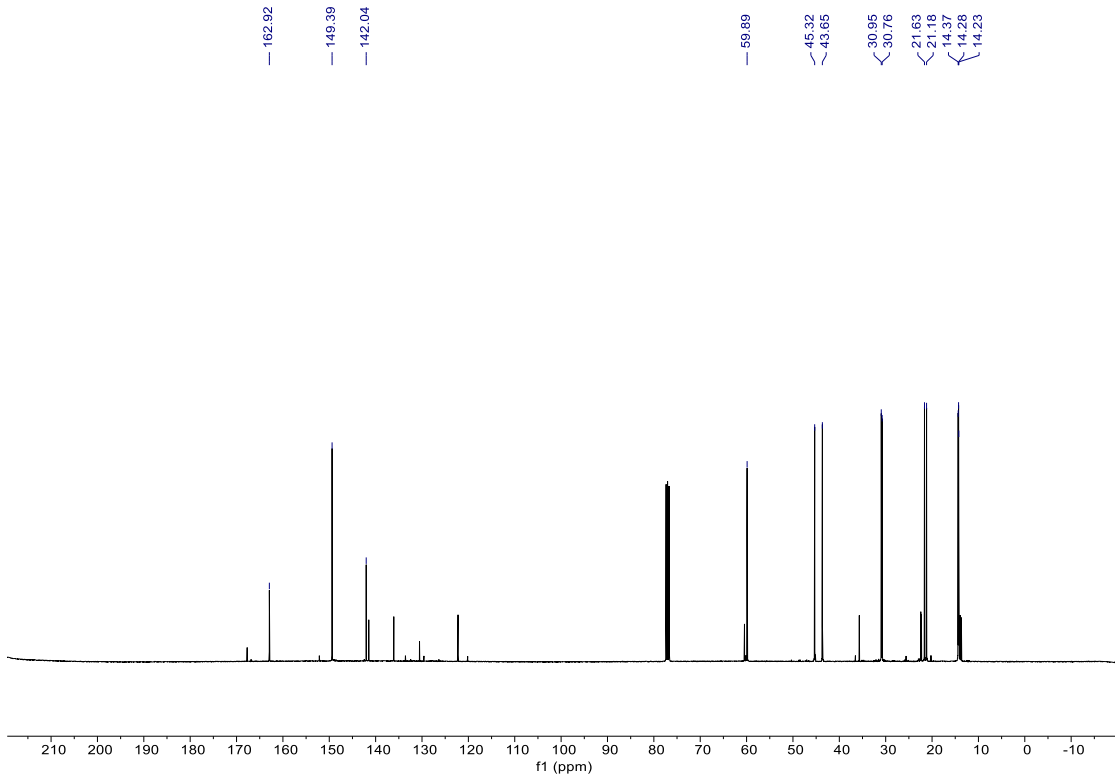


Fig. S124 ¹³C NMR spectrum (101 MHz, CDCl₃) of CBO.

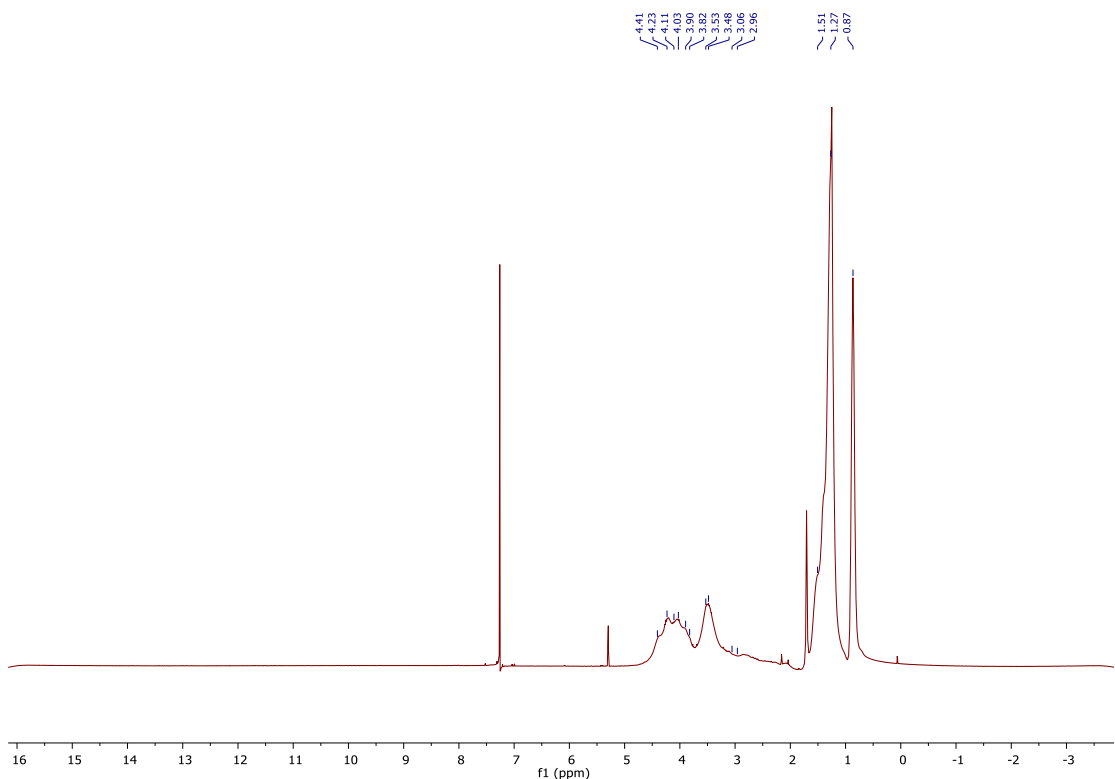


Fig. S125 ¹H NMR spectrum (400 MHz, CDCl₃) of PHCBI.

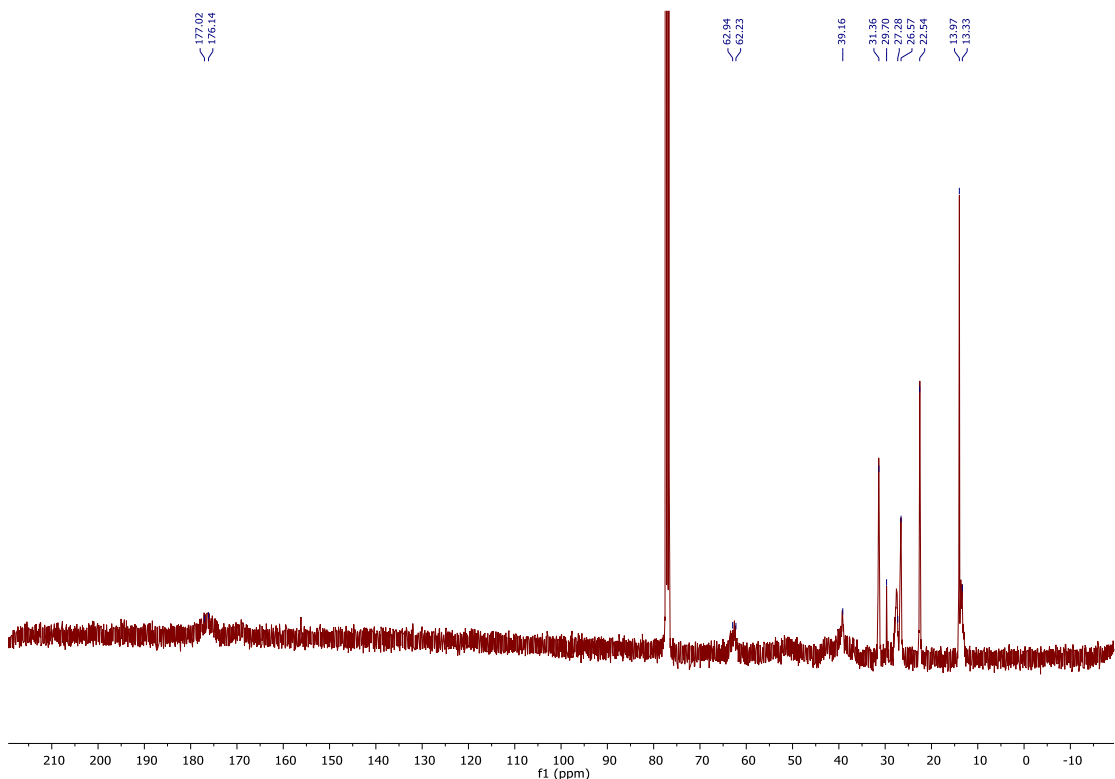


Fig. S126 ^{13}C NMR spectrum (101 MHz, CDCl_3) of PHCBI.

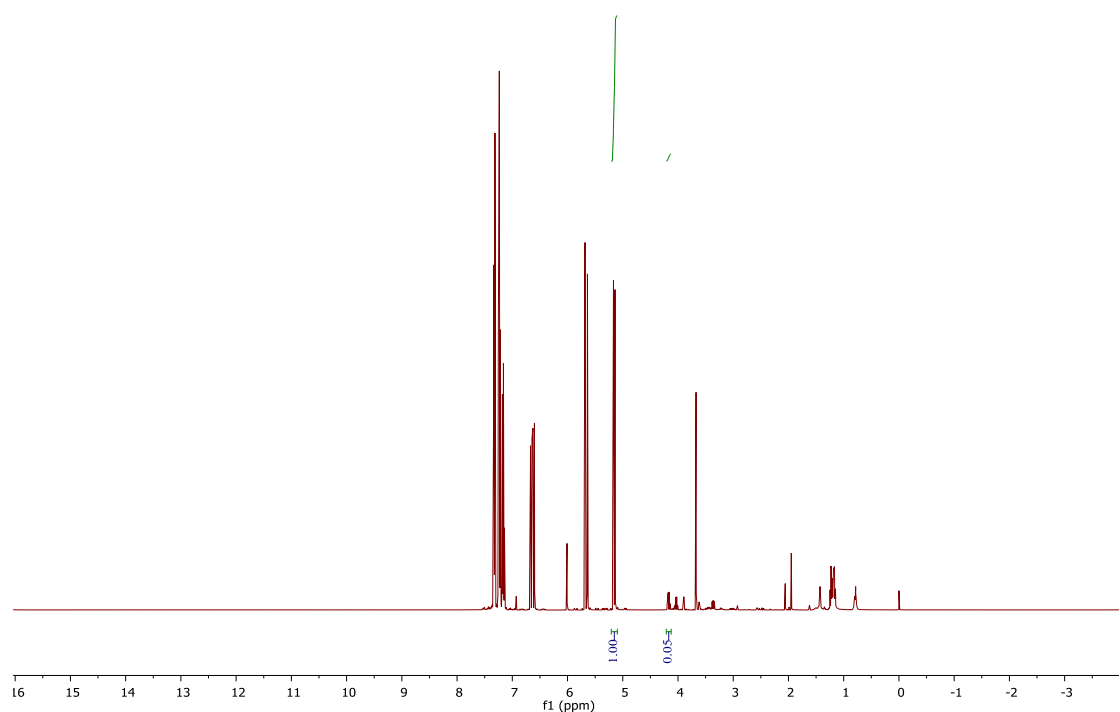


Fig. S127 ^1H NMR spectrum (400 MHz, CDCl_3) of reaction feed mixture for the synthesis of $\text{PS}_{82}\text{-}co\text{-}\text{PHCBI}_{18}$. (The fraction HCBI in feed is $(0.05/2)/(0.05/2+1) \approx 0.02$. Therefore, the fraction of styrene in feed is 0.98.)

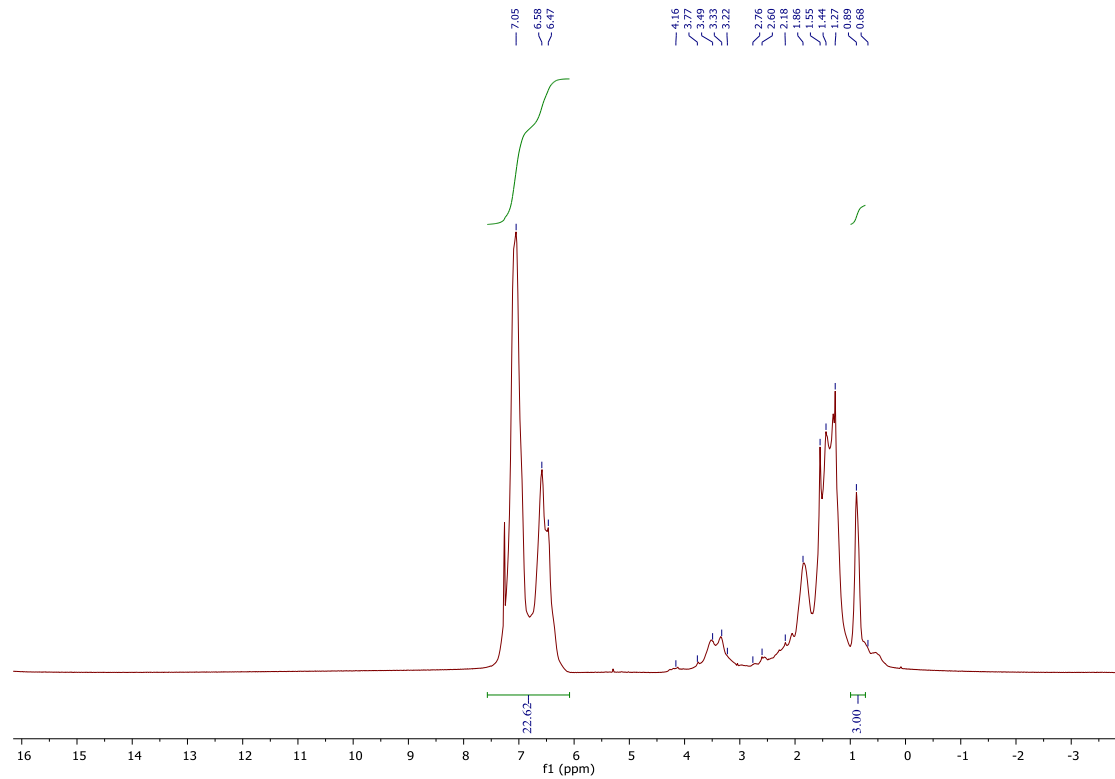


Fig. S128 ^1H NMR spectrum (400 MHz, CDCl_3) of $\text{PS}_{82}\text{-}co\text{-}\text{PHCBI}_{18}$. (The fraction of HCBI in copolymers is $1/(22.62/5+1)*100\% \approx 18\%$. Therefore, the fraction of styrene in copolymer is 82%).

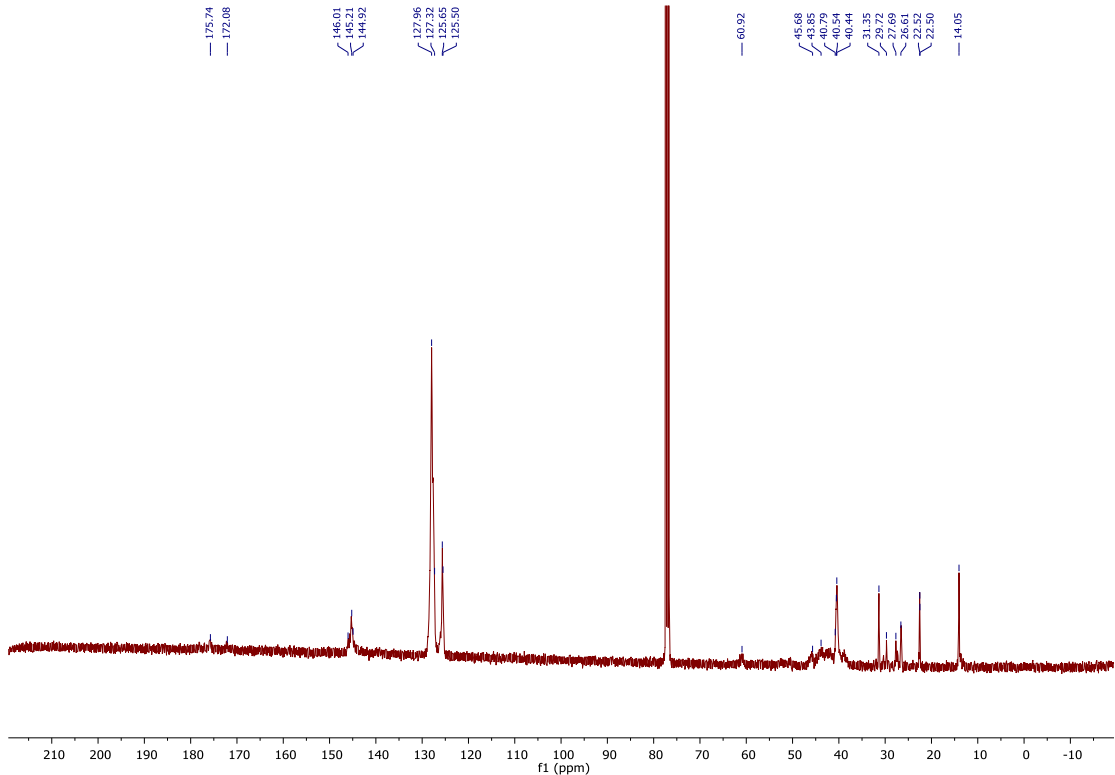


Fig. S129 ^{13}C NMR spectrum (101 MHz, CDCl_3) of $\text{PS}_{82}\text{-}co\text{-}\text{PHCBI}_{18}$.

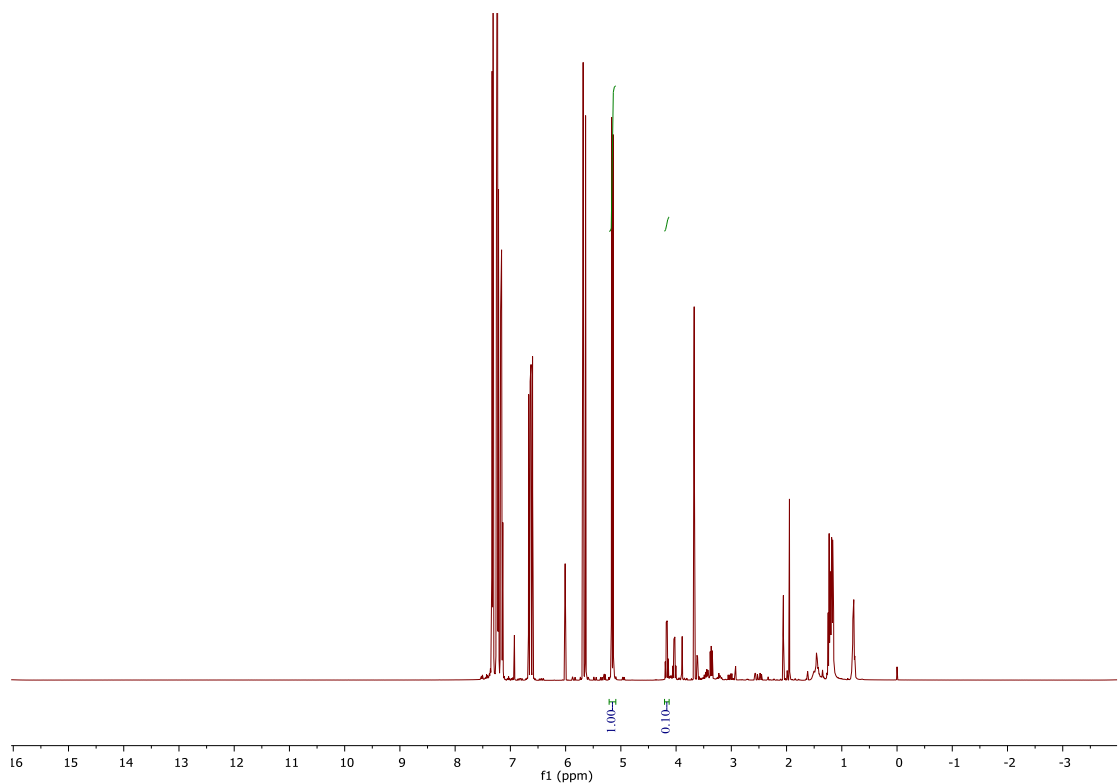


Fig. S130 ^1H NMR spectrum (400 MHz, CDCl_3) of reaction feed mixture for the synthesis of $\text{PS}_{75}\text{-}co\text{-}\text{PHCBI}_{25}$. (The fraction of HCBI in feed is $(0.10/2)/(0.10/2+1) \approx 0.05$. Therefore, the fraction of styrene in feed is 0.95.)

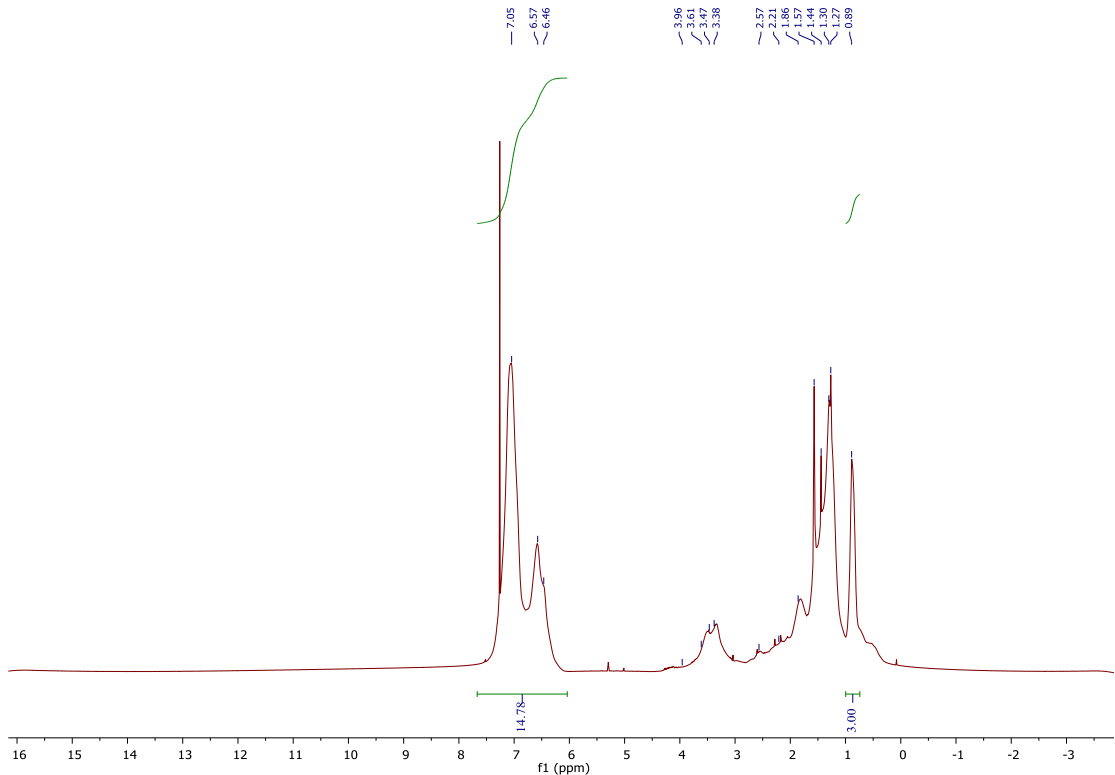


Fig. S131 ^1H NMR spectrum (400 MHz, CDCl_3) of $\text{PS}_{75}\text{-}co\text{-}\text{PHCBI}_{25}$. (The fraction of HCBI in copolymers is $1/(14.78/5+1)*100\% \approx 25\%$. Therefore, the fraction of styrene in copolymer is 75%).

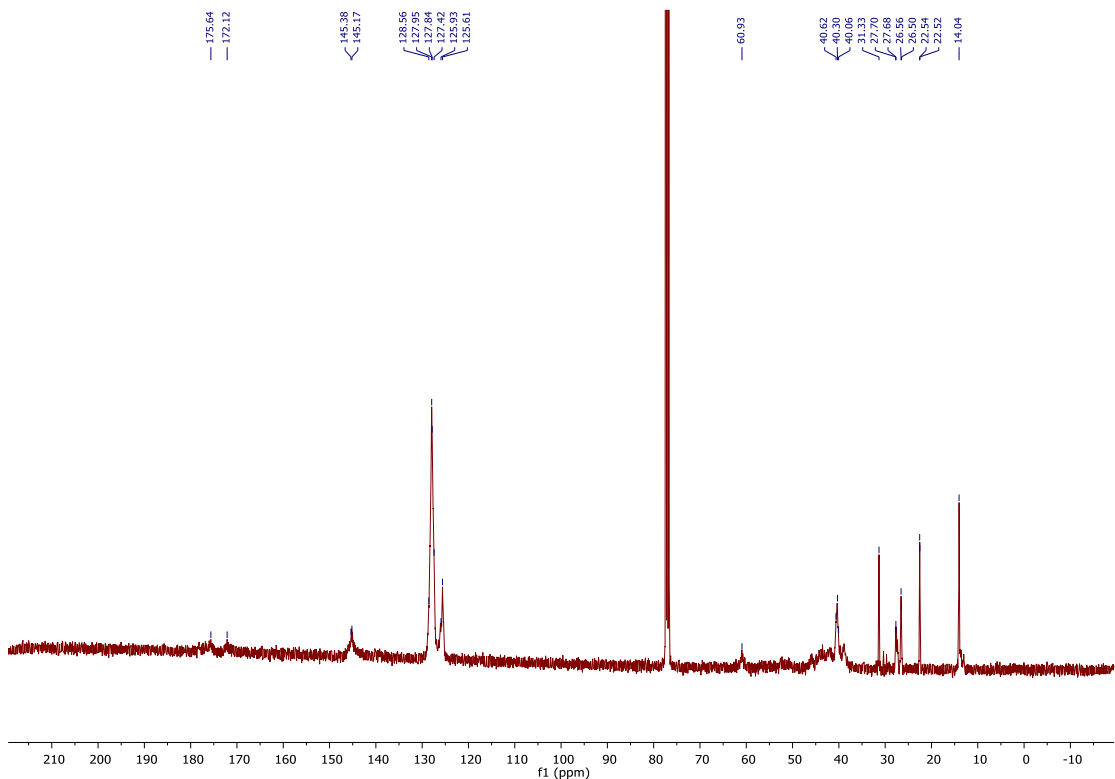


Fig. S132 ^{13}C NMR spectrum (101 MHz, CDCl_3) of $\text{PS}_{75}\text{-}co\text{-}\text{PHCBI}_{25}$.

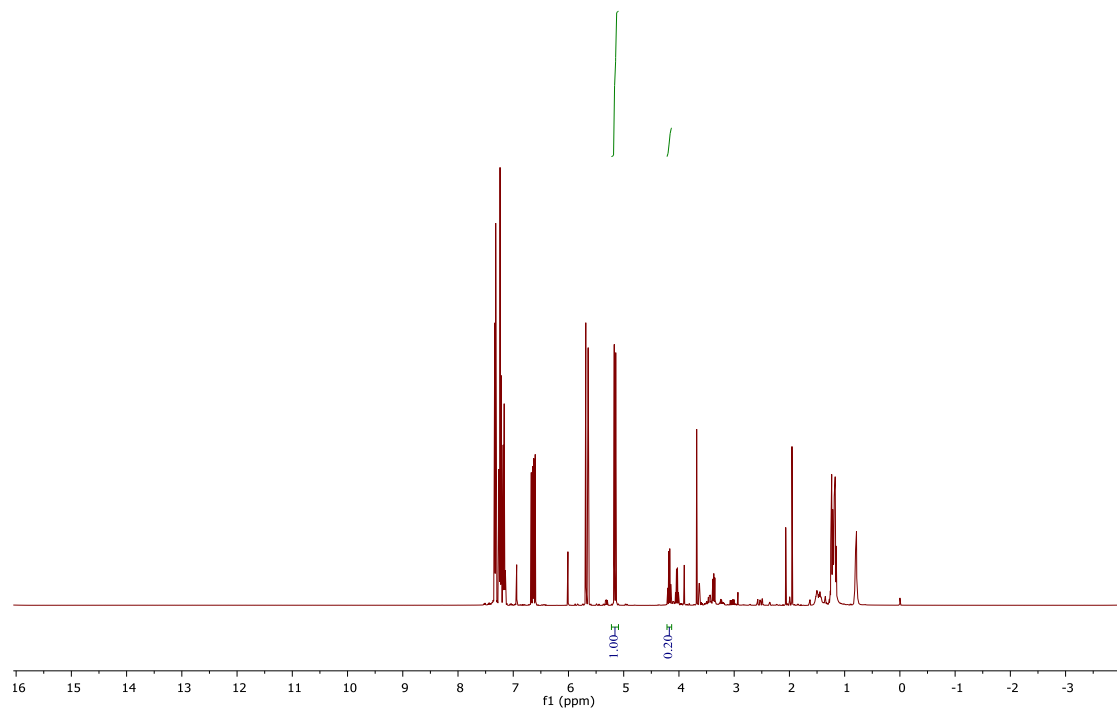


Fig. S133 ¹H NMR spectrum (400 MHz, CDCl₃) of reaction feed mixture for the synthesis of PS₆₀-co-PHCBI₄₀. (The fraction of HCBI in feed is (0.20/2)/(0.20/2+1) ≈ 0.09. Therefore, the fraction of styrene in feed is 0.91.)

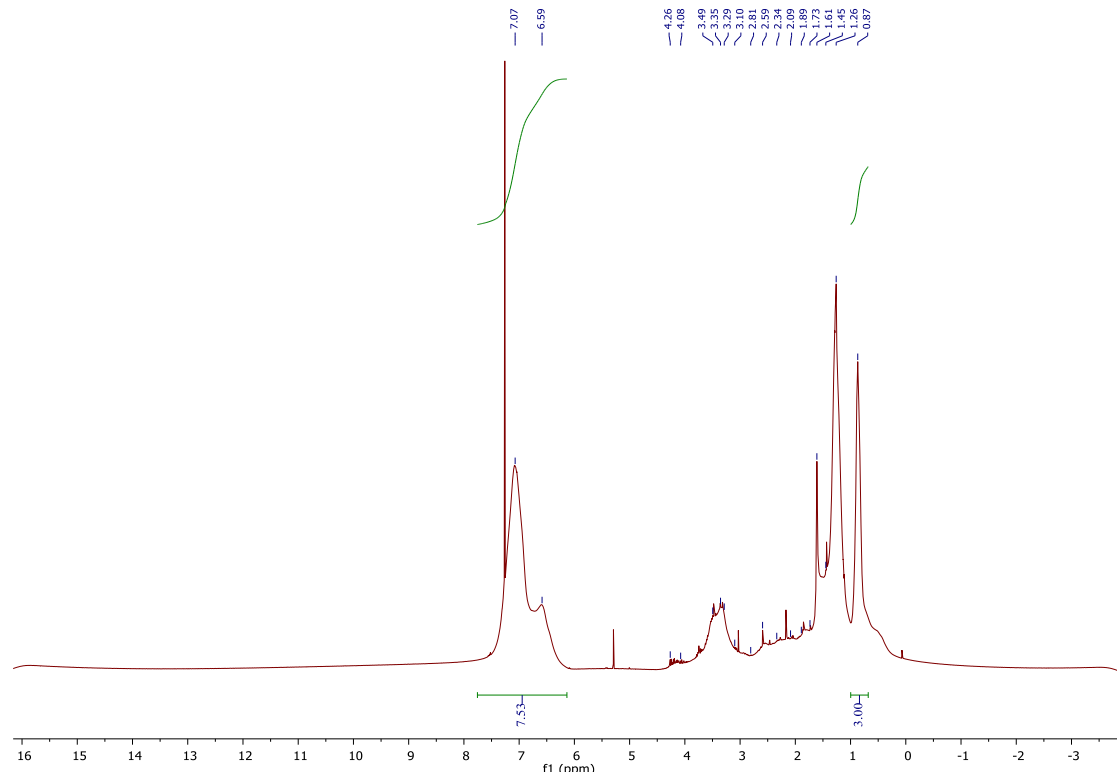


Fig. S134 ¹H NMR spectrum (400 MHz, CDCl₃) of PS₆₀-co-PHCBI₄₀. (The fraction of HCBI in copolymers is 1/(7.53/5+1)*100% ≈ 40%. Therefore, the fraction of styrene in copolymer is 60%.)

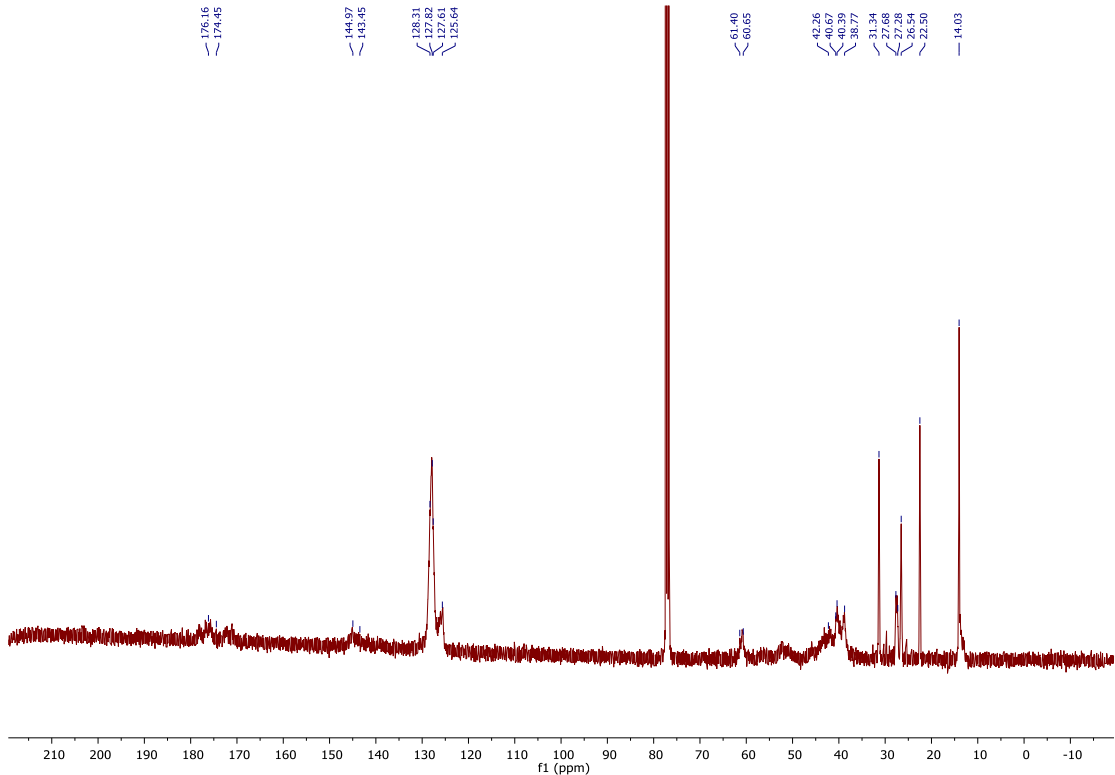


Fig. S135 ^{13}C NMR spectrum (101 MHz, CDCl_3) of $\text{PS}_{60}\text{-}co\text{-}\text{PHCBI}_{40}$.

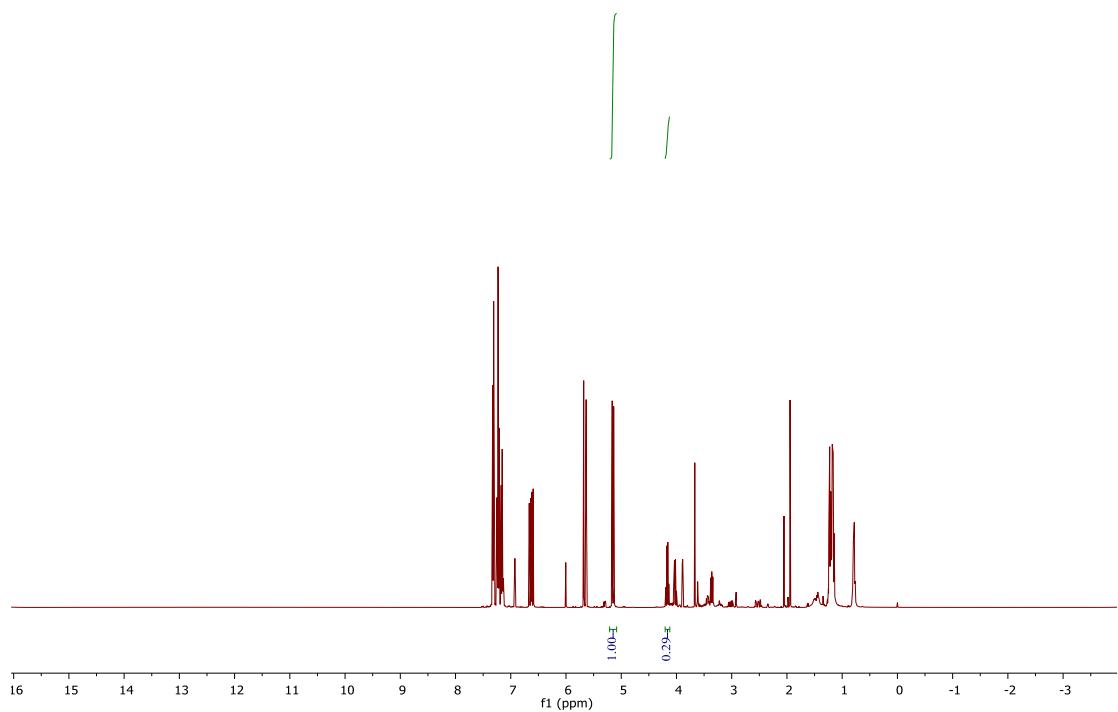


Fig. S136 ^1H NMR spectrum (400 MHz, CDCl_3) of reaction feed mixture for the synthesis of $\text{PS}_{55}\text{-}co\text{-}\text{PHCBI}_{45}$. (The fraction of HCBI in feed is $(0.29/2)/(0.29/2+1) \approx 0.13$. Therefore, the fraction of styrene in feed is 0.87.)

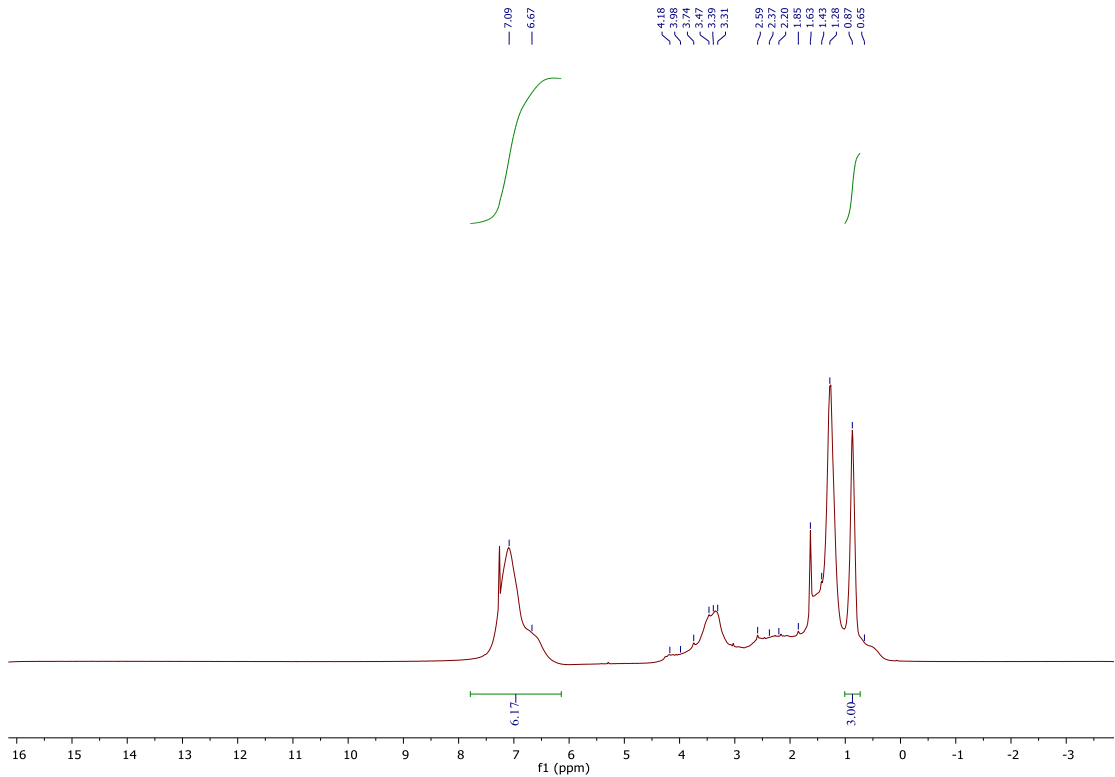


Fig. S137 ^1H NMR spectrum (400 MHz, CDCl_3) of $\text{PS}_{55}\text{-}co\text{-}\text{PHCBI}_{45}$. (The fraction of HCBI in copolymers is $1/(6.17/5+1)*100\% \approx 45\%$. Therefore, the fraction of styrene in copolymer is 55%).

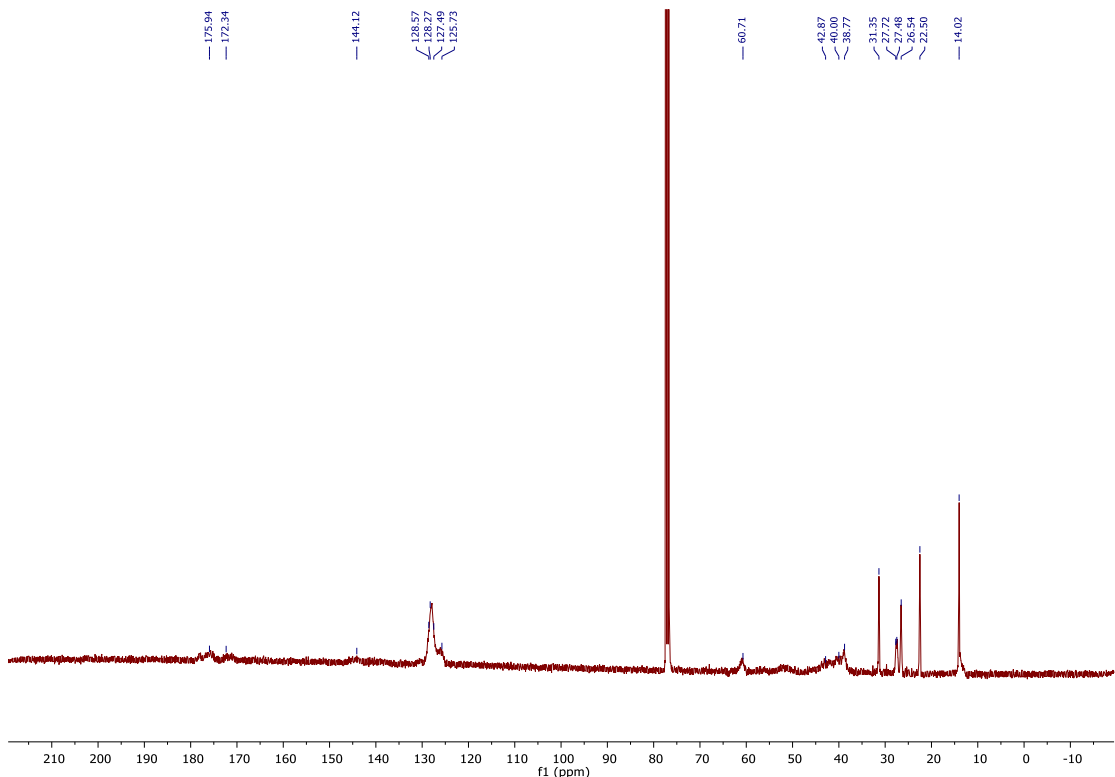


Fig. S138 ^{13}C NMR spectrum (101 MHz, CDCl_3) of $\text{PS}_{55}\text{-}co\text{-}\text{PHCBI}_{45}$.

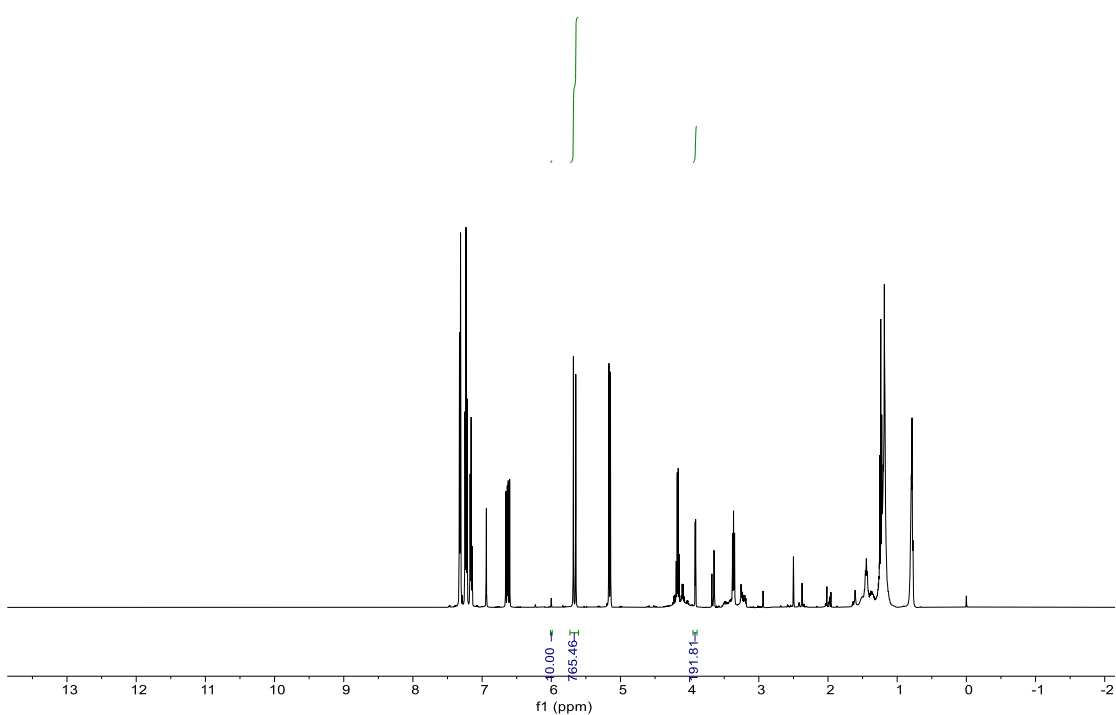


Fig. S139 ^1H NMR spectrum (500 MHz, CDCl_3) of reaction monomer feed mixture for the synthesis of $\text{PS}_{50}\text{-}co\text{-}\text{PHCBI}_{50}$. (The fraction of HCBI in feed is $(191.81/(191.81+765.46)) \approx 0.2$. Therefore, the fraction of styrene in feed is 0.8.)

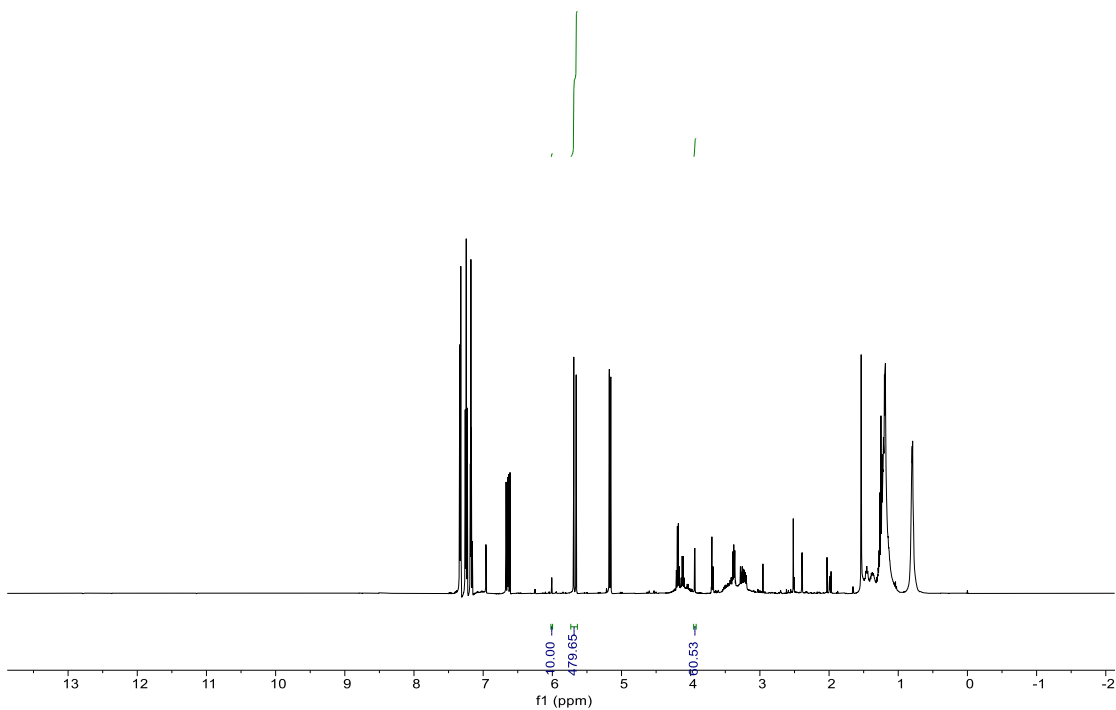
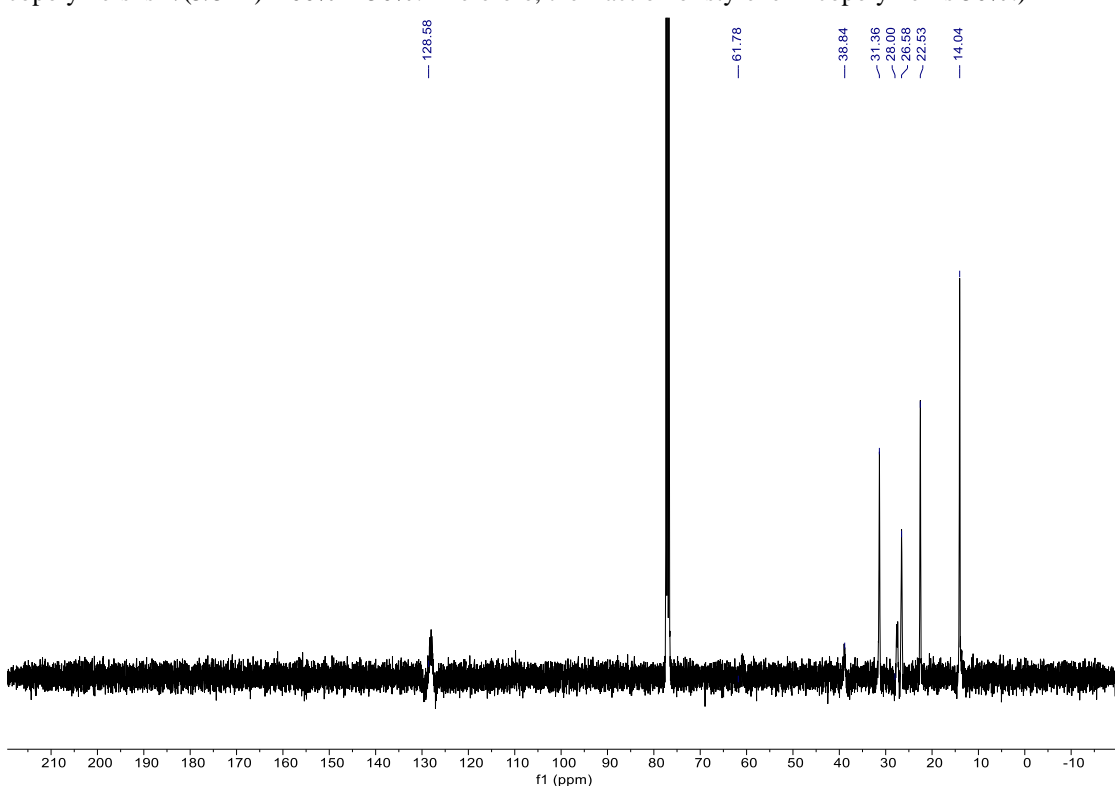
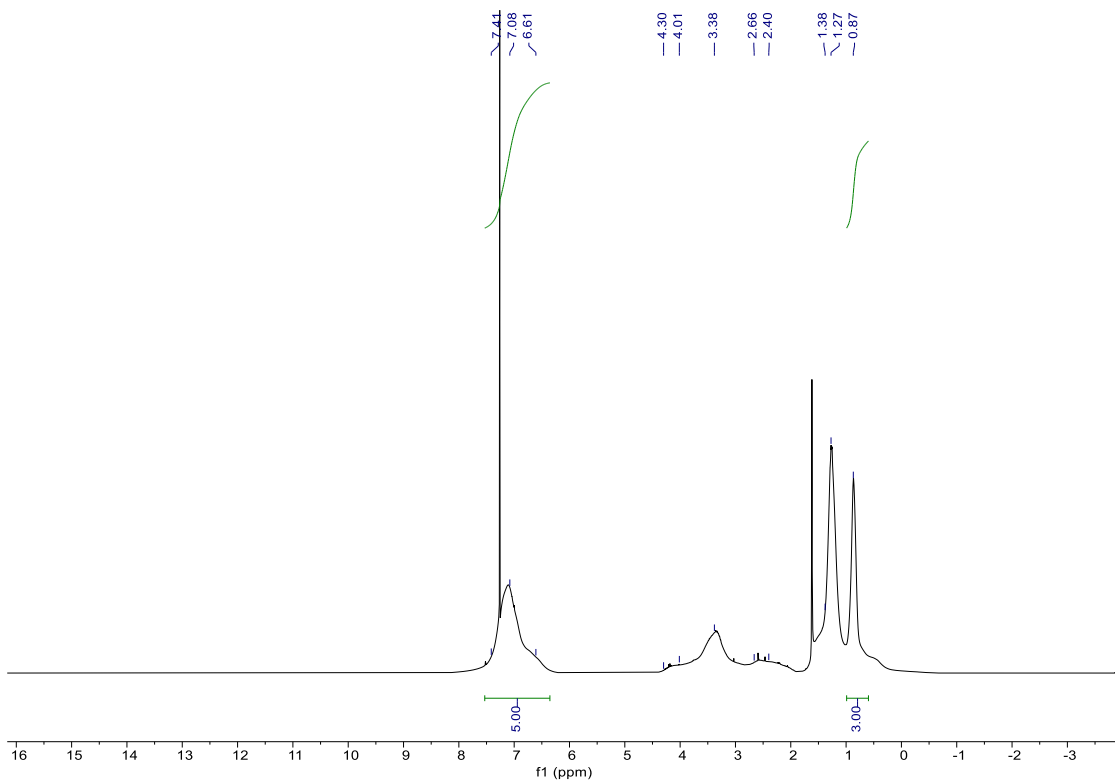


Fig. S140 ^1H NMR spectrum (500 MHz, CDCl_3) of monomers conversion for the synthesis of $\text{PS}_{50}\text{-}co\text{-}\text{PHCBI}_{50}$. (Monomers conversion after polymerization is $((191.81+765.46)-(479.65+60.53))/(191.81+765.46) \approx 44\%$.)



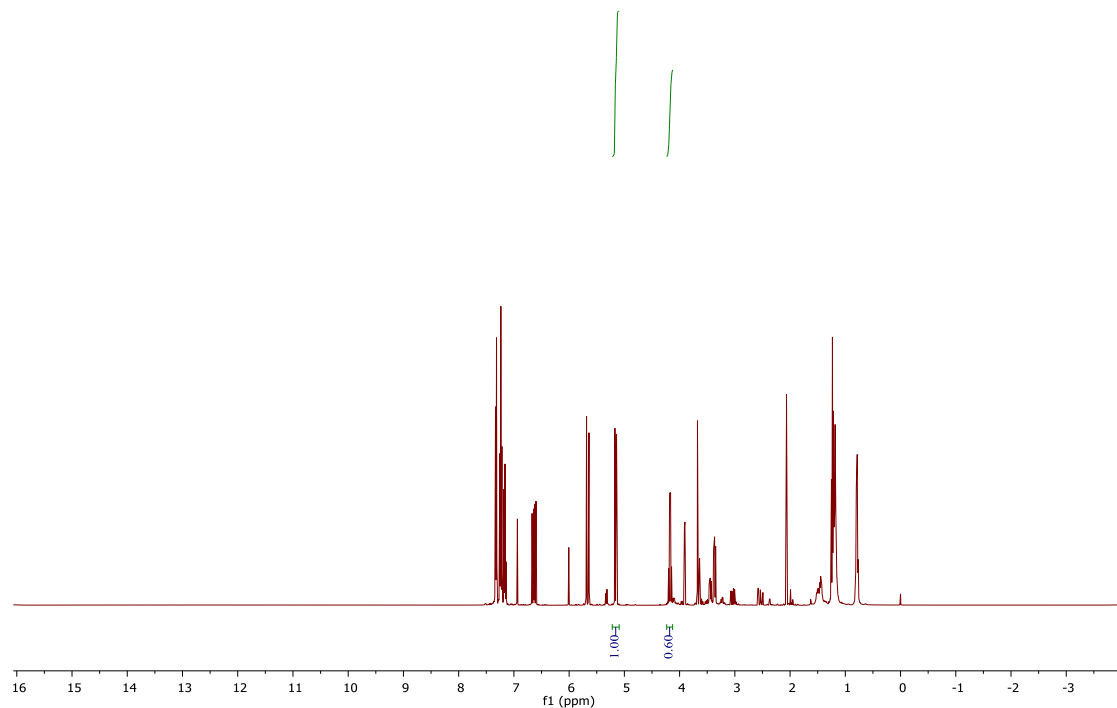


Fig. S143 ^1H NMR spectrum (400 MHz, CDCl_3) of reaction feed mixture for the synthesis of $\text{PS}_{49}\text{-}co\text{-}\text{PHCBI}_{51}$. (The fraction of HCBI in feed is $(0.60/2)/(0.60/2+1) \approx 0.23$. Therefore, the fraction of styrene in feed is 0.77.)

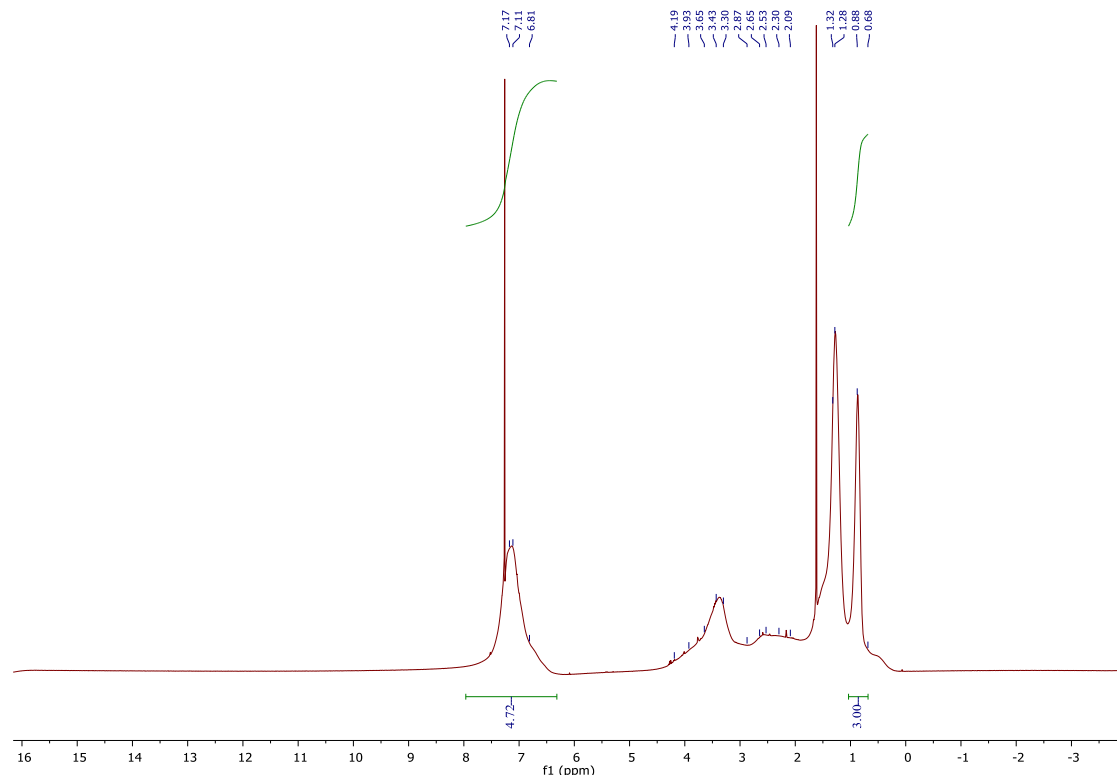


Fig. S144 ^1H NMR spectrum (400 MHz, CDCl_3) of $\text{PS}_{49}\text{-}co\text{-}\text{PHCBI}_{51}$. (The fraction of HCBI in copolymers is $1/(4.72/5+1)*100\% \approx 51\%$. Therefore, the fraction of styrene in copolymer is 49%).

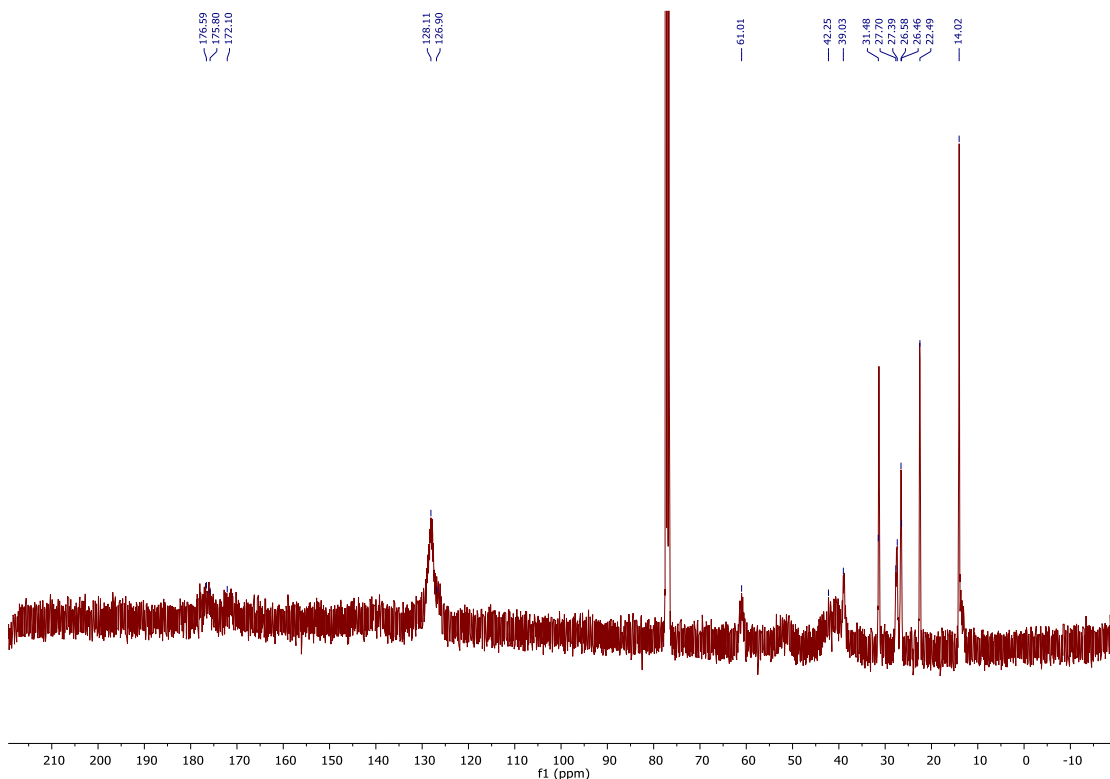


Fig. S145 ^{13}C NMR spectrum (101 MHz, CDCl_3) of $\text{PS}_{49}\text{-}co\text{-}\text{PHCBI}_{51}$.

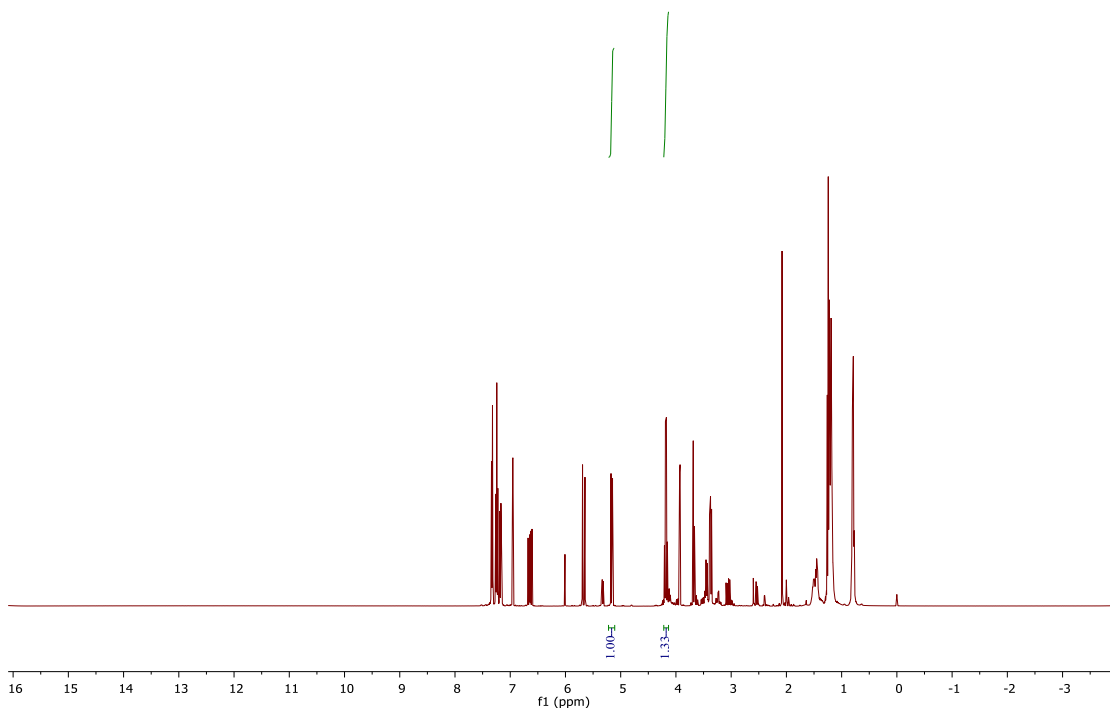


Fig. S146 ^1H NMR spectrum (400 MHz, CDCl_3) of reaction feed mixture for the synthesis of $\text{PS}_{45}\text{-}co\text{-}\text{PHCBI}_{55}$. (The fraction of HCBI in feed is $(1.33/2)/(1.33/2+1) \approx 0.4$. Therefore, the fraction of styrene in feed is 0.6.)

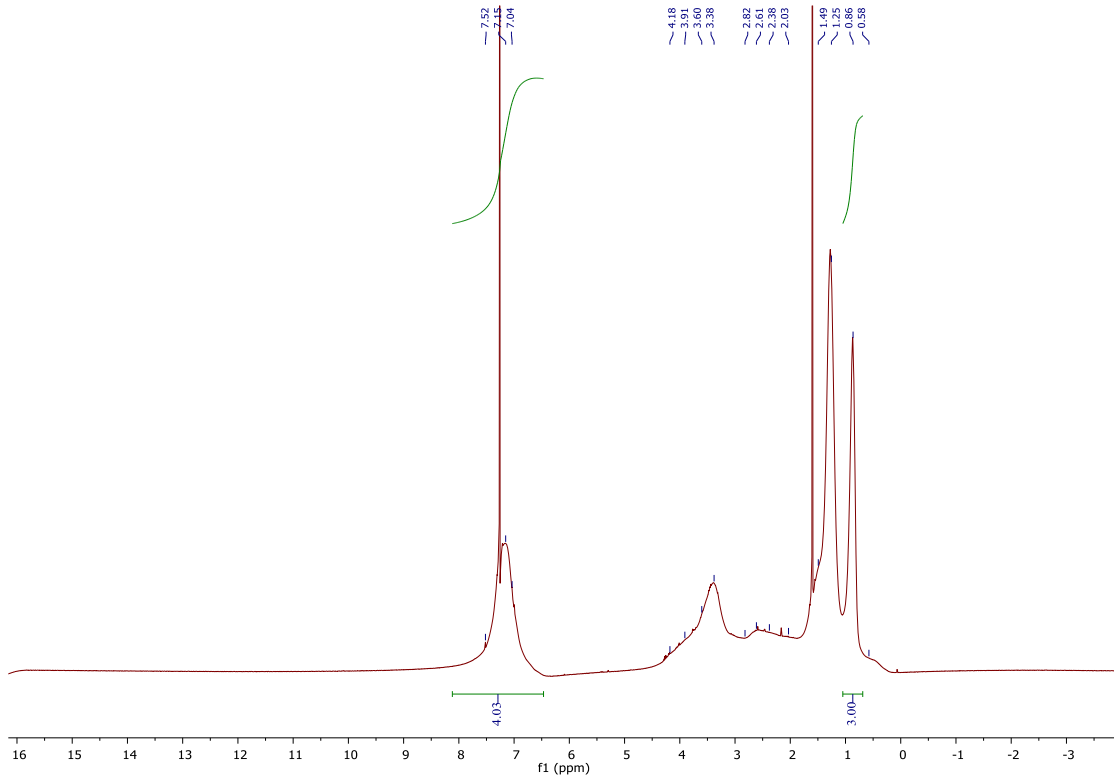


Fig. S147 ^1H NMR spectrum (400 MHz, CDCl_3) of $\text{PS}_{45}\text{-}co\text{-}\text{PHCBI}_{55}$. (The fraction of HCBI in copolymers is $1/(4.03/5+1)*100\% \approx 55\%$. Therefore, the fraction of styrene in copolymer is 45%).

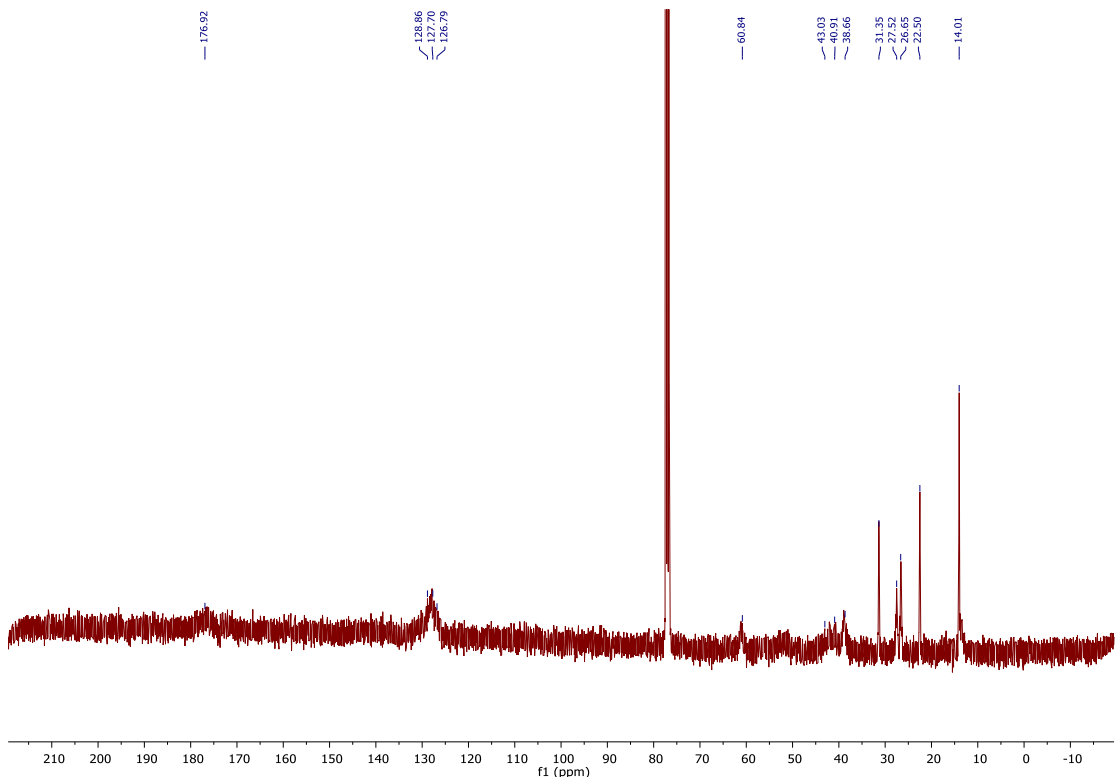


Fig. S148 ^{13}C NMR spectrum (101 MHz, CDCl_3) of $\text{PS}_{45}\text{-}co\text{-}\text{PHCBI}_{55}$.

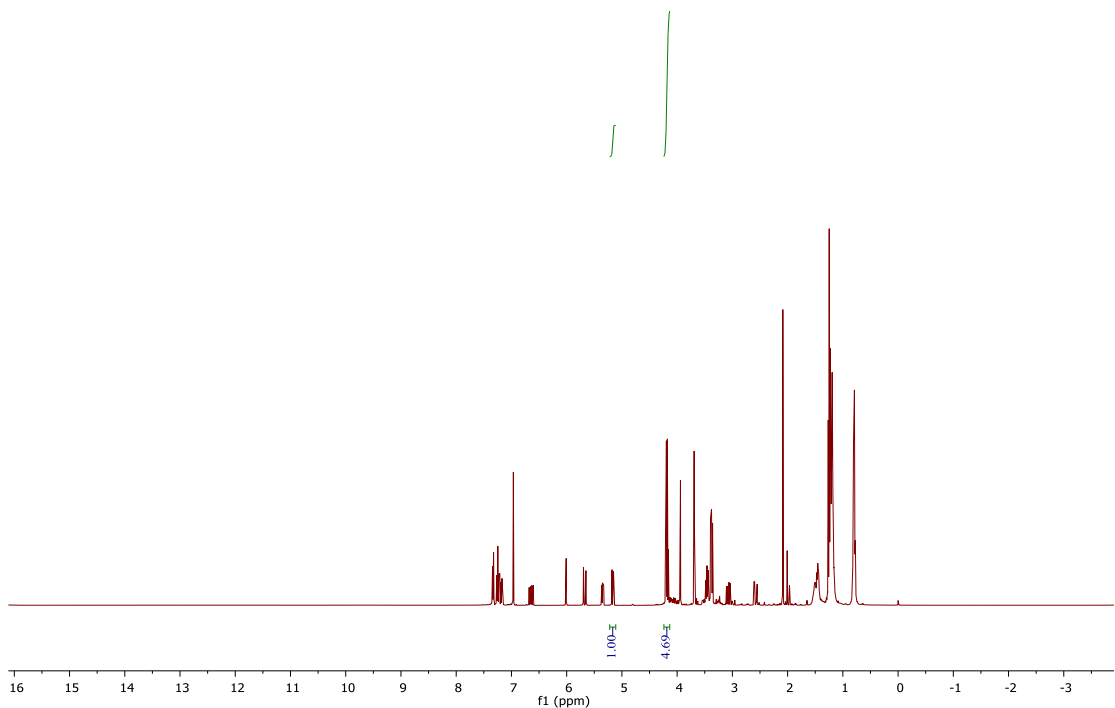


Fig. S149 ¹H NMR spectrum (400 MHz, CDCl₃) of reaction feed mixture for the synthesis of PS₃₈-co-PHCBI₆₂. (The fraction of HCBI in feed is (4.69/2)/(4.69/2+1) ≈ 0.7. Therefore, the fraction of styrene in feed is 0.3.)

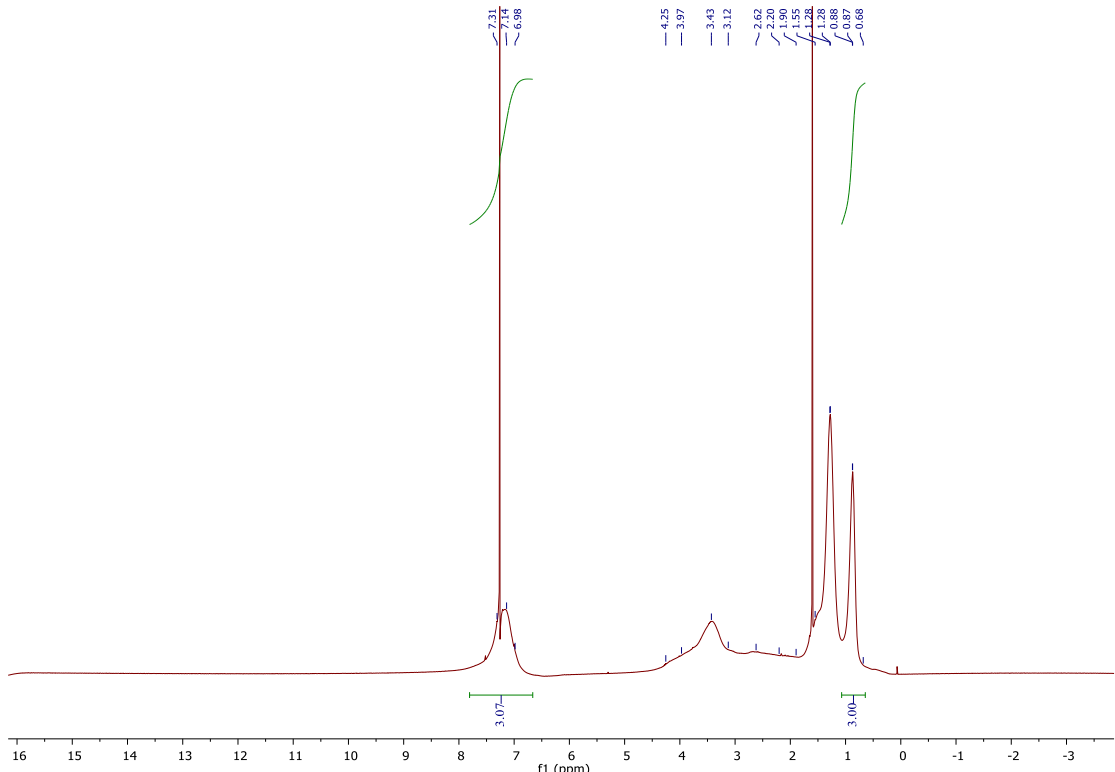


Fig. S150 ¹H NMR spectrum (400 MHz, CDCl₃) of PS₃₈-co-PHCBI₆₂. (The fraction of HCBI in copolymers is 1/(3.07/5+1)*100% ≈ 62%. Therefore, the fraction of styrene in copolymer is 38%.)

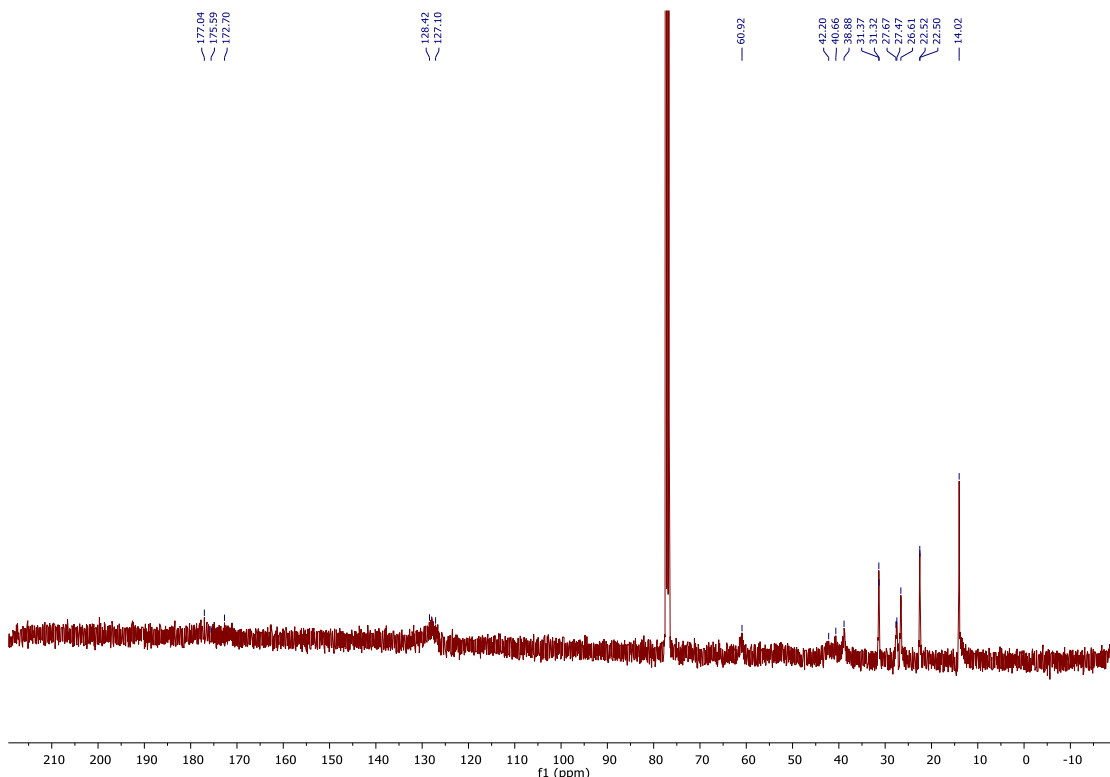


Fig. S151 ¹³C NMR spectrum (101 MHz, CDCl₃) of PS₃₈-co-PHCBI₆₂.

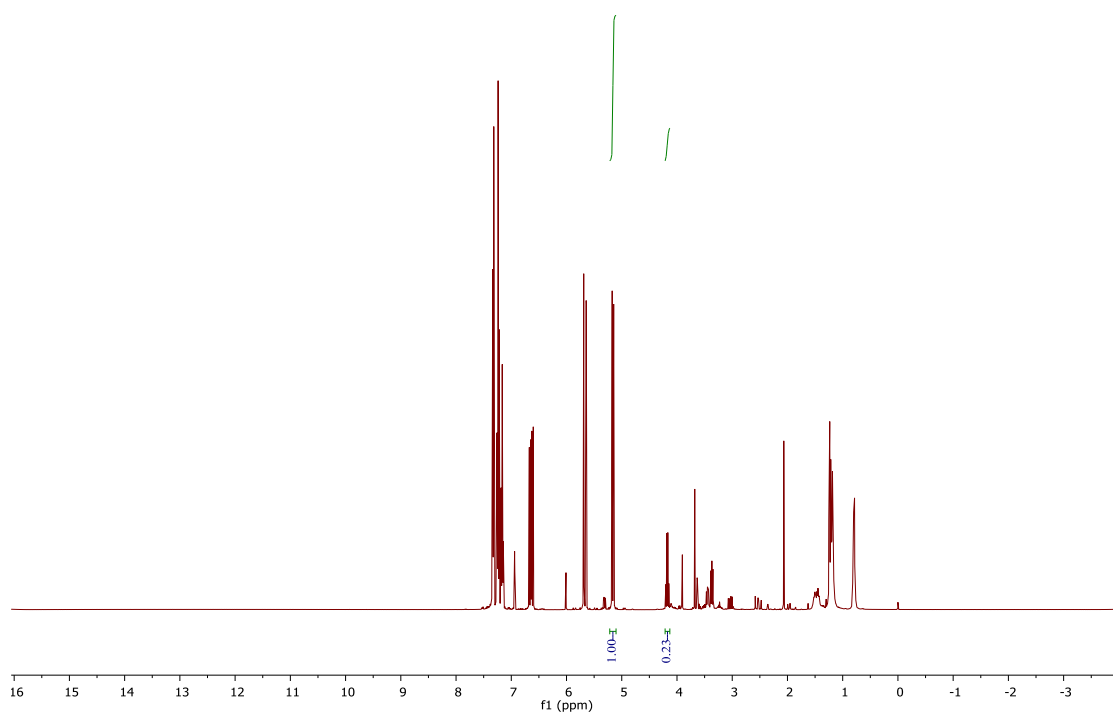


Fig. S152 ¹H NMR spectrum (400 MHz, CDCl₃) of reaction feed mixture for the synthesis of PS₇₃-co-PHCBI₂₇. (The fraction of HCBI in feed is (0.23/2)/(0.23/2+1) ≈ 0.1. Therefore, the fraction of styrene in feed is 0.9.)

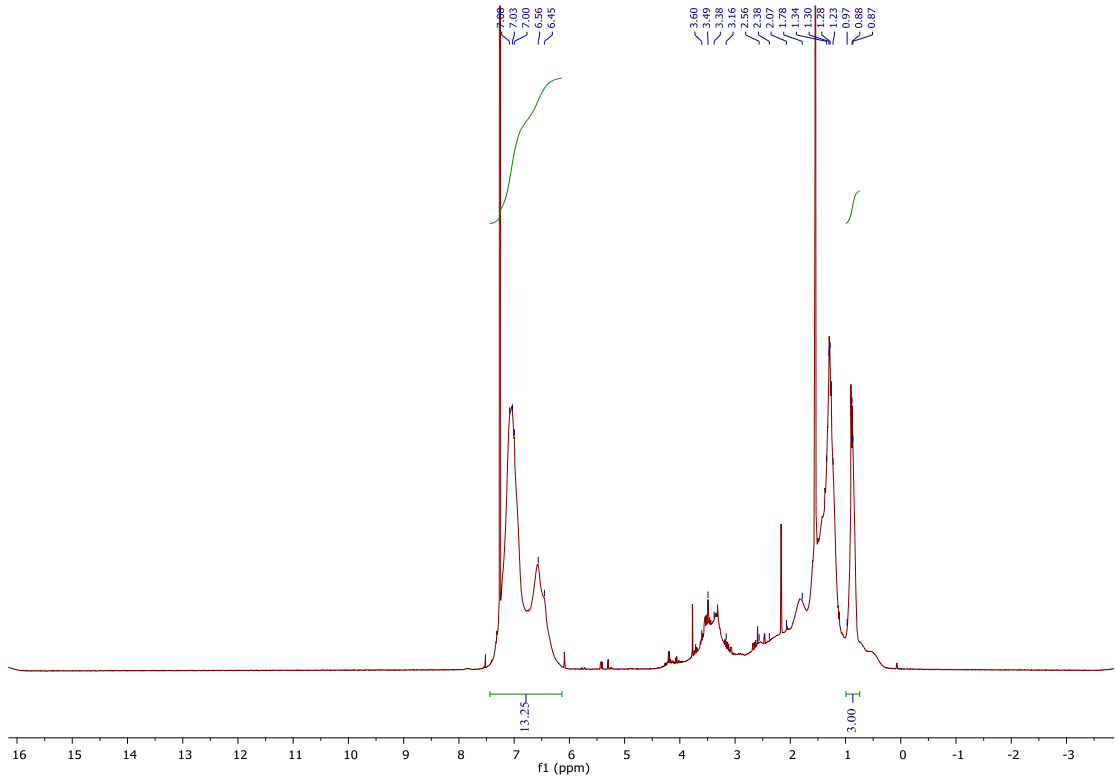


Fig. S153 ^1H NMR spectrum (400 MHz, CDCl_3) of $\text{PS}_{73}\text{-}co\text{-}\text{PHCBI}_{27}$. (The fraction of HCBI in copolymers is $1/(13.25/5+1)*100\% \approx 27\%$. Therefore, the fraction of styrene in copolymer is 73%).

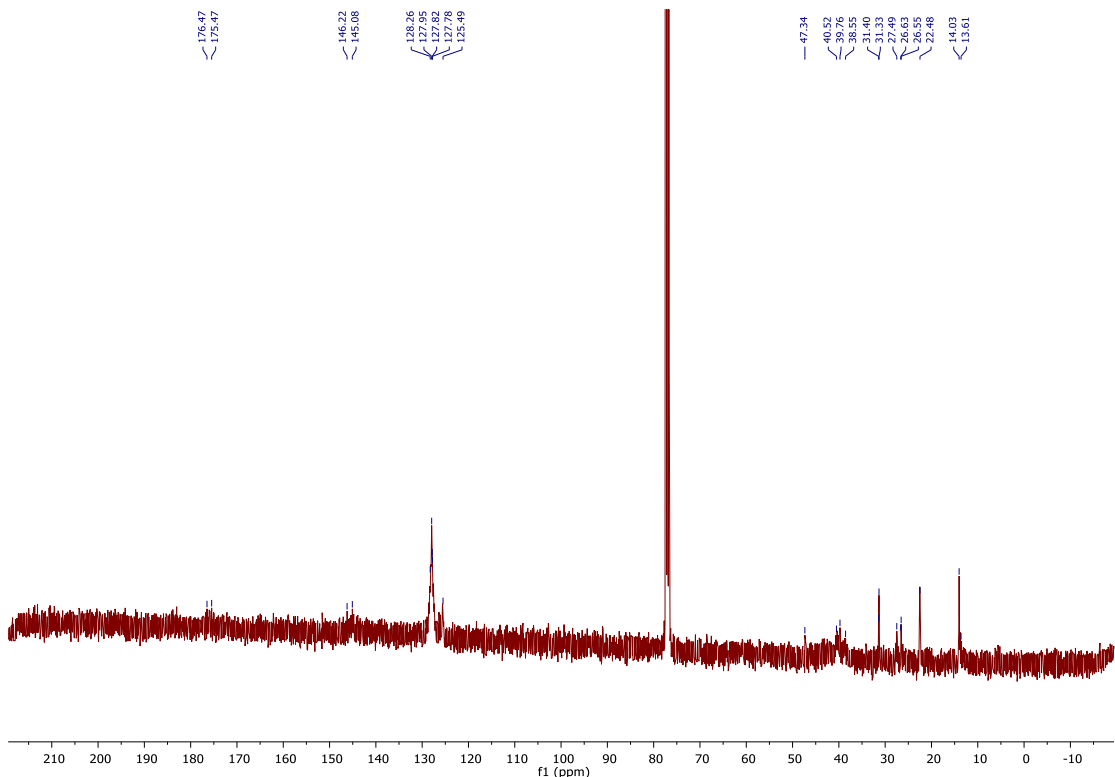


Fig. S154 ^{13}C NMR spectrum (101 MHz, CDCl_3) of $\text{PS}_{73}\text{-}co\text{-}\text{PHCBI}_{27}$.

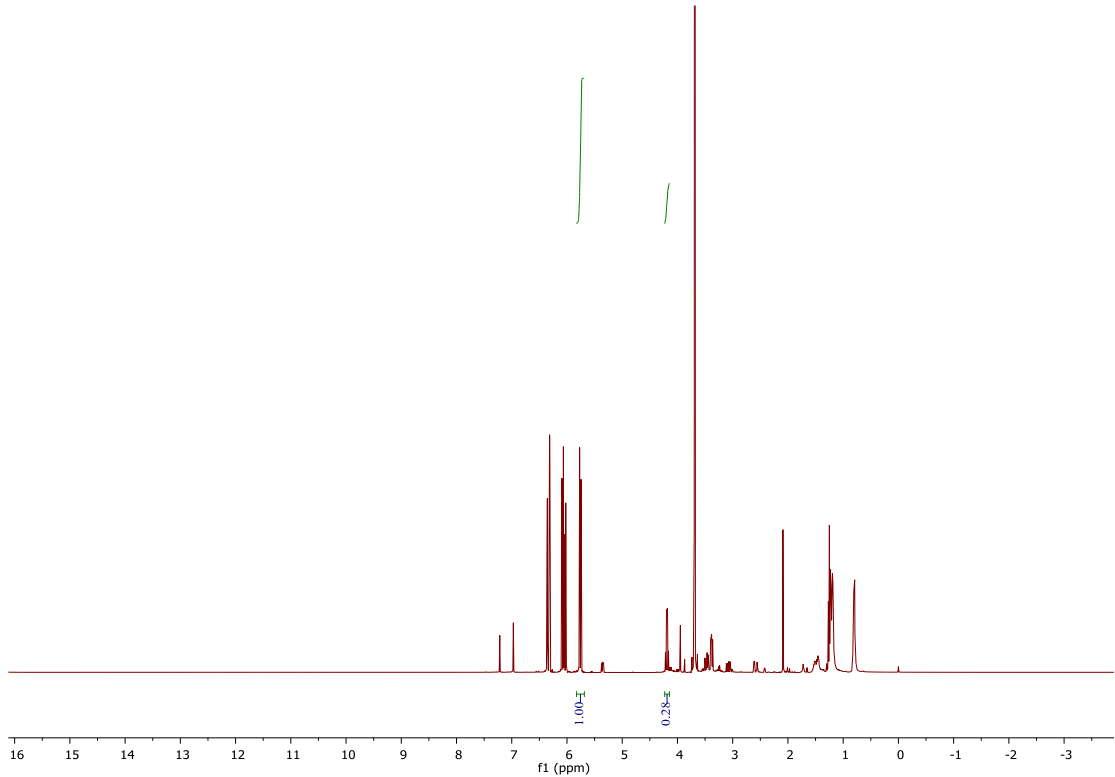


Fig. S155 ¹H NMR spectrum (400 MHz, CDCl₃) of reaction feed mixture for the synthesis of PMA₈₇-co-PHCBI₁₃. (The fraction of HCBI in feed is (0.28/2)/(0.28/2+1) ≈ 0.12. Therefore, the fraction of methyl acrylate in feed is 0.88.)

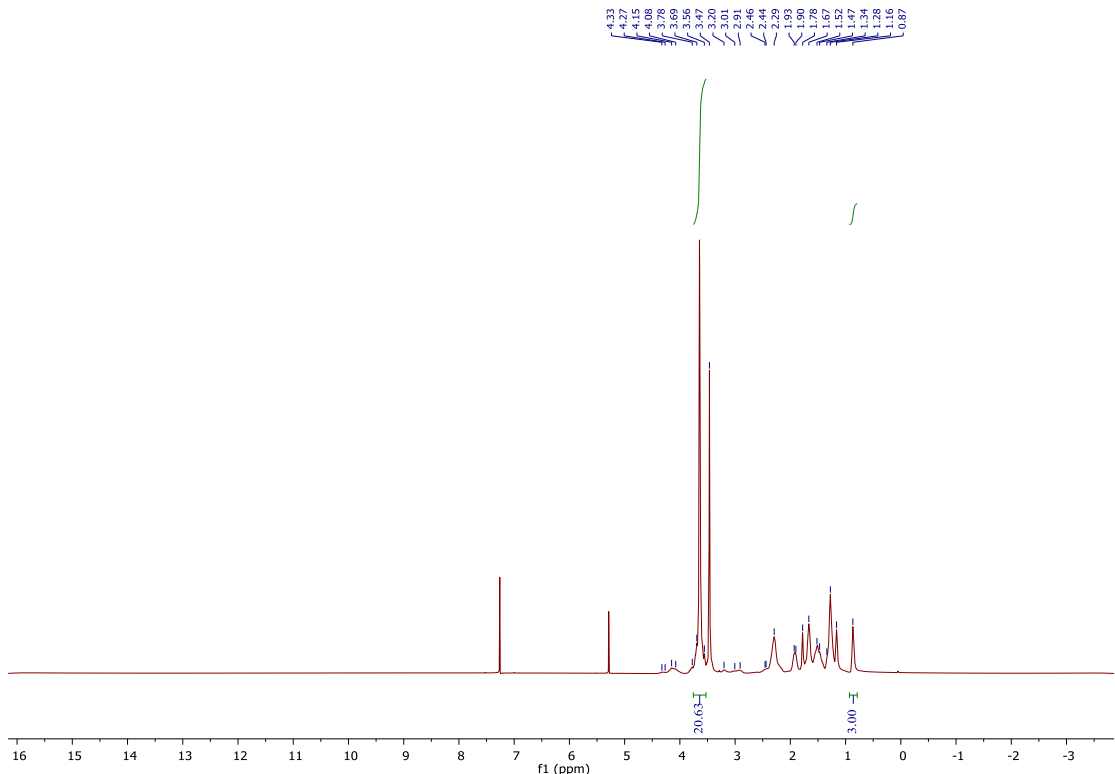


Fig. S156 ¹H NMR spectrum (400 MHz, CDCl₃) of PMA₈₇-co-PHCBI₁₃. (The fraction of HCBI in copolymers is 1/(20.63/3+1)*100% ≈ 13%. Therefore, the fraction of methyl acrylate in copolymer is 87%.)

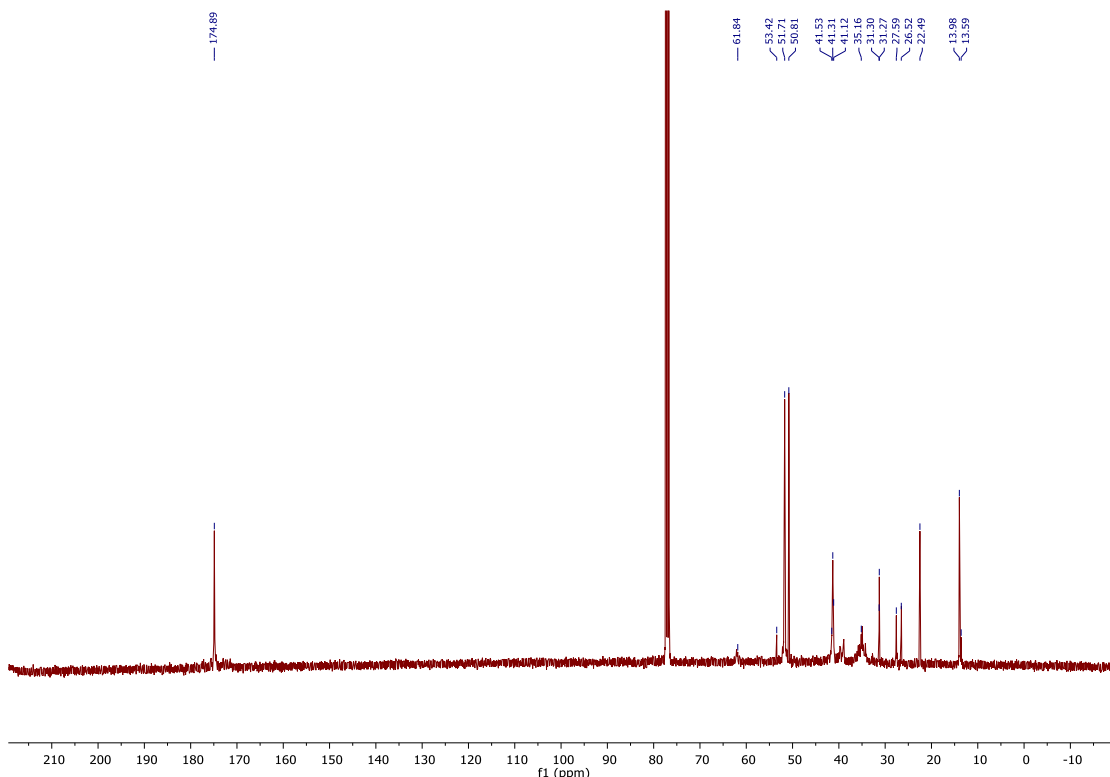


Fig. S157 ^{13}C NMR spectrum (101 MHz, CDCl_3) of $\text{PMA}_{87}\text{-}co\text{-}\text{PHCBI}_{13}$.

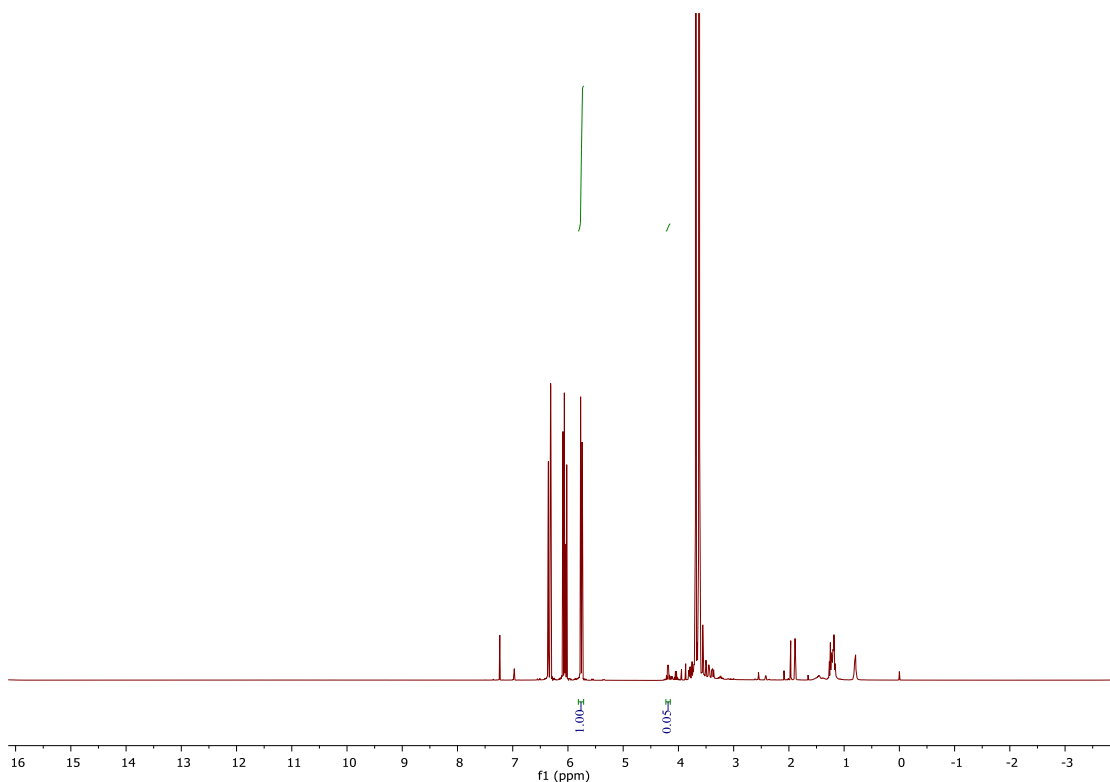


Fig. S158 ^1H NMR spectrum (400 MHz, CDCl_3) of reaction feed mixture for the synthesis of $\text{PMA}_{97}\text{-}co\text{-}\text{PHCBI}_3$. (The fraction of HCBI in feed is $(0.05/2)/(0.05/2+1) \approx 0.02$. Therefore, the fraction of methyl acrylate in feed is 0.98.)

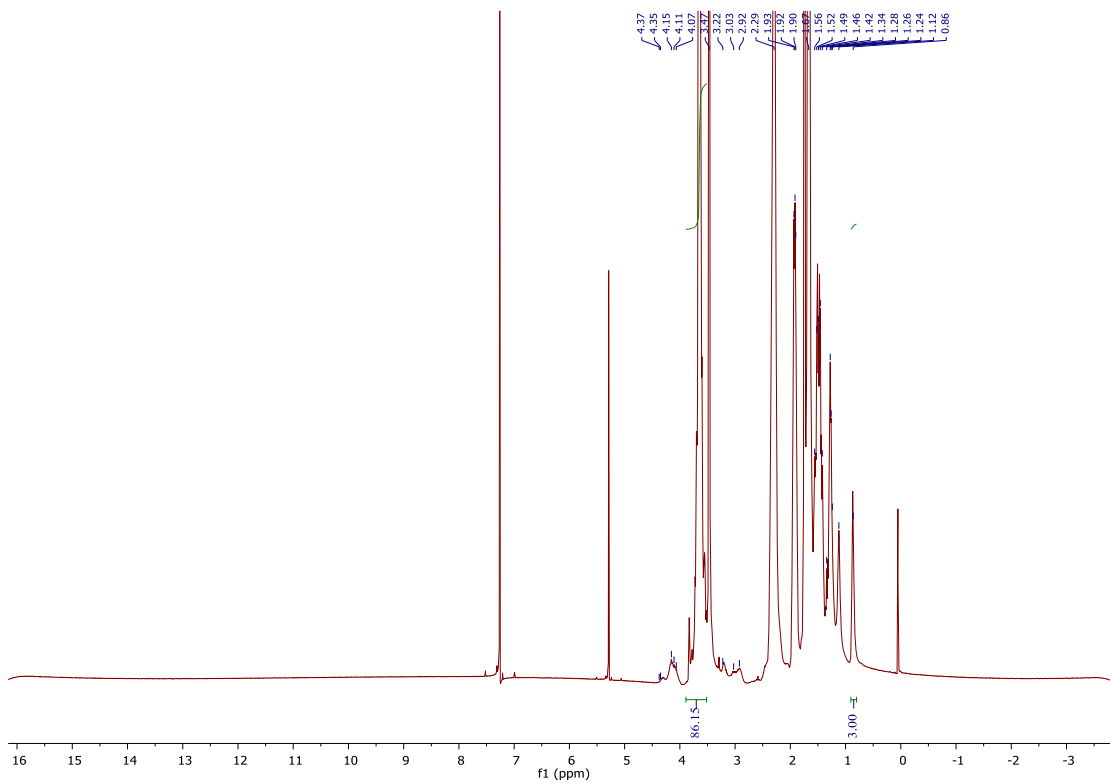


Fig. S159 ^1H NMR spectrum (400 MHz, CDCl_3) of $\text{PMA}_{97}\text{-}co\text{-}\text{PHCBI}_3$. (The fraction of HCBI in copolymers is $1/(86.15/3+1)*100\% \approx 3\%$, therefore, the fraction of methyl acrylate in copolymer is 97%).

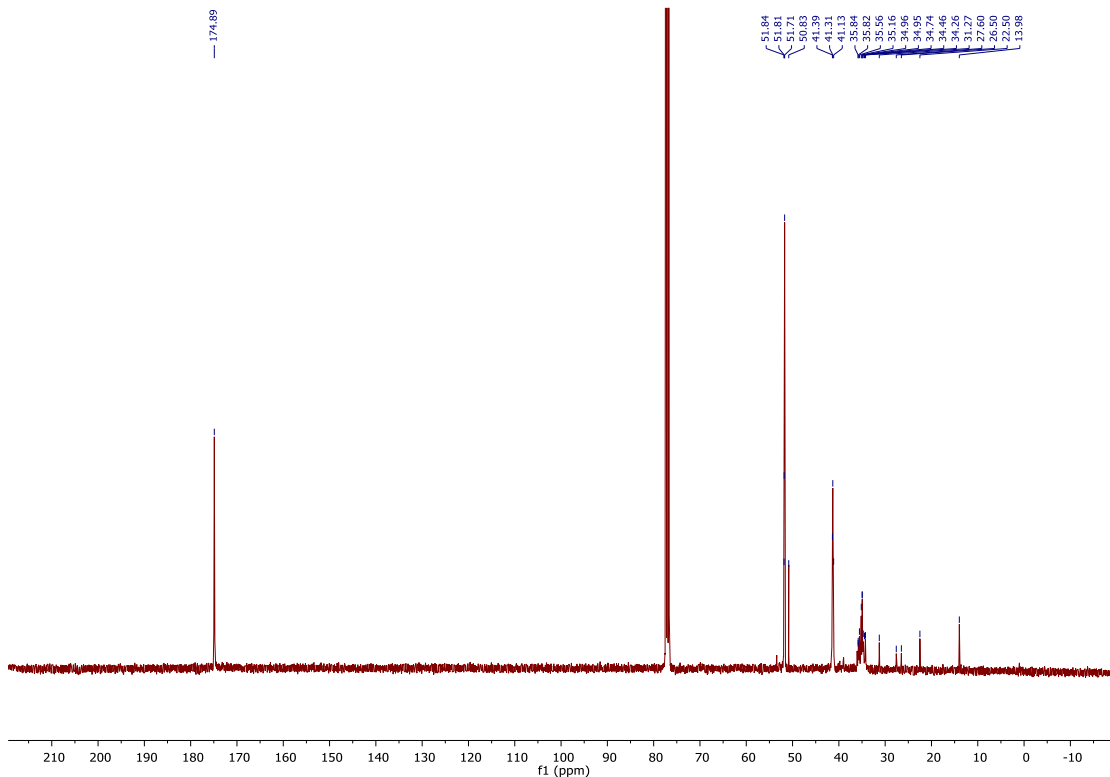


Fig. S160 ^{13}C NMR spectrum (101 MHz, CDCl_3) of $\text{PMA}_{97}\text{-}co\text{-}\text{PHCBI}_3$.

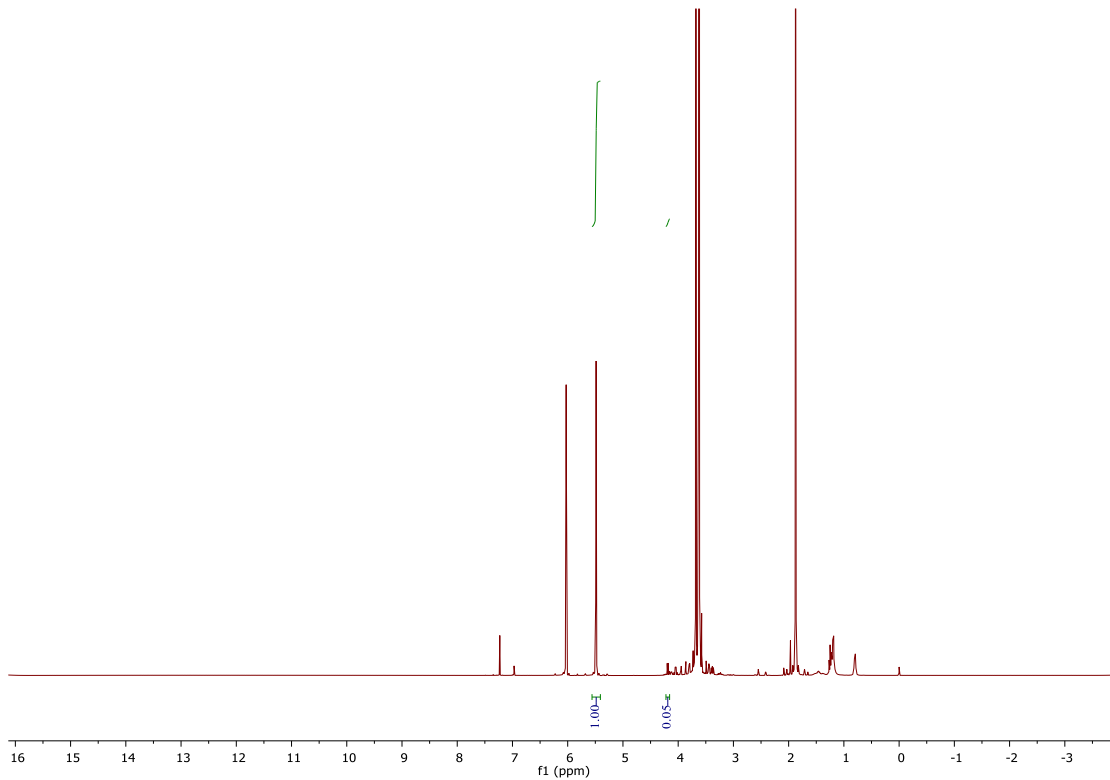


Fig. S161 ^1H NMR spectrum (400 MHz, CDCl_3) of reaction feed mixture for the synthesis of PMMA₉₈-*co*-PHCBI₂. (The fraction of HCBI in feed is $(0.05/2)/(0.05/2+1) \approx 0.02$. Therefore, the fraction of methyl methacrylate in feed is 0.98.)

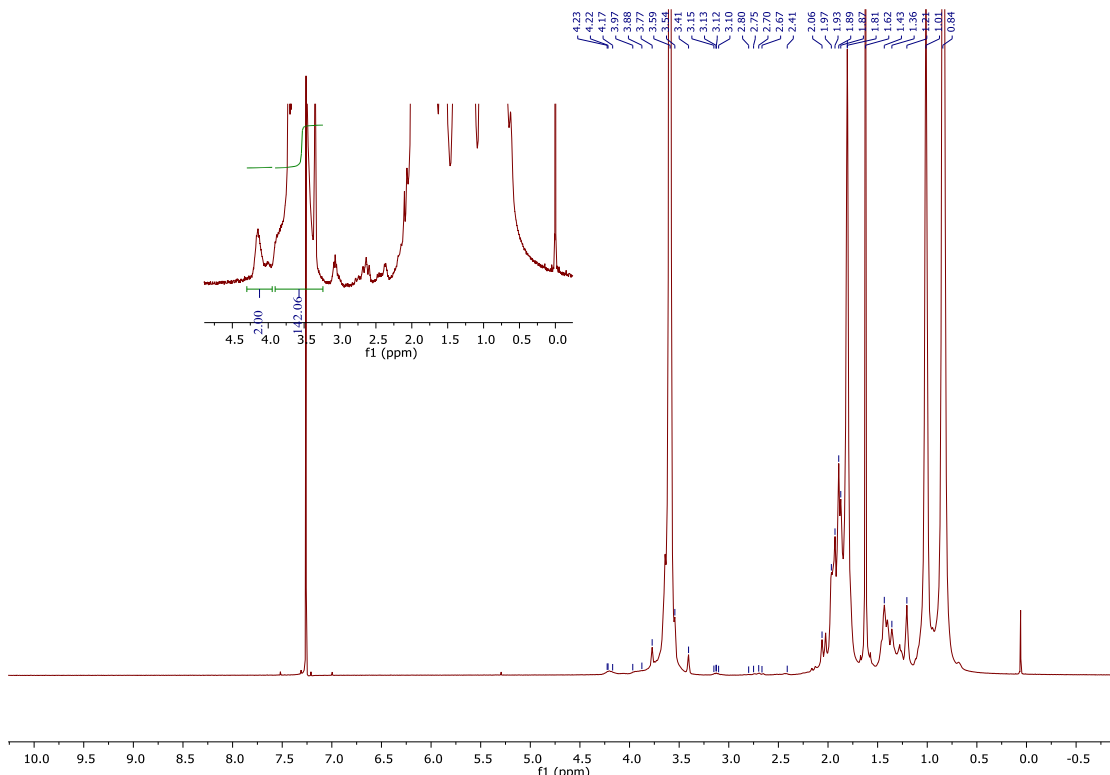


Fig. S162 ^1H NMR spectrum (400 MHz, CDCl_3) of $\text{PMMA}_{98}-co-\text{PHCBI}_2$. (The fraction of HCBI in copolymers is $1/(142.06/3+1)*100\% \approx 2\%$, therefore, the fraction of methyl methacrylate in copolymer is 98%).

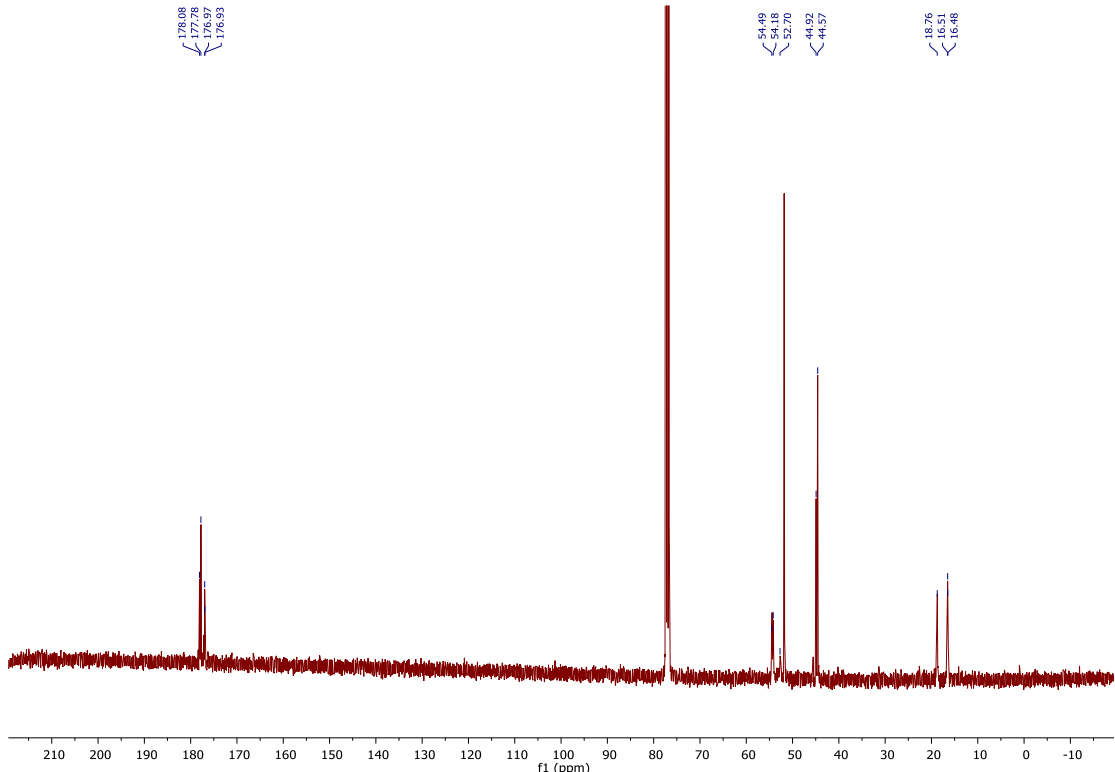


Fig. S163 ^{13}C NMR spectrum (101 MHz, CDCl_3) of $\text{PMMA}_{98}\text{-}co\text{-}\text{PHCBI}_2$.

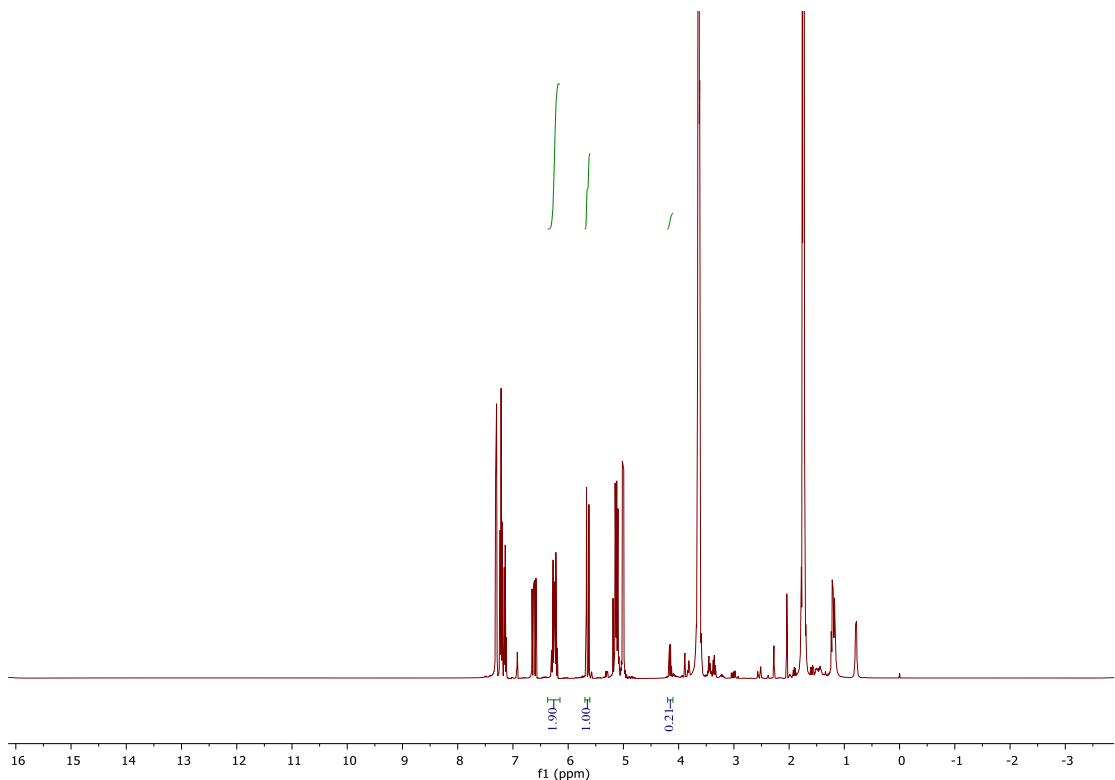


Fig. S164 ^1H NMR spectrum (400 MHz, CDCl_3) of reaction feed mixture for the synthesis of $\text{PS}_{34}\text{-}co\text{-}\text{PB}_{49}\text{-}co\text{-}\text{PHCBI}_{17}$. (The fraction of HCBI in feed is $(0.21/2)/(1.9/2+0.21/2+1) \approx 0.05$. The fraction of styrene in copolymers is $(1/(1.9/2+0.21/2+1)) \approx 0.49$. Therefore, the fraction of butadiene in copolymer is 0.46.)

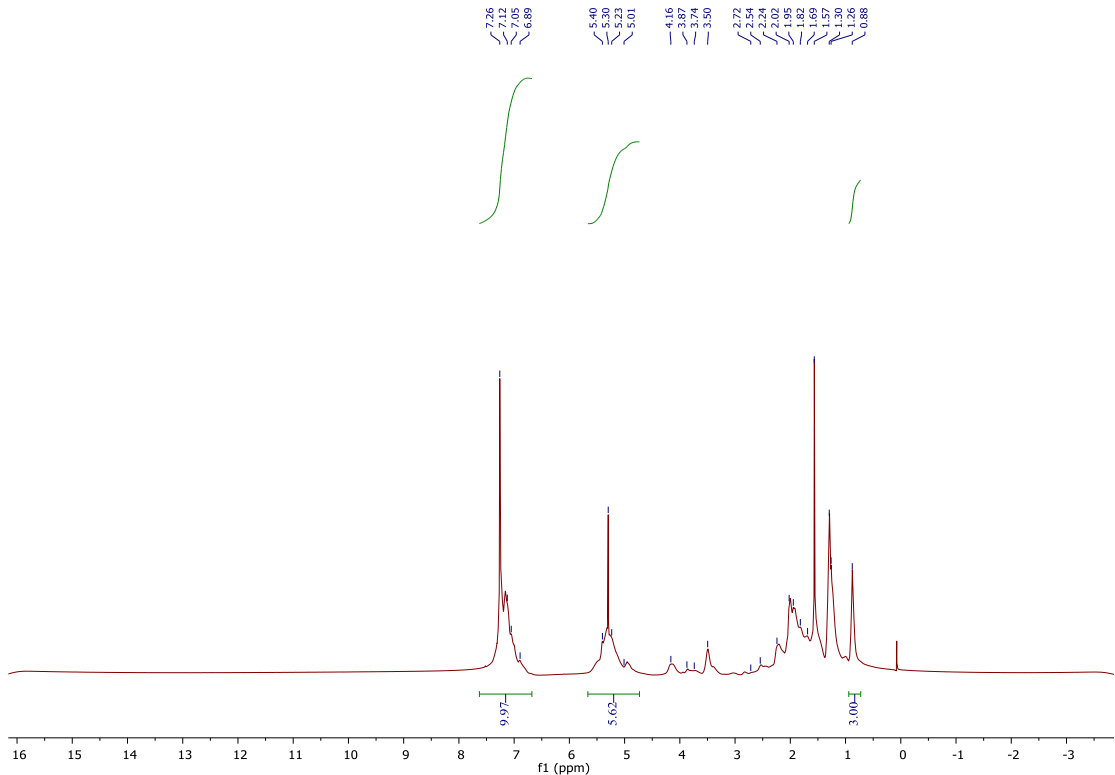


Fig. S165 ^1H NMR spectrum (400 MHz, CDCl_3) of $\text{PS}_{34}\text{-}co\text{-}\text{PB}_{49}\text{-}co\text{-}\text{PHCBI}_{17}$. (The fraction of HCBI in copolymers is $1/(9.97/5+5.62/2+1)*100\% \approx 17\%$. The fraction of styrene in copolymers is $(9.97/5)/(9.97/5+5.62/2+1)*100\% \approx 34\%$. Therefore, the fraction of butadiene in copolymer is 49%.)

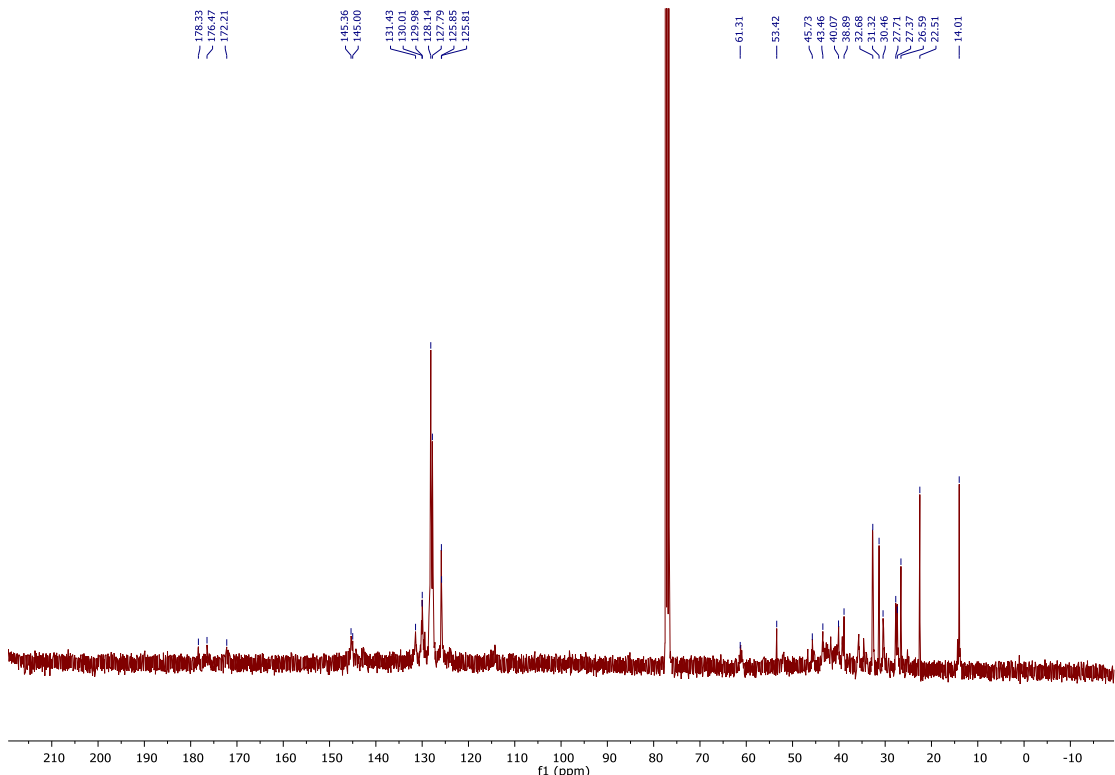


Fig. S166 ^{13}C NMR spectrum (101 MHz, CDCl_3) of $\text{PS}_{34}\text{-}co\text{-}\text{PB}_{49}\text{-}co\text{-}\text{PHCBI}_{17}$.

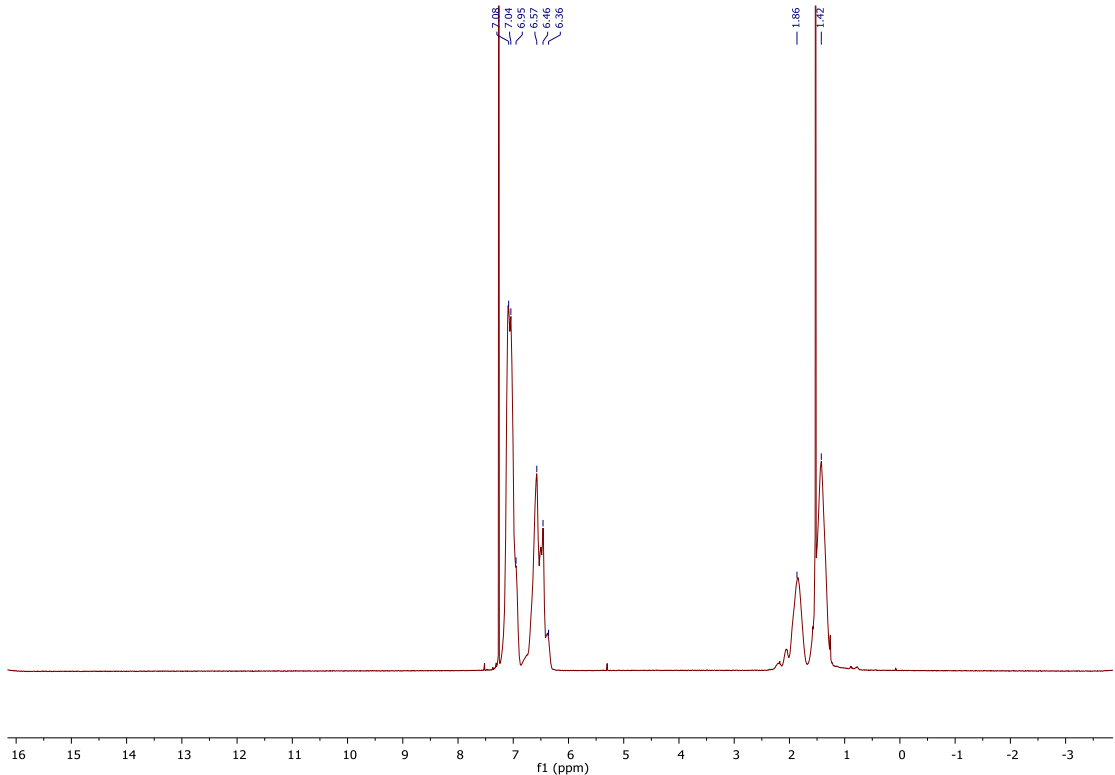


Fig. S167 ¹H NMR spectrum (400 MHz, CDCl₃) of PS.

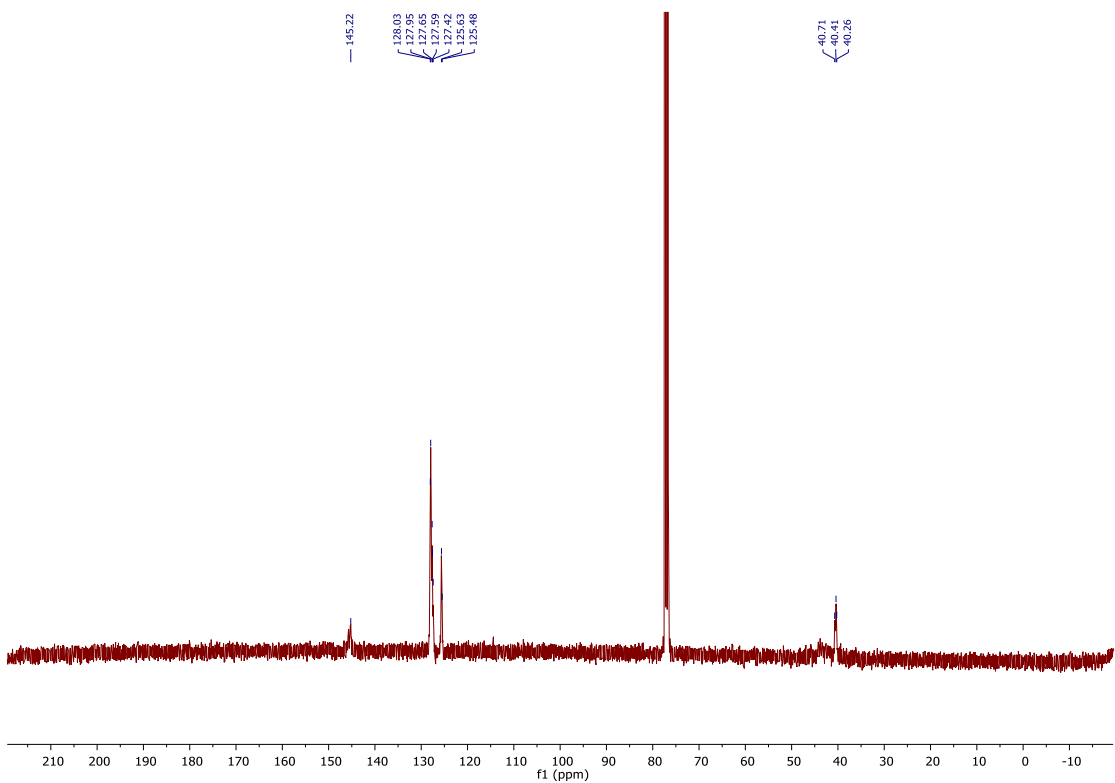


Fig. S168 ¹³C NMR spectrum (101 MHz, CDCl₃) of PS.

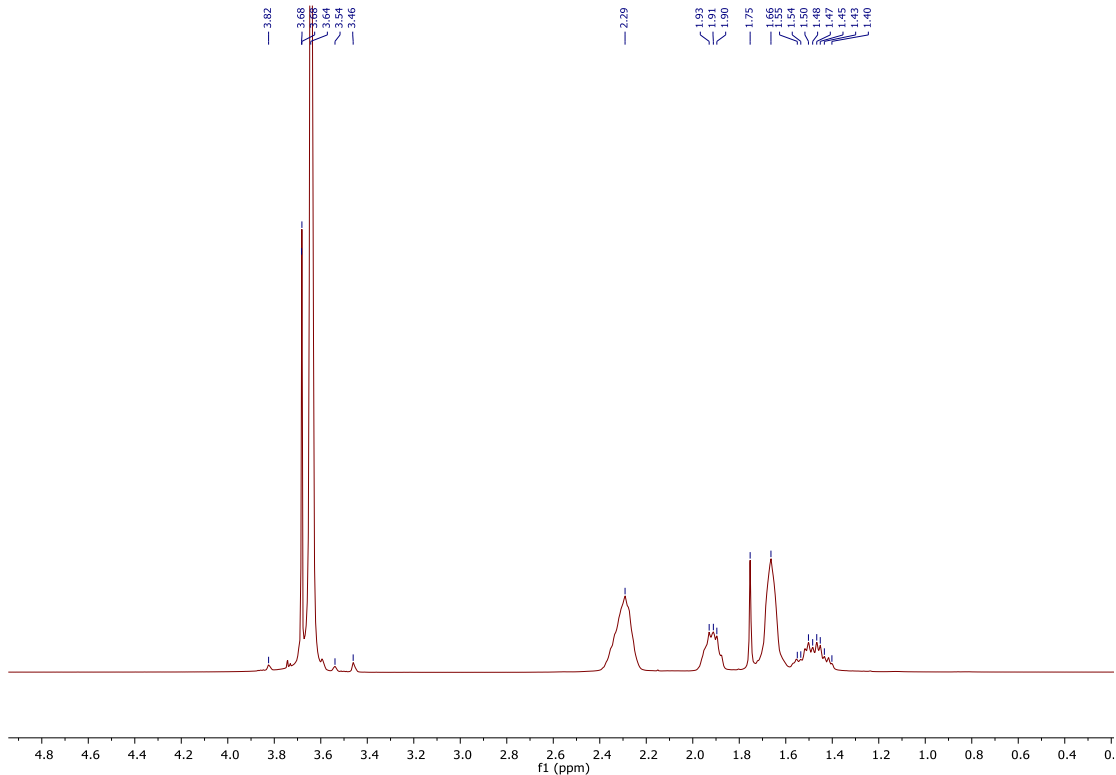


Fig. S169 ¹H NMR spectrum (400 MHz, CDCl₃) of PMA.

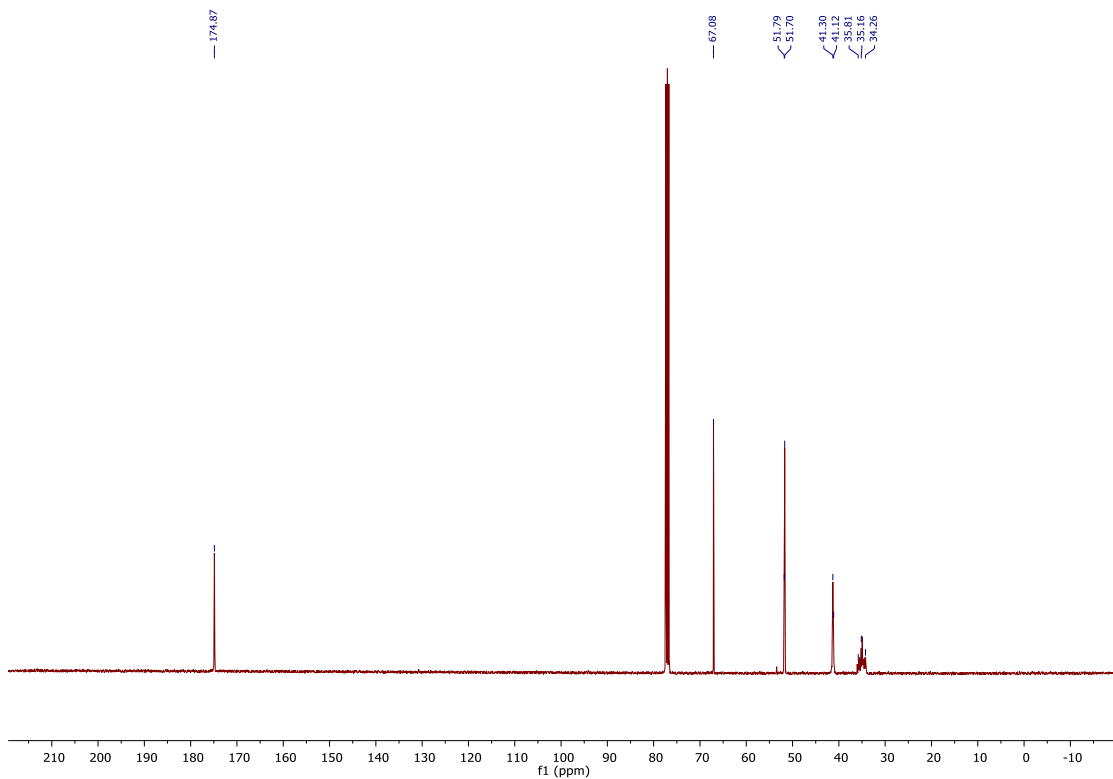


Fig. S170 ¹³C NMR spectrum (101 MHz, CDCl₃) of PMA.

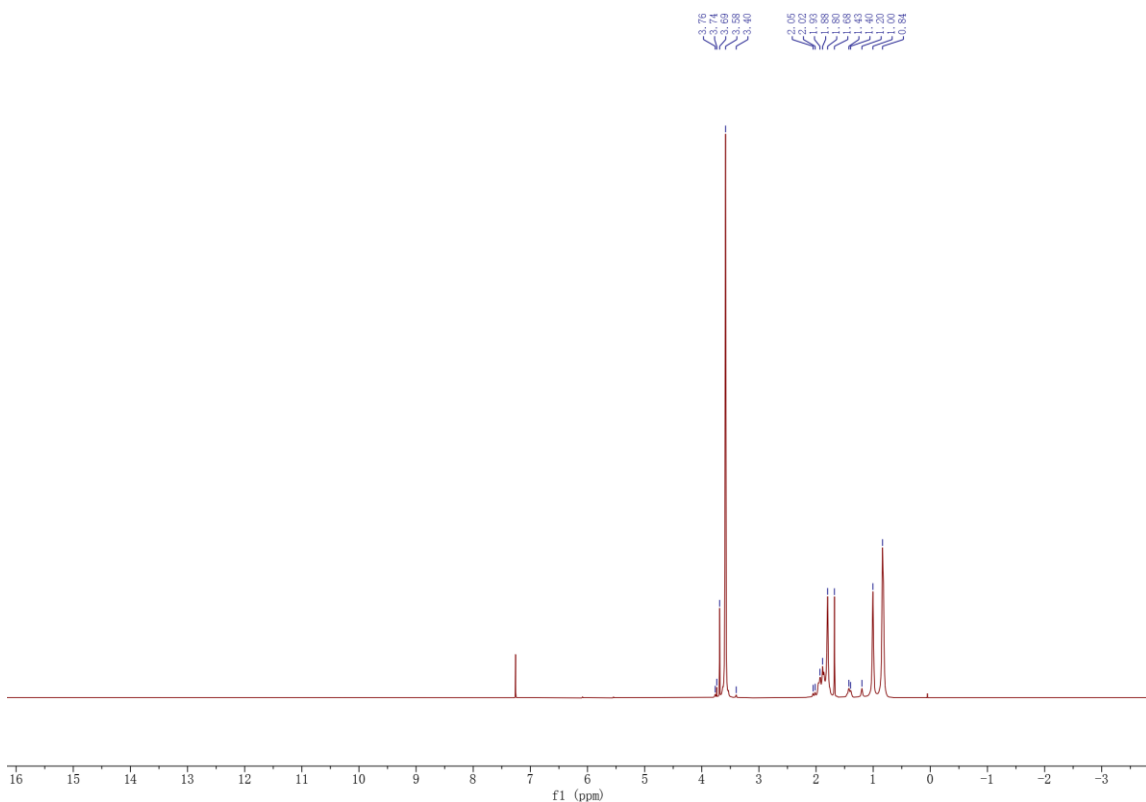


Fig.S171 ^1H NMR spectrum (400 MHz, CDCl_3) of PMMA.

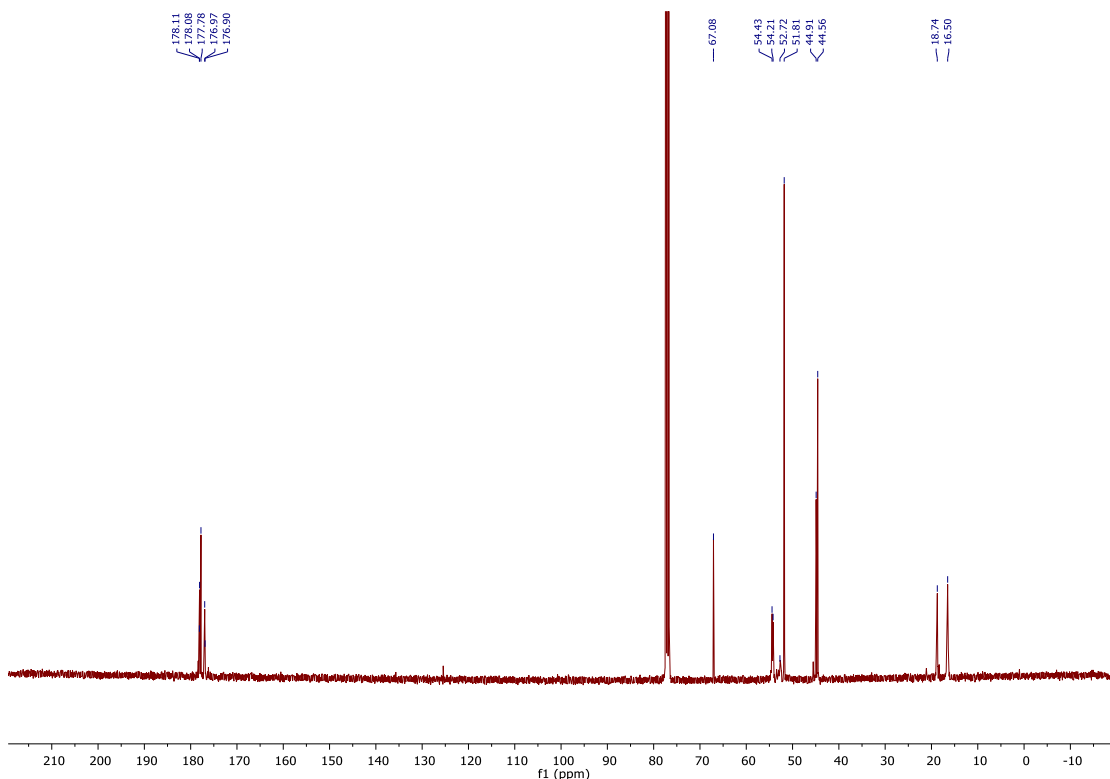


Fig. S172 ^{13}C NMR spectrum (101 MHz, CDCl_3) of PMMA.

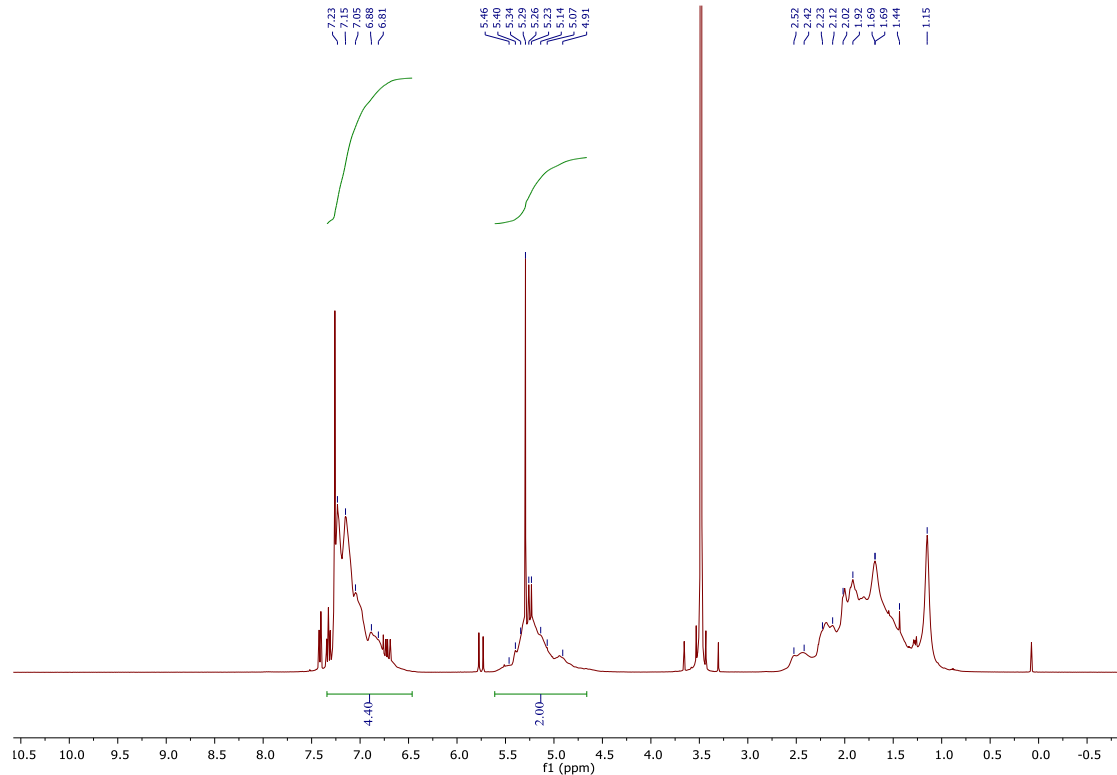


Fig. S173 ^1H NMR spectrum (400 MHz, CDCl_3) of $\text{PS}_{47}\text{-}co\text{-}\text{PB}_{53}$. (The fraction of styrene in copolymers is $(4.4/5)/(4.4/5+1)*100\% \approx 47\%$. Therefore, the fraction of butadiene in copolymer is 53%).

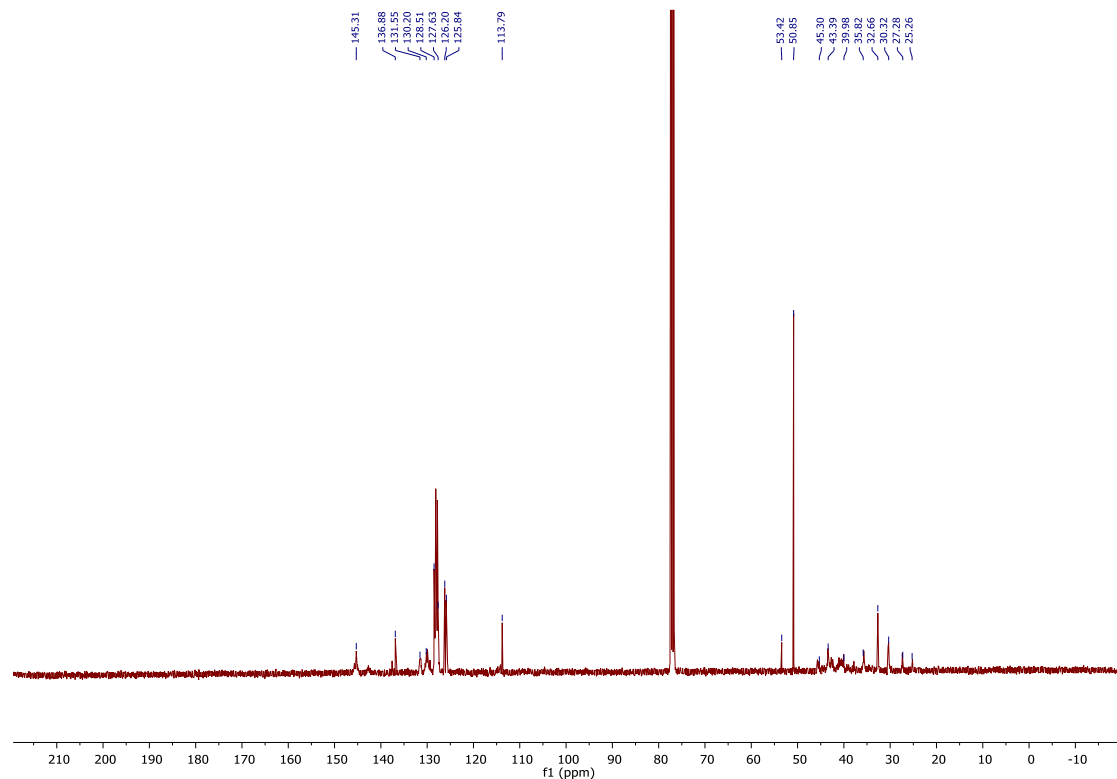


Fig. S174 ^{13}C NMR spectrum (101 MHz, CDCl_3) of $\text{PS}_{47}\text{-}co\text{-}\text{PB}_{53}$.

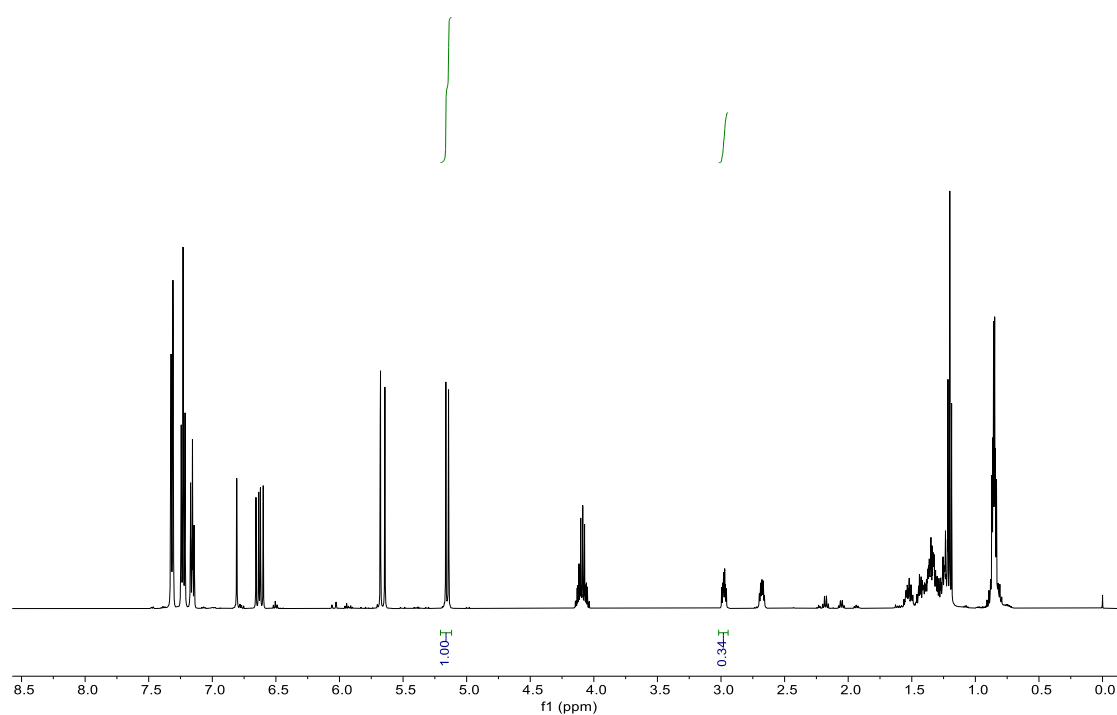


Fig. S175 ^1H NMR spectrum (500 MHz, CDCl_3) of reaction feed mixture for the synthesis of $\text{PS}_{65}\text{-}co\text{-}\text{PCBO}_{35}$. (The fraction of CBO in feed is $0.34/(1+0.34) \approx 0.25$. Therefore, the fraction of styrene in feed is 0.75.)

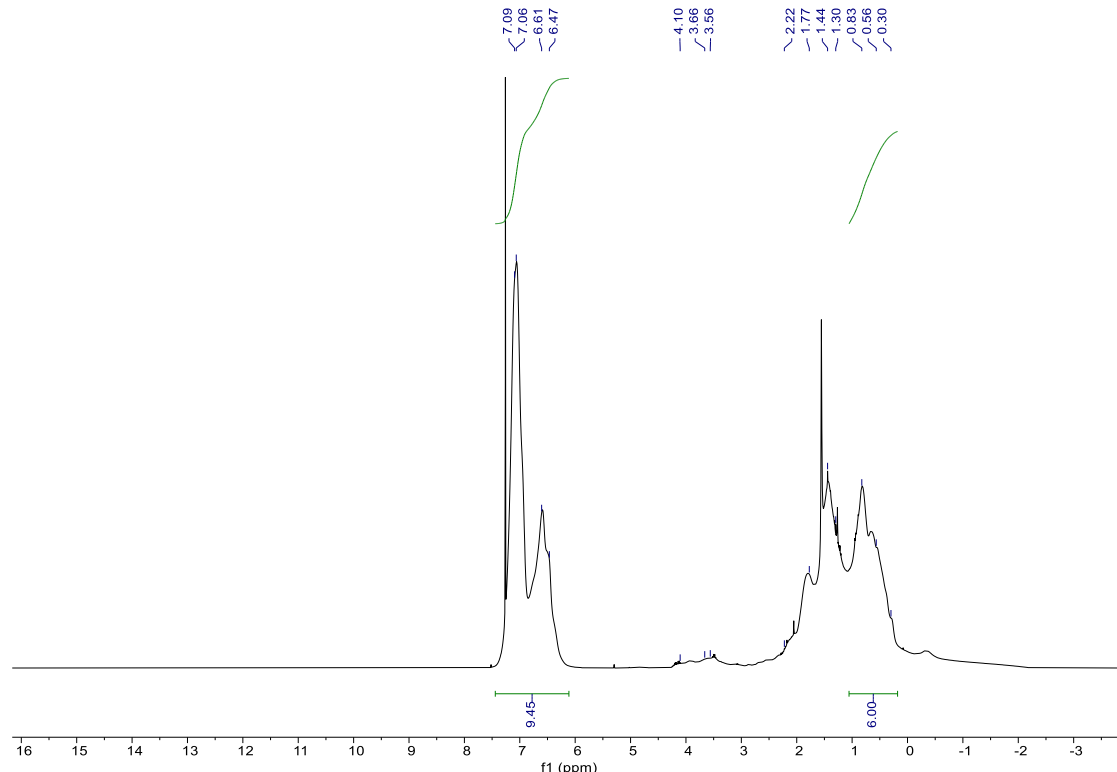


Fig. S176 ^1H NMR spectrum (400 MHz, CDCl_3) of $\text{PS}_{65}\text{-}co\text{-}\text{PCBO}_{35}$, (The fraction of styrene in copolymers is $(9.45/5)/(9.45/5+1)*100\% \approx 65\%$. Therefore, the fraction of CBO in copolymer is 35%).

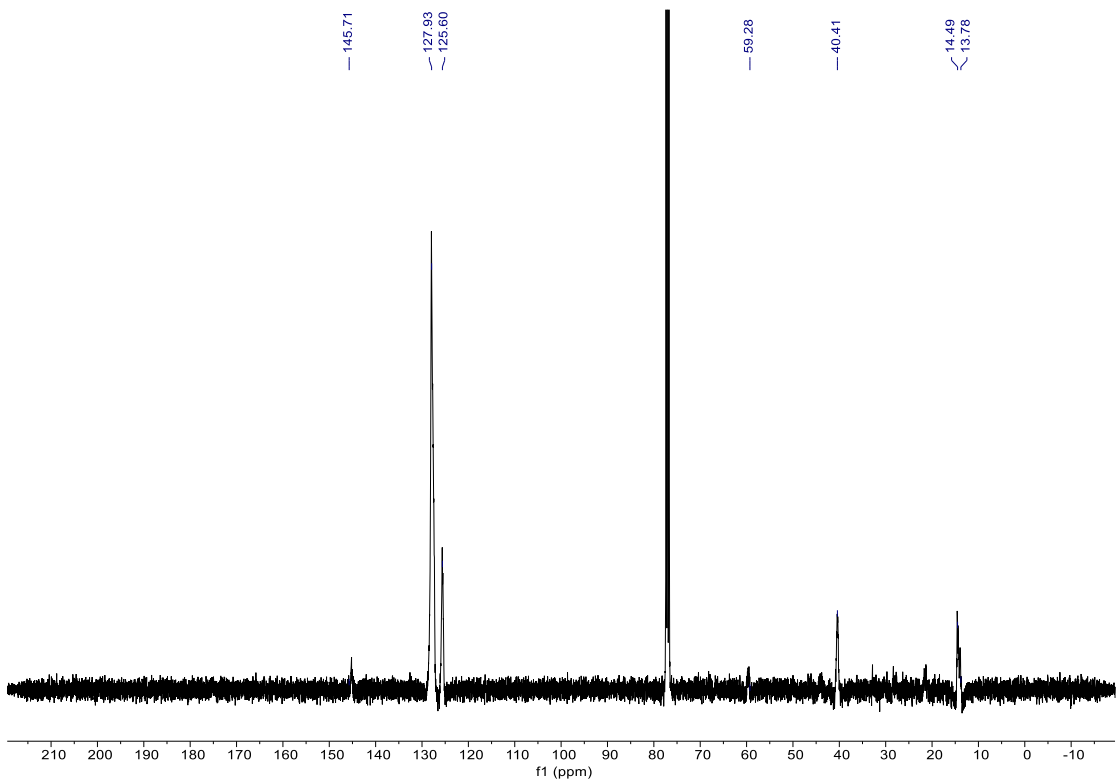


Fig. S177 ¹³C NMR spectrum (101 MHz, CDCl₃) of PS₆₅-co-PCBO₃₅

Reference

1. Khayum, M. A.; Kandambeth, S.; Mitra, S.; Nair, S. B.; Das, A.; Nagane, S. S.; Mukherjee, R. & Banerjee, R. Chemically delaminated free-standing ultrathin covalent organic nanosheets. *Angew. Chem. Int. Ed.* **55**, 15604-15608 (2016).
2. Asadirad, A. M.; Boutault, S.; Erno, Z. & Branda, N. R. Controlling a polymer adhesive using light and molecular switch. *J. Am. Chem. Soc.* **136**, 3024-3027 (2014).
3. White paper as a reference www.waters.com/webassets/cms/library/docs/720005480en.pdf
4. Triandafyllidi, I.; Nikitas, N.; Gkizis, P. L.; Spiliopoulou N. & Kokotos, C. G. Hexafluoroisopropanol-promoted or Brønsted acid-mediated photochemical [2+2] cycloadditions of alkynes with maleimides. *ChemSusChem* **15**, e202102441 (2022).
5. Snider, B. B.; Rodini, D. J.; Conn, R. S. E. & Sealfon, S. Lewis acid catalyzed reactions of methyl propiolate with unactivated alkenes. *J. Am. Chem. Soc.* **101**, 5283-5293 (1979).
6. Fineman, M. & Ross, S. D. Linear method for determining monomer reactivity ratios in copolymerization. *J. Polym. Sci.* **5**, 259–262 (1950).
7. Kelen, T. & Tudos, F. Analysis of the linear methods for determining copolymerization reactivity ratios. I. A new improved linear graphic method. *J. Macromol. Sci., Chem.* **9**, 1–27 (1975).
8. Scholten P. B. V.; Demarteau, J. ; Gennen, S. ; Winter, J. D. ; Grignard, B. ; Debuigne, A. ; Meier, M. A. R. & Detrembleur, C. Merging CO₂-based building blocks with cobalt-mediated radical polymerization for the synthesis of functional poly(vinyl alcohol)s. *Macromolecules*, **51**, 3379-3393 (2018).
9. Drean, M.; Guegan, P.; Detrembleur, C.; Jerome, C.; Rieger, J. & Debuigne, A. Controlled synthesis of poly(vinylamine)-based copolymers by organometallic-mediated radical polymerization. *Macromolecules*, **49**, 4817-4827 (2016).
10. Klein, I. M.; Husic, C. C.; Kovács, D. P.; Choquette, N. J.; Robb, M. J. Validation of the CoGEF Method as a Predictive Tool for Polymer Mechanochemistry. *J. Am. Chem. Soc.* **142**, 16364-16381 (2020).
11. Stauch, T.; Dreuw, A. Advances in Quantum Mechanochemistry: Electronic Structure Methods and Force Analysis. *Chem. Rev.* **116**, 14137-14180 (2016).
12. Caruso, M. M.; Davis, D. A.; Shen, Q.; Odom, S. A.; Sottos, N. R.; White, S. R.; Moore, J. S. Mechanically-Induced Chemical Changes in Polymeric Materials. *Chem. Rev.* **109**, 5755-5798 (2009).
13. Chen, Z.; mercer, J. A. M.; Zhu, X.; Romaniuk, J. A. H.; Pfattner, R.; Cegelski, L.; Martinez, T. J.; Bruns, N. Z.; Xia, Y. Mechanochemical Unzipping of Insulating Polyladderene to Semiconducting Polyacetylene. *Science* **357**, 475-479 (2017).
14. Ong, M. T.; Leiding, J.; Tao, H.; Virshup, A. M.; Martinez, T. J. First rinciples Dynamics and Minimum Energy Pathways for Mechanochemical Ring Opening of Cyclobutene. *J. Am. Chem. Soc.* **131**, 6377-6379 (2009).

15. Kryger, M. J.; Munaretto, A. M.; Moore, J. S. Structure-mechanochemical Activity Relationship for Cyclobutane Mechanophores. *J. Am. Chem. Soc.* **133**, 18992-18998 (2011).
16. Brown, C. L.; Bowser, B. H.; Meisner, J.; Kouznetsova, T. B.; Seritan, S; Martinez, T. J.; Craig, S. L Substituent Effects in Mechanochemical Allowed and Forbidden Cyclobutene Ring-Opeing Reactions. *J. Am. Chem. Soc.* **143**, 3846-3855 (2021).
17. Yang, Q. Z.; Huang, Z.; Kucharski, T. J.; Khvostichenko, D.; Chen, J.; Boulatov, R. A Molecular Force Probe *Nature Nanotech.* **4**, 302-306 (2009).
18. Ong, M. T.; Leiding, J.; Tao, H.; Virshup, A. M.; Martínez, T. J. First Principles Dynamics and Minimum Energy Pathways for Mechanochemical Ring Opening of Cyclobutene. *J. Am. Chem. Soc.* **131**, 6377-6379 (2009).
19. Hickenboth, C. R.; Moore, J. S.; White, S. R.; Sottos, N. R.; Baudry, J.; Wilson, S. R. Biasing reaction pathways with mechanical force. *Nature* **446**, 423-427 (2007).
20. Frisch, M. J.; Trucks, G. W.; Schlegel, H. B.; Scuseria, G. E.; Robb, M. A.; Cheeseman, J. R.; Scalmani, G.; Barone, V.; Mennucci, B.; Petersson, G. A.; et al. Gaussian 09 Revision A.01. 2009.
21. Halgren, T. A.; Lipscomb, W. N. The synchronous-transit method for determining reaction pathways and locating molecular transition states. *Chem. Phys. Lett.* **49**, 225-232 (1977).
22. Peng, C.; Bernhard Schlegel, H. Combining Synchronous Transit and Quasi-Newton Methods to Find Transition States. *Isr. J. Chem.* **33**, 449-454 (1993).
23. Stauch, T.; Dreuw, A. On the use of different coordinate systems in mechanochemical force analyses. *J. Chem. Phys.* **143**, 074118 (2015).